Design and Construction of
A Parallel Axes Gear Research Test Rig

M.Sc. Thesis

In

Mechanical Engineering

University of Gaziantep

Supervisor
Prof.Dr.Nihat YILDIRIM

By

Ömer UÇTU

July 2015

REPUBLIC OF TURKEY
UNIVERSITY OF GAZIANTEP
GRADUATE SCHOOL OF NATURAL & APPLIED SCIENCES
MECHANICAL ENGINEERING

Name of the thesis: Design and Construction of a Parallel Axes Gear Research Test Rig
Name of Student : Ömer UÇTU
Exam Date : 27.07.2015

Approval of the Graduate School of Natural and Applied Sciences

Prof. Dr. Metin BEDİR
Director

I certify that this thesis satisfies all the requirements as a thesis for the degree of Master of Science.

Prof. Dr. M.Sait SÖYLEMEZ
Head of Department

This is to certify that we have read this thesis and that in our opinion it is fully adequate, in scope and quality, as a thesis for the degree of Master of Science.

Prof. Dr. Nihat YILDIRIM
Supervisor

Examining Committee Members	Signature
Prof. Dr. Mustafa YAŞAR	....
Prof. Dr. Nihat YILDIRIM	....
Asst. Prof. Dr. Abdullah AKPOLAT	....

I hereby declare that all information in this document has been obtained and presented in accordance with academic rules and ethical conduct. I also declare that, as required by these rules and conduct, I have fully cited and referenced all material and results that are not original to this work.

Ömer UÇTU

ABSTRACT

DESIGN AND CONSTRUCTION OF A PARALLEL AXES GEAR RESEARCH TEST RIG

UÇTU, Ömer
M.Sc. in Mechanical Engineering
Supervisor: Prof. Dr. Nihat YILDIRIM
July 2015
188 pages

In this thesis, a back to back type research test rig is designed and manufactured to study on the transmission error, wear, pitting and oil performance of the gears under controllable conditions. The back to back test rig have test and slave gearboxes connecting with rod and couplings. Static torque is locked into the system via torque clutch mechanism. Power of electric motor only compensates system power losses. Its speed is variable between 0-3000 rpm. Speed of the system can be increased by belt-pulley system. Lubrication of gears and bearings is provided from an oil tank whose capacity is 30 lt/min. On test rig, in addition to these, there are 4 thermocouples, an oil pressure gauge and an oil pump (20 cc).

In analytical design of parts, all calculations of test gears, shafts, bearings, torsion rods, couplings and similar are made by using computer programme Ms Excel®. All 3-D and 2-D drawings of test rig components are made by using computer programme Catia® and AutoCAD®. Finite element analysis of some parts are made by using computer programme MSC SimXpert®. All parts of the test rig are manufactured in high precision machines.

Key words: Gear test rig design, gear test rig manufacturing, finite element analysis, gearbox design, gearbox manufacturing.

ÖZET

PARALEL EKSENLİ DİŞLİLER İÇİN DİŞLİ ARAŞTIRMA TEST DÜZENEĞİ TASARIMI VE İMALATI

UÇTU, Ömer
Yüksek Lisans Tezi, Mak. Müh. Bölümü
Tez Yöneticisi: Prof. Dr. Nihat YILDIRIM
Temmuz 2015
188 sayfa

Bu çalışmada, dişlilerdeki iletim hataları, aşınma, korozyon ve yağ performansı üzerinde çalışma yapmak üzere kapalı devre tip dişli test düzeneği tasarlanmış ve üretimi yapılmıştır. Düzenek kaplin ve rodlarla birbirine bağlanmış test ve sürücü dişli kutularından oluşmaktadır. Sisteme statik tork, tork yükleme mekanizması ile yapılmaktadır. Elektrik motoru sadece sistem içerisindeki kayıpları karşılamaktadır. Elektrik motorun hızı 0 ile 3000 rpm arasında değişmektedir. Kayış kasnak mekanizması ile şaftların hızı arttırılabilmektedir. Dişli ve rulmanların yağlanması 30 lt/dak yağ basma kapasitesine sahip yağ tankından sağlanmaktadır. Ayrıca düzenekte 4 adet sıcaklık ölçer, 1 adet yağ basınçölçer ve 1 adet yağ pompası bulunmaktadır.

Sistemde kullanılan parçaların; test dişlileri, şaftlar, rulmanlar, tork rodları, kaplinler ve benzerlerinin analitik tasarımları Ms Excel® programı kullanılarak yapılmıştır. Üç boyutlu ve iki boyutlu çizimleri Catia®, ve AutoCad® programı kullanılarak çizilmiştir. Sonlu elemanlar analizi ise MSC SimXpert® programı kullanılarak yapılmıştır. Deney düzeneği parçaların üretiminde ise ağırlıklı olarak hassas işleme makinelerinden faydalanılmıştır.

Anahtar kelimeler: Dişli test düzeneği tasarımı, dişli test düzeneği üretimi, sonlu elemanlar analizi, dişli kutusu tasarımı, dişli kutusu üretimi.

ACKNOWLEDGEMENT

The author is grateful to. Prof. Dr. Nihat YILDIRIM for his encouragements and suggestions throughout the study of this thesis as the supervisor.

I would like to thank to Assist. Prof. Dr. Abdullah AKPOLAT for his valuable support

I would like to thank to Research Asst. BURAK ŞAHİN.

I would like to thank to all BCS Metal family, especially, Bülent KARATAŞ and Kerem ELİBAL.

I would like to thank to my brother, Ramazan UÇTU for his support.

I would like to express my gratitude to my wife, Hacer, and my daughter, Azra and my son, A.Cemil for their support, patience and encouragement.

TABLE OF CONTENTS

LIST OF TABLES

LIST OF FIGURES

CHAPTER 1

INTRODUCTION

1.1.GENERAL INFORMATION ABOUT THESIS SUBJECTS

Gears are one of the most important power transmission elements required to transmit both torque and motion between parallel and non-parallel shafts. Those parallel axes ones including spur and helical gears are the most widely used types of gears. They are used in a large spectrum of the applications ranging from simple kitchen utensils to hydraulic pumps, from conventional speed reduction units used in combination with most electric motors to almost all automotive vehicles having multiple speed gearboxes, from energy conversion units of turbine gearboxes to critical applications of waterborne and airborne vehicles of ships, aeroplanes and helicopters. Among those fields, transportation vehicles of both ground wheelded vehicles and the airborne types are the most widely used and most critical applications requiring reliable, well designed and suitably tested gears.

A faulty gear system could result in serious damage in such critical applications if defects occur in any of the gears during operation. Early detection of the defects, or prevention of those defects via design process are crucial to prevent the system from malfunction that could cause damage or entire system halt. Therefore both a sound design theory and an experimental work to verify the design theories are essential steps towards a reliable gear system design.

Gears (and gear designers) are under a non-stop pressure (get gears) to run at higher speeds and under more loads than ever before. Not only the load and speed capacities are required to be increased but also the vibration and noise performances of those high speed gears are required to be improved. These load and vibration-noise requirements are related to two performances of gears namely the static and dynamic performances. This second requirement (better vibration and noise levels) is called the dynamic performance of gears which is not as clearly identified as the static performance. Even the static performance of gears is not so straight forward. Failure possibilities and performance ratings of meshing gears covers many parameters including bending and contact stresses, tooth friction, lubrication, tooth surface imperfections, geometric inaccuracies, heat treatment, system resonances, structural integrity (gear-shaft-bearing-housing), internal excitations and others.

Such complex and inter related parameter variations cannot always be modelled analytically or numerically and even if they are assumed to be modelled such models require an experimental verification for validating the proposed models. Therefore, an universal gear research test rig is an essential tool from the point of view of improving both static and dynamic performances when designing gears for critical applications such as aerospace and automotive industries.

For years, design and manufacture of those heavy load and high speed gears used in both aerospace and automotive industries were all performed outside of Turkey. Gear and gearbox design industry for such critical sectors were not established at home till today. However, fast growing industry of local automotive manufacturers and the newly emerging local aerospace industries of Turkey has made a big step into requirement of design and manufacture of reliable gears and gearboxes. Such incentives of both private sector and state development plans brings the requirement of providing gear designers a universal gear research test rig on which different tests and measurements can be performed to validate their design before huge investments are made to manufacture them.

During past 30 years it has become increasingly recognized that the dynamic performance of gears matters more than the static performance since most gears do run at relatively high speeds. At such high speeds also under relatively high tooth loads, the torsional vibration of gears become an important cause of gearbox vibration and noise (and also dynamic tooth stresses). Researchers and designers began to pay their attention to the dynamic behaviors of gear systems operating at high speeds. The main goal of their research is to study the reasons for the noise and vibrations of gear systems to ensure quality product. The first simple mass-spring model was introduced in 1950's [1]. Researchers, thereafter, improved the mass-spring model by adding modified physical factors such as damping and friction coefficients. These modifications increase the reliability of the model. Özgüven and Houser [1] presented a thorough review on these mathematical models used in gears dynamic analyses. Some of the researchers proposed a large-scale digitized approach for an interrupted static and dynamic analyses of spur gearing.

The phenomenon of (static and dynamic) transmission error(s) is agreed upon to be one of the main gear vibration and noise sources. Transmission Error (TE) illustrated in Figure1.1 is defined [2] as "the difference between the actual position of the output gear and the position it would occupy if the gear drive were perfectly conjugate." Therefore measurement of both static and dynamic TE's is important to support any gear design and gear system model to be used in research and development works. Most efforts to experimentally measure transmission errors have been initially devoted to their measurement under very light loads at very slow speeds. These efforts have been primarily directed towards using transmission error as a gear screening measurement or quality control and most commercial developments have been for this purpose. For quality control, light loads are desirable, since profile errors, run out and gear tooth nicks can be detected for all teeth by simply rolling the test gear against a master gear. Likewise, the test gear's rotational speed must be low enough to avoid any system dynamic effects.

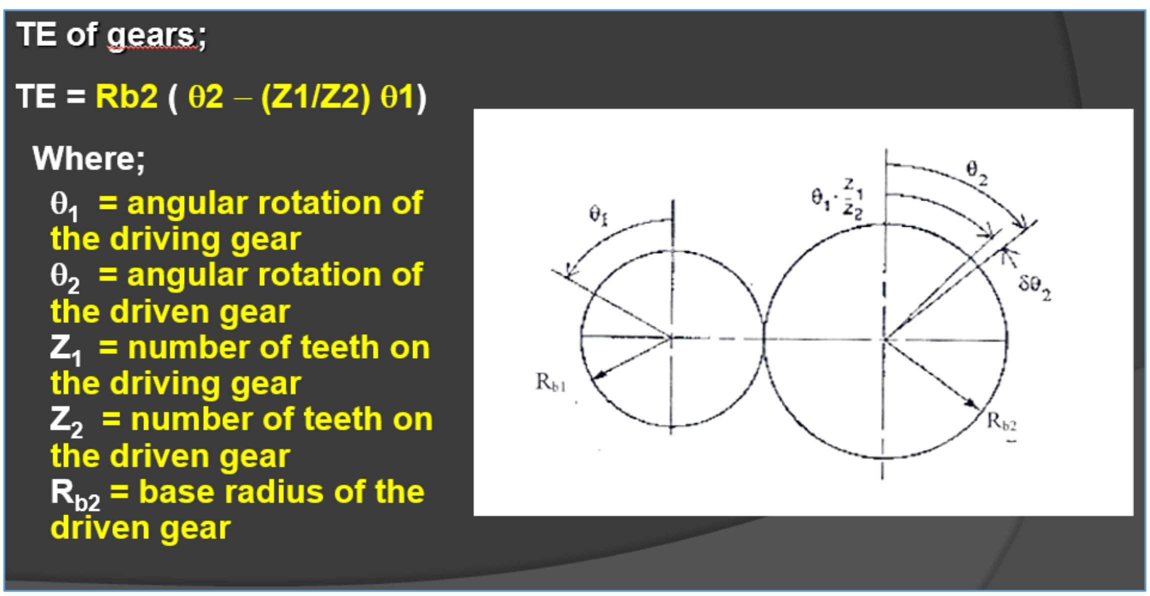

Figure 1.1: Mathematical formula of TE

In addition to manufacturing inconsistencies which may be detected by slow speed transmission error measurement, when gears are loaded, an additional component of transmission error arises due to deflections of the gear teeth and their supporting structure like shafts and bearings under load.

Diagnosing a gear system by examining vibration signals is the most commonly used method for detecting gear failures. The conventional methods for processing measured data contain the frequency domain technique, time domain technique, and time-frequency domain technique. These methods have been widely employed to detect gear failures. However, they all have some limitations and cannot be applied to all conditions; that is, some types of failures cannot be detected by these methods. Many articles have been published to compare these techniques. Among many of the theoretically possible transmission error measurement techniques, the following are the ones practically used and mentioned in the literature with some limitations.

- Magnetic signal methods
- Torsional vibration transducers of the seismic type
- Tachometer type devices
- Tangential accelerometer devices
- Grating (rotary encoder) systems for digital use
- Grating systems for analogue use

Because of the inaccessibility of free shafts, there have seldom been TE measurements performed on unmodified production gearboxes. A combination system which utilizes both an optical encoder and a torsional induction accelerometer was used by Milenkoviç, Shmuter et al.[3,4] to measure dynamic TE at operating speeds on an axle inspection system. Through all of these attempts, optical encoders have repeatedly been selected as a favorable means of measuring TE. Several manufacturers build commercial systems using encoders for TE measurement, but as mentioned earlier, these systems are typically designed for unloaded measurements.

There are three types of common test stands;

1. Back-to-Back tester

2. Loaded transmission error tester

In most cases of the TE measurement of both unloaded and loaded gears, a power circulating (Back-to-back) test setup which used special gear housings was used.

1.2.PURPOSE OF THESIS

Gears are one of the most important elements among similar machine elements. They lead to positive and continuous transmission of motion, power and force at different directions. So, they promote invention of different machines and equipments. Today gears are used in many kinds of machines and equipments like as, simple home and office machines, every kind of transports, heavy machines, tanks, helicopters, submarines and etc. Especially, gears transmit high power without rival in most application. Gears supply the highest efficiency and highest working life among similar for minimum and maximum speeds. Also gears are the cheapest machine elements among similar.

There are gear research centers, like AGMA, BGA, FZG, CETIM and etc, in many European countries, because gears are important elements for technological development. For modern gear design theoretical researches only are not enough. Experimental research results have to support the theoretical findings. Experimental research results do activate the research subjects beyond the theoretical limits too.

In other words, advantages of experimental works about gears can be expressed according to theoretical studies below;

- Although theoretical studies are necessary before any manufacture and use, experimental studies are also necessary to validate the theoretical studies.
- Experimental studies are generally valid all over the world.
- Actual working conditions can be set or determined with high accuracies during experimental studies.
- It is not always possible theoretically, to evaluate and describe, effects of some mechanism such as lubricating the gears on gear performance.
- Parameters such as noise and vibration are easily measured on test rigs.
- More complex the mechanism, more difficult the theoretical analysis with high confidence.

Disadvantages of experimental works can be expressed below;

- Gear test rigs require high cost.
- Experimental researches consume a lot of time and effort.

In the subject of gear design, both in our university and other university in Turkey and in the world a lot of researches are made by academicians but there is a clear need for the more experimental work. Design of this such a test rig will help to start doing experimental work and supply actual test results about gear researches. Mutual relations between our university and other universities of the world based on the experimental work being planned will improve too.

At the end of thesis some parameters will be measured. These parameters are;

- Lubrication oil temperature
- Torque measurement

If the designed and manufactured gear test rig (a schematic view of which is shown in Figure 1.2) is equipped and modified with required equipments, lots of different parameters could be measured.

Some of these parameters are;

- Gear tooth stresses and strains
- Gear tooth deflections
- Gear tooth static and dynamic loads
- Bearing deflections and loads
- Gear shaft vibrations
- Gear torsional vibrations
- Gear case vibrations
- Noise radiated from a test gearbox
- Etc.

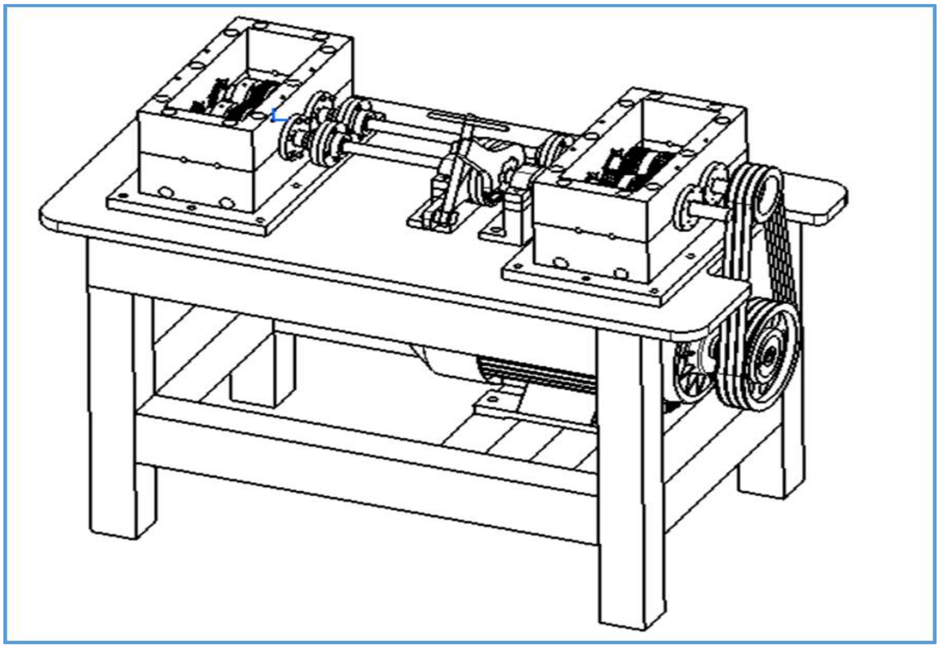

Figure 1.2: Test Rig

The aim of this thesis is to perform necessary research and development work for design, production and basic instrumentation (thermocouple for oil, strain gauges) of a functional Parallel Axes Gear Test System.

Such a test system will enable designers and researchers do research work for development of quitter, safer, long life gear design procedures by studying static, dynamic and fatigue characteristics of spur and helical gears used in different industries.

The same test system to be designed, manufactured and instrumented, will also serve other critical sectors like automotive and energy where parallel axis gears are also used widely.

CHAPTER 2

LITERATURE SURVEY

2.1.LITERATURE SURVEY

The gears, which are the most basic elements of the organs of power transmission, related research and development work were always carried out in the form of prove and support the theoretical studies with experimental studies. Because, most of the time, theoretical studies were conducted based on some preliminary acceptance and predictions. This preliminary acceptance with the accuracy of the predictions/hypothesis is however approved by experimental studies. New theory and hypothesis are developed through the results are obtained from conducted systematic experimental study. In this way, the great improvements have been achieved on the gears, which are the most critical elements of the many applications, design and manufacturing methods

In conducted experimental studies abovementioned, many other topics are included such as the gear wear down, the gear surface fatigue, the formation of a dynamic force at high speeds, vibration and noise in the gear, the effects of the gear profile geometry to gear strength, lubrication system efficiency, the different oil performances of additives, the effects of the gear surface hardness on the material strength and life etc.

The gears are used in many critical applications such as defense industry (space, air, land and sea), energy sector (steam and wind turbine gear boxes) and the automotive sector. Gears used in these areas without experimental confirmation can be contained high risks for designer and manufacturer. Because of these reasons the country and institutions conducted years of scientific and technological R&D activities to develop gear design and manufacturing technology. They established one or few types of gear experimental test rigs to check and confirm theoretical studies.

These kinds of gear test rigs are designed and manufactured within R & D activities. They are used to make experiments for parallel-axis and non-parallel axes gears' performance evaluation. These are braked gear test rig and the closed circuit (back-to-back) gear test rig. In braked type gear test rig (Figure 2.1 and 2.2), gears and gearbox to be tested should be driven by electric motor at one side whereas different kinds of braking system such as magnetic, eddy current, hydraulic, etc can be loaded at other side to create a reaction torque.

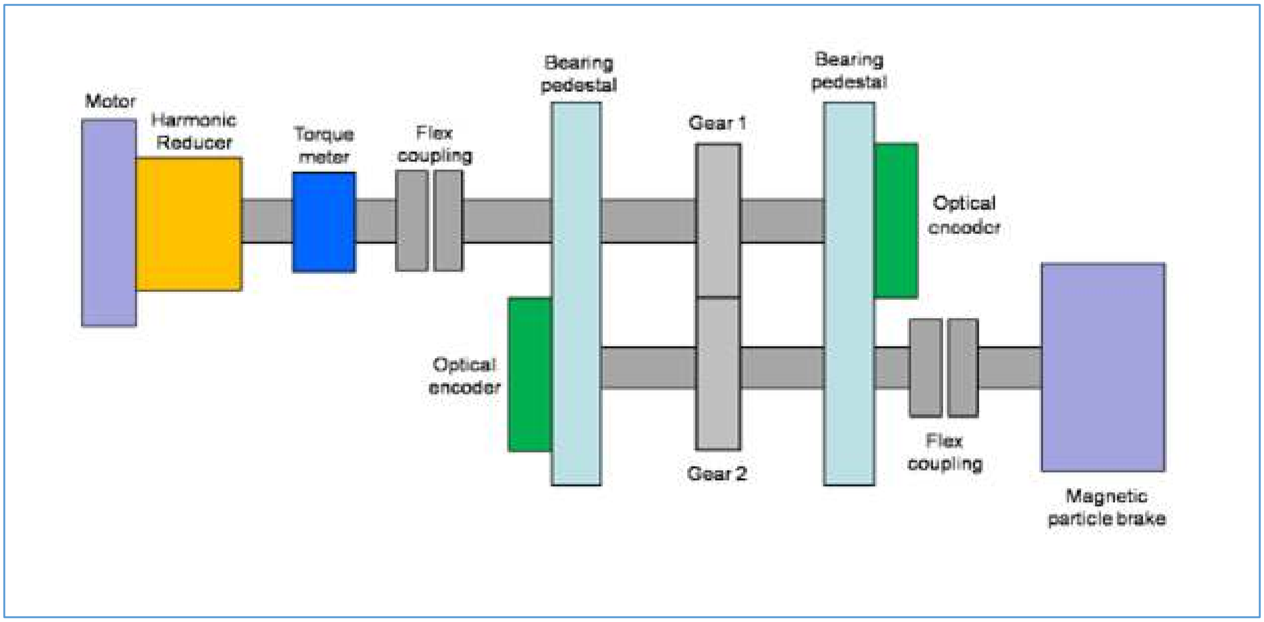

Figure 2.1: Braked Gear Test Rig

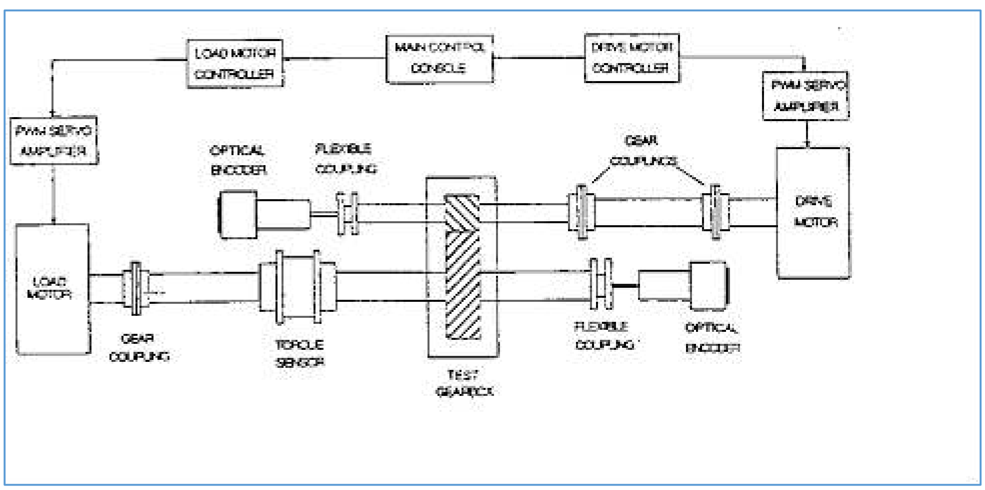

Figure 2.2: Braked System

In these systems the amount of gear transfer torque and rotational speeds (within the boundaries of the system) can be adjusted at the desired value. This type of control of speed and torque values can be adjusted while driving is an important advantage. However, changing or not changing the reaction torque of the brake system while driving after adjusting desired value sometimes is a problem parameter. This parameter must be observed nearly. It directly affects the test performance of gear. Main problem of this type of test systems is being waste of all gear transfers power.

On the other hand test gearbox and similar support gearbox (slave gearbox) are used as back to back on "closed circuit" gear test rig (Figure 2.3 and 2.4) and a torque can be fixed between them.

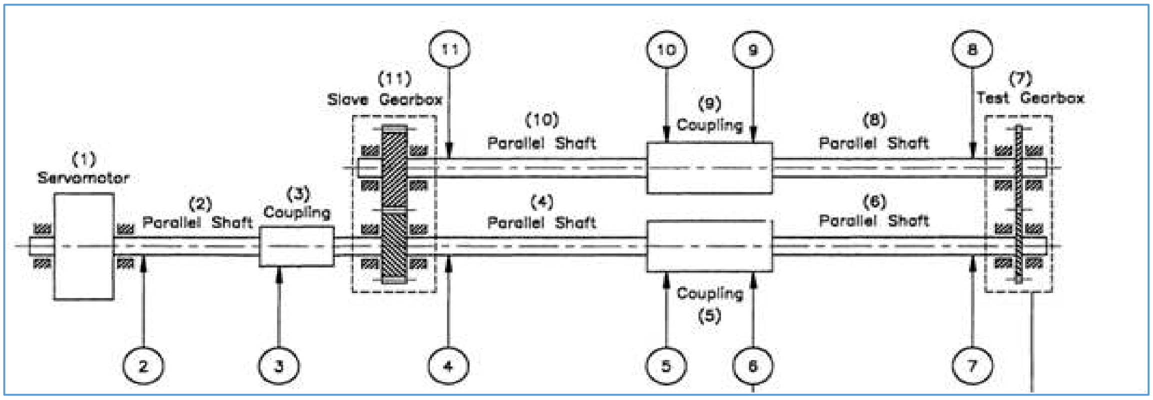

Figure 2.3: Closed circuit test rig

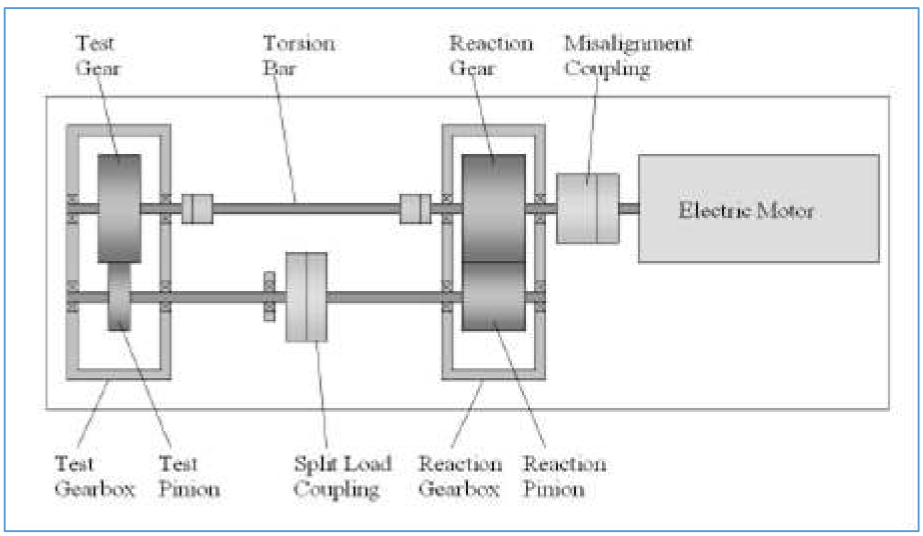

Figure 2.4: Closed circuit test rig

This torque can be applied and removed by adjusting angular positions of coupling or similar torque loading mechanisms in the system. In this way, between both the gearbox, and also between gears (and teeth), a fixed torque is installed, regardless of the speed.

A braking system is not required for loading of torque like the braked loading test rig. But a driver (usually an electric motor) is needed to operate the systems. However, this is not as high as required motor power. It is nearly 1/10 of transmitted power (10%). Because this motor power is required only for compensating friction (and inertia) in the system.

However, this mechanism has some disadvantages too. Not changing of torque during operation is disadvantages. However, it is possible to change torque during operation with the R & D works. Especially slave gear box needs to be isolated to eliminate vibration and noise which negatively affect the behavior of test gear box. This is other difficulty for back to back test rig. All kinds of dynamic (high speeds) testing and experiments on the gears can be made much easier and cheaper with back to back test rig.

Tooth root stresses, tooth surface fatigue, micro pitting, macro pitting, scuffing, scoring, oil and lubricating system, effects of new gear materials performance, effects of new manufacturing methods, surface quality, gear vibrations and noise, the dynamic modeling of gear, dynamic forces of gear, bearing forces and etc. can be studied on the back to back test rig;

Main countries and institutions designed and operated of this type of test rigs are USA (NASA, Ohio State University), Germany (FZG, WZL, and Munich Technical University), and England (BGA, Cambridge University, Newcastle University) ve France (CETIM). In recent years, Japan, Australia, and China are followed to this countries.

Studies starting with Opitz and Dudley at 1940 and 1950 has been formed to systematic researches in established unit in NASA. This unit has been most important center of gear studies of both USA and all countries result of R&D works together with American Universities. Scientific studies carried out in this unit or similar units are published and serviced to national gear design and manufacturing industry.

Approximately the late 1960s or early 1970s, experimental studies working on gear test rig designed and manufactured in NASA as shown in Figure 2.5. From 1970 to 2010 different versions of this test rig has been designed and manufactured to perform experimental studies as parallel to last studies. Scientific studies on similar mechanisms have been gone and serviced to in aerospace, defense, air, sea and land transportation, the energy sector, the automotive sector.

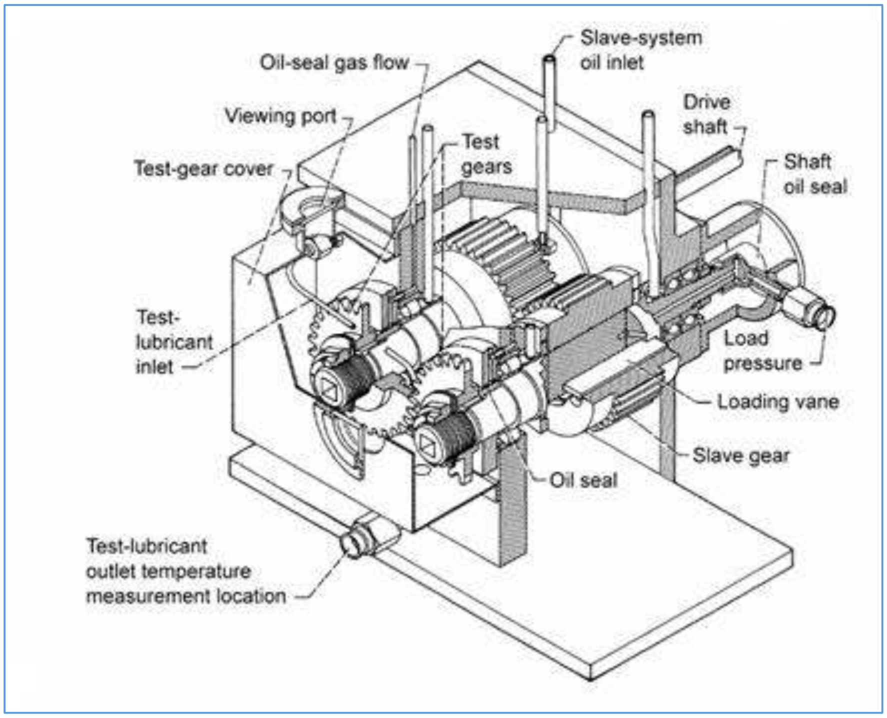

Figure 2.5: Designed test rig in NASA

Some studies performed by using some of the test rig are:

- Krantz and Kahraman, 2005, in their research, investigated experimentally the influence of lubricant viscosity and additives on the wear rate of spur gear pairs. The gear specimens from a comprehensive gear durability test program that includes seven different lubricants were inspected to demonstrate the influence of the lubrication condition on gear tooth surface wear. Krantz and Kahraman, 2005, found that the wear rates are strongly related to the viscosity of the lubricant. Lubricants with larger viscosity result in larger lambda ratios and lower wear rates. A similar strong influence of the lubricant viscosity was previously observed for surface fatigue lives as well. An exponential relationship between the surface fatigue lives and the average wear rates was found. The data suggest that viscosity plays a dominant role. There were also considerable differences in wear amounts for three lubricants with differing additive packages but similar compositions and viscosities [5].

- Krantz, 2005, focused in his project was gear surface fatigue, with special attention given to the influence of surface roughness. He grouped his research in three categories: (1) assessments and developments of statistical methods for gear fatigue data, (2) experimental evaluation of the fatigue lives of super finished gears relative to ground gears, and (3) evaluation of the experimental condition by use of elasto hydrodynamics, stress analysis, and surface topography inspections [6].

- Krantz and Tufts, 2007, compared their results with past works done using the same test apparatus and test methods. For surface fatigue testing, the present results were compared to previous works testing AISI 9310 and Pyro wear 53 (AMS 6308B), two alloys used in production today as aircraft steels. Surface fatigue testing was done at a contact stress of 1.7 GPA (250 ksi). For bending fatigue testing, the present results were compared to previous works testing AISI 9310. Krantz and Tufts conducted testing using the single tooth bending method, load control, and a crack initiation definition of a 2 percent increase in the test load stroke relative to the stroke of the initial loadings. In this study, Krantz and Tufts quantified some performance characteristics of the new alloy and has provided guidance for the design and development of next generation gear steels [7].

- Handschuh, Timothy and Krantz, 2010, conducted some experiments to provide an understanding of the engagement of metal debris into a gear mesh. They used gears for testing were case-carburized 12-pitch spur gears made from the steel alloy AISI 9310. The metal debris that was engaged into the pair of meshing test gears was shim stock, drill bit shanks, and chips of gears liberated from a test gear. Handschuh, Timothy and Krantz found that the peak torque required to rotate the gears with the object engaged was proportional to the size (mass) of the engaged object. Engaging objects of higher hardness required a significantly greater peak torque relative to an equivalent sized object of lesser hardness. For the largest chip sizes tested, sufficient deformation occurred to the gear teeth to prevent smooth motions of the gear when the damaged tooth is engaged. During this study, no new chips and no obvious tooth fracture occurred [8].

As we have seen, gear life-strength relations, tooth stresses under load, surface abrasion - life properties, lubricating oil and effects, the effects of the quality of the surface, the effects of material properties and many issues and their R&D studies have been done with experimental works on this type of gear test rigs.

Different gear test rigs have been designed and manufactured for similar studies. This type of academic research and development studies about gears is mainly carried out in the Ohio State University.

Some academic researches of universities are:

- Chase, 2005, in his thesis developed a methodology to test the efficiency of high speed gearboxes. A specially designed test machine was developed and procured to be able to independently control the speed, input torque, lubes temperature, and lube flow rate. A systematic approach to calibrating, mounting/removal of test specimens as well as methodology for testing of the high-speed gearboxes has been developed. The effect of surface roughness, surface coatings, diametric pitch, rotational speed, load, lubricant viscosity, and temperature and face width has been studied. A variety of gear sets have been designed and procured for the experiments. The surface roughness of the gears have been measured and tabulated. Correlations between the previously mentioned tests parameters to the efficiencies have been outlined [9].

- Klein, 2009, his thesis was based on experimental studies involving two modes of gear contact fatigue failure: gear pitting (spalling) and gear scuffing. Klein, 2009, performed the standard ISO 14635-1 FZG Scuffing Test on AISI 8620 type a spur gears. These experiments included four uncoated gear pairs and one gear pair coated with an experimental PVD coating. Uncoated gears encountered scuffing during Stages 11 and 12. In the study, a high correlation between temperature and scuffing results was detected for both coated and uncoated specimens [10].

- Vaidyanathan, 2009, in his study, developed a test methodology for measuring load-dependent (mechanical) and load-independent power losses of helical gear pairs. For this purpose, he adapted a high-speed four-square type test machine. Several sets of helical gears having varying module, pressure angle and helix angle are procured, and their power losses under jet-lubricated conditions are measured at various speed and torque levels. Vaidyanathan, 2009, compared the experimental results to a helical gear mechanical power loss model from a companion study to assess the accuracy of the power loss predictions. The validated model is then used to perform parameter sensitivity studies to quantify the impact of various key gear design parameters on mechanical power losses and to demonstrate the tradeoff that must take place to arrive at a gear design that is balanced in all essential aspects including noise, durability (bending and contact) and power loss [11].

- Rossi, 2010, on his PhD thesis he focused on ınfluence of profile modifications on Transmission Error and noise of spur gears. He studied theoretical and experiments. According his thesis, profile modifications can be improved minimizing TE at the desired torque. Both of theoretical simulation and experimental validation seems to be the right way to design quieter gear and transmissions [12].

- Milliren, 2011, in his study, performed an experimental investigation to investigate the impact of various gear errors on transmission error and root fillet stresses. Method is as follows; a test set-up is devised to operate a pair of spur gears under loaded, low-speed conditions. Two measurement systems; one an optical encoder-based transmission error measurement system and the other a multi-channel strain measurement system, are developed and implemented with the test set-up. A set of test gears having various types and tightly-controlled magnitudes of manufacturing errors are designed and procured. These errors include indexing errors of different tooth sequences, pitch line run-out errors and lead wobble errors. An extensive test matrix is executed to quantify the impact of these errors on the loaded static transmission error and the root stresses of the spur gears. At the end, the same test conditions are simulated by using a recent feature of gear analysis model (LDP) to assess the accuracy of its predictions [13].

AGMA (American Gear manufacturers ' Association) is the biggest supporters of R &D studies about gear such as NASA and OHIO State University. AGMA products better designed and better manufactured gears with using the results of the supported projects (theoretical and experimental). Furthermore, AGMA turns these studies to gear software for gear designers and manufacturers [13].

- McPherson, and Sroka, 2005, found that superfinishing process helps to remove minor foreign object damage by uniformly removing a minimal amount of material on the gear teeth, while meeting original manufacturing specifications for geometry. According to McPherson, and Sroka, the process also resulted in enhanced surface quality and did not exhibit detrimental metallurgical effects on the surface or sub--surface of the teeth. Furthermore, the process was found to eliminate gray staining, an early precursor to pitting. McPherson, and Sroka, described the results of the helicopter gear repair project and included the geometry and metallurgical evaluations on the repaired gear. Further effort to characterize the durability and strength characteristics of the repaired gear is ongoing [14].

Research studies about gears in the UK are similar in USA. These studies were started as invudual between 1940 and1950 (H E Merritt, S L Harris) and following years they were carried out in cooperation between Industry and University. Manufacturers represents British Gear Association (BGA).University of Cambridge, University of New Castle and University of Huddersfield focus on gear researches.

- Yıldırım 1994, studied on a closed circuit test rig for experiments, the mechanism has been designed, produced and operated by MUNRO 1962 at University of Cambridge for Ph.D. project of him, which experimentally verified the Transmission errors theory put forward by HARRIS in the 1950's. The mechanism was modified and equipped with new instrumentation for testing heavy duties, high performance HCR spur gears, based on the theory [15].

- Britton, Elcoate, Alanou, Evans and Snidle, 2000, studied on a special four-gear rig to determine gear tooth frictional losses at loads and different speeds using a gas-turbine engine oil. They investigated the effect of surface finish by comparing the frictional losses of conventionally ground teeth with those of teeth [16].

As can be seen from the publications, theoretical and (mainly) experimental studies were conducted at dynamic performance of gears (dynamic forces, vibration, noise, etc.). It also experimental methods have been researched and designed to measure the dynamic forces and vibrations.

Theoretical and experimental R & D studies have been researched in both America and Britain. They had some results based on gear design, fabrication and performance analyses. Ohio state University, Newcastle University and private organizations have been prepared commercial software for gear design, production and performance analyses according to these results.

In Germany gear research work has been started to gain importance with Niemann G and following years theoretical and experimental R & D studies have been researched with some universities and private organizations as the same of America and England. FZG (Munich Technical University Gear Research Center), WZL Aachen University, have conducted gear research actively.

There are some of these studies as shown in below. These focus on dynamic forces, lubricating oil temperature rise, the bottom teeth and tooth surface stresses and tooth surface fatigue and wear, effects of tooth surface micro-correction, surface hardening method and etc.

- Otto, 2009, studied on a FZG back-to-back test rig. They observed power losses by minimized lubrication. They investigated the limits concerning possible reduction of lubricant quantity [17].
- Höhn, Otto and Thoma, 2010, focus on spur and helical gears. They calculated load carrying and load distribution capacity for spur and helical gears. They solved these parameters by analytical and compared with experiments [18].
- Höhn, Oster and Otto, 2010 used a FZG test rig to observe tooth bending strength on helical gears. Different loads have been applied on helical gears. At the same time speed value has been changed and the results have been observed [19].
- Klocke, Gorgels and Vasiliou, 2010studien on influence of gear properties induced by Hard Finishing Processes on the Load Carrying Capacity of Gears .The aim of their research project was to induce residual stresses of the gears by different hard finishing processes. The other aim was analyze residual stresses' influence on the durability of the gears. They manufactured tested gears by gear honing, profile grinding and generating grinding. The results of the load carrying capacity tests showed depending on the values of the residual stresses [20].
- Brecher, Gorgels and Bagh, 2009, studied on Improvement of the Efficiency of Parallel-Axis Transmissions by Means of PVD-Coatings [21].

In France some of the gear research are carried out in CETIM (Technical Centre for Mechanical Industry). This Centre redesigns and improves power transmission elements including gears. UNITRAM in France (Union National des Industries de Transmission Mechaniques) is similar to America (AGMA), and England (BGA).UNITRAM represents French gear and power transmission manufacturers.

EUROTRANS (European Committee of Associations of Manufacturers of Gears and Transmission Parts) represents European manufacturers of power transmission elements.

In our country (in Turkey) gear researches are more theoretical level. Mainly these researches are gear manufacture simulation and concentrated on dynamic performance of gear and modeling of gear. Some of these works follows.

- Fetvacı and Imrak, 2008, focused on mathematical modelling and cutting simulation of spur gear with asymmetric involute teeth. Their research gives a mathematical model of spur gears with asymmetric involute teeth. This study is based on the generating mechanism and gear theory. The designed profile of rack cutter equations with asymmetric teeth, the coordinate transformation principle, the differential geometry theory, and the gearing theory have been applied and computer graphs is illustrated [22].At the same year, Fetvacı and Imrak computerized cutting simulation of involute helical gears generated rack cutters. Their research studies the rack cutters equations for generating helical gears within involute teeth. They have been given the equations of designed profile of rack cutter, the principle of coordinate transformation, the theory of differential geometry and the theory of gearing, the mathematical models of involute helical gear. In addition, they developed a computer simulation program to generate the tooth profile of involute gears and to illustrate the effect of tool geometry on generated surfaces. Also, they illustrated the simulation of the generating process [23]. Fetvacı at 2010, has studied on Computer Simulation of Helical Gears with Asymmetric Involute Teeth. His research studies the computerized tooth profile generation of involute helical gears cut by rack cutters with asymmetric teeth. He investigated undercutting analysis also by considering the relative velocity and equation of meshing. He developed a computer program to generate the tooth profile of helical gears with asymmetric involute teeth [24].

- Karpat, Ekwaro-Osire, Cavdar, and Babalik, 2008 studied on dynamic analysis of involute spur gears with asymmetric teeth. Their study offers preliminary results to designers for understanding dynamic behavior of spur gears with asymmetric teeth. They have developed a dynamic model with using MATLAB, and used for the prediction of the instantaneous dynamic loads of spur gears with symmetric and asymmetric teeth. In addition, they developed a 2-D three-tooth model to use for finite element analysis [25].

- Bozca and Fietkau, 2009 studied on an empirical model based optimization of gearbox geometric design parameters to reduce rattle noise in an automotive transmission. They calculated and simulated rattle noise based on design parameters of five speed gearbox. All gears were helical in this study. They analyzed effect of design parameters on rattle noise. They observed optimization of rattle noise profiles depending on design parameters [26].

Although some studies have supported experimental studies and these are usually done with opportunities or resources of foreign countries. Some of these are:

- With reference to the previous researches [15] of Yildirim based on the systematic approach to the profile relief design of both low contact ratio and high contact ratio spur gears, Yildirim at 2005, illustrated some guidelines for the use of short and double reliefs of the HCRG profile design under the effect of realistic parameters like variable tooth stiffness and manufacturing errors regarding the profile relief values. According to Yildirim, root stress of the double relief can be minimized by optimizing the maximum tooth load value, hence the tooth load diagram with constant and variable tooth stiffness [28].

- Düzcükoglu and Imrek, 2005, investigated experimentally relation between wear and tooth width modification in spur gears. They carried out test on a FZG back to back test rig (91,5 mm center distance). They used gear specimen (mn: 6 mm, z1, z2:15, fw: 10 mm-20 mm) which made of AISI 4140 steel (carburized, quenched and oil annealed). They subjected the gear pairs to operational torques of 183.4 Nm and revolutions of small gear was 250 rev/min. They operated the FZG test rig for a total of 3.6×105 cycles for both modified and unmodified gears, and in every 0.9×105 cycle, then they stopped the test rig [29].

- Yildirim, Gasparini and Sartori, 2008, studied on helicopter transmission that had improved performance in terms of vibration and noise behavior, in compliance with surface durability requirement, compared with what was achievable with previous designs. Some scholars already designed and tested the different spur gears of both low and high contact ratios (HCRs) in helicopter transmissions with different profile modifications but with limited performance improvement [30].

- Düzcükoglu and Imrek, 2008, studied on spur gears experimentally to prevent premature pitting formation. The aim of their study is to delay the formation of pitting in the single tooth meshing region by means of decreasing the Hertzian surface pressure by increasing tooth width. They used a FZG back to back test rig which its center distance 91, 5 mm. Both of Test gears' specifications are normal module is 6mm, number of teeth is 15mm and face width is between 10mm and 20mm.They subjected to gears two different torques(183,4 Nm and 239,3 Nm) at 650rpm.Their experiments show that pitting appearance is delayed for the width-modified gear wheels with respect to the gears having no such modifications [31].

Studies about design and development gear test rigs

- Başaran, 2001, investigated pitting on helical gears in his master thesis. He has designed back to back type gear test rig (Figure 2.6.) and has produced in Gazi University. Furthermore, he design helical test gears and he has done fatigue test on these helical gears. He has investigated the change of the Hertz pressure of the active profile. He has tried by different profile shift factor, different helical angle under different loads on helical gears. He has fixed materials, lubricants and surface roughness parameters. In the light of the calculations and the experimental results showed the effect of the parameters examined pitting damage. In this study, all the characteristics of these three groups, were studied in order to understand the effects on the overall performance of the base fluid [32].

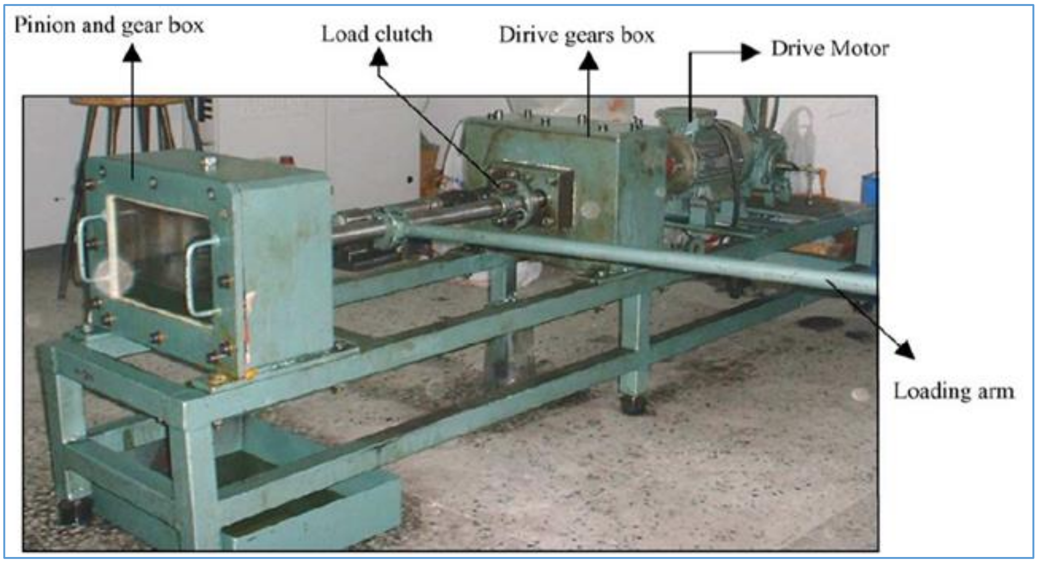

Figure 2.6: Designed and produced in Gazi University [32].

- Imrek and Özkasap, 2001, focused on experimental investigation of spur gear wear. They used a back to back test rig as FZG (the test rig was designed by Imrek) which center distance is 91,5 mm. According their experimental studies, they observed wear of gears at different speed (750 rpm and 1500 rpm) and torque values (25 Nm-175 Nm) and they observed oil temperature at different load (546 N-3825 N) value with different oils (SAE 140 and base oil). They used 3,5mm normal module, 26 teeth number (z1, z2) and 10mm face width [27].

- Manoj, Gopinath and Muthuveerappan, 2002, designed and developed a power re-circulating test rig (Figure 2.7) which center distance 94.5 mm, drive motor is 5hp and 1440 rpm. The test rig have one pair of test spur gears and one pair of helical loading gears. The variation in gear loading is achieved by axial loading of the helical gear using a pneumatic actuator. The no load-starting feature in the test rig reduces the size of the motor. They modified the test rig with multimode condition monitoring unit and computer data acquisition system. Continuous multimode monitoring, online data analysis and post data analysis make the system more versatile in accurately predicting the failure. They discussed the features of the test rig and advantages.

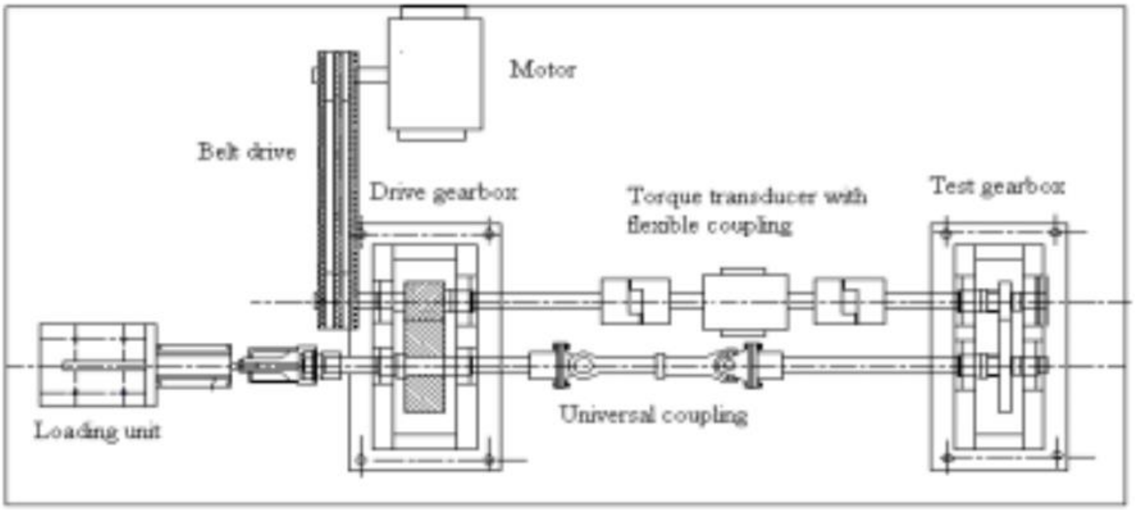

Figure 2.7: A Back to Back Test Rig Designed by Manoj, Gopinath and Muthuveerappan

- ÇAKIR, 2003, designed a back to back gear test rig. He used a maximum tooth load 300 N/mm and face width of gears 30 mm. He defined center distance of gears as 120 mm. Spur gears for test are 40 teeth number, 3mm normal module and 20 degree pressure angle. Helical gear for slave gearboxes are 23 teeth number, 3.75 mm normal module and 45 degree helical angle. Maximum shaft speed is 6000 rpm.He designed test rig at these conditions [33].

- Korka and Vela, 2008, focused on design and development of a gear test rig to study vibration of gear boxes. They designed a gear test rig shown in Figure 2.8. The gearbox is driven an electric motor which its rated power 2.5 kW, nominal speed is 1500 rpm and maximum torque is 16 Nm. They used an oil pump for the breaking system of test rig. They used the test rig for studying the influence of the superficial fluoropolymer coatings on the level of vibrations and noise [34].

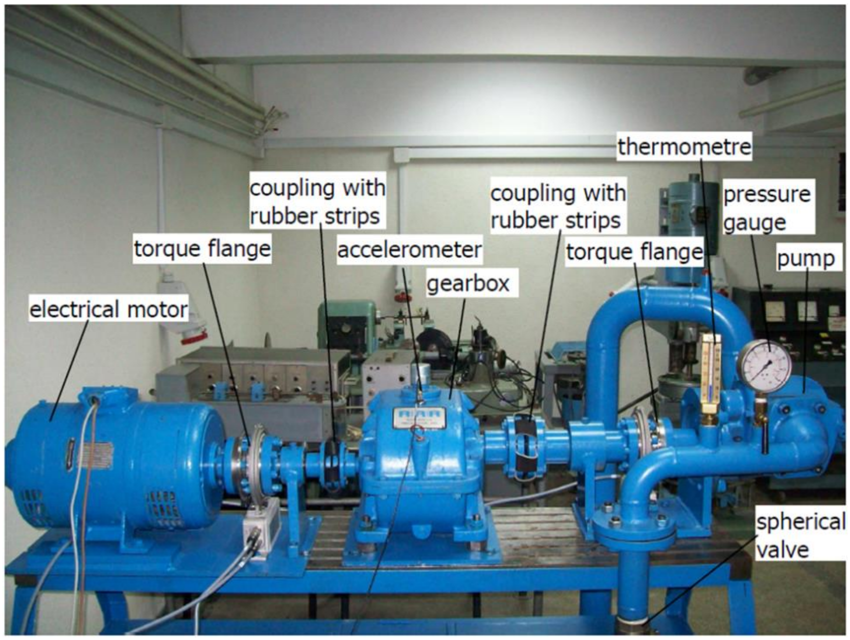

Figure 2.8: A Braked Test Rig Designed by Korka and Vela

- Lomate, Mohite, and Shinde, 2010, studied on design and development a torque test rig in Figure 2.9. They designed a hydraulically actuated multi-plate brake system torque test rig which is torque values between 0.5 kNm and 10 kNm with rated speed. Calibration of gear torque test rig is supported with theoretical values. While calibration of mechanism, they observed that maximum error torque of system within measured torque is 50 Nm. The mechanism can be operated to test peak load, duty cycle and temperature of cooling water for some of gear boxes [35].

Figure 2.9: A Multi-Plate Brake Torque Test Rig Designed by Lomate, Mohite and Shinde

- Åkerblom, 2010, designed a power circulation test rig (Figure 2.10) to test gears under controlled conditions. He used FEM to detect the dynamical properties of mechanism. Experimental modal analysis has been provided on the gearbox housing to verify the theoretical predictions of natural frequencies. He used the test rig to test noise and vibration of gears with different manufacturing errors and design parameters. In addition to noise testing, the mechanism can be operated to test gear life and measurement of efficiency. Technical data of test gears are that teeth number of test gears are 49 and 55, normal module is 3.5 mm, pressure angle and helical angle are 20degreee, face width is 35 and 33 mm. Center distance of gear pair is 191.9 mm. Technical data for the test rig are that Torque is 0–5000 Nm, Rotation speed is 0–2800 rpm, Power of electric motor is 110 kW, Maximum power through gearboxes is 1400 kW and oil temperature is 20–100 ^{0}C [36].

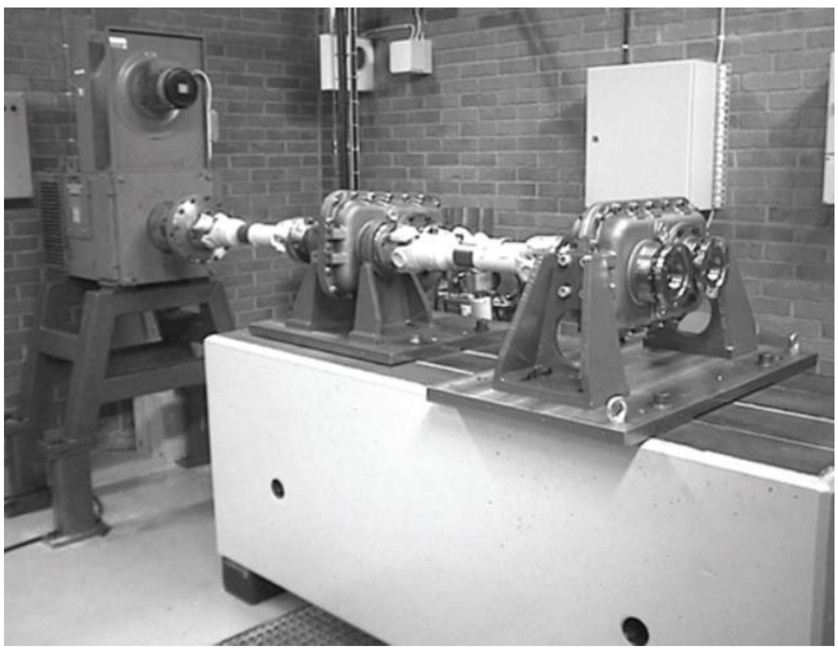

Figure 2.10: A Power Circulation Test Rig Designed By Åkerblom

- Sachidananda, Gonsalvis, Prakash and Rajesh, 2011, designed a simple power Recirculating Gear Test Rig as shown in Figure 2.11. Main components of their test rig are Gear Housing, Vernier Coupling, Loading Torque Meter, Input Torque Meter, DC electric motor and spur gears. The torque meter consists of four spiral springs. Its maximum torque capacity is 3.6×10^4 Nmm. Thus while the drive shaft is rotating at 150 rad/s, the power locked in the system will be equal to 33 kW [37].

Figure 2.11: A Power Circulation Test Rig Designed by Sachidananda, Gonsalvis, Prakash and Rajesh

- Tunalıoğlu and Tuç, 2012, designed a back to back test rig for sun gear in planetary gear systems (Figure 2.12). They studied on wear experiments to investigate wear on internal gears by manufacturing pinion-internal gear whose working system. During test, they used pinion and internal gears made of St 37 material loaded with different torques. Wear measures in surface of pinion and internal gear were investigated at different load recurrence. They used for gears 3 mm normal module, 17 and 75 number of teeth, 10mm face width of gear and 87 mm center distance. They used two electric motors, ones is 7.5 kW and 3000 rpm to drive system, and other is used for cooling of lubrication oil [38].

Figure 2.12: Back to Back Test Rig Designed by Tunalıoğlu and Tuç

- Kimura, Minami and Kondo, 2013, studied on the testing rig belongs to Osaka Steel Works [41] which is developed in order to analyze the noise spectrum from gear unit itself under loading condition. KIMURA, MINAMI and KONDO installed the test rig in an anechoic chamber. Result of this is to eliminate the background noise. So they have developed a low noise type gear unit which is changed the tooth profile by using this testing rig.

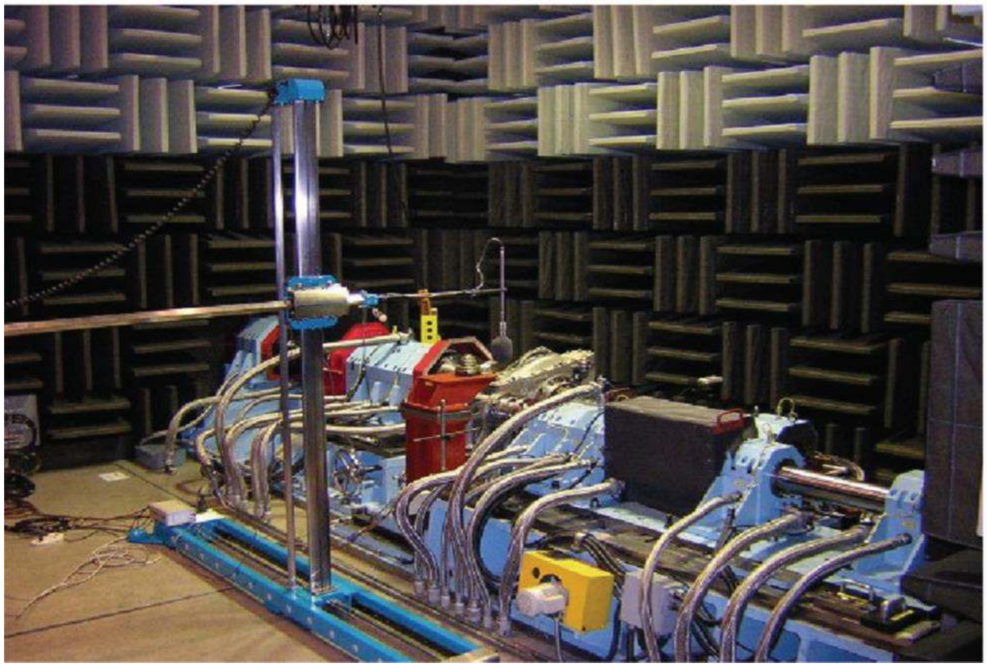

Figure 2.13: A Loading Test Rig in the Anechoic Chamber Designed In Osaka Steel Work

- Lijesh, 2015, designed and developed a gear test rig to obtain realistic (in-situ) conditions for spur gear. The designed and developed test setup can be used to vary the speed from 600 rpm to 24,000 rpm. He used an Accelerometer to measure the vibration of the system and the acquired signals are analyzed to predict the system performance. To confirm the conclusions from the vibration results, inspection using optical microscope on the gear surface were carried out before and after performing experiments. He operated the test gears for $1.5x10^6$ and $3x10^6$ cycles (Figure 2.14).

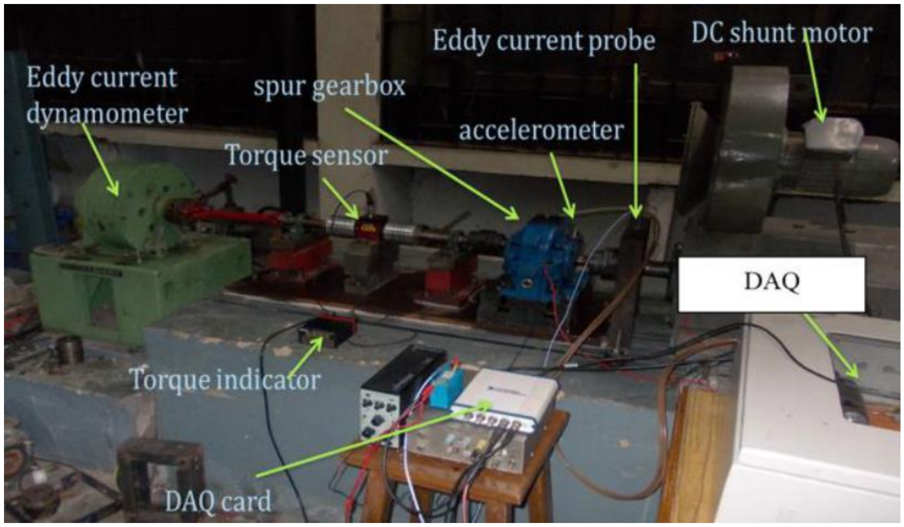

Figure 2.14: A Braked Test Rig Designed by Lijesh

Apart from these studies, generally, five FZG test rigs are used in the world [39].

These are;

- **Standard FZG test rig** is a back to back gear test rig with a mechanical power circuit. The maximum transmitted load can be between 0 Nm and 1000 Nm. It means that load delivers some 150 kW at 1500 rpm and 300 kW at 3000 rpm. Lubrication tip is spray. Electric motor speed is between 100-3000 rpm.

- **Modified FZG test rig** is modification of standard FZG test rig. Modifications are done with measure instruments.

- **Load spectra FZG test rig** is computer controlled. It is suitable for in-depth analysis of gears and lubricants, particularly for assessing pitting capacity. Torque, speed and oil temperature can be changed during the actual test run. Pinion speed is +/- 6000 rpm, pinion torque +/- 600 Nm. Rig has a Hydraulic unit for torque clutch.

- **Special gear test rig** is produced for Customer requires. Center Distance may be up to 200mm, tooth width may be up to 100 mm, gear speed may be up to 6000 rpm, transmitted torque may be up to 6000 Nm and electric motor capacity may be up to 2600 kW.

Newcastle University have some gear test rig [40] as in the FZG. Their design unit designed and built many types of test rig for:

- Research into gear surface fatigue – back-to-back rigs and disc rigs.
- Life testing
- Efficiency measurements
- Wear testing (including low speed, high temperature gear testing).
- Noise and vibration measurements
- Lube oil studies
- Coupling performance.

Back to back test rig in Newcastle University is classified three types according to CD.

- 75 mm Center Distance test rig features in Table 2.1.

Table 2.1: 75 mm test rig specifications

Centre Distance:	75 mm
Speed:	0 to 6000 rpm
Gear Ratio:	1.5:1
Max. Torque:	400 Nm
Face width:	10 & 15 mm
Max. Power at 6000rpm:	250 kW
Module :	1 to 4 mm
Drive Motor:	5.5 kW

- 91.5 mm Center Distance test rig features in Table 2.2.

Table 2.2: 91.5 mm test rig specifications

Centre Distance:	91.5 mm
Speed:	0 to 6000 rpm
Gear Ratio:	1:1 and 1.5:1
Max Torque:	1400 Nm
Face width:	30 mm Max.
Max. Power:	880 kW
Module:	2 to 6 mm
Drive Motor:	30 kW
Helix Angle:	0…30°

- 160 mm Center Distance test rig features in Table 2.3

Table 2.3: 160 Mm Test Rig Specifications

Centre Distance:	160 mm
Speed:	0 to 4500 rpm
Gear Ratio:	1:1
Max. Torque:	6000 Nm
Face width:	45 mm Max.
Max. Power:	2800 kW
Module:	4 to 10 mm
Drive Motor:	75 kW
Helix Angle:	0…30°

The Marine Gearing Research Rig (MGRR) was designed and built at the Design Unit in Newcastle University, with MOD (N) funding, to investigate noise excitation of marine sized gears at tooth contact frequency and associated harmonics. The rig consists of a test box and a slave box in back to back configuration.

The specifications are in Table 2.4:

Table 2.4: Marine Test Rig Specifications

Centre Distance: 400 mm
Speed: 0 to 5500 rpm
Gear Ratio: 3:1
Max. Torque: 15000 Nm
Face width: 200 mm
Max. Power: 8000 kW
Drive Motor: 200 kW

2.2.DISCUSSING OF LITERATURE SURVEY

According to literature survey all over the world, there are many researches experimental and analytical about gears. But studies of design and development of gear test rig is not much more. Generally, center distances of designed test rig are between 87 mm and 160 mm. Mostly use is 91.5 mm. But according to special center distance, new test rig can be design and produce. Heavily system speed range are between 0 and 6000 rpm. But different speed can be set. Transmitted torque is between 0-6000 Nm. Spur gears and helical gears were mostly used as test gears. Gear test specimen are made of different material and different modules, number of teeth and pressure, helical angle. Torque clutches were designed different concept. Lubrication oils were different quality.

Particularly, studies oriented to dynamic performance in Turkey (dynamic forces, angular and axial vibrations, noise, precision and high speed chopper and turbine gear profile design effects, effects of assembly errors to performance, etc) does not seem possible on these mechanisms. This type mechanism must be more precision to use in critical areas like aerospace and similar industry. But designed mechanisms in Turkey aren't precision enough due to manufacturing and assembly errors.

Especially design, manufacturing and development of heavy loaded and high speed gear used for the defense industry, energy, automotive and other critical sectors in our country is not yet enough. Needs in this topic usually are met which deal with overseas countries such as USA, France, UK and Germany. Turkey have the automotive sector, but design and manufacturing operations of current gears and similar parts in this sector are carried out with international licenses. In this area, if domestic R & D works for design and manufacture in Turkey has not been started, our dependence on overseas will be continued. Experimental studies carried out by various research centers around the world need to be launched in our country. So necessary test equipments must be designed and produced. In addition these test equipments are necessary to support the theoretical studies in our country.

The production of such mechanisms is not possible just about anywhere. It requires custom design, fabrication and measurement instruments and equipment. Since its inception, the experimental R & D efforts with both design/software, will be able to serve manufacturing sector. NASA and OHIO State University (and similar to other research centers and universities) as well as numerous scientific, technological and academic (MSC, PhD etc) will be doing R & D work on gear test rigs. Theoretical design and analysis of studies conducted experiments on the mechanisms to be obtained will be compared with experimental study. As a result, reliable design, analysis, and manufacturing softwares can be presented to national (and international) gear designers and manufacturers. In this way, our country will make a major contribution to the development of national technological infrastructure.

In fact, this type of experimental test rigs are not commonly produced or used products. Therefore, design and manufacturing of this mechanism is an R & D work. Because research-design and development work needs to be done according to the requirements of the measurement, kind and sensitivity of measured parameters.

This type of experimental test rigs and research labs should be designed and set by each country for their manufacturing, machinery, defense, automotive, energy and other industries. This Centre is going to be started with the successive and complementary features projects.

After completing test rig, some experiments and measurements can be performed on it. Then so many research activates can be possible for spur and helical gears by using this rig. In addition, similar experimental studies are going to be possible on bearings, shafts, couplings and lubricating system.

CHAPTER 3

TEST RIGS

3.1.GENERAL INFORMATION

Gears are very important power transmission elements for different sectors like automotive, energy, machines, aero planes and helicopters. Leader countries in these sectors such as USA, Germany, France and England have worked on gear design and manufacturing technology for years. At the same time, they have set gear test rigs to prove their theoretical studies with experimental studies. The following tests have been studied by many researchers by means of the test rigs that they have designed and constructed;

- Pitting
- Micro-Pitting
- Scuffing
- Wear
- Tooth Root Breakage
- Efficiency
- Excitation

On the same test rigs, the following parameter influences have also been studied;

- Gear geometry
- Material
- Heat Treatment
- Manufacturing Related Product Properties
- Lubricant

- Operating Conditions
- Laboratory

Generally, there are two types of test stands for these types of experimental studies;

- Back-to-Back Test Rig (closed circle test rig, power circulating test rig)
- Braked Test Rig.

3.2.BACK-TO-BACK TESTER

Back-to-back research rigs shown in Figure 3.1 is very often used for testing power transmission systems as they offer very low power consumption compared to braked and other non-generative test systems. A conventional back-to-back configuration, consists of a test gearbox and a slave gearbox of identical gear ratio, which are coupled together.

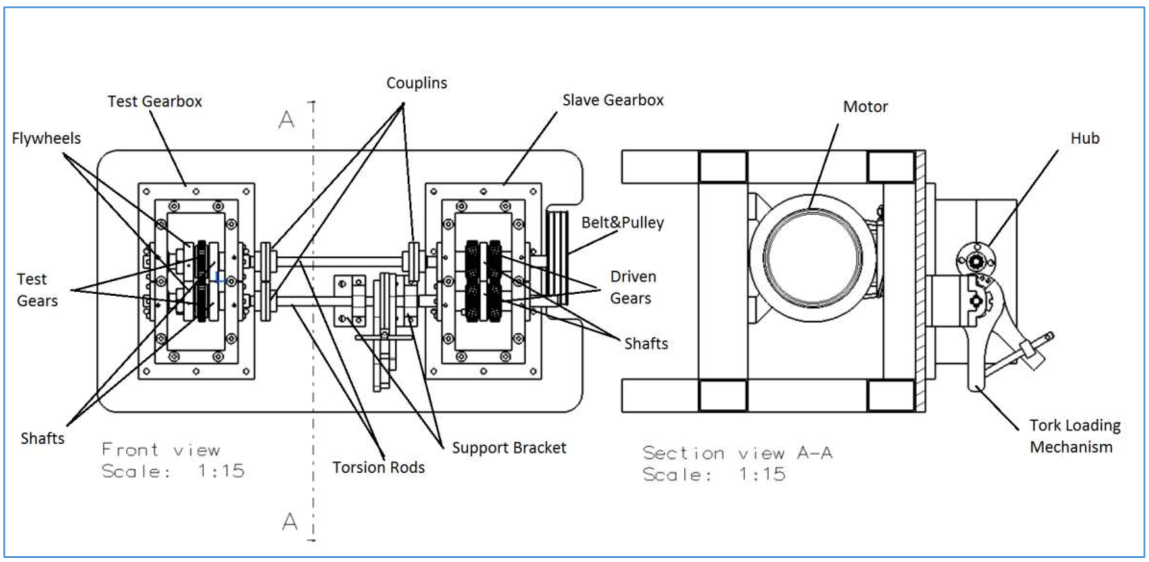

Figure 3.1: Back-to-Back Test Rig

The test and slave gearboxes are generally similar in design. Both are split about the center line into top and bottom halves. Flywheels are put in to the system to bring the natural frequency of the torsional vibration of the gears down to a convenient speed range, so that the gears could run up to and above sub harmonic resonant speeds.

The test gearbox and the slave gearbox are connected to each other by two shafts. One shaft is divided in three parts. Test gear shaft and torsion rod are fixed by rigid coupling. Torsion rod and slave gear shaft are coupled with the load clutch in between. One side of the load clutch can be fixed to the foundation with the locking pin while the other side is twisted e.g. by means of a lever and weights or hydraulic system or mechanic system. After bolting the clutch together the load can be removed and the shaft be unlocked. Thus a static torque is applied to the system which can be checked in the torque measuring clutch as the twist of a calibrated torsion shaft. The rig can be operated with an AC motor at 3000 rpm. The speed of motor is increased or decreased with belt-pulley system to desired value. The gears are normally lubricated with an additional oil supply device also spray lubrication can be applied.

There are two methods of setting the shaft torque, e.g. static (winding up the shaft mechanically when the rig is stopped) and dynamic (winding up the shaft while rotating) which is developed by Smith [42].

The dynamic method offers significant advantages, e.g.

- Low start-up torques (especially important when hydrodynamic bearings are used in the system).
- No danger of scuffing of gear teeth at high torque on start-up.
- The ability to change torque while running.
- Computer control of torque can be easily realized.

In spite of the significant advantages of dynamic torque actuation relatively few gear research rigs have this facility yet.

Back-to-back tester is important due to following advantages;

- Constant torque can be loaded unrelated from speed.
- Not need to an extra braked system
- Reduced noise emission level and precision noise measurement
- Reduced energy consumption
- Reduced installation costs due to need a single drive motor for system losses.
- System is simple and understandable.

- No issues with heat dissipation.
- All failure modes can be verified.

At the same time back to back tester has some disadvantages;

- Not possible to change system torque while gears are rotating (static type).
- Torque variation control requires test interruption.

3.3.BRAKED TEST RIG

Bench equipped with a motor and a brake, in an open loop layout. Motor has to supply all the power under which the gearbox has to be tested; Brake has to simulate resistance efforts and transform it to heat.

In this gear test rig illustrated in Figure 3.2 there is a gearbox or test gears. Gears are connected together with two shafts. The gearbox or gears with the drive unit are fixed on a rigid concrete chassis.

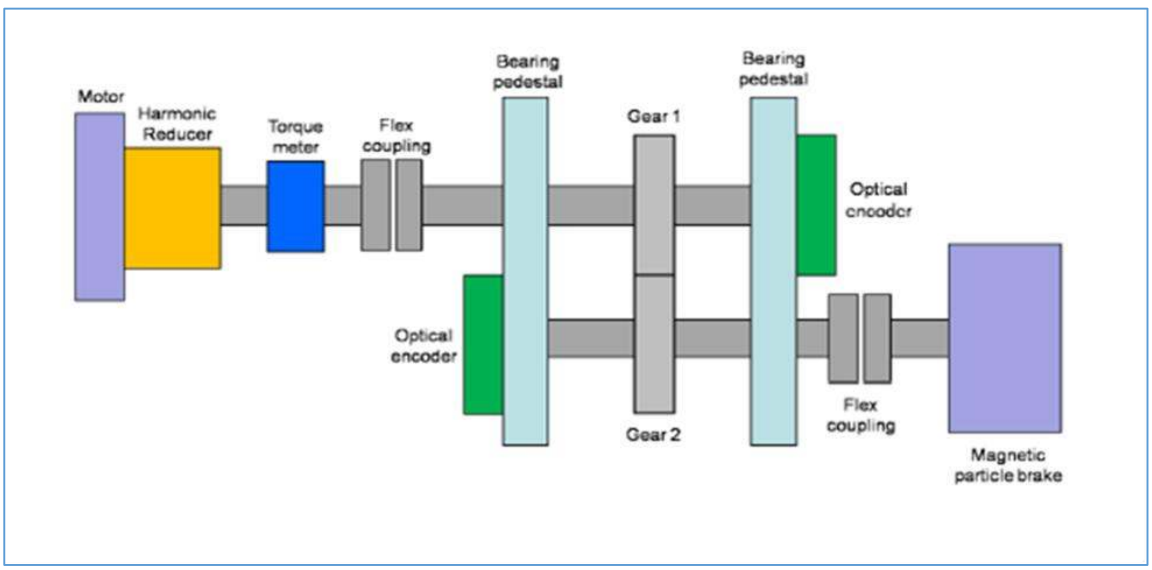

Figure 3.2: Braked Test Rig

Motors and shafts are connected through flex coupling. A non-contact torque transducer is connected on shafts to measure the torque and speed of the pinion side of the gear test rig.

While test gears or gearbox of braked test rig is driven by an electrical motor at one side, at the other side they are loaded with a braked system (magnetic, eddy current, hydraulic, etc.) to form a reaction torque.

Torque and speed range of this systems can be set easily in the system limits during operations. This is an important advantage of braked test rig. But, changing reaction torque during operations after setting affects the test performance directly. So torque range should be observed not to be problem.

In this system first and mainly problem is wasting of entire transmission power. For example, transmission power of a gear pair transmitted 500 Nm and rotated 5000 rpm is approximately 500x500=250 kW. All power has to be destroyed as heating or another energy type.

Advantages of braked test rig;

- Torque variation control without test interruption and simple architecture.
- Most of failure modes can be verified.

Disadvantages of braked test rig;

- High installation cost.
- High energy consumption
- High noise emission level
- Difficulty to dissipate brake heat.

3.4.MAIN COMPONENTS OF THE TEST RIG TO BE DESIGNED

In previous section, advantages and disadvantages of two system (Back-to-Back Test Rig and Braked Test Rig) have been mentioned. Back-to-Back Test Rig was preferred to design and produce. Result of this, back to back test rig operates silently, so precision noise and vibration test can be done. There is only one driving electric motor to compensate power losses. In addition this electric motor has low capacity than braked tester. This means, system has low power consumption and system is cheaper than braked system. Back to back test rig is simple and easy to understand.

Main Components of Back to Back test rig are illustrated in Figure 3.3 and components on the test and slave shaft are in Figure 3.4 and Figure 3.5.

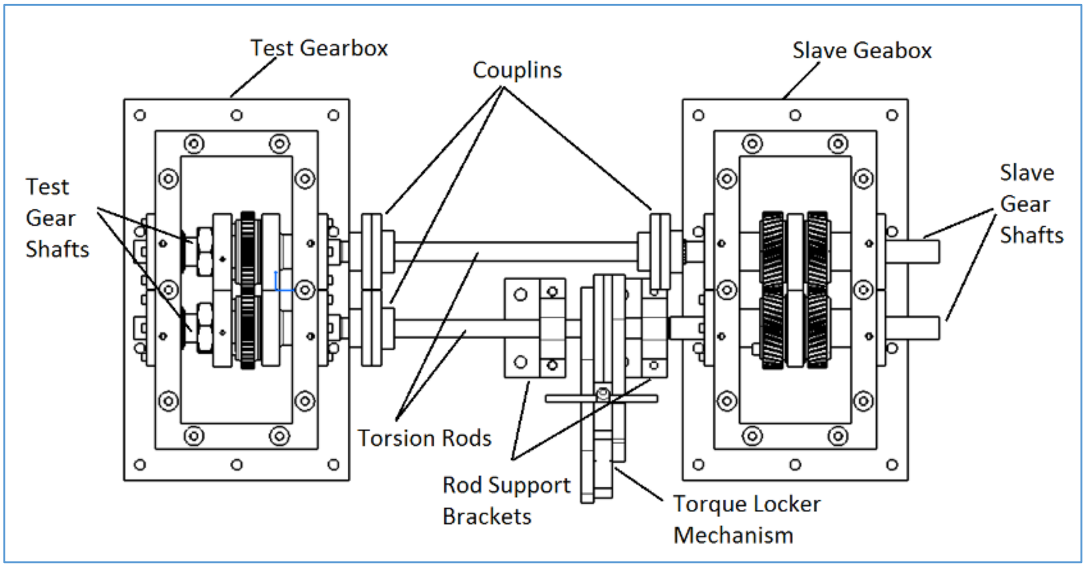

Figure 3.3: Test Rig Components

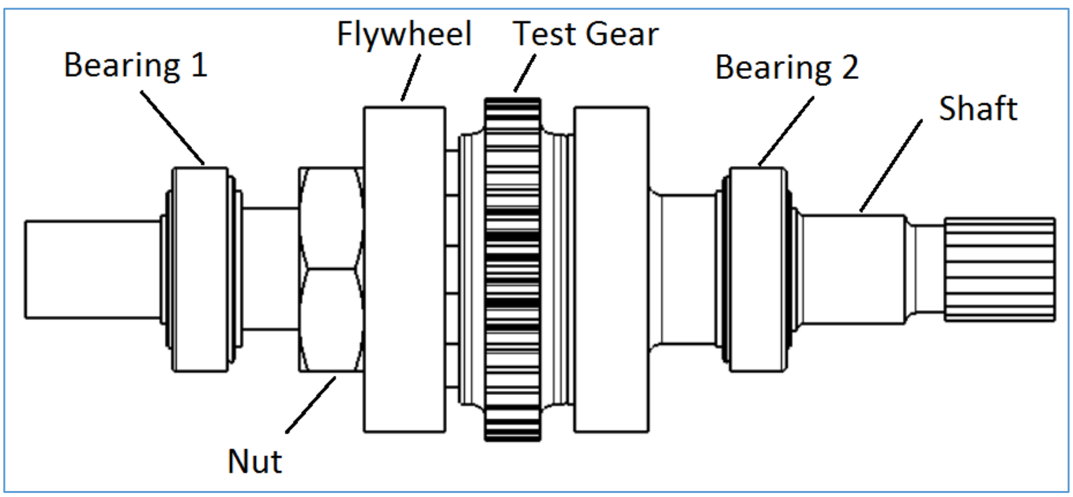

Figure 3.4: Test Gear Shaft Components

Shaft: A shaft is a rotating machine element which is used to transmit power from one place to another. The power is delivered to the shaft by some tangential force and the resultant torque (or twisting moment) set up within the shaft permits the power to be transferred to various machine linked up to the shaft.

The following stresses are induced in the shafts:

- Shear stresses due to the transmission of torque (i.e. due to torsional load).
- Bending stresses (tensile or compressive) due to the forces acting upon machine element like gears, pulleys etc.
- Stresses due to combined torsional and bending loads.

Flywheels: were put into the system to bring the natural frequency of the torsional vibration of the gears down to a convenient speed range, so that the gears could run up to and above sub-harmonic resonant speed (Figure 3.4).

Bearings: A bearing is a machine element that constrains relative motion between moving parts to only the desired motion. The design of the bearing may, for example, provide for free linear movement of the moving part or for free rotation around a fixed axis; or, it may prevent a motion by controlling the vectors of normal forces that bear on the moving parts. Bearings are classified broadly according to the type of operation, the motions allowed, or to the directions of the loads (forces) applied to the parts.

Pin joint: In mechanical engineering, there are multiple methods for fastening objects together. A pin joint is a solid cylinder-shaped device, similar to a bolt, which is used to connect objects at the joint area. This type of joint connection allows each object to rotate at the point of joint connection. Most mechanical devices that require bending or opening typically use a pin joint.

Pins on the test or slave shafts are connected between shaft and gears meets the shear stress caused by the gear load.

Bolt: A bolt is a type of threaded hardware fastener that is used to position two work pieces in specific relation to each other. Bolts come in several configurations for their application and specification variances.

Nut: Flywheel is connected to the shaft by nut.

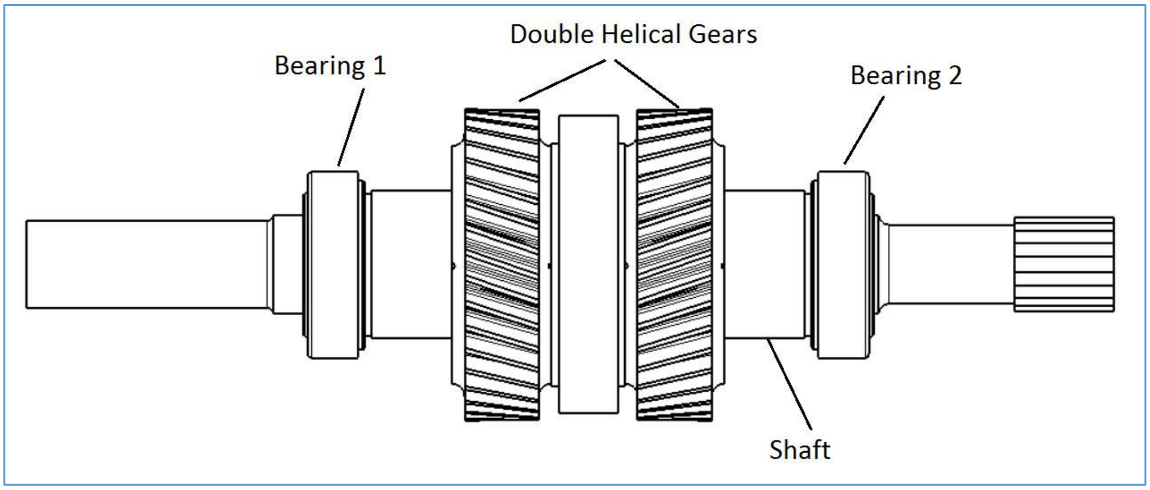

Figure 3.5: Slave Gear Shaft Components

Double Helical (Herringbone) Gears: Since the main interest is in the vibration of the test gears, a pair of high accuracy double helical gears are used in the slave gearbox to minimize sources of excitation in the slave gearbox side.

Highly Flexible Torsion Rods (Torsional soft Shafts): must be efficient in helping to isolate the two gearboxes dynamically. The shaft flexure vibration is discouraged by using large shaft diameters.

Slave Gearbox & Test Gearbox (or Gear cases): they are very massive, to reduce gearbox resonances and minimize gearbox vibration amplitudes.

Electric Motor: mainly compensates for the losses in the system and overcoming the inertial resistance.

Couplings: A coupling makes a semi-permanent connection between two shafts. There are two rotational plates. Torsion rod and shafts are connected using pins by couplings.

Rod Support Bracket: It supports to the torsion rod and slave gear shaft to avoid bending stress on the rods while loading torque.

Torque Locker Mechanism (Figure 3.6): It consists of two circular plates fastened to the shaft ends using pins. One of these plates has any number of holes and the other has less one hole than the first. This rotational arrangement permits achieving a definite angular increment for every successive hole as it coincides with the reference hole. It gives an incremental value of angular rotation when one plate is rotated in relation to the other. This feature enables achieving accurate control over the amount of torque applied.

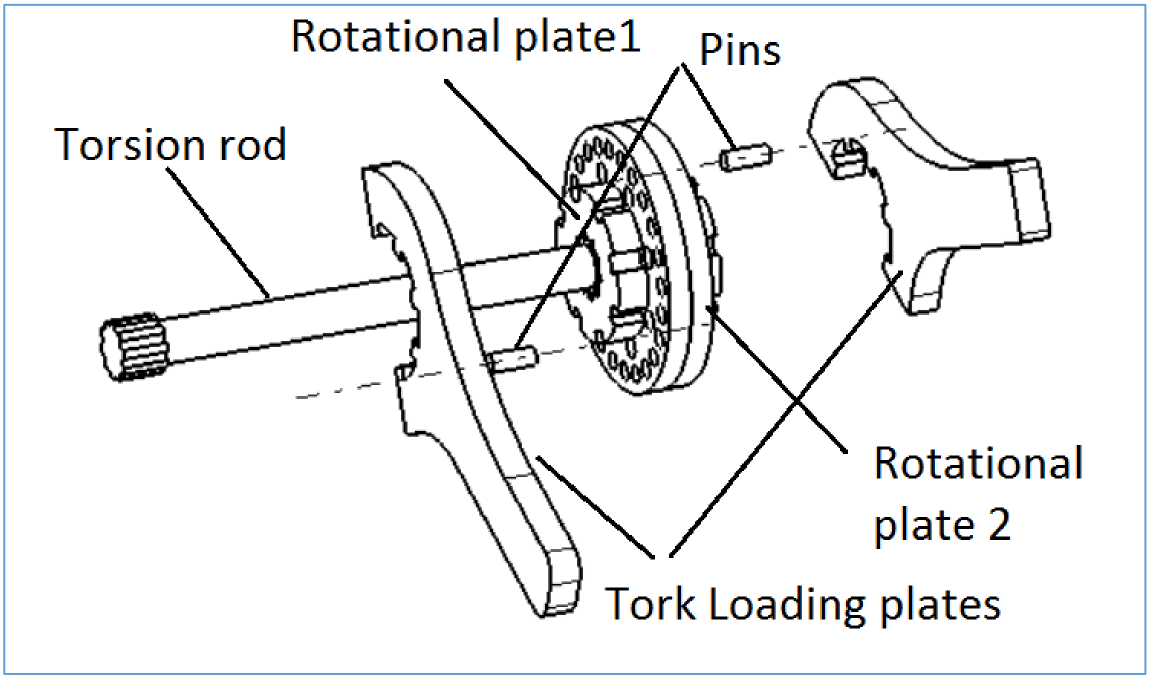

Figure 3.6: Torque Loading Mechanism

The one half of the rotational plate is held while the other half is acted upon by a lever loaded by dead weights of desired value effecting the torque required to cause angular twist of a long shaft. The mechanism halves are then clamped so that the applied torque is locked between the gear pairs.

CHAPTER 4

DESIGN OF TEST RIG

4.1.DEFINITION OF THE DESIGN TASKS

Generally, at any product design some questions relating with product have to be answered. Test rig can be designed by focus on these questions. Following questions were considered and some answers are provided as listed below is necessary and important for the test rig design:

- Which gear types will be tested?

Parallel axis gears were discussed in chapter one will be tested. These gears are spur and helical. As well as their failures are subject of thesis. In this point spur and helical gear's parameters affect the test rig parameters and test results. So design, manufacturing process and heat treatment process of them require attention. Any errors of process caused review of other components or redesign or reproduce. Detailed information about parallel axis gears are described in Appendix A. In addition computer aided design of parallel axis gears is explained step by step in Appendix B. In Appendix C, linear static analysis of spur gear is done with FEM.

- Which parameters will be measured?

Torsional and axial vibrations, oil temperature, transmitted torque, speed of systems, mass of wear particles, noise of system will be measured.

- Which test rig should be used and why?

Back-to-Back Test Rig will be used to design and produce. Result of this, back to back test rig operates silently, so precision noise and vibration test can be done. There is only one driven electric motor to compensate power losses. In addition this electric motor has low capacity than braked tester. This means, system has low power consumption and system is cheaper than braked system. Back to back test rig is simple and easy to understand.

- What are the boundary conditions (loads, speed and others)?

Maximum tooth load will be 500 N/mm, system speed will be between 0-6000 rpm, center distance of shaft will be 120 mm.

- Which components on the test rig are safety parts and requires attention?

All rotational components on the test rig are safety parts and requires attention. But especially components that transmitted power and torque are more important than the others. So for these parts, factor of safety need to be higher (>2)

4.2.CENTER DISTANCE

Center distance is the shortest distance between centers of parallel axis gears. It is very important parameter for the test rigs to test gears with many different properties. These properties may be different modules or may be different tooth number at the same center distance.

Center distance is calculated as dividing by 2 sum of both gear pitch diameters. Its formula for calculating the center distance of pinion and gear can be written;

$$\mathrm{CD} = \frac{\mathrm{D_1}+\mathrm{D_2}}{2} \tag{4.1}$$

To test gears with many different properties at the test rig design, modules and tooth number should be added to calculations. In this point for center distance, following equation can be used, where m is “module” and Z is “tooth number”;

$$CD = 0.5 * m * (Z1 + Z2) \tag{4.2}$$

Standard modules should be selected from manufacturer catalogues or gear standards to produce gear by using standard cutters. Because many gear manufacturers work in standard modules. If nonstandard module is used, extra cutting tool is necessary to product or cost of gear may be increased. Center distance or tooth number can be assumed. Some standard modules illustrated in Table 4.1 are used at design.

Table 4.1: Some of Standard Modulus

m(mm)	1	1.25	1.5	1.75	2	2.25	2.5	2.75	3	3.25	3.5	3.75	4	4.5	4.75	5

Some of center distance used in the literature are 75 mm, 87 mm, 91.5 mm, 94.5 mm, 120 mm and 160 mm and 191.9 mm. Differently, following center distances are assumed (Table 4.2). Because they have more than the number of multipliers to study different module and different teeth number (Table 4.3).

Table 4.2: Assumed center distances

Center Distance (mm)	120	100	90	60

Table 4.3: Calculated tooth number for 120 mm center distance and standard modules.

Center distance	Z (tooth number)	module (mm)
120.00	120.00	1.00
120.00	96.00	1.25
120.00	80.00	1.50
120.00	68.57	1.75
120.00	60.00	2.00
120.00	53.33	2.25
120.00	48.00	2.50
120.00	43.64	2.75
120.00	40.00	3.00
120.00	36.92	3.25
120.00	34.29	3.50
120.00	32.00	3.75
120.00	30.00	4.00
120.00	26.67	4.50
120.00	25.26	4.75
120.00	24.00	5.00

Table 4.4: Calculated tooth number for 100 mm center distance and standard modules.

Center distance	Z (tooth number)	module (mm)
100.00	100.00	1.00
100.00	80.00	1.25
100.00	66.67	1.50
100.00	57.14	1.75
100.00	50.00	2.00
100.00	44.44	2.25
100.00	40.00	2.50
100.00	36.36	2.75
100.00	33.33	3.00
100.00	30.77	3.25
100.00	28.57	3.50
100.00	26.67	3.75
100.00	25.00	4.00
100.00	22.22	4.50
100.00	21.05	4.75
100.00	20.00	5.00

Table 4.5: Calculated tooth number for 90 mm center distance and standard modules.

Center distance	Z (tooth number)	module (mm)
90.00	90.00	1.00
90.00	72.00	1.25
90.00	60.00	1.50
90.00	51.43	1.75
90.00	45.00	2.00
90.00	40.00	2.25
90.00	36.00	2.50
90.00	32.73	2.75
90.00	30.00	3.00
90.00	27.69	3.25
90.00	25.71	3.50
90.00	24.00	3.75
90.00	22.50	4.00
90.00	20.00	4.50
90.00	18.95	4.75
90.00	18.00	5.00

Table 4.6: Calculated tooth number for 60 mm center distance and standard modules.

Center distance	Z (tooth number)	module (mm)
60.00	60.00	1.00
60.00	48.00	1.25
60.00	40.00	1.50
60.00	34.29	1.75
60.00	30.00	2.00
60.00	26.67	2.25
60.00	24.00	2.50
60.00	21.82	2.75
60.00	20.00	3.00
60.00	18.46	3.25
60.00	17.14	3.50
60.00	16.00	3.75
60.00	15.00	4.00
60.00	13.33	4.50
60.00	12.63	4.75
60.00	12.00	5.00

Selecting center distance is the most important parameter, because amount of testing gears are directly related to this and of course all components design changes with this value. Thus, selected module value must supply possibility of large amount test gear and easy design of components (e.g., shaft, couplings...).

Center distance is chosen as 120 mm which supplies integer tooth numbers 24, 30, 32, 40, 48, and 60 (Table 4.7) between 2mm and 5mm normal modules for spur gears. Furthermore 29 favorable test helical gears were the possibilities which have normal modules from 2 to 5 mm. 90 mm center distance has same number of integer (Table 4.7) as 120 mm. But 90 mm center distance affects assembly of bearings, couplings and housings. It makes it difficult to assembly.

Table 4.7: Discussing Of Center Distance between 2 mm and 5 mm Normal Modules

m(mm)	CD(mm)	Z
2	120	60
	100	50
	90	45
	60	30
2.25	120	-------
	100	-------
	90	40
	60	-------
2.5	120	48
	100	40
	90	36
	60	24
2.75	120	-------
	100	-------
	90	-------
	60	-------

m(mm)	CD(mm)	Z
3	120	40
	100	-------
	90	30
	60	20
3.25	120	-------
	100	-------
	90	-------
	60	-------
3.5	120	-------
	100	-------
	90	-------
	60	-------
3.75	120	32
	100	-------
	90	24
	60	16

m(mm)	CD(mm)	Z
4	120	30
	100	25
	90	---------
	60	15
4.5	120	---------
	100	---------
	90	20
	60	---------
4.75	120	---------
	100	---------
	90	---------
	60	---------
5	120	24
	100	20
	90	18
	60	12

In the literature for helical gears helix angle (ψ) is usually recommended to be between 8° and 30°. Allowable helix angles at 120 mm center distance are shown in Table 4.8 for helical gears.

Table 4.8: Allowable helix angles at 120 mm center distance

d(mm)	Z	m(mm)	ψ(degree)
120	56	2	21.04
120	57	2	18.19
120	58	2	14.84
120	59	2	10.48
120	50	2.25	20.36
120	51	2.25	17.01
120	52	2.25	12.84
120	45	2.5	20.36
120	46	2.5	16.60
120	47	2.5	11.72
120	41	2.75	20.02
120	42	2.75	15.74
120	43	2.75	9.80
120	37	3	22.33
120	38	3	18.19
120	39	3	12.83
120	34	3.25	22.95
120	35	3.25	18.57
120	36	3.25	12.83
120	32	3.5	21.03
120	33	3.5	15.74
120	30	3.75	20.36
120	31	3.75	14.36
120	29	4	14.83
120	28	4	21.03
120	25	4.5	20.36
120	26	4.5	12.83
120	22	5	23.55
120	23	5	16.59

In Table 4.8 for helix angle following equation is used.

$$m_t = \frac{m}{\cos\psi} \tag{4.3}$$

m_t =? and $\cos\psi$ =?

$$d = m_t . Z \tag{4.4}$$

This equation includes three parameters where "m_t" is transverse module, "m" is normal module and "ψ" is helix angle. But transverse module and helix angle are unknown. To calculate transverse module next formula can be used. According to formula "d" is pitch diameter of helical gear and "Z" is tooth number of it. If tooth number is assumed, transverse module can be calculated. Then, transverse module value by adding the first equation, helix angle is calculated.

4.3.TOOTH FORCE IN A GEAR PAIR

Gear test rig design is imagined as a ladder, unit tooth load (*Tl in N/mm*) is the first ladder of the design. Because all of structural deflections and stresses occur from tooth loads. Design of parts builds depending on tooth load. In this thesis tooth loads are assumed between 0 and 500 N/mm. Then design parameters are calculated one by one.

Firstly face width of gears (F_w) is calculated. In the literature face width is between three time's circular pitch of gear (p) and five times of circular pitch of gear. Normally, circular pitch is equal to multiplied of normal module and pi (3.14). If normal module is assumed as 3 mm, face width is between 28.26 mm and 47.10 mm. In this design face width was assumed 30mm.

$$3p < F_w < 5p \tag{4.5}$$

$$p = m * pi \tag{4.6}$$

At design for loading maximum value is always used. Then, 500 N/mm tooth load should be used at this design. Tooth force of gear (W) is calculated in below equation. According to this equation tooth force is 15000 N.

$$W(\text{Tooth force}) = \text{unit tooth load} * \text{face width}(F_w) \tag{4.7}$$

4.3.1. Tooth Force of Spur Gear

Tooth Force of Spur Gear is illustrated in Figure 4.1 where W is tooth force, W_t is tangential force, W_r is radial force and φ is pressure angle of spur gear.

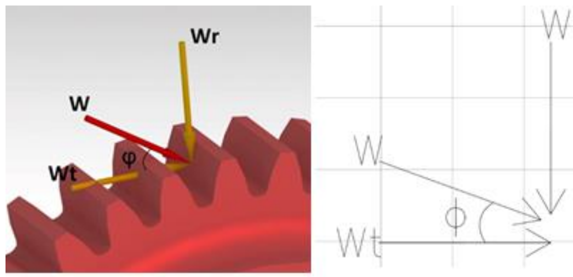

Figure 4.1: Tooth Force of Spur Gear

These parameters of spur gear;

$$W = Tl * F_w \tag{4.8}$$

$$W = \frac{500\ N}{mm} * 30mm \qquad W = 15000\ N$$

$$W_t = W.\cos\varphi \tag{4.9}$$

$$W_t = 15000 * \cos 20\, W_t = 14095\ N$$

$$W_r = W.\sin\varphi \tag{4.10}$$

$$W_r = 15000 * \sin 20\, W_r = 5130\ N$$

4.3.2. Tooth Force of Helical Gear

Tooth Force of Helical Gear is illustrated in Fig where W is tooth force, W_t is tangential force, W_r is radial force, W_a is axial force, ψ is helix angle and φ is normal pressure angle of helical gear.

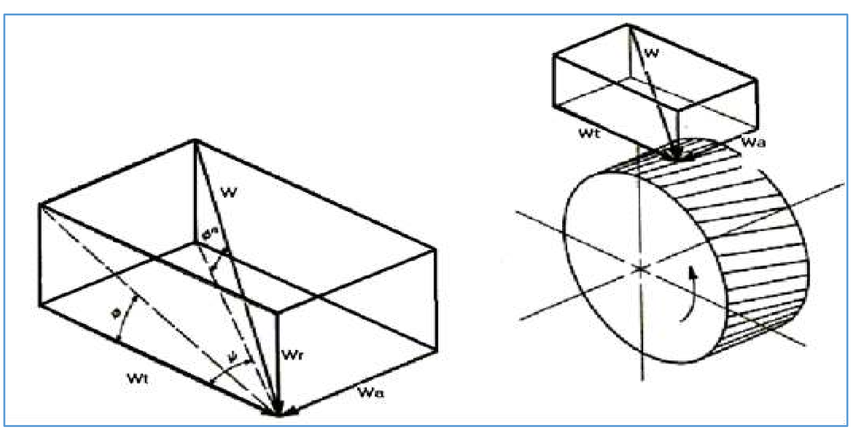

Figure 4.2: Tooth Force of Helical Gear

These parameters of helical gear; (in Table 4.8 for 38 teeth number and 3mm module helix angle 18.2 degree)

$$W_t = W.\cos\varphi.\cos\psi \tag{4.11}$$

$W_t = 15000 * \cos 20 * \cos 18.2 \;\; W_t = 13390$ N

$$W_r = W.\sin\varphi \tag{4.12}$$

$W_r = 15000 * \sin 20 \; W_r = 5130$ N

$$W_a = W.\cos\varphi.\sin\psi \tag{4.13}$$

$W_a = 15000 * \cos 20 * \sin 18.2 \; W_a = 4402$ N

4.4.REACTION FORCES OF BEARING

The magnitudes and directions of the tangential, radial and axial components of gear forces are important because they act on the shafts that the gears are mounted on and contribute to the forces acting on the bearings that support the shafts. Since the conditions of static equilibrium will be used to determine bearing reactions, correct directions for the gear forces acting on a shaft must be established.

The reaction forces and its directions depending on spur gear forces are illustrated in Figure 4.3 below. Here, reaction forces must be calculated on the xy and xz plane. Firstly forces on xy planes are defined, after reaction forces on same plane are calculated.

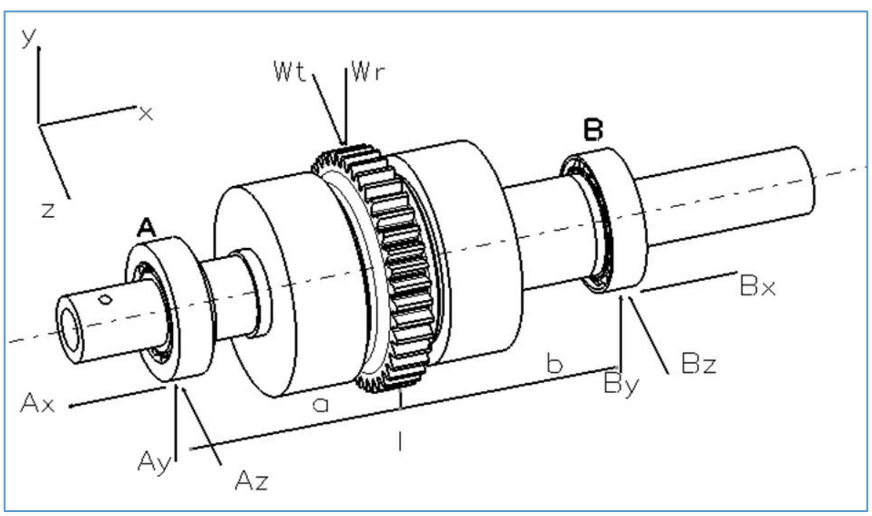

Figure 4.3: The reaction forces and its directions of spur gear forces

For spur gear, forces on the xy plane as shown in Figure 4.4 below. Here, A and B points are place where mounted bearing. W_r is radial force, A_y and B_y are reaction forces in y direction.

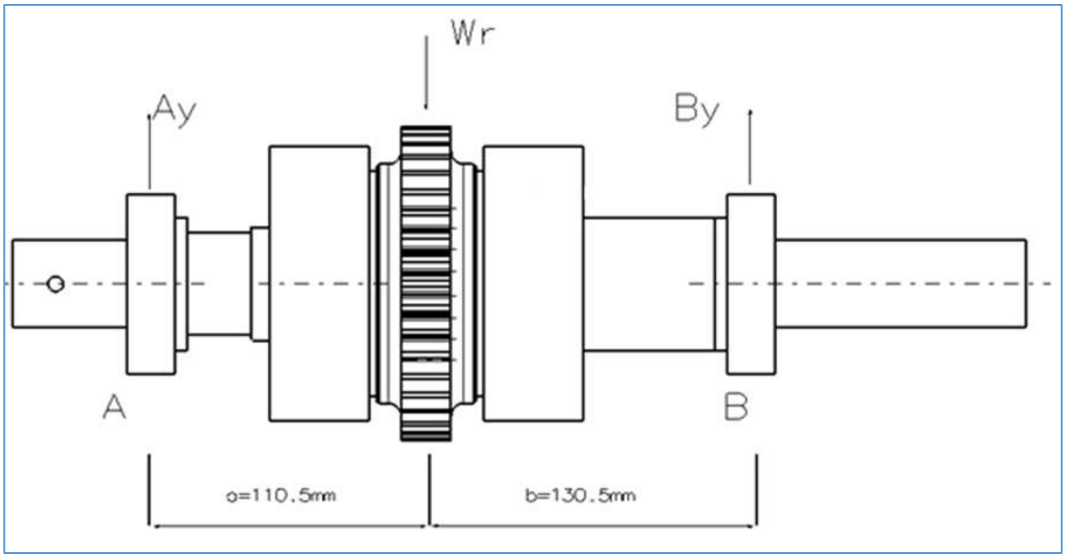

Figure 4.4: For spur gear, forces on the xy plane

This shaft like a simple support beam. To calculate unknown A_y and B_y reaction forces, an obvious assumption of static equilibrium is necessary. In the absence of any horizontal forces, the equation is sum of all forces in x directions equal to zero. However, since there are two unknown forces, one at each support; two equations are sufficient, i.e. sum of all forces in x directions equal to zero and sum of all moments to zero.

In the design, equations and reaction forces in y direction are below.

$$\Sigma \mathrm{MA} = 0 \tag{4.14}$$

$$\mathrm{B}_y.(\mathrm{a}+\mathrm{b}) - \mathrm{W}_r.\mathrm{a} = 0 \tag{4.15}$$

$$\mathrm{B}_y * (241) - 5130 * 110.5 = 0$$

$$\mathrm{B}_y = 2352\mathrm{N}$$

$$\mathrm{W}_r - \mathrm{B}_y = \mathrm{A}_y \tag{4.16}$$

$$\mathrm{A}_y = 2778\ \mathrm{N}$$

$$\mathrm{A}_x \text{ or } \mathrm{B}_x = 0$$

For spur gear, forces on the xz plane as shown in Figure 4.5 below. Here, A and B points are place where mounted bearing. Wt is tangential force, A_z and B_z are reaction forces in z direction.

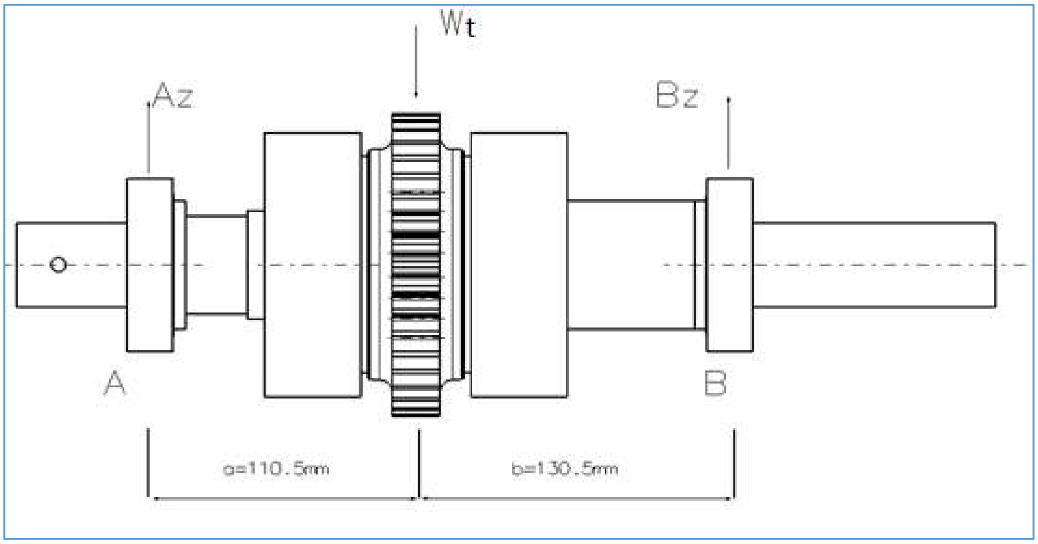

Figure 4.5: For spur gear, forces on the xz plane

Equations and reaction forces in z direction are below.

$\Sigma MA = 0$

$$B_z * (a + b) - W_t * a = 0 \tag{4.17}$$

$B_z * (241) - 14095 * 110.5 = 0$

$B_z = 6462N$

$$W_t - B_z = A_z \tag{4.18}$$

$A_z = 7633\ N$

The reaction forces and its directions depending on helical gear forces as shown in Figure 4.6 below. As spur gear, Reaction forces are studied on xy and xz planes.

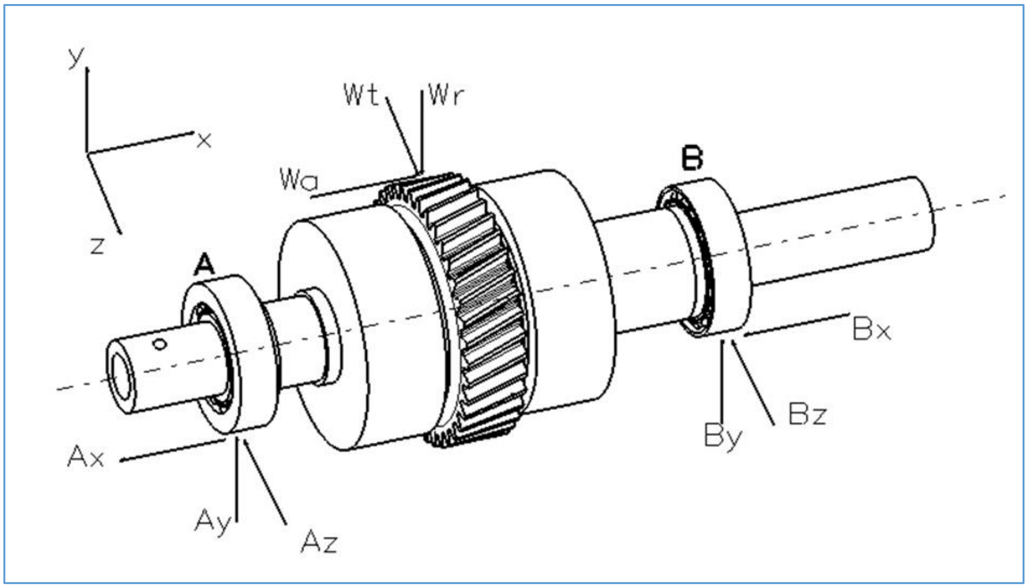

Figure 4.6: The reaction forces and its directions depending on helical gear

For helical gear, forces on the xy plane as shown in Figure 4.7 below. Here, A and B points are place where mounted bearing. W_a is axial force, W_t is tangential force, A_y and B_y are reaction forces in y direction, A_x and B_x are reaction forces in z direction and W_a*r is moment which is occurred by axial force.

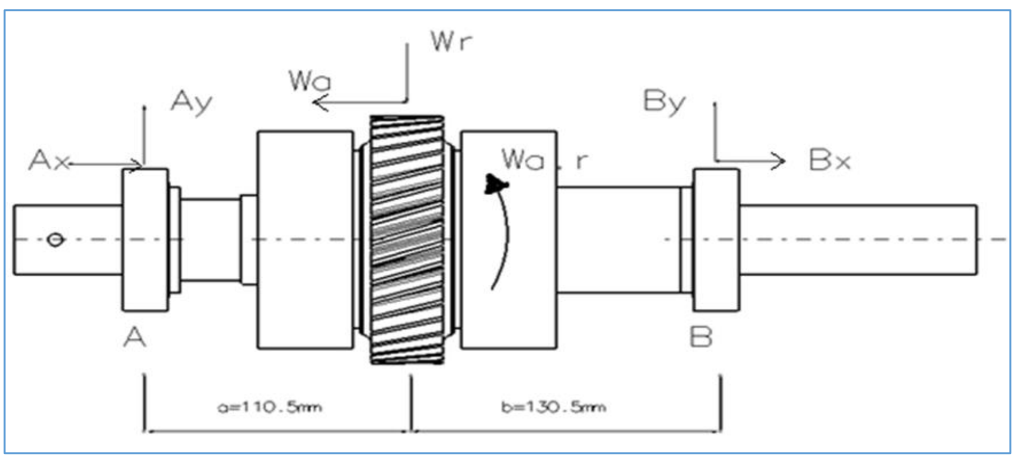

Figure 4.7: For helical gear, forces on the xy plane

Equations and reaction forces in y and x directions are below.

$\Sigma MA = 0$

$$B_y.(a + b) - W_r.a + W_a.r = 0 \tag{4.19}$$

$B_y * (241) - 5130 * 110.5 - 4402 * 60 = 0$

$B_y = 1256N$

$W_r - B_y = A_y$ (4.20)

$A_y = 3784$ N

$A_x = W_a$

For helical gear, forces on the xz plane as shown in Figure 4.9 below.

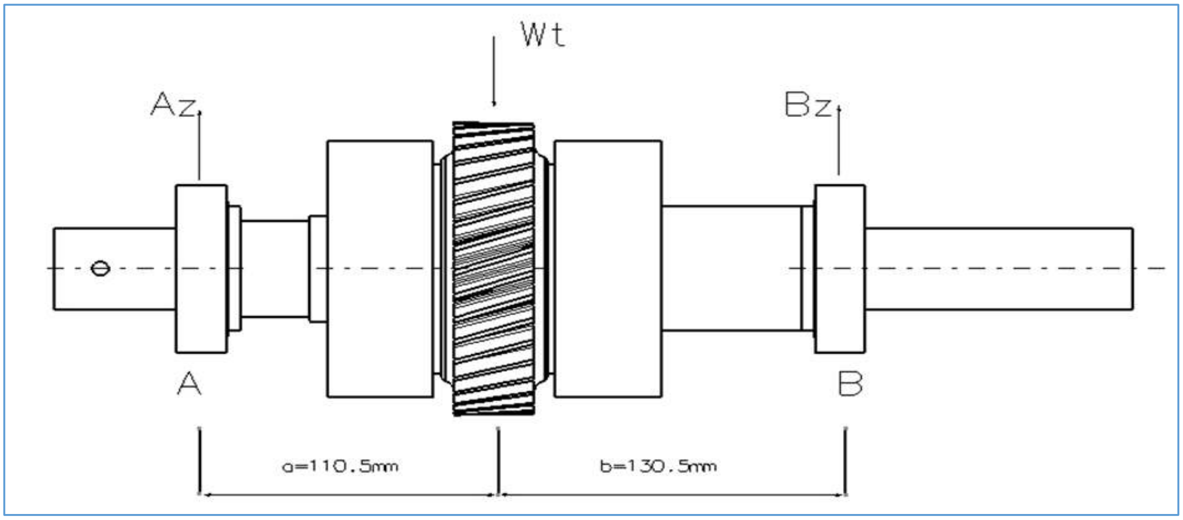

Figure 4.8: For helical gear, forces on the xz plane

A and B points are place where mounted bearing. W_t is tangential force, A_z and B_z are reaction forces in z direction.

$\Sigma MA = 0$

$B_z * (a + b) - W_t * a = 0$ (4.21)

$B_z * (241) - 13390 * 110.5 = 0$

$B_z = 6139\ N$

$W_t - B_z = A_z$ (4.22)

$A_z = 7251\ N$

4.5.BENDING MOMENTS ON THE SHAFT

Generally, forces on the shaft occur bending moment and shear force. Practically, there are two load types affected the shaft. They are distributed loads and concentrated loads. To analyses effect of these loads, shear force and bending moment diagram are drawn. The conditions of static equilibrium is used to draw these diagrams.

Following steps can be generalized to draw shear force and bending moment diagrams.

- Firstly, reaction forces of bearing are calculated. It is studied in previous title.
- Shaft is divided into sections. For this steps, the most appropriate method is selecting a region between the forces. For example; two regions affected to the middle of shaft by only one force is enough. It is shown in Figure 4.9

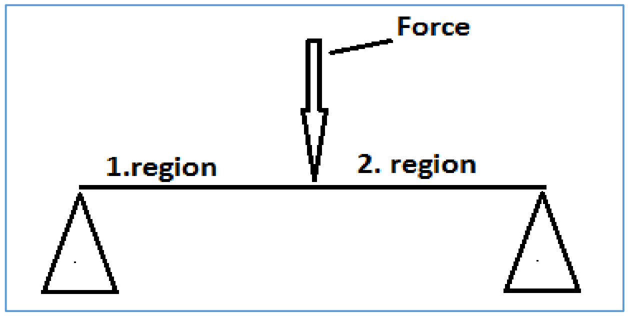

Figure 4.9: Divided shaft

- Assuming cut the beam of x distance, shear force and bending moment are applied on this point.(V=shear force, M=bending moment)

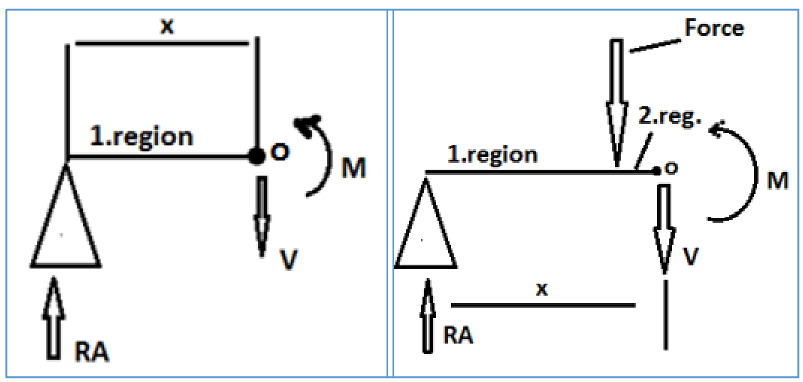

Figure 4.10: Cutting of beam

- The conditions of static equilibrium is used. This conditions are;

$$\Sigma Mo = 0 \tag{4.23}$$

$$\Sigma F = 0 \tag{4.24}$$

- Finally, calculated values are transported to the diagram.

4.5.1. Bending moment for spur gear

Forces affected to the shaft and its values is shown in Figure 4.3. Bending moments is needed to study for two regions on xy plane and xz plane.

$B_y = 2352$ N, $A_y = 2778$ N, $A_x = B_x = 0$ N, $B_z = 6462$ N, $A_z = 7633$ N

$W_r = 5130$ N $W_t = 14095$ N, $W_a = 0$ N

xy plane;

First region on xy plane is between point A and point O. It is illustrated in Figure 4.11. According to point O, bending moment's formula multiply by Ay and x distance. Minimum bending moment value is at point A, maximum bending moment is at point O.

if $0 < x < a$ $M = A_y * x$ (4.25)

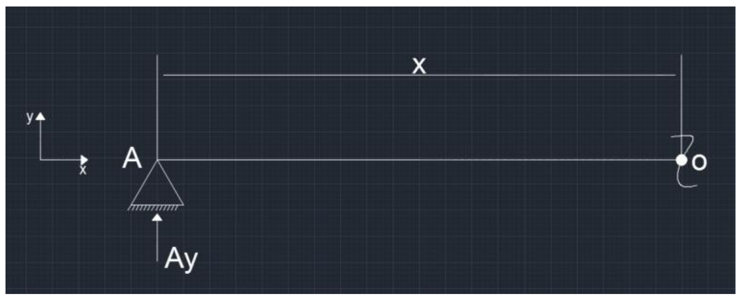

Figure 4.11: First region on xy plane

Second region on xy plane is between point A and point O. It is illustrated in Figure 4.12. Bending moment's formula is shown below. Minimum bending moment value is at point A, maximum bending moment is at point O.

if $a < x < l$ $M = A_y * x - W_r * (x - a)$ (4.26)

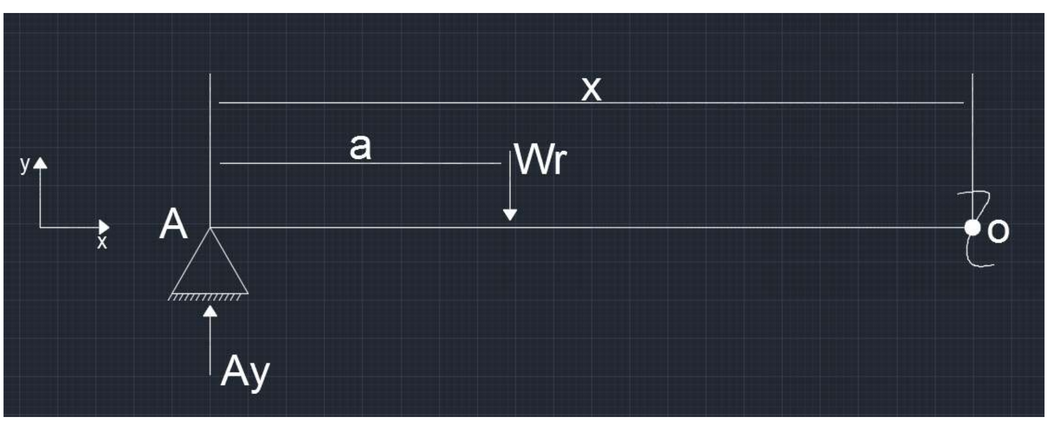

Figure 4.12: First region on xy plane

If moment values at y direction are added to the diagram (Figure 4.13);

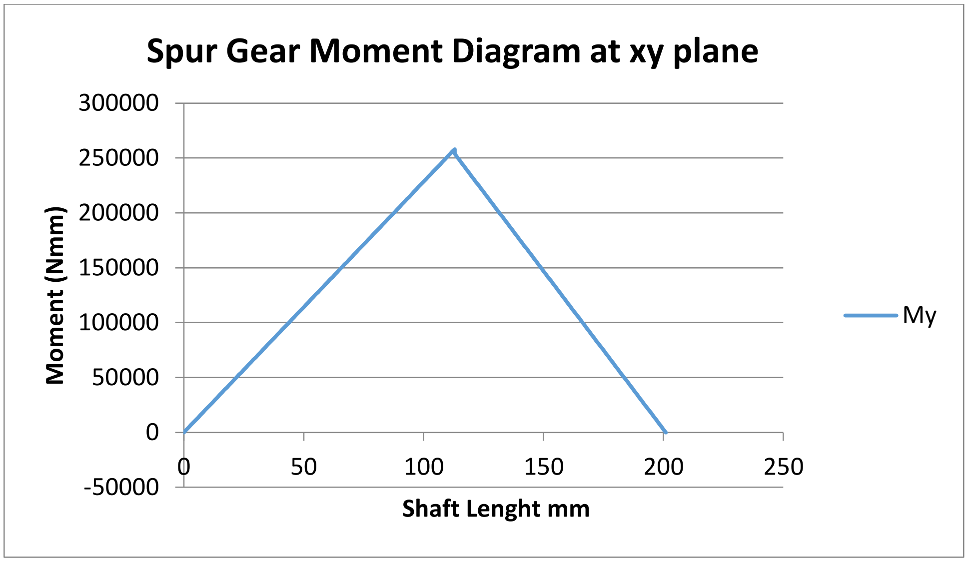

Figure 4.13: Spur gear Moment Diagram at xy plane

xz plane

First region on xz plane is between point A and point O. It is illustrated in Figure 4.14. According to point O, bending moment's formula multiply by A_z and x distance. Minimum bending moment value is at point A, maximum bending moment is at point O.

$$\text{if } 0 < x < a \qquad M = A_z * x \tag{4.27}$$

Figure 4.14: First region on xz plane

Second region on xz plane is between point A and point O. It is illustrated in Figure 4.15. Bending moment's formula is shown below. Minimum bending moment value is at point A, maximum bending moment is at point O.

$$\text{if } a < x < l \qquad M = A_z * x - W_t * (x - a) \tag{4.28}$$

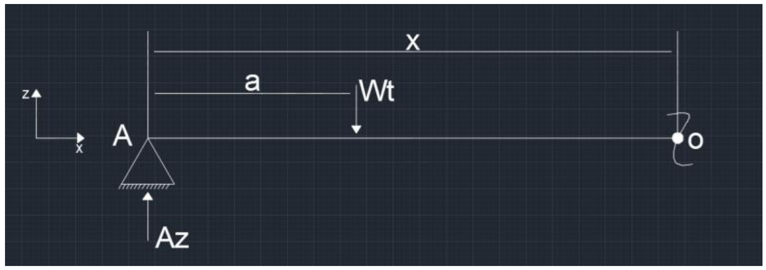

Figure 4.15: First region on xz plane

If moment values at z direction are added to the diagram (Figure 4.16);

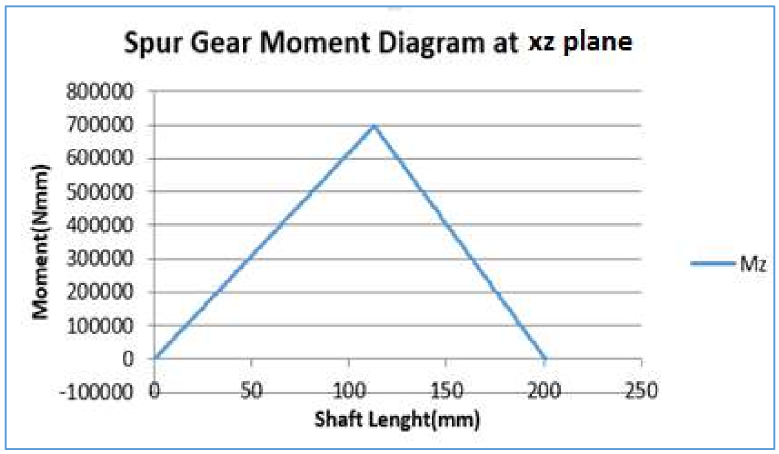

Figure 4.16: Spur gear Moment Diagram at xz plane

Total moment (M_t) diagram (Figure 4.17) is drawn by below equation. Where "M_y" is bending moment at y direction and "M_z" is at z direction.

$$M_t = \sqrt{{M_y}^2 + {M_z}^2} \tag{4.29}$$

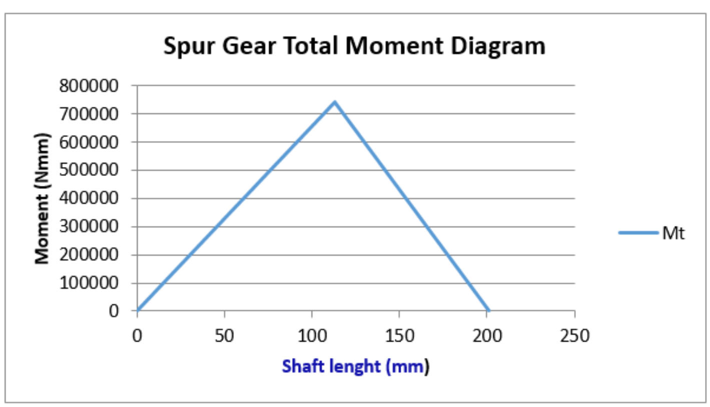

Figure 4.17: Spur Gear Total Moment Diagram

4.5.2. Bending moment for helical gear

Forces affected to the shaft and its values is shown in Figure 4.6. Bending moments is needed to study for two regions on xy plane and xz plane.

$B_y = 1256$ N, $A_y = 3874$ N, $A_x = B_x = 4402$ N, $B_z = 6139$ N, $A_z = 7253$ N

$W_r = 5130$ N , $W_t = 13390$ N, $W_a = 4402$ N

xy plane;

First region on xy plane is between point A and point O. It is illustrated in Figure 4.18. According to point O, bending moment's formula multiply by Ay and x distance. Minimum bending moment value is at point A, maximum bending moment is at point O.

$$\text{if } 0 < x < a \qquad M = A_y * x \tag{4.30}$$

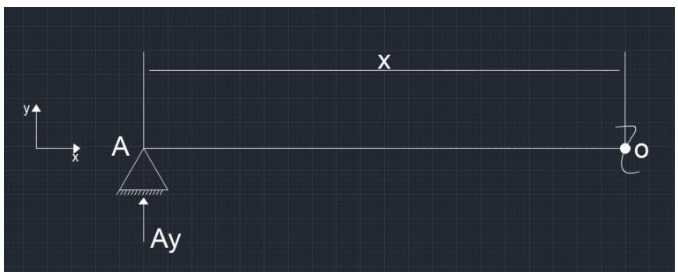

Figure 4.18: First region on xy plane of helical gears

Second region on xy plane is between point A and point O. It is illustrated in Figure 4.19. Bending moment's formula is shown below. Minimum bending moment value is at point A, maximum bending moment is at point O.

$$\text{if } a < x < l \qquad M = A_y * x - W_r * (x - a) - W_a * r \tag{4.31}$$

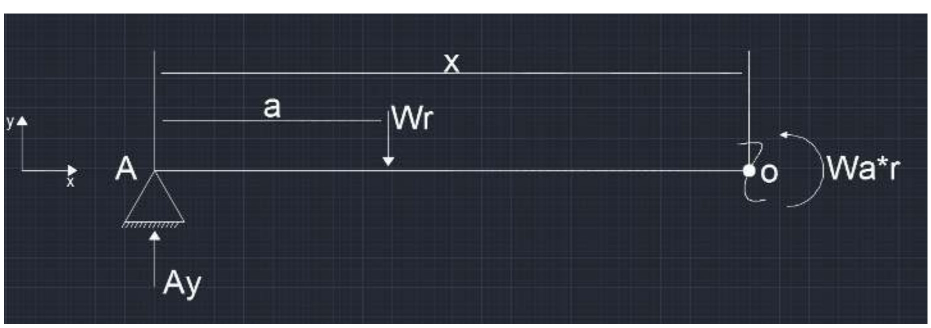

Figure 4.19: First region on xy plane of helical gears

If moment values at y direction are added to the diagram (Figure 4.20);

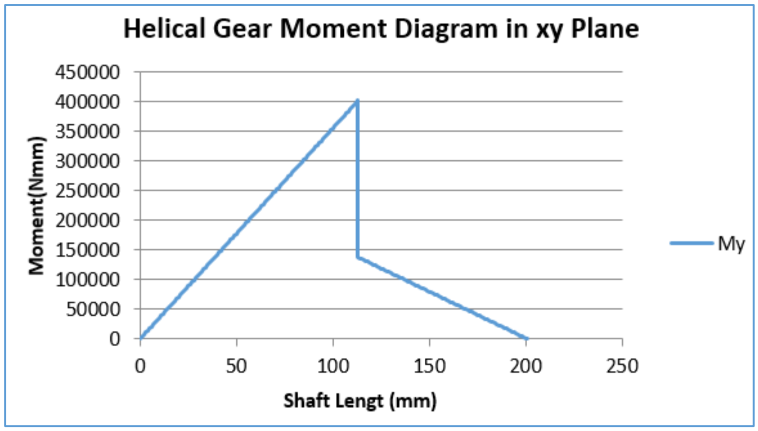

Figure 4.20: Helical gear Moment Diagram at xy Plane

xz plane

First region on xz plane is between point A and point O. It is illustrated in Figure 4.21. According to point O, bending moment's formula multiply by A_z and x distance. Minimum bending moment value is at point A, maximum bending moment is at point O.

if $0 < x < a$ $\qquad M = A_z * x \qquad (4.32)$

Figure 4.21: First region on xz plane of helical gears

Second region on xz plane is between point A and point O. It is illustrated in Figure 4.22. Bending moment's formula is shown below. Minimum bending moment value is at point A, maximum bending moment is at point O.

if $a < x < l$ $\qquad M = A_z * x - W_t * (x - a) \qquad (4.33)$

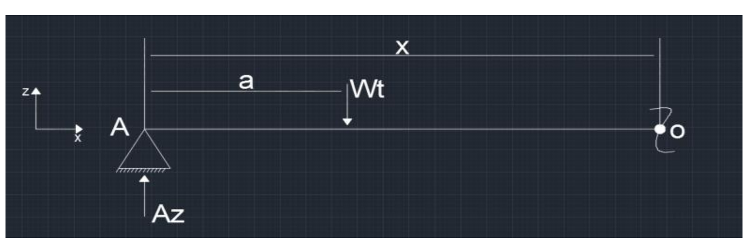

Figure 4.22: Second region on xz plane of helical gears

If moment values at z direction are added to the diagram (Figure 4.23);

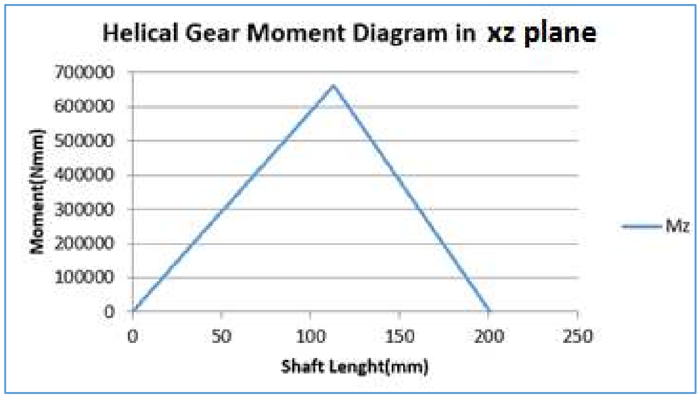

Figure 4.23: Helical Gear Moment Diagram at xz Plane

Total moment (M_t) diagram (Figure 4.24) is drawn by below equation. Where M_y is bending moment in y direction and M_z is in z direction.

$$M_t = \sqrt{{M_y}^2 + {M_z}^2} \tag{4.34}$$

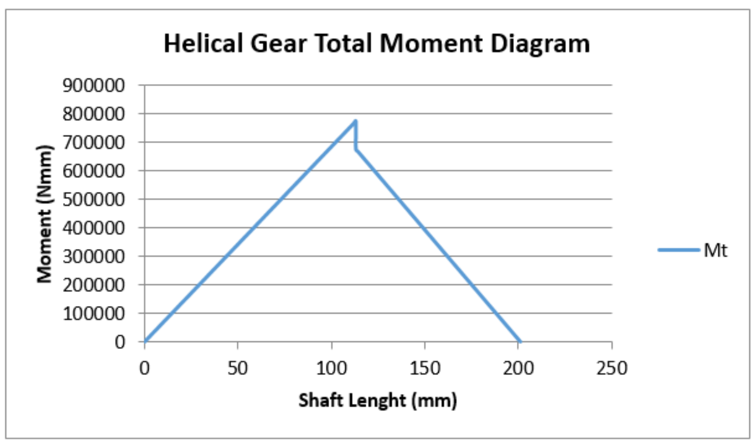

Figure 4.24: Helical Gear Total Moment Diagram

4.6.CRITICAL SECTION DETERMINATION OF SHAFT

Critical sections are sections likely to be subjected to high stresses. Locate critical sections by inspection, with reference to the applied loads. Critical sections are usually associated with changes of shaft section or points of load application. When considering fluctuating loads, features which produce high stress concentrations are particularly critical. More than one potentially critical section may be needed to consider.

Potential critical points are generally points where the load is applied and changes of shaft sections in the region where the torque circulate. At design,2 points are defined as potential critical points as shown in Figure 4.25.

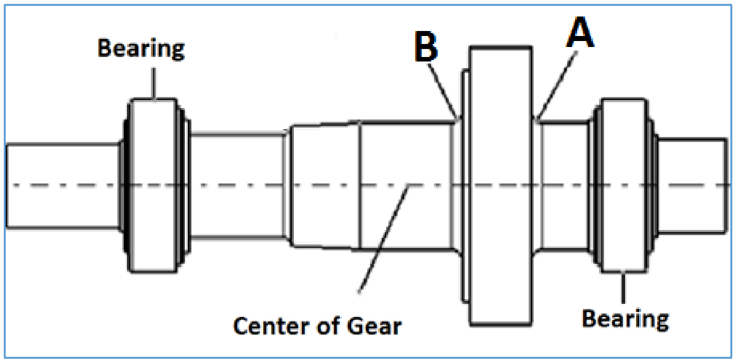

Figure 4.25: Critical Points of Shaft

Practically, potential critical points are found by calculating Von-Mises Stress. According to the von Mises's theory, a ductile solid will yield when the distortion energy density reaches a critical value for that material. Since this should be true for uniaxial stress state also, the critical value of the distortional energy can be estimated from the uniaxial test.

According to von Mises's failure criterion, the material under multi-axial loading will yield when the distortional energy is equal to or greater than the critical value for the material.

Thus, the distortion energy theory can be stated that material yields when the von Mises stress exceeds the yield stress obtained in a uniaxial tensile test. The von Mises stress in Equation (4.35) can be rewritten in terms of general stress components as

$$\sigma' = \sqrt{\sigma_t^2 + 3 * \tau^2} \tag{4.35}$$

In this equations "σ'" represents Von-Misses Stress, "σ_t" represents total normal stress and "τ" represents shear stress. When the shaft considered in terms of normal stresses due to gear loads, bending moment and axial force affect to the shaft. So at this study total normal stress is calculated by the sum of bending stress "σ_{bend}" and normal stress "σ_n" as shown in below equation.

$$\sigma_t = \sigma_{bend} + \sigma_n \tag{4.36}$$

At bending stress calculation, Equation (4.37) is used where M=bending moments specified in bending moment section, c= distance to the central axis of shaft and I=inertia.

$$\sigma_{bend} = \frac{M * c}{I} \tag{4.37}$$

Below equation is used for normal stress. Here, F is force, W_a is axial force and A is area of shaft critical section, D is outer diameter of shaft critical section.

$$\sigma_n = \frac{F}{A} = \frac{4 * W_a}{\pi * (D^2)} \tag{4.38}$$

Torque occurs to shear stress. So at shear stress calculation, equation (4.39) is used where T is expressed with torque, r is expressed with Radius of shaft critical section, J is expressed with polar moment of inertia. Torque equal to multiply by tangential force "W_t" and pitch radius of gear "r_p".

$$\tau = \frac{T * r}{J} = \frac{T * r}{\frac{\pi}{32}(D^4)} \tag{4.39}$$

$$T = W_t * r_p \tag{4.40}$$

According to these equations von misses values are calculated for 2 potential critical sections illustrated in Table 4.9 both of spur and helical gear one by one. Most critical point is determined as B point. At the same time potential critical section of shaft is found with FEM in Appendix C.

Table 4.9: Potential Critical Sections of Spur and Helical Gear

SPUR	Point	σb(N/mm2)	σ'(N/mm2)	n(assumed safety factor)	Sy(N/mm2)(Yield stress)
	A	21	52.5	3	157.5
	B	38.5	62.5	3	187.5
HELICAL	Point	σt(N/mm2)	σ'(N/mm2)	n(assumed safety factor)	Sy(N/mm2)(Yield stress)
	A	19.2	50.5	3	151.7
	B	35.1	60.1	3	180.3

At B point von mises stress is calculated as 60.1 MPa. If safety factor "n" is assumed as 3, yield strength can be as 180.3 MPa for necessary shaft material due to below equation.

$$S_{yD} = \sigma' * n \tag{4.41}$$

Due to found critical point, shaft material may be A-20 Steel 1050 CD (According to AISI). It is often used for shaft material in application. Yield strength and tensile strength of this material are 580 MPa and 690 MPa.

4.7.FATIGUE DESIGN OF SHAFT

Fatigue failures occur related to fluctuating stresses. Fluctuating stresses are much lower than the stress which are result of a static application loads. Approximately 90% of all mechanical service failures' reason is fatigue. Fatigue is a problem for any part or component that moves. Vehicles on roads, aircraft wings and fuselages, ships at sea, nuclear reactors, jet engines, and land-based turbines are all subject to fatigue failures. It has been recognized, since 1830 that a metal subjected to a repeated or fluctuating load will fail at a stress level lower than that required to cause fracture on a single application of the load. Firstly it is observed in Europe by researchers. They found that bridge and railroad components were cracking due to repeated loading. As the century progressed and the use of metals expanded with the increasing use of machines, more and more failures of components subjected to repeated loads were recorded. Now, structural fatigue has assumed an even greater importance as a result of the ever-increasing use of high-strength materials and the desire for higher performance from these materials.

Most determinations of fatigue properties have been made in completely reversed bending by means of the so-called rotating bend test. The usual laboratory procedure for determining an S-N curve (as shown in Figure 4.20.) is to test the first specimen at a high stress, about two thirds of the static tensile strength of the material, where failure is expected in a fairly small number of cycles. The test stress is decreased for each succeeding specimen until one or two specimens do not fail before at least 10^7 cycles. For materials which exhibit it, the highest stress at which no failure occurs, a run out is taken to be the fatigue limit. For situations where an infinite life design requires a probability of survival to be associated with it, more complex testing and analysis procedures, such as the Prot and staircase methods, have been developed to determine the mean and variance of the fatigue limit. For materials which do not exhibit a fatigue limit, tests are usually terminated between 10^7 and 10^8 cycles, and the concept of an endurance limit at either 10^7 or 10^8 cycles defined.

The S-N curve (Figure 4.26) is usually determined through the use of about 15 specimens. However, it is generally found that results are accompanied by a large amount of scatter and some form of statistical analysis should be applied.

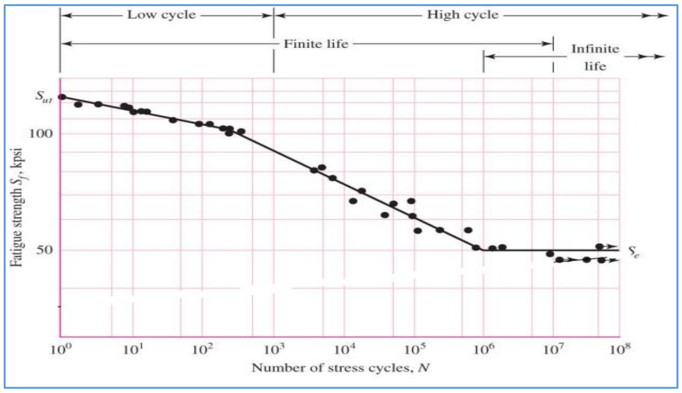

Figure 4.26: S-N Curve

Fatigue design is analyzed as “infinite life” and “finite life” illustrated in Figure 4.27. Failure Theories approaches are categorized five titles. They are Modified Goodman Approach, Soderberg Approach, Gerber Approach, Keçecioğlu's Approach and Baci's Approach. In this thesis for fatigue design of shaft Modified Goodman Approach is used.

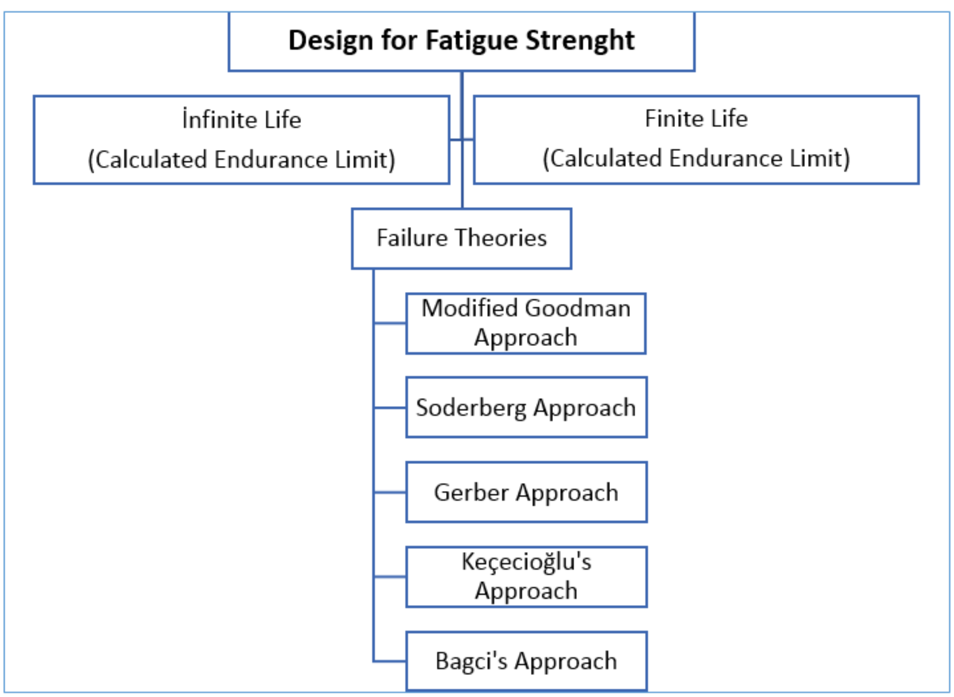

Figure 4.27: Failure Theories Approaches

According to Modified Goodman Approach safety factor "n" is calculated in equation (4.43) is regulating of equation (4.42).

$$n = \frac{1}{\frac{\sigma_a}{S_e} + \frac{\sigma_m}{S_u}} \tag{4.42}$$

$$n = \frac{1}{\frac{\sigma'_a}{k_a * k_b * k_c * k_d * S'_e} + \frac{\sigma'_m}{S_u}} \tag{4.43}$$

In these equations;

$n = \text{factorofsafety}$

$\sigma_a = \text{Alternatingstress}$

$\sigma_m = \text{MeanStress}$

$S_e = \text{Endurancelimit}$

$S_u = \text{UltimateStrenght}$

$k_a = \text{Surfacefactor}$

$k_b = \text{Sizefactor}$

$k_c = \text{Reliabilityfactor}$

$k_d = \text{Temperaturefactor}$

$k_e = \text{Modifyingfactor}$

$k_f = \text{Miscellaneouseffectsfactor}$

$S'_e = \text{Endurancelimitofrotating} - \text{beamspecimen}$

Endurance Limit formula is;

$$S_e = k_a * k_b * k_c * k_d * k_e * S'_e \tag{4.44}$$

Surface factor formula is below. According this formula "a" and "b" are constants associated with surface operation type. "a" is equal to 4.51 and b is equal to -0.265 to operate surface of shaft with machining.

$$k_a = aS_{ut}^b \tag{4.45}$$

$$k_a = 4.51(690)^{-0.265} = 0.797$$

Size factor formula is in equation. In this, d is the critical section diameter of shaft.

$$k_b = (d/7.62)^{-0.107} \tag{4.46}$$

$$k_b = (\frac{1}{7.62})^{-0.107} * d^{-0.107} = 1.24 * 55^{-0.107} = 0.81$$

For %99 reliability, reliability factor is 0.814.

$$k_c = 0.814$$

T_c is operation temperature. It is assumed that 50 degree below temperature factor formula can be used;

$$k_d = 0.9877 + 0.6507(10^{-3})T_C - 0.3414(10^{-5}){T_C}^2 + 0.5021(10^{-8}){T_C}^3$$

$$-6.246(10^{-12}){T_C}^4 \quad (4.47)$$

$k_d = 1$

The Modifying factor formula is following equation. Instead of modifying factor at endurance limit equation directly "$1/K_f$" is suggested. "K_f "is notch factor.

$$k_e = \frac{1}{K_f} \quad (4.48)$$

K_f is calculated in Equation 4.49. According to this equation "K_t" is geometric stress calculation factor and "q" is notch-sensitivity factor. Geometric stress calculation factor is taken from moment, axial and torsion load graph. In these graph, the diameter change ratio "D/d" and ratio of shoulder fillet to small diameter "r/d" at critical point must be known as shown in Figure 4.28. Notch-sensitivity factor is similar as geometric stress calculation factor. Its value is taken from graph. But to take this value, ultimate tensile strength of shaft material and shoulder fillet must be known.

$$K_f = 1 + q(K_t - 1) \quad (4.49)$$

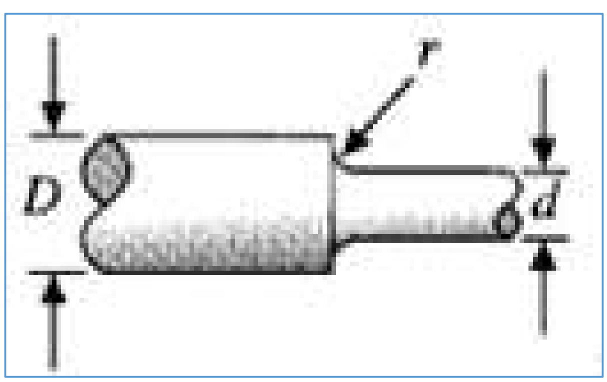

Figure 4.28: Size values of the shaft.

On the shaft, the diameter change ratio “D/d” is “110 mm/55 mm=2” and ratio of shoulder fillet to small diameter “r/d” is “5 mm/55 mm=0.09” at critical point.

According to these value;

For bending moment from moment graph, geometric stress calculation factor “K_t” and notch-sensitivity factor “q” and calculated notch factor “K_t” are (Figure 4.29 and 4.30);

$q = 0.7$, (r=5, S_{UT}=680 MPa=0.7 GPa)

$K_t = 1.8$ (Dependent On D/d=2, r/d=0.09)

$K_{f(mom)} = 1+0.7(1.8-1)=1.56$

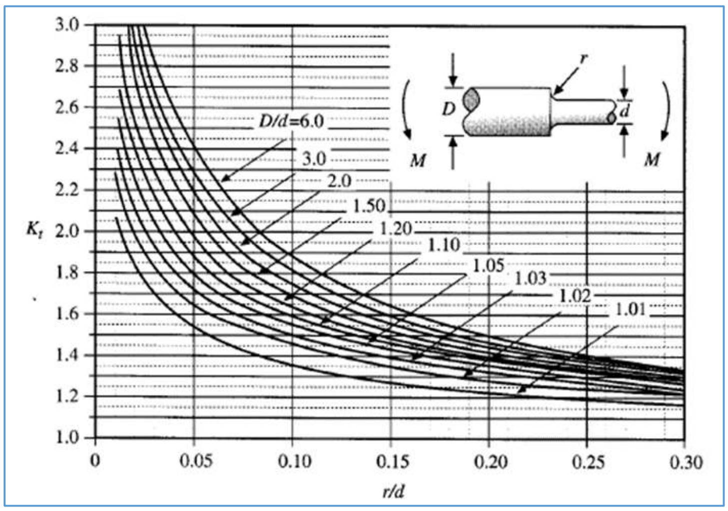

Figure 4.29: Geometric Stress Calculation Factor for Bending Moment

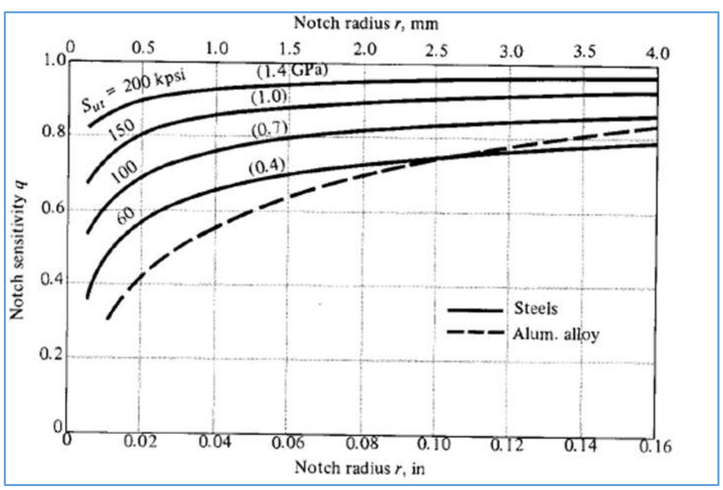

Figure 4.30: Notch-Sensitivity Factor Graph

For axial loading from axial loading graph, geometric stress calculation factor "K_t" and notch-sensitivity factor "q" and calculated notch factor "K_t" are (Figure 4.31);

$q = 0.7$ (r=5, SUT=680 MPa=0.7 GPa)

$K_t = 2$ (Dependent On D/d=2, r/d=0.09)

$K_{f(ax.)} = 1.7$

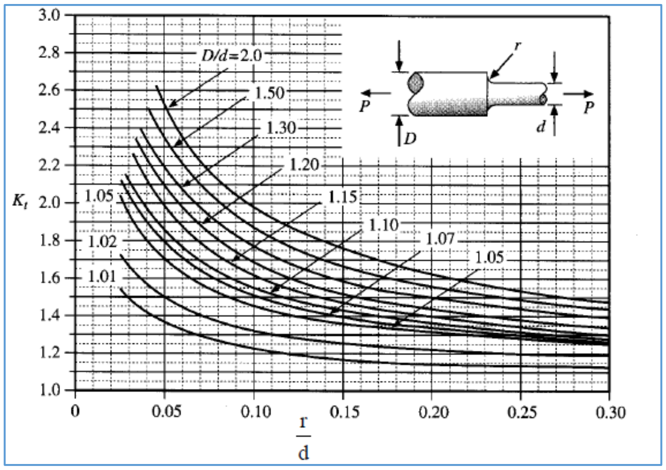

Figure 4.31: Geometric Stress Calculation Factor for Axial Loading

For torsion loading from torsion graph, geometric stress calculation factor "K_t" and notch-sensitivity factor "q" and calculated notch factor "K_t" are (Figure 4.32);

q =0.7 (r=5, S_{ut}=680 MPa=0.7 GPa)

$K_t = 1.5$ (Dependent On D/d=2, r/d=0.09)

$K_{ft} = 1.34$

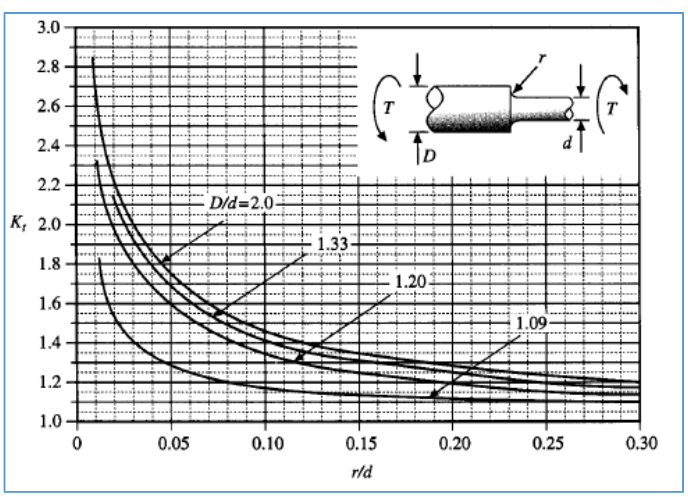

Figure 4.32: Geometric Stress Calculation Factor for Torsion

The shaft material is ductile. For ductile materials, if ultimate strength is small than 1400 MPa, following equation is used. Shaft material is A-20 Steel 1050 CD and its yield strength “S_y”=580 MPa and ultimate strength S_{ut}=690 MPa. So endurance limit of rotating-beam specimen “S'_e” is;

$$S'_e = 0.5S_u \qquad \text{if } S_u < 1400 \text{ MPa} \tag{4.50}$$

$$S'_e = 0.5 * 690 = 345 \text{ MPa}$$

At bending moments and axial loadings, following equations is used for alternating stress. In this, there are two stresses called maximum and minimum stress. Loading on the shaft occur these stresses. Maximum stress is equal to tensile stress, minimum stress is equal to compressive stress as shown in Figure 4.33. Maximum stress direction is positive, minimum stress direction is negative.

$$\sigma_{a(mom,eks)} = \frac{\sigma_{max} - \sigma_{min}}{2} \tag{4.51}$$

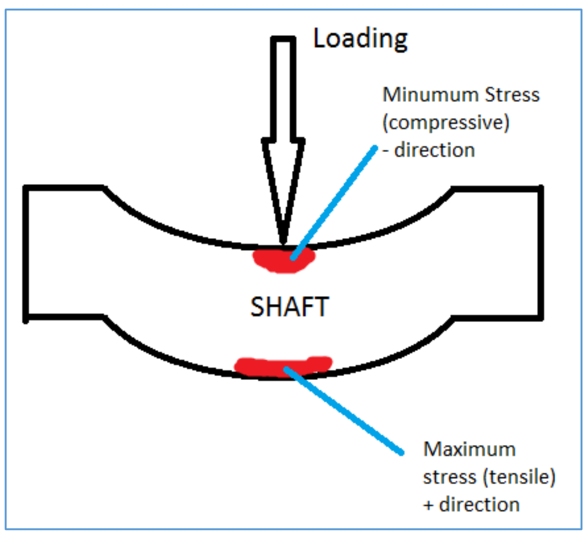

Figure 4.33: Maximum stress and minimum stress of shaft

At bending moment, alternating stress is;

$$\sigma_{a(mom.)} = \frac{35.1-(-35.1)}{2} = 35.1 \text{ MPa (Table 5.9, helical gears ben. stress is 35.1 MPa)}$$

No alternating stress is occurred at axial loading.

$$\sigma_{a(axial)} = 0$$

Total alternating stress is;

$$\sigma_{a(t)} = K_{f(mom)}\sigma_{a(mom.)} + K_{f(axial)}\sigma_{a(axial)} \tag{4.52}$$

$$\sigma_{a(t)} = 1.56 * 35.1 = 54.7 \text{ MPa}$$

Alternating Von-Mises stress is calculated according to below equation. In thus, alternating shear stress is equal to zero.

$$\sigma'_a = \sqrt{\sigma_{a(t)}^2 + 3 * \tau_a{}^2} \tag{4.53}$$

$$\sigma'_a = \sqrt{54.7^2 + 3 * 0} = 54.7 \text{ MPa}$$

At bending moments and axial loadings, following equations is used for mean stress. In this, there are two stresses called maximum and minimum stress like alternating stress.

$$\sigma_{m(mom,eks.)} = \frac{\sigma_{max}+\sigma_{min}}{2} \tag{4.54}$$

At bending moment, mean stress is;

$$\sigma_{m(mom.)} = \frac{35.1 + (-35.1)}{2} = 0 \text{ MPa}$$

At axial loading, mean stress is

$\sigma_{m(eks.)} = 2.6$ MPa(Table 5.9, helical gears normal stress is 2.6 MPa)

Mean stress for torsion loading is;

$$\tau_m = K_{ft} * \tau \tag{4.55}$$

$\tau_m = 1.35 * 27 = 36.45$ MPa (Table 5.9, helical gears shear stress is 27 MPa)

Total mean stress is;

$$\sigma_{m(t)} = K_{f(mom)}\sigma_{m(mom.)} + K_{f(eks.)}\sigma_{m(eks.)} \tag{4.56}$$

$$\sigma_{m(t)} = 1.56 * 0 + 2 * 2.6 = 5.2 \text{ MPa}$$

Mean Von-Mises stress is calculated according to below equation. In thus, mean normal stress is equal to axial mean stress.

$$\sigma'_m = \sqrt{\sigma_{m(t)}^2 + 3 * \tau_m{}^2} \tag{4.57}$$

So mean Von-Mises is

$$\sigma'_m = \sqrt{5.2^2 + 3 * 36.45^2} = 63.3 \text{ MPa}$$

According to Equation 5.43, safety factor is calculated for fatigue design as 2.55.

n=2.55

4.8.DEFLECTIONS OF SHAFT

Shaft under the influence of external forces and moments indicates a relative change at various points. These changes are called deformation. Each element under the external forces and moments which is used in practice replaces more or less.

In this regard, stiffness at techniques, is limiting of deflections. Working conditions, has led to the need to limit the deformation. For example, there is a gear pair on the two shafts under the loads. If this loads occur the large deflection on shafts, the contact between the gears become in the tooth gap, and this jeopardizes the operation and the safety mechanism. So deflections of shaft must be calculated.

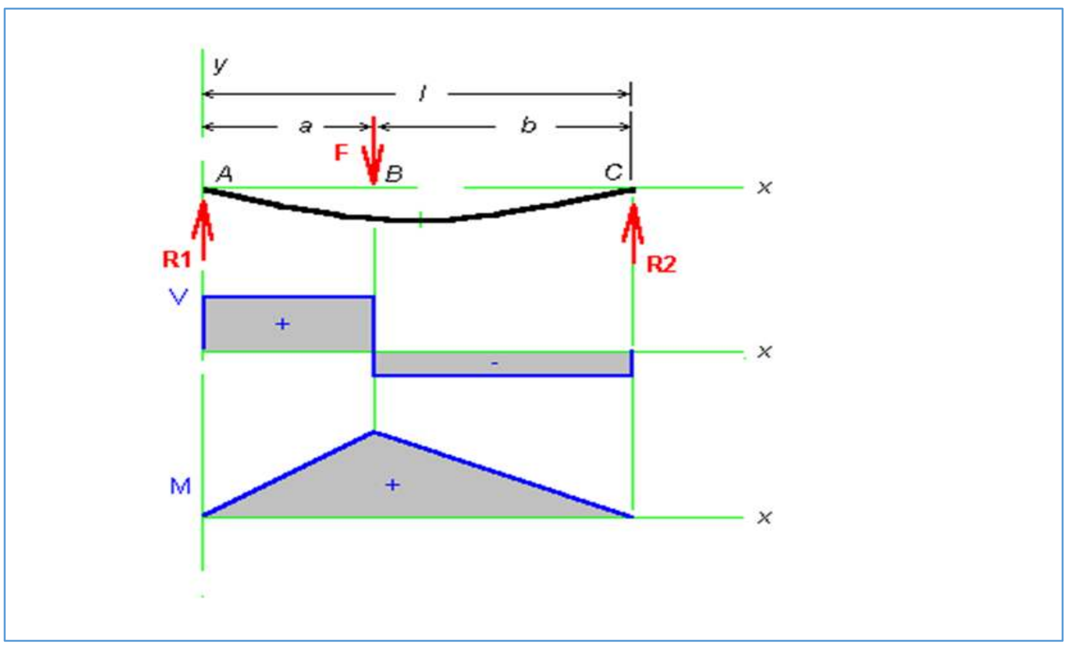

Figure 4.34: Deflection of Simple Supported Beam

Shafts at this study can be considered as simple supported beam illustrated in above graph.R_1 and R_2 are reaction forces, F is load, a and b are distances between supports and load and l is length of shaft (Figure 4.34).

Reaction forces can be calculated below equations;

For R_1, moment equations at C point is;

$$R_1 * l = F * b \tag{4.58}$$

$$R_1 = \frac{F*b}{l} \tag{4.59}$$

For R_2, moment equations at A point is;

$$R_2 * l = F * a \tag{4.60}$$

$$R_2 = \frac{F*a}{l} \tag{4.61}$$

Moment between A and B points is; where x is any point between A and B.

$$M_{AB} = R_1 * x \tag{4.62}$$

$$M_{AB} = \frac{F*b*x}{l} \tag{4.63}$$

Moment between B and C points is; where x is any point between B and C.

$$M_{BC} = R_1 * x - F * (x - a) \tag{4.64}$$

$$M_{BC} = \frac{F*b*x}{l} - F * x + F * a \tag{4.65}$$

$$M_{BC} = F(\frac{b*x}{l} - x + a) \tag{4.66}$$

So deflection between A and B can be calculated below equation.

$$Y_{AB} = \frac{F*b*x}{6*E*I*l}(x^2 + b^2 - l^2) \tag{4.67}$$

If $M_{AB} = \frac{F*b*x}{l}$, equation can be derived below.

$$Y_{AB} = \frac{M_{AB}}{6*E*I}(x^2 + b^2 - l^2) \tag{4.68}$$

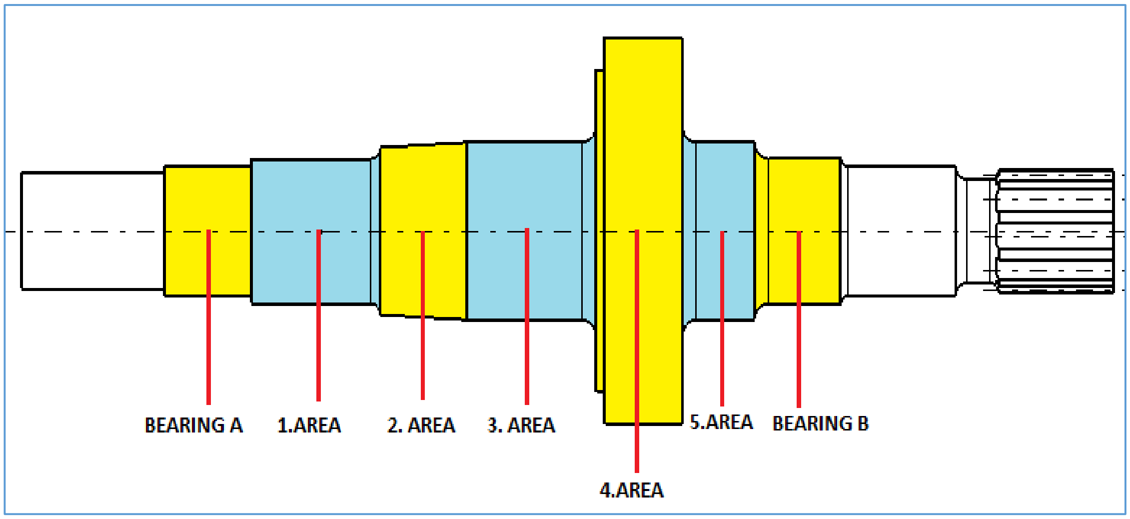

Figure 4.35: Areas of Shaft

Shaft is totally divided 7 areas between centers of bearings with bearing areas in illustrated Figure 4.35. Center of per areas is signed and moment values of this center points are taken from section 1.4. Moment values in equation are calculated in section 1.4.Deflection is calculated for per areas. This deflection formula should be calculated in Microsoft excel as shown in Table 5.10.

Table 4.10: Deflection calculations of MS Excel

Bearing A		1. Area		2. Area		3. Area	
Definition	Dimesion	Definition	Dimesion	Definition	Dimesion	Definition	Dimesion
a(mm)	0	a(mm)	37,8	a(mm)	73	a(mm)	113
b(mm)	201	b(mm)	163,2	b(mm)	128	b(mm)	88
l(mm)	201	l(mm)	201	l(mm)	201	l(mm)	201
E(Gpa)	207	E(Gpa)	207	E(Gpa)	207	E(Gpa)	207
E(N/mm2)	207000	E(N/mm2)	207000	E(N/mm2)	207000	E(N/mm2)	207000
D(mm)	40	D(mm)	44,75	D(mm)	53,43	D(mm)	55
d(mm)	0	d(mm)	0	d(mm)	0	d(mm)	26
I (mm4)	125600	I (mm4)	196753,2128	I (mm4)	399843,8042	I (mm4)	426532,1541
M113 (Nmm)	0	M38 (Nmm)	260625,7982	M73 (Nmn	500675,8754	M113 (Nm	775018,8209
Deflection	Result	Deflection	Result	Deflection	Result	Deflection	Result
YAB(mm)	0,000	YAB(mm)	-0,013	YAB(mm)	-0,019	YAB(mm)	-0,029
YAB(μ)	0,000	YAB(μ)	-13,159	YAB(μ)	-18,841	YAB(μ)	-29,096
YBC(mm)	0,000	YBC(mm)	-0,013	YBC(mm)	-0,019	YBC(mm)	-0,029
YBC(μ)	0,000	YBC(μ)	-13,159	YBC(μ)	-18,841	YBC(μ)	-29,096
wi (kg)	0,296	wi (kg)	0,556	wi (kg)	0,529	wi (kg)	0,673
yi (mm)	0,000	yi (mm)	0,013	yi (mm)	0,019	yi (mm)	0,029
yi2 (mm2)	0,000000	yi2 (mm2)	0,000173	yi2 (mm2)	0,000355	yi2 (mm2)	0,000847
wi*yi	0	wi*yi	0,007316287	wi*yi	0,009966971	wi*yi	0,019581459
wi*yi2	0	wi*yi2	9,62735E-05	wi*yi2	0,000187789	wi*yi2	0,000569738

4. Area		5. Area		Bearing B	
Definition	Dimesion	Definition	Dimesion	Definition	Dimesion
a(mm)	128	a(mm)	140,5	a(mm)	201
b(mm)	73	b(mm)	69,5	b(mm)	0
l(mm)	201	l(mm)	210	l(mm)	201
E(Gpa)	207	E(Gpa)	207	E(Gpa)	207
E(N/mm2)	207000	E(N/mm2)	207000	E(N/mm2)	207000
D(mm)	60	D(mm)	55	D(mm)	40
d(mm)	28	d(mm)	26	d(mm)	28
I (mm4)	605693,44	I (mm4)	426532,1541	I (mm4)	95443,44
M128 (Nm	561347,46	M140,5 (N	469071,1795	M197,25 (Nmm)	0
Deflection	Result	Deflection	Result	Deflection	Result
YAB(mm)	-0,014	YAB(mm)	-0,017	YAB(mm)	0,000
YAB(μ)	-13,945	YAB(μ)	-17,292	YAB(μ)	0,000
YBC(mm)	-0,014	YBC(mm)	-0,017	YBC(mm)	0,000
YBC(μ)	-13,945	YBC(μ)	-17,292	YBC(μ)	0,000
wi (kg)	2,249	wi (kg)	0,346	wi (kg)	0,151
yi (mm)	0,014	yi (mm)	0,017	yi (mm)	0,000
yi2 (mm2)	0,000194	yi2 (mm2)	0,000299	yi2 (mm2)	0,000000
wi*yi	0,031362421	wi*yi	0,005983187	wi*yi	0
wi*yi2	0,000437351	wi*yi2	0,000103464	wi*yi2	0

If shaft deflections are calculated according to these values, In Figure 4.36 is obtained. Maximum deflection is 29 micrometer at center of gear at applying load point.

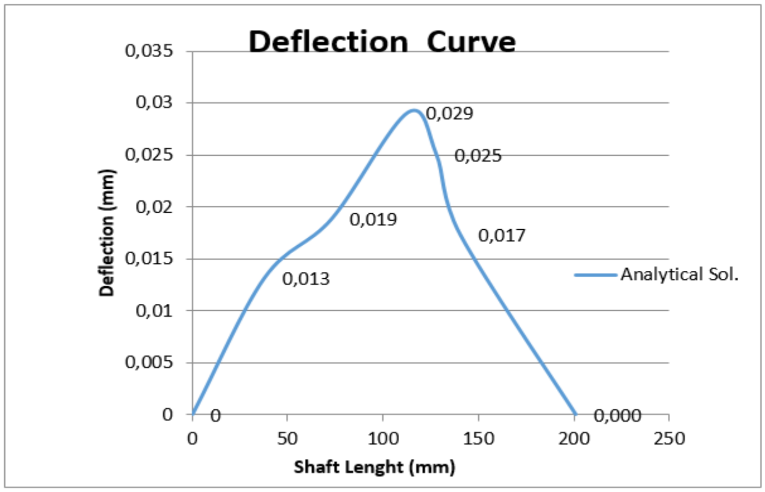

Figure 4.36: Deflection Curve of Analytical Solution

4.9.CRITICAL SPEED OF SHAFTS

It is necessary to explain some of the terms before critical speed of shaft. These terms are natural frequency and resonance. Natural frequency is a frequency that related to mass and elasticity of part and part gets damaged and continuously vibrated when it is warned at this frequency. Resonance is warn of parts with natural frequency or equivalent frequency.

Shafts deflect in the absence of external load when it rotates. Mass of a shaft can cause deflection at certain speeds that will create resonant vibration. This is Critical Speed.

Below equation is used for stepped shafts.

$$w_c = \sqrt{\frac{g * \sum w_i * Y_i}{\sum w_i * Y_i^2}} \tag{4.69}$$

Where is;

w_c = Critical speed

g = Gravity

w_i = Weight of the ith location

Y_i = Deflection at the ith body location

In this study, shaft can be defined as 5 areas not bearing areas and white areas as shown in Figure 4.29. Reason of this assuming of deflection as zero at bearing and white areas.

Firstly, mass of per areas is found or calculated. This can be in two ways. First, volume is calculated, then it is multiplied by the density of shaft.

$$\text{Mass}=\text{volume}*\text{density} \tag{4.70}$$

Others, material is applied to the shaft in a 3D cad program like Catia. After, mass of per area is read from software is illustrated in Figure 4.37.

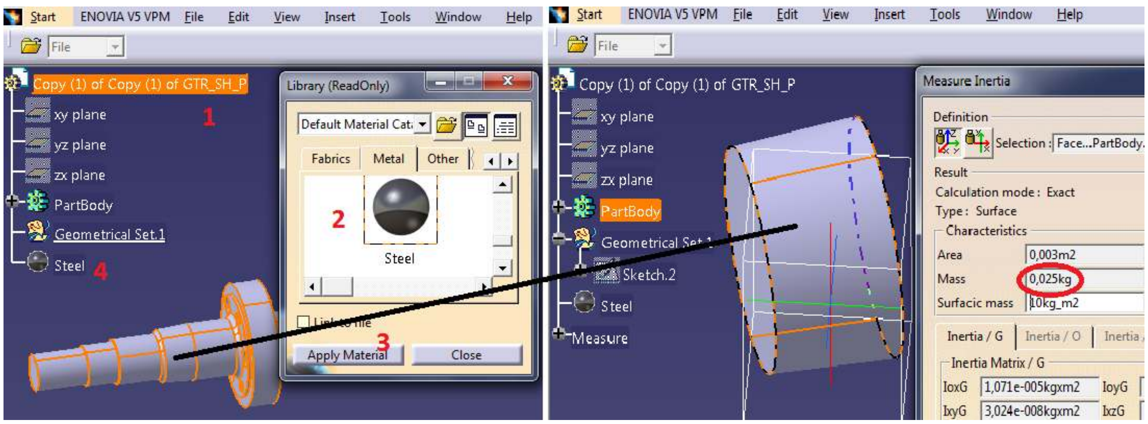

Figure 4.37: Mass calculation in Catia

These masses and calculated deflections in previous sections are added in excel and formulas are written in it. Then critical speed of shaft is calculated as 43326 rpm as shown in Figure 4.38.

Bearing A		1. Area		2. Area		3. Area		4. Area		5. Area		Bearing B	
Definition	Dimesion	Definition	Dimesion	Definition	Dimesion	Definition	Dimesion	Definition	Dimesion	Definition	Dimesion	Definition	Dimesion
a(mm)	0	a(mm)	37,8	a(mm)	73	a(mm)	113	a(mm)	128	a(mm)	140,5	a(mm)	201
b(mm)	201	b(mm)	163,2	b(mm)	128	b(mm)	88	b(mm)	73	b(mm)	69,5	b(mm)	0
l(mm)	201	l(mm)	201	l(mm)	201	l(mm)	201	l(mm)	201	l(mm)	210	l(mm)	201
E(Gpa)	207	E(Gpa)	207	E(Gpa)	207	E(Gpa)	207	E(Gpa)	207	E(Gpa)	207	E(Gpa)	207
E(N/mm2)	207000	E(N/mm2)	207000	E(N/mm2)	207000	E(N/mm2)	207000	E(N/mm2)	207000	E(N/mm2)	207000	E(N/mm2)	207000
D(mm)	40	D(mm)	44,75	D(mm)	53,43	D(mm)	55	D(mm)	60	D(mm)	55	D(mm)	40
d(mm)	0	d(mm)	0	d(mm)	0	d(mm)	26	d(mm)	28	d(mm)	26	d(mm)	28
I (mm4)	125600	I (mm4)	196753,2128	I (mm4)	399843,8042	I (mm4)	426532,1541	I (mm4)	605693,44	I (mm4)	426532,1541	I (mm4)	95443,44
M113 (Nmm)	0	M38 (Nmm)	260625,7982	M73 (Nmn	500675,8754	M113 (Nm	775018,8209	M128 (Nm	561347,46	M140,5 (N	469071,1795	M197,25 (Nmm)	0
Deflection	Result	Deflection	Result	Deflection	Result	Deflection	Result	Deflection	Result	Deflection	Result	Deflection	Result
YAB(mm)	0,000	YAB(mm)	-0,013	YAB(mm)	-0,019	YAB(mm)	-0,029	YAB(mm)	-0,014	YAB(mm)	-0,017	YAB(mm)	0,000
YAB(μ)	0,000	YAB(μ)	-13,159	YAB(μ)	-18,841	YAB(μ)	-29,096	YAB(μ)	-13,945	YAB(μ)	-17,292	YAB(μ)	0,000
YBC(mm)	0,000	YBC(mm)	-0,013	YBC(mm)	-0,019	YBC(mm)	-0,029	YBC(mm)	-0,014	YBC(mm)	-0,017	YBC(mm)	0,000
YBC(μ)	0,000	YBC(μ)	-13,159	YBC(μ)	-18,841	YBC(μ)	-29,096	YBC(μ)	-13,945	YBC(μ)	-17,292	YBC(μ)	0,000
wi (kg)	0,296	wi (kg)	0,556	wi (kg)	0,529	wi (kg)	0,673	wi (kg)	2,249	wi (kg)	0,346	wi (kg)	0,151
yi (mm)	0,000	yi (mm)	0,013	yi (mm)	0,019	yi (mm)	0,029	yi (mm)	0,014	yi (mm)	0,017	yi (mm)	0,000
yi2 (mm2)	0,000000	yi2 (mm2)	0,000173	yi2 (mm2)	0,000355	yi2 (mm2)	0,000847	yi2 (mm2)	0,000194	yi2 (mm2)	0,000299	yi2 (mm2)	0,000000
wi*yi	0	wi*yi	0,007316287	wi*yi	0,009966971	wi*yi	0,019581459	wi*yi	0,031362421	wi*yi	0,005983187	wi*yi	0
wi*yi2	0	wi*yi2	9,62735E-05	wi*yi2	0,000187789	wi*yi2	0,000569738	wi*yi2	0,000437351	wi*yi2	0,000103464	wi*yi2	0
Total wi*yi	0,074210325												
Total wi*yi2	0,001394615												
g(mm/s2)	9810												
wc (rad/sec)	4537,317169												
wc (rpm)	43326,84165												

Figure 4.38: Calculation of Critical Speed of Shaft in Excel

Practically, the maximum shaft speed should not exceed 75 percent of the critical speed is suggested. Test rig max speed is 6000 rpm and calculated critical speed is 39535 rpm.

Maximum operation speed = 43326 x 0.75

Maximum operation speed = 32494 rpm

Test rig max speed is very low from maximum operation speed. So there isn't any problem on the test rig about resonance.

4.10. BEARING SELECTION

In this test rig tapered roller bearings should be used due to radial loads and axial (thrust) loads or combination of radial & axial loads.

Tapered roller bearings can carry both

- Radial loads and
- Axial (thrust) loads or
- Combination of radial & axial loads

In relatively high capacities compared with other bearings.

4.10.1. Selection procedure for TIMKEN Tapered Roller Bearings

- Calculated radial loads at bearing points

These values were calculated in gear design sections as reaction forces illustrated in below Figure 4.17. This forces are A_y, A_z, B_y and B_z.

- Calculated thrust load (Te) and set the direction. Thrust load is equal axial load is calculated in gear design section.

  $\mathrm{T_e} = \mathrm{W_a}$
- Assume K value of nearly 1.5 for both bearing
- Calculate equivalent force at A point asF_{eA} andequivalent force at B point asF_{eB} values.

  $$\mathrm{F_{eA}} = 0.4\frac{\mathrm{F_{rA}}}{\mathrm{n}} + \mathrm{K_A}\left(\frac{0.47*\mathrm{F_{rB}}}{\mathrm{n}*\mathrm{K_B}} \pm \mathrm{T_e}\right) \tag{4.71}$$

  $$\mathrm{F_{eB}} = 0.4\frac{\mathrm{F_{rB}}}{\mathrm{n}} + \mathrm{K_B}\left(\frac{0.47*\mathrm{F_{rA}}}{\mathrm{n}*\mathrm{K_A}} \pm \mathrm{T_e}\right) \tag{4.72}$$

Where F_{rA} is combination of radial & axial loads at A point and F_{rB} is combination of radial & axial loads at B point. These values are written as;

$$F_{rA} = \sqrt{A_y^2 + A_z^2} \tag{4.73}$$

$$F_{rB} = \sqrt{B_y^2 + B_z^2} \tag{4.74}$$

If F_{eA} or $F_{eB} < F_{rA}$ or F_{rB} ; $F_{eA} = F_{rA}$ and $F_{eB} = F_{rB}$

- Use F_{eq} values in load-life along with L_d *and* n_d values (selection catalogue)

$$C_R = Feq * \left[\frac{L_d * n_d}{L_R * n_R}\right]^{1/a} \tag{4.75}$$

Where

L_d =design (required) life of bearing in hrs

n_d = design speed (in rpm) of the shaft

L_R (rating life) = 3000 hrs

n_R (rating speed) =500 rpm

F_{eq} =radial equivalent load to be carried

C_R= rating load for bearing

a=10/3

- Choose a bearing from catalogue bases both diameter and rating (C_R)

  $C_{Rat} > C_R$

- Use new correct K values of selected bearing (K_A , K_B) in step 4 to recalculated F_{eA} and F_{eB}
- Use the $F_{eq\,A,B}$ values in life equation to calculate the new life (with %90 relialibility)

$$L_D = L_R * \frac{n_R}{n_D} * \left(\frac{C_R}{F_{eqnew}}\right)^a_{A,B} \tag{4.76}$$

- Compare the new calculated life

  if $L_{Dnew} > L_D$ selection is 0k

  if $L_{Dnew} < L_D$ re − try a stranger bearing

Formula of Selection procedure for TIMKEN Tapered Roller Bearings section is added to excel software as shown in Figure 4.39. From Timken catalogue inner 420 –outer 414X tapered roller bearing is selected.

Definition	Normal Calculation	New Calculation
Ay(N)	3560	3560
Az(N)	5862,288557	5862,288557
By(N)	1570	1570
Bz(N)	7527,711443	7527,711443
FrA (N)	6858,573257	6858,573257
FrB (N)	7689,690473	7689,690473
Te=Wa (N)	4402	4402
KA	1,5	2,22
KB	1,5	2,22
FeA (N)	-245,4161748	-3414,856175
FeA real (N)	6858,573257	6858,573257
FeB (N)	12902,40562	16071,84562
FeB real (N)	12902,40562	16071,84562
LR (hour)	3000	3000
nR (rpm)	500	500
LD (hour)	3000	3000
nd (rpm)	5000	5000
a(10/3)	3,33	3,33
CRA (N)	13684,65276	
CRB (N)	25743,68371	
	CR(timken catologue)	30000
	Ldnew(hours)	4003,947242
	Bore d (mm)	40
		OK

Figure 4.39: Solution of Bearing Formulation in Excel

4.11. BOLT DESIGN

In this study gear is connected to the shaft with three bolts ant three pins as shown in Figure 4.40. Bolts carry the axial loads occurred from helical gear in this test rig. 10.9 grade M12 bolts was used.

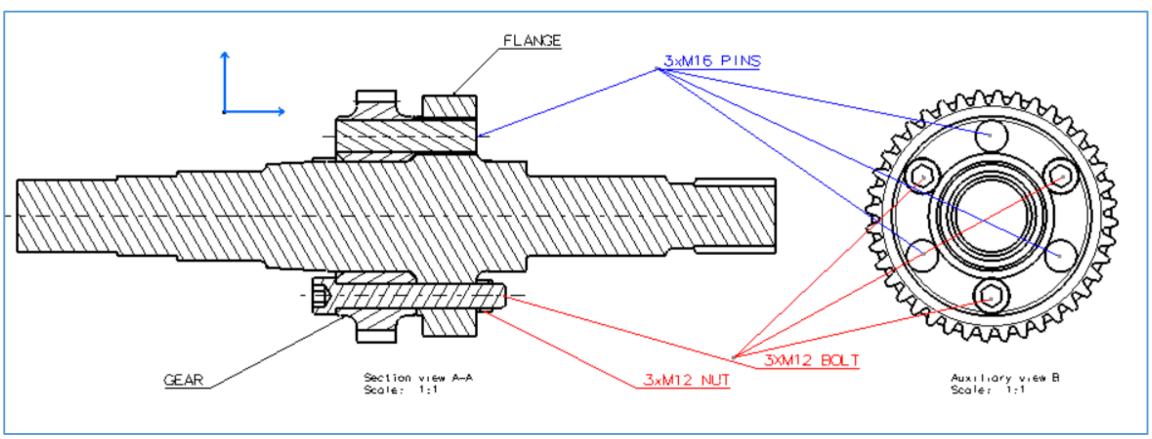

Figure 4.40: Bolts and Pins on the Shaft

Safety factor formula of bolts can be written as

$$n = \frac{[A_t * S_{ut} - F_i]}{\left[\frac{C * P_{max}}{2*(N)} * \left(\frac{S_{ut}}{S_e} + 1\right)\right]} \tag{4.77}$$

Where;

A_t=Tensile stress area

S_{ut}=Minimum tensile strength of bolt

F_i=Preload

P_{max}=Maximum external load

N=Number of bolt

S_e=Endurance strength

C=Stiffness constant of the joint

Tensile stress area and minimum tensile strength of bolt can be taken from literature. In practical application of preload can be used as,

$$0.5F_p \leq F_i \leq 0.9F_p \tag{4.78}$$

Where F_p is proof load and it is calculated as,

$$F_p = A_t * S_p \tag{4.79}$$

Where S_p is proof strength and it is taken from table 8.11 of Shigleys' Mechanical Engineering Book and A_t is taken from table 8.1;

A_t=84.3 mm^2

$S_p = 830$ MPa $\quad S_y = 940$ MPa $\quad S_{ut} = 1040$ MPa

F_p=69969 N

Assumed that

$F_i = 0.7F_p$

$F_i = 0.7 * 69969$

$F_i = 48978$ N

$F_{max} = F_i + C * P_{max}$

$F_{max} = 48978 + 0.09 * 4402$

$F_{max} = 49418.5$ N

$$F_{min} = F_i + C * P_{min}$$

$$F_{min} = 48978 \text{ N}$$

$$F_a = \frac{F_{max} - F_{min}}{2}$$

$$F_a = \frac{49418.5 \text{ N} - 48978 \text{ N}}{2}$$

$$F_a = 220 \text{ N}$$

$$F_m = \frac{F_{max} + F_{min}}{2}$$

$$F_m = \frac{49418.5 \text{ N} + 48978 \text{ N}}{2}$$

$$F_m = 49198.5 \text{ N}$$

Stiffness constant of the joint is written as,

$$C = \frac{k_b}{k_b + k_m} \tag{4.80}$$

Where k_b is the estimated effective stiffness of the bolt and k_m is member stiffness of bolt and estimated effective stiffness is calculated as,

$$k_b = \frac{A * E}{l} \tag{4.81}$$

$$k_b = \frac{\pi * 12^2 * 207000}{4 * 83} = 282062 \text{ N/mm}$$

Where E is Young’s modulus, l is total thickness of the parts which have been fastened together and A is major diameter area of bolt calculated as;

When half-apex angle is 30degree and diameter of the washer face is 1.5d, member stiffness is written as,

$$k_m = \frac{0.5774 * \pi * E * d}{2 * \ln\left(5 \frac{0.5774l + 0,5d}{0.5774l + 2,5d}\right)} \tag{4.82}$$

$$k_m = \frac{\pi * 207000 * 12}{2 * \ln\left(\frac{5 * (83 + 0.5 * 12)}{83 + 2.5 * 12}\right)}$$

$k_m = 2846645 \text{ N/mm}$

$$\mathbf{C} = \frac{k_\mathbf{b}}{k_\mathbf{b} + k_\mathbf{m}} = \frac{282062}{282062 + 2846645}$$

$\mathbf{C} = 0.09$

Maximum external load is taken from gear axial forces. Endurance strength is written as;

$S_e = k_e * S_e'$ (4.83)

$S_e' = 0.5 * S_{ut}$ (≤1400 MPa estimated Shigley's Equation 6-8) (4.84)

$S_e' = 0.5 * 1040$

$S_e' = 520 \text{ MPa}$

$k_e = \frac{1}{K_f}$ (4.85)

From Shigley's Table 8-6 $K_f = 3$

$k_e = \dfrac{1}{3} = 0.333$

$S_e = 0.333 * 520$

$S_e = 171 \text{ MPa}$

Where S_e' is endurance limit of rotating-beam specimen?

In this conditions for 3 bolt fatigue safety factor is calculated as n=83.7 and for one bolt fatigue safety factor is calculated as n=27.9

4.11.1. Static Factor of Safety of Bolt

Static Factor of Safety of Bolt formula is given as;

$n_{stc} = \frac{S_y}{\sigma_{bolt}}$ (4.86)

Where S_y is yield strength of bolt taken from table, σ_{bolt} is normal stress of bolt and it is calculated with below equation.

$\sigma_{bolt} = \frac{F_{bolt}}{A_t}$ (4.87)

Where F_{bolt} is resultant load on the bolt and it is equal to maximum resultant load on the bolt.

$$F_{bolt} = F_{max} \tag{4.88}$$

Maximum resultant load on the bolt is calculated in following equations.

$$F_{max} = F_i + C * P_{max} \tag{4.89}$$

$$\sigma_{bolt=} \frac{49418.5}{84.3} = 586.2\ N/mm^2$$

Static Factor of Safety of Bolt is found as 1.6 in this conditions.

$$n_{stc} = \frac{940}{586.2}$$

$$n_{stc} = 1.6$$

4.11.2. Stress in Threads

Safety factor of the threads on the screw is calculated as;

$$n = \frac{S_{sy}}{\tau_{th}}$$

Where S_{sy} is max shear stress and it is written as;

$$S_{sy} = 0.5 * S_y \tag{4.90}$$

τ_{th} is shear stress of the threads on the screw is calculated as;

$$\tau_{th} = \frac{2*F}{\pi * d_r * h} \tag{4.91}$$

Where;

d_r = minor diameter of the screw thread

h = the nut height

F = maximum resultant load

For M12 minor diameter of the screw thread and the nut height is taken from table;

$d_r = 9.853$ mm and $h = 10$ mm

Safety factor of the threads on the screw is calculated as 1.5

$n_{th} = 1.5$

Safety factor of the threads on the nut can be calculated as previous formulas. But minor diameter of the nut thread is taken as 12mm and safety factor is as 1.8.

$n_{nt} = 1.8$

Safety factor of average bearing stress on screw and nut threads is written as

$$n = \frac{S_{uc}}{\sigma_b} \tag{4.92}$$

Where;

$S_{uc} = compressivestrenght$

$\sigma_b = bearingstress$

Bearing stress formula as shown in below equation.

$$\sigma_b = \frac{4 * p * F}{\pi * h * (d^2 - d_r^2)} \tag{4.93}$$

Where

$p = pitch$

$d = majordiameterofscrewthread$

Safety factor is calculated as 5.17

$n_{br} = 5.17$

4.12. PIN JOINTS DESIGN

Pin is a cylindrical or conical machine element which connects the parts as removable. The task of the pin; to fix position of the components at same center, to connect them together and to carry and transmit the loads of components.

On the test rig, there are three pin joints. One of them, connecting gear to shaft, second, connecting couplings together, third connecting torque loading mechanism together. They are illustrated in Figure 4.41.

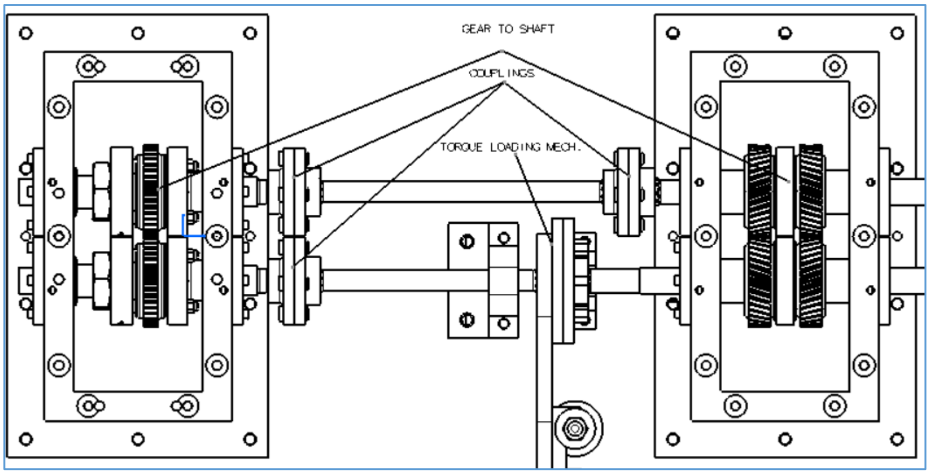

Figure 4.41: Pin Joints on the Test Rig.

4.12.1. Pin Joint of Gear to Shaft

Three M16 pins were used to connect gear to the shaft as shown in Figure 4.42. Two shear forces occurred from gear forces effect these pins.

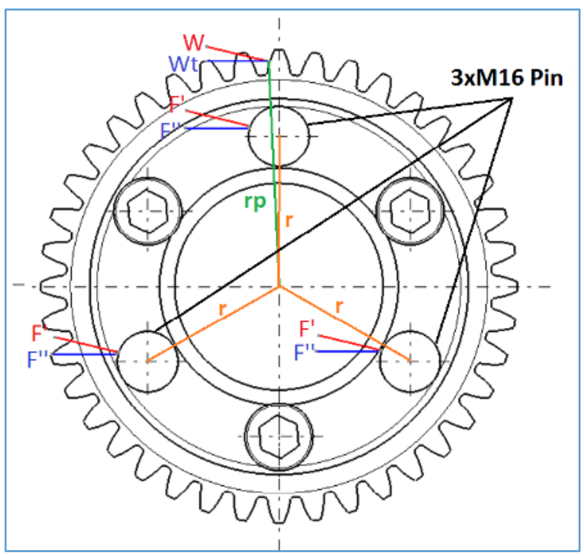

Figure 4.42: Pin Joints of Gear

Safety factor of these pins is calculated in below equation.

$$n = \frac{0.5 * S_y}{\tau} \tag{4.94}$$

Where Sy is? Yield strength of pin material as "4140 steel" and its yield strength is 880MPa (AFTER HEAT TREATMENT), τ is shear stress and it can be written as;

$$\tau = 1.5 \frac{F_A}{A_p} \tag{4.95}$$

Where A_p is pin section area, F_A is equivalence force of pin shear forces and they are calculated as;

$$A_p = \pi * r^2 \tag{4.96}$$

$$F_A = F'^2 + F''^2 - 2 * F' * F'' * \cos\theta \text{ (Cosines theory Figure 4.43)} \tag{4.97}$$

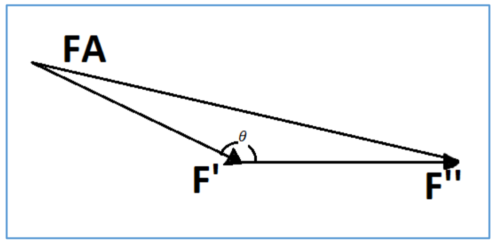

Figure 4.43: Cosines Theory for Pins

According to equivalence force formula,

F'=Primary shear and it is written as;

$$F' = \frac{W}{n} \tag{4.98}$$

W=tooth forces and n=number of pins

F''=Secondary shear or moment load it is written as;

$$F'' = \frac{M*r}{3*r^2} \tag{4.99}$$

M=Resultant moment on the centroid and r=Radial distance from the centroid to the center pin. Resultant moment on the centroid is calculated as;

$$M = W_t * r_p \tag{4.100}$$

$W_{t.}$ =Tangential force of gear and r_p=pitch radius of gear

In these conditions for one pin safety factor is calculated as 1.7 and for three pins safety factor is calculated as 5.07

4.12.2. Pin Joint of Couplings

Four M18 pins were used to connect couplings together as shown in Figure 4.44. One shear forces occurred from system torque effect these pins.

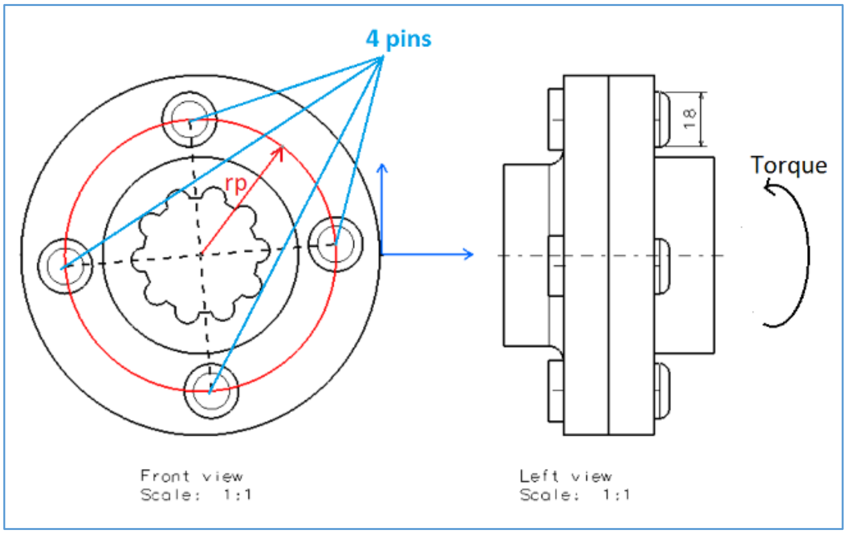

Figure 4.44: Pin Joints of Couplings

Safety factor of these pins is calculated in below equation.

$$n = \frac{0.5 * S_y}{\tau} \quad (4.101)$$

Where S_y is yield strength of pin material as "4140 steel" and its yield strength is 880 MPa, τ is shear stress and it can be written as;

$$\tau = 1.5 \frac{F}{A_p} \quad (4.102)$$

Where A_p is pin section area, F is shear force of pin and they are calculated as;

$$A_p = \pi * r^2 \quad (4.103)$$

$$F = \frac{T * r_p}{4 * r_p{}^2} \quad (4.104)$$

Where T is system torque and r_p is radial distance from the centroid to the center pin. In these conditions for one pin safety factor is calculated as 4.17 and for four pins safety factor is calculated as 16.7

4.12.3. Pin Joint of Torque Loading Mechanism

Two M12 pins were used to connect couplings together as shown in Figure 4.45. One shear forces occurred from system torque effect these pins.

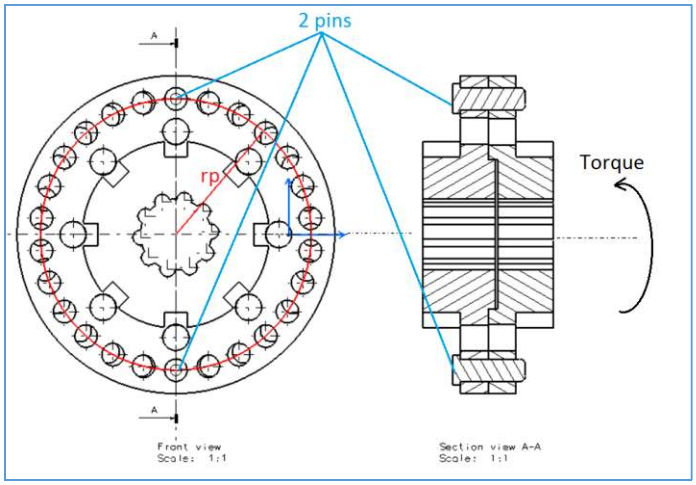

Figure 4.45: Pin Joints of Torque Loading Mechanism

Safety factor of these pins is calculated in below equation.

$$n = \frac{0.5 * S_y}{\tau} \tag{4.105}$$

Where Sy is yield strength of pin material as "4140 steel" and its yield strength is 880MPa, τ is shear stress and it can be written as;

$$\tau = 1.5 \frac{F}{A_p} \tag{4.106}$$

Where A_p is pin section area, F is shear force of pin and they are calculated as;

$$A_p = \pi * r^2 \tag{4.107}$$

$$F = \frac{T * r_p}{2 * {r_p}^2} \tag{4.108}$$

Where T is system torque and r_p is radial distance from the centroid to the center pin

In these conditions for one pin safety factor is calculated as 2.99 and for two pins safety factor is calculated as 5.9. In addition linear static analysis of torque loading coupling is tested with FEM in Appendix C and Von Misses Stress is controlled.

4.13. DESIGN OF TORSION RODS

A torsion rod is a flexible spring that can be elastically deformed about its axis via twisting. Torsion rods are designed to hold required torque to twist the spring according to the angle of the twist.

A torsion rod works by resisting the torque placed on it. One end of the torsion bar is fixed and the other side is twisted via moment, thus causing torque to build up. When this happens, the torsion rod is resistant to the torque and will quickly go back to its starting position once the torque is removed.

On the test rig two torsion rods have been used as shown in Figure 4.46.These torsion rods are analyzed with FEM in Appendix C. In analysis, rods are fully fixed from one side of coupling connecting and torque applied from other side of rod. Von misses stress is observed at the end of analysis.

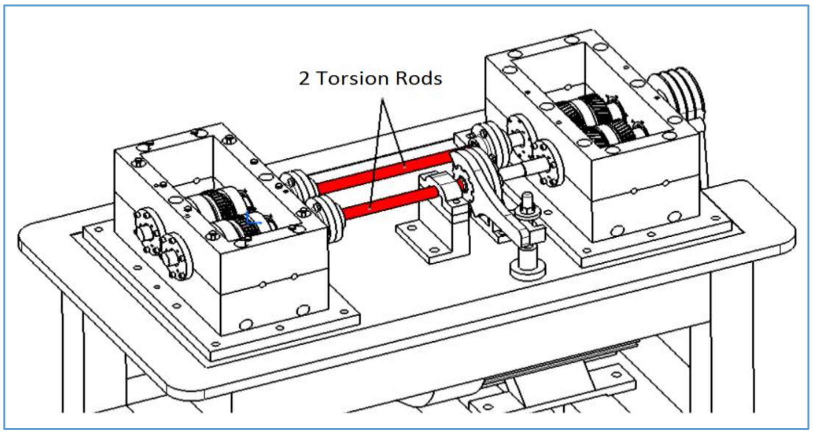

Figure 4.46: Torsional Rods

The angle of the twist formula of torsion rod is written as;

$$\emptyset = \frac{T*L}{J*G} \tag{4.109}$$

Where;

$\emptyset$=Angle of Twist

J=Polar area moment of inertia

T=Torque

G=Modulus of rigidity

L=Length of torsion rod (Figure 4.47)

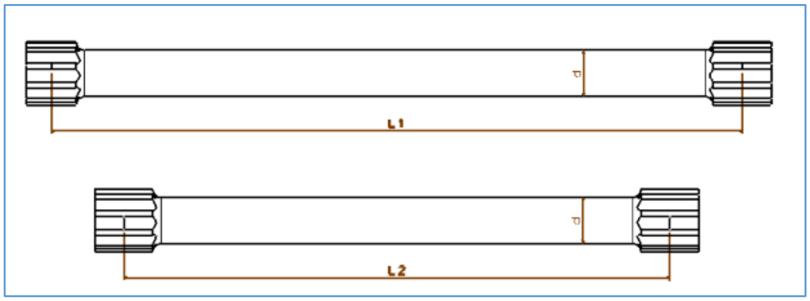

Figure 4.47: Sizes of Torsional Rods

Below equation can be used for torque;

$$T = \frac{J * \tau_{nominal}}{r} \tag{4.110}$$

Where;

r=Radius of the outer surface of torsion rods

$\tau_{nominal}$=Nominal shear stress

Polar area moment of inertia for circular section is;

$$J = \frac{\pi * d^4}{32} \tag{4.111}$$

$$J = \frac{\pi * 28^4}{32}$$

J= 60313.12 mm^4

Where d (28 mm) is radius of the outer surface of torsion rods.

Nominal shear stress is written as;

$$\tau_{nominal} = \frac{\tau_{max}}{n} \tag{4.112}$$

$$\tau_{nominal} = \frac{880}{2} = 440 \text{ N/mm2}$$

$$T = \frac{60313.12 \ * 440}{14} = 1895555.2 \text{ Nmm}$$

Where

n=Safety factor and τ_{max}= S_y (yield strength of material)

Length of torsion rod is total length of two rods and it is;

$$L=L1+L2 \tag{4.113}$$

L=417.5+330=747.5 mm

Modulus of rigidity is calculated as;

$$G=\frac{E}{2*(1+v)} \tag{4.114}$$

G=79 GPa

Where E is young's modulus and v is poison ratio. They are based on rod material. Rod material is 4140 steel and E=205 GPa, v=0.3, Sy=880 N/mm^2

If safety factor is assumed as 2, angle of twist is calculated as 0.5959 rad.

Radians to degree conversion is;

$$0.5959 * \frac{360}{2\pi} = 34°$$

Torque loading mechanism is illustrated in Figure 4.48. System is fixed via fixed part from right coupling and then torque is applied via arm from left coupling.

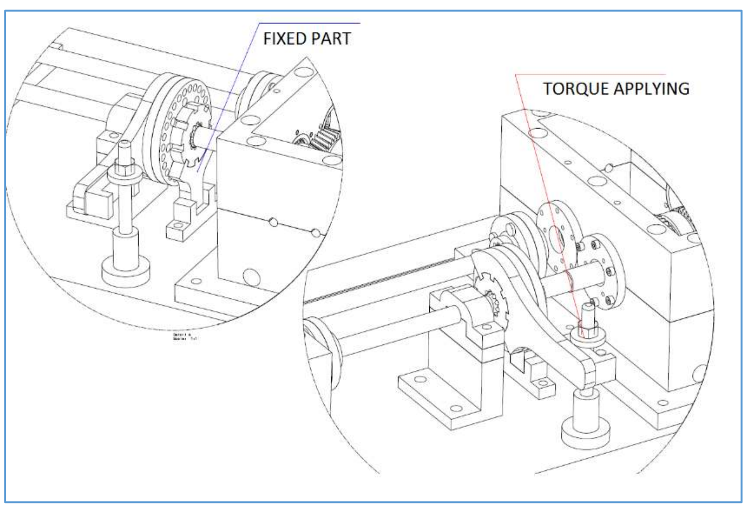

Figure 4.48: Torque Loading Mechanism

Right and left torque couplings as shown in Figure 4.49. Left coupling has 24 pin holes and right coupling has 26 pin holes. Angle between per pin holes of left coupling according to center axis is α_1 and angle between per pin holes of right coupling according to center axis is α_2.

And they are calculated as;

$$\alpha_1 = \frac{360}{24(\text{holes})} = 15° \text{ and } \alpha_2 = \frac{360}{26(\text{holes})} = 13.8°$$

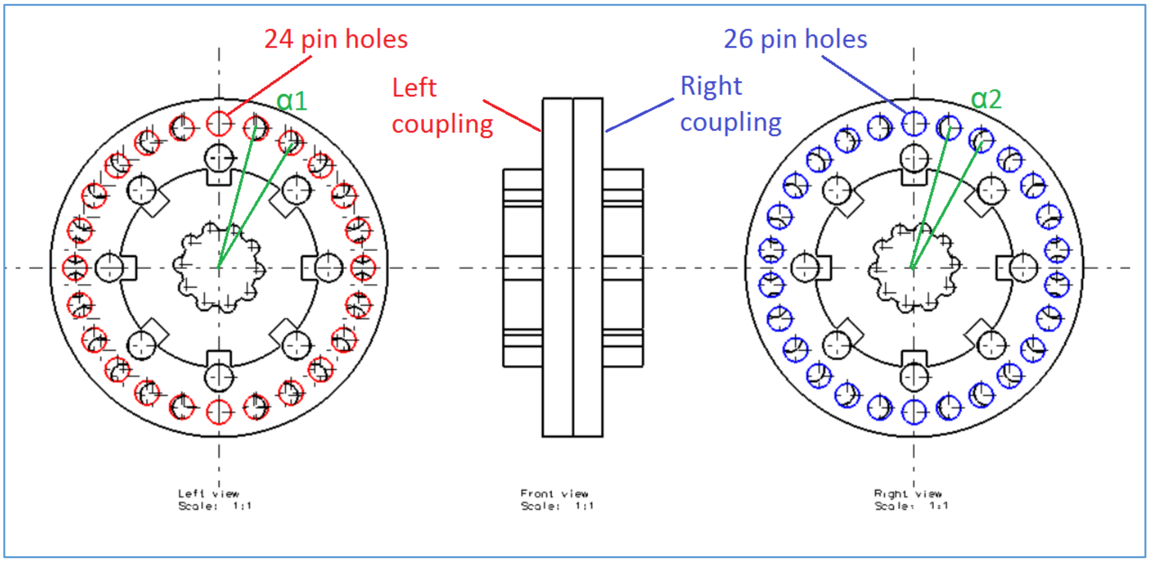

Figure 4.49: Right and left torque couplings of Torque Loading Mechanism

Angle between α_1 and α_2 is;

$$\alpha = \alpha_1 - \alpha_2 \tag{4.115}$$

$$\alpha = 15° - 13.8°$$

$$\alpha = 1.2° = 0.02 \text{ rad}$$

Per 0.02 rad twist of rod is equal a torque value. This value can be calculated as below equation;

$$\emptyset = \frac{T * L}{J * G}$$

And if this equation is arranged as;

$$T = \frac{\emptyset * \mathbf{J} * \mathbf{G}}{\mathbf{L}} \tag{4.116}$$

Per 0.02 rad twist of rod is equal to 128 Nm

4.14. TOOTH FORCE IN A GEAR PAIR

Tooth force is 500 N/mm and Face width= 30mm so the maximum torque of torsion rod is calculated 803400 Nmm (equation 5.11) but is seemed that applicable gear tooth load is 1128N/mm with 30 mm face width for maximum applicable torque is $1.9*10^6$Nmm.

$$\text{Gear tooth load(N/mm)} = \frac{\text{T(Nmm)}}{\text{Gear Facewidth(mm)}*\text{dp}} \qquad (4.117)$$

$d_p=(d-(2*1.25*mn))$ (4.118)

$d_p=(120-(2*1.25*3))$

$d_p=56$ mm

$$\text{Gear tooth load(N/mm)} = \frac{1.9 * 10^6 \text{ Nmm}}{30(\text{mm}) * 56(\text{mm})}$$

$$\text{Gear tooth load(N/mm)} = 1128 \text{ N/mm}$$

4.15. MOTOR SELECTION

Relation between system torque and motor power can be written as;

$$T = 9550 * \frac{P}{n} \qquad (4.119)$$

Where

$T = \text{Torque (Nm)}$

$P = \text{Power (kW)}$

$n = \text{speed (rpm)}$

And this equation is arranged as;

$$P = \frac{T*n}{9550} \qquad (4.120)$$

In this study system torque is calculated as 800 Nm and speed is considered as 5000rpm. So motor power is defined as 420 kW. But at back to back test rig, motor is only compensated system power losses. If these losses is assumed as %10, the required engine power is calculated as 42 kW.

$$P_r = P * \text{system power losses} \qquad (4.121)$$

$$P_r = P * \frac{10}{100} \qquad (4.122)$$

4.16. BELT AND PULLEY SELECTION

Placing of belt and pulley on the test rig is illustrated in Figure 4.50. In previous section, motor power is defined 42 kW and its speed is 3000 rpm from motor catalogue. So small diameter of pulley is 100 mm and large diameter of pulley is 200 mm. Center distance of pulleys is 500 mm.

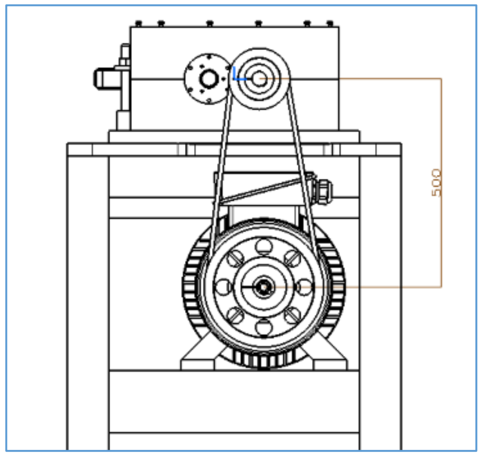

Figure 4.50: Placing of belt and pulley on the test rig

Belt and pulley selection is made using Opti belt software as shown in Figure 4.51. Inputs of this software are drive power, type of driver unit and driven unit, driver and driven speed, center distance and service factor.

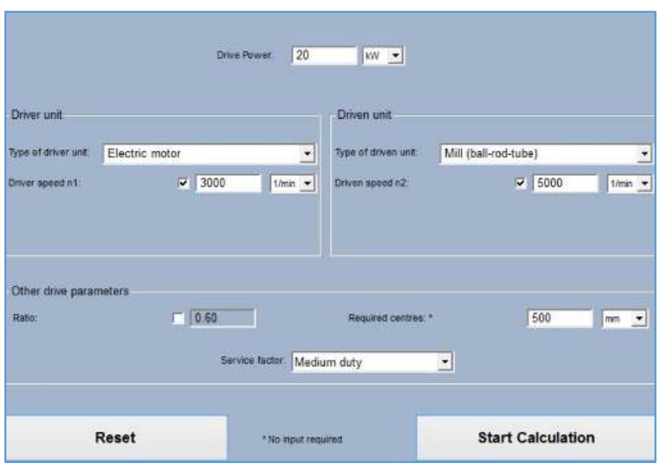

Figure 4.51: Main Page of Opti Belt

After calculation drive requires window is opened. In this window which belt, pulley, bushes can be used and which needed tension recommendation are defined as shown in Figure 4.52.

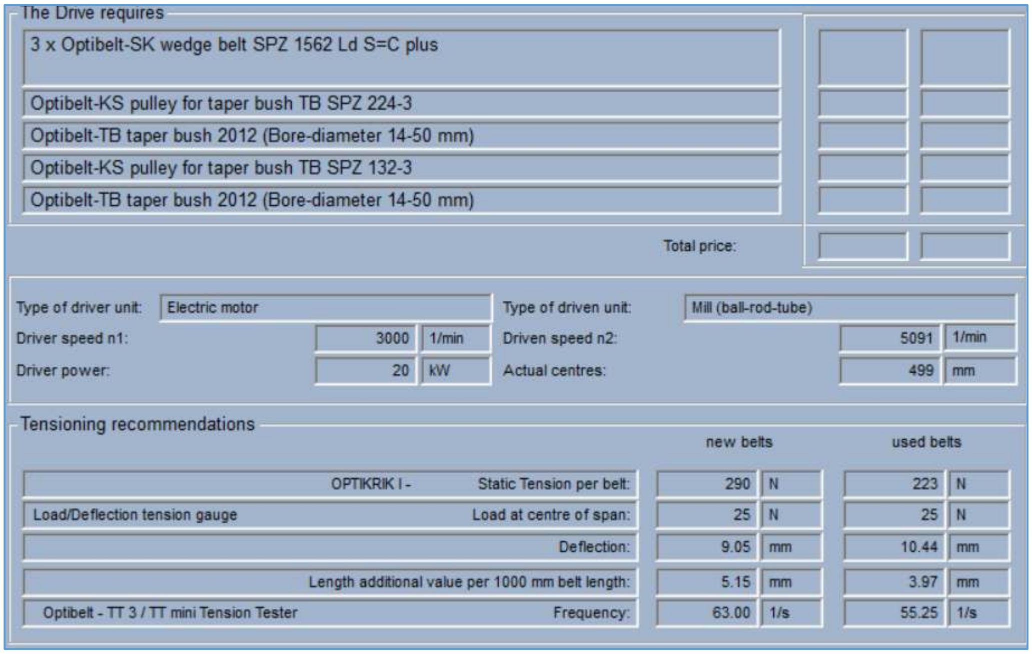

Figure 4.52: Drive requires

Outputs of parameters can be shown in Detail tab as Figure 4.53.

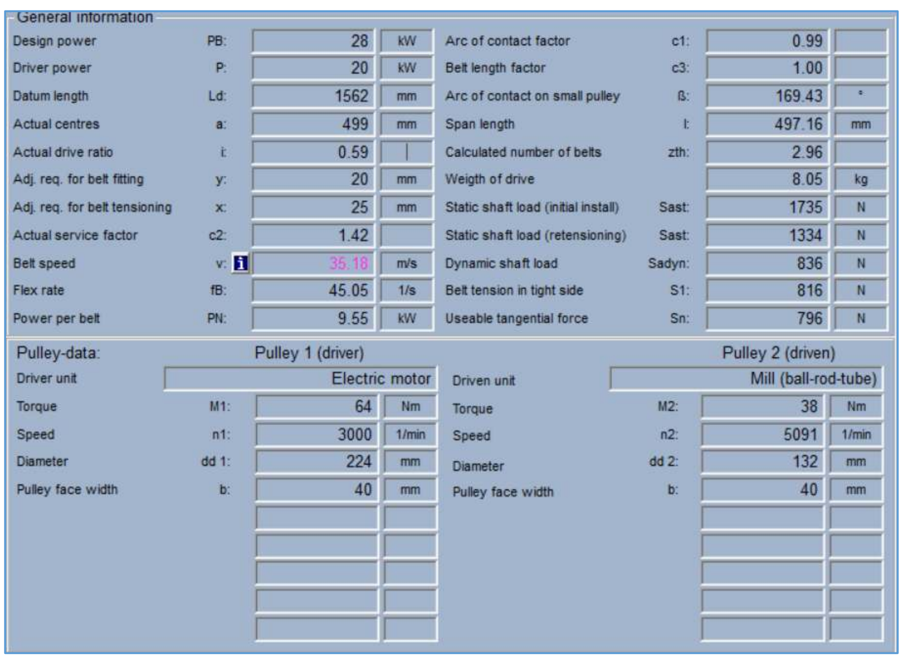

Figure 4.53: Outputs of parameters of belt-pulley

Result list is shown in Figure 4.54.

General view | Details | result list

N..	Section	Length [mm]	z	d1 [mm]	d2 [mm]	a [mm]	n2eff [1/min]	v [m/s]	c2 real.	Sa stat. [N]	Price [€]
1	SK-SPZ	1487	4	200	100	505	6000	31.41	1.43	1465	---
2	SK-SPZ	1600	3	250	125	502	6000	39.27	1.37	1375	---
3	SK-SPZ	1437	5	180	90	504	6000	28.27	1.52	1574	---
4	SK-SPZ	1662	3	280	140	496	6000	43.98	1.48	1458	---
5	SK-SPZ	1537	4	224	112	501	6000	35.18	1.64	1506	---
6	SK-SPA	1600	3	250	125	502	6000	39.27	1.42	1834	---
7	SK-SPZ	1400	5	170	85	498	6000	26.70	1.38	1573	---
8	SK-SPZ	1762	3	315	160	502	5906	49.48	1.55	1597	---
9	SK-SPZ	1462	5	190	95	505	6000	29.84	1.66	1584	---
10	SK-SPA	1507	4	212	106	501	6000	33.30	1.45	1922	---
11	SK-SPA	1682	3	280	140	506	6000	43.98	1.59	2033	---
12	SK-SPA	1532	4	224	112	499	6000	35.18	1.61	1998	---
13	SK-SPA	1482	5	200	100	503	6000	31.41	1.59	2093	---
14	SK-SPA	1557	4	236	118	497	6000	37.07	1.75	2085	---
15	SK-SPA	1757	3	315	160	499	5906	49.48	1.70	2322	---

Figure 4.54: Result List of Belt-Pulley

4.17. LUBRICATION SYSTEM DESIGN

On the test rig, there are two parts for lubricating. These are gears and tapered roller bearings. For gear, oil should be preferred for lubrication. Tapered roller bearings are generally lubricated with grease. But, for many critical tapered roller bearing applications (heavy duty), a common oil circulation system need to be lubricated with oil. So for tapered roller bearing, lubricant type should be selected.

4.17.1. Selection between Grease and Oil for Lubrication for Bearings

Table 4.11 Provides the guidelines for selection between grease or oil as the lubricant.

Bearing type	Bearing D_i mm	Limit of DmN factor for grease lub.
Ball & cyl. Roller, needle roller brgs. Without inner race	Up to 50	350,000
	Over 50	$350,000/(D_i/50)^{0.5}$
Tapered & spherical roller, needle roller with inner race	Up to 50	175,000
	Over 50	$175,000/(D_i/50)^{0.5}$
Full complement cyl. Roller brg, multi row Tapered roller and cyl. Bearing, thrust bearing	Up to 50	120,000
	Over 50	$120,000/(D_i/50)^{0.5}$

In table 4.11:

D_i = Inner diameter of the bearing (mm)

D_o = Outer diameter of the bearing (mm)

$D_m = (D_i+D_o)/2$

N = RPM of the bearing

If the DmN factor is more than that indicated in Table 4.11, oil should be used for the lubrication of the bearing.

Our selected tapered roller bearing parameters are;

D_i: 40mm
D_o: 75mm
N: 6000rpm
D_m= (40+75)/2=57.5 mm
DmN=57. 5*6000=345000
Due to D_i=40 mm, according to table DmN=175,000/ (D_i/50)0.5
DmN=156524
Our calculated DmN factor (345000) is more than that indicated in Table 4.11 (156524). So oil should be used for the lubrication.

4.17.2. Selection of Oil Viscosity for Antifriction Bearings

Viscosity at working temperature (cSt) = k*14.8936*(Max. catalogue speed /Actual speed)^{0,7}

The value of k should be taken from Table 4.12.

Table 4.12 Provides the guidelines for selection between grease or oil as the lubricant.

Bearing operating condition	**Factor k**
Normal operation, bearing equivalent load less than 18% of the C-Rating	1.00
Normal operation, bearing equivalent load equal to or more than 18% of the C-Rating (heavily loaded bearing)	1.50
Shock and vibration, bearing load less than 18% of the C-Rating	1.50
Shock and vibration, bearing load equal to or more than 18% of the C-Rating	1.75
Very low speed (less than or equal to 10% of the maximum catalogue speed for oil lubrication)	2.00

Max. Catalogue speed is 9000 rpm for bearing

Actual speed is 6000 rpm

Viscosity at working temperature = k*14.8936*(Max. catalogue speed /Actual speed)^{0,7}

Viscosity at working temperature =1.5*14.8936*(9000/6000)$^{0.7}$

Viscosity at working temperature =29.6 cSt

4.17.3. Estimation of Required Flow Rate of Bearings

For spherical roller, angular contact, taper roller and thrust roller bearings:

Oil flow rate, q (litre per minute) = Antilog ((2*log D_o) – 3.602)

q= Antilog ((2*log 75) – 3.602)=1.4 lt/min.

For 8 bearings, 1.4*8=11.2 lt/min.

4.17.4. Selection of Lubricant Viscosity of Gears

The pitch line velocity of the gears is a good index of the required viscosity. The following empirical relation is used to determine the required viscosity:

Viscosity at 40^0 C (cSt) = 498.92/$V^{0.5}$, where V=pitch line velocity of gear or pinion in m/s.

V= (π*d*n)/60

n: speed of gear (rpm)

d: pitch diameter of gear (m)

V= (π*0. 12*6000)/60

V=37.6 m/s

Table 4.13 Application of lubricant to gear train

Pitch line velocity (m/s)	**Method of application**	**Remarks**
Up to 16	Splash lubrication	Gear to dip in oil up to twice the tooth depth
More than 16 up to 26	Splash lubrication	Use baffles and oil pans to reduce churning
More than 26 up to 36	Pressure fed	Oil jets before the mesh approach
More than 36 upto 72	Pressure fed	Oil jets after the gears leave the mesh
More than 72	Pressure fed	Oil jets at both sides of the mesh, 2/3 rd of oil to be supplied to the outgoing side and 1/3 rd to the incoming side.

Viscosity at 40^0 C (cSt) = $498.92/V^{0.5}$

Viscosity at 40^0 C =$498.92/37.6^{0.5}$

Viscosity at 40^0 C=91.36 CSt

4.17.5. Lubricant Flow Rate of Gears

The following empirical relation gives the required flow rate of lubricant to the gear train:

q = pxc (litre/min) where p = transmitted power (kW), c is the factor given in Table 4.13

p=420 kW

c=0.0250

q=420*0.0250

q=10.5 lt/min.

For two gearbox= 2*10.5=21 lt/min

Table 4.14 Factor c

Application	lpm per kW	Flow condition
Heavy duty	0.0250	Copious
Moderate duty	0.0170	Adequate
Light duty	0.0125	Boundary lubrication

Total Flow rate of both gear and Bearing

$Q_t = q_b + q_g$

$Q_t = 11.2 + 21 = 32.2$ lt/min

Pomp and Motor Selection for Lubrication

For 32.2 lt/min flow rate, 1.1 kW 20cc hydraulic pomp with electric motor is selected.

For Lubricant oil SAE 80 oil is selected (Figure 4.55).

SAE Viscosity Grade		80	90	140	MB 80
Density, @ 15°C g/ml	ASTM 4052	0,888	0,896	0,907	0,890
Flash Point COC, °C	ASTM D 92	228	230	258	238
Kinematic Viscosity 40°C mm²/s 100°C mm²/s	ASTM D 445	85,22 10,14	163,56 15,42	398,8 27,21	112,1, 12,18
Viscosity Index	ASTM D 2270	99	95	93	98
Pour Point, °C	ASTM D 97	-30	-21	-9	-27

Figure 4.55: Typical specifications of Oil

Oil capacity

For 32.2 lt/min flow rate,

32.2*3=96.6 lt/dk capacity reservoir oil tank is designed.

4.17.6. Design of Forced Lubrication System

Designed lubrication system is illustrated in Figure 4.56.

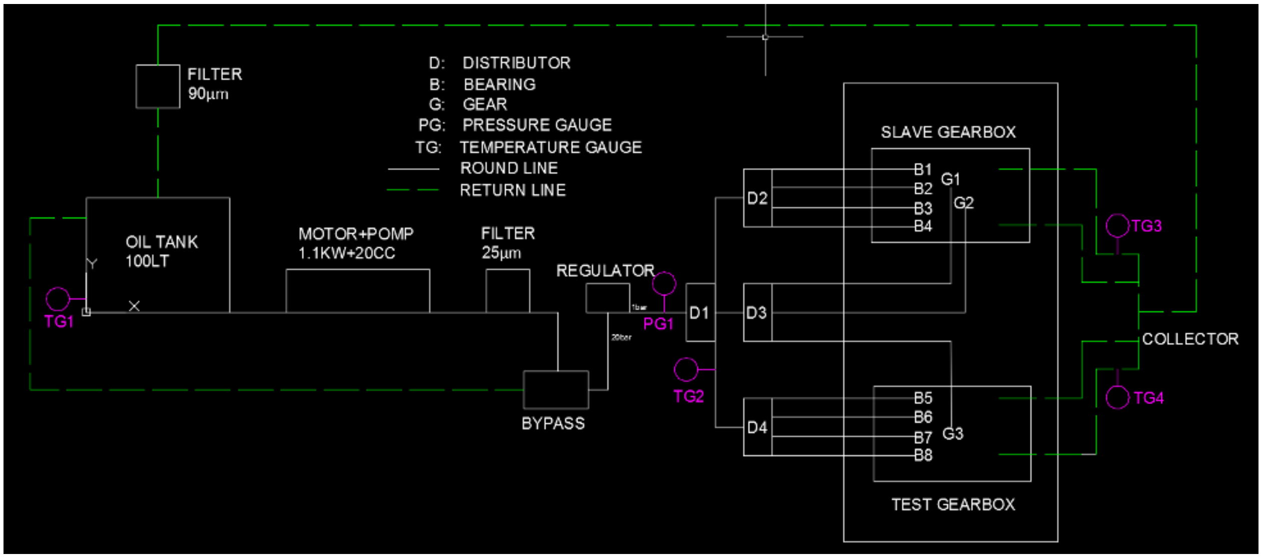

Figure 4.56: Lubrication System of Test Rig

4.18. IMPORTANT POINTS FOR TEST RIG DESIGN

4.18.1 Misalignment of Shafts or Center Distance of Gears

A designer designs a test rig correctly as 3D model. Measurements, distance, diameter, thickness and the other sizes can be correct. In short, everything okay in a virtual environment. But during production something can be wrong. For example, as below figure 4.57 center distance of gears or shaft is 120 mm.

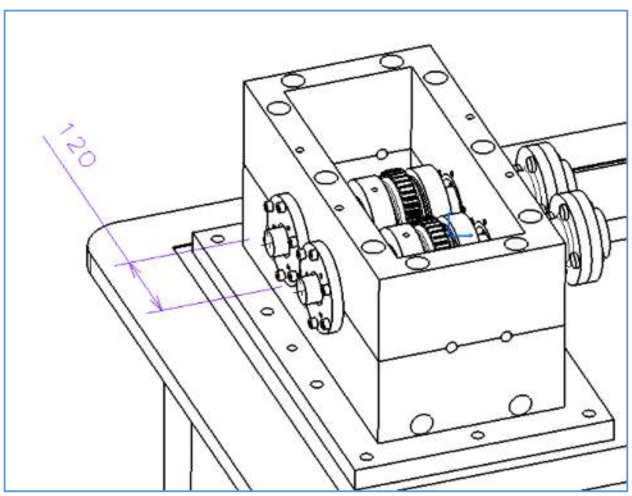

Figure 4.57: Center Distance of Gears

After production this distance can be measured as 119.5 mm or 120.5 mm or other measures not 120 mm. It is illustrated in Figure 4.58.

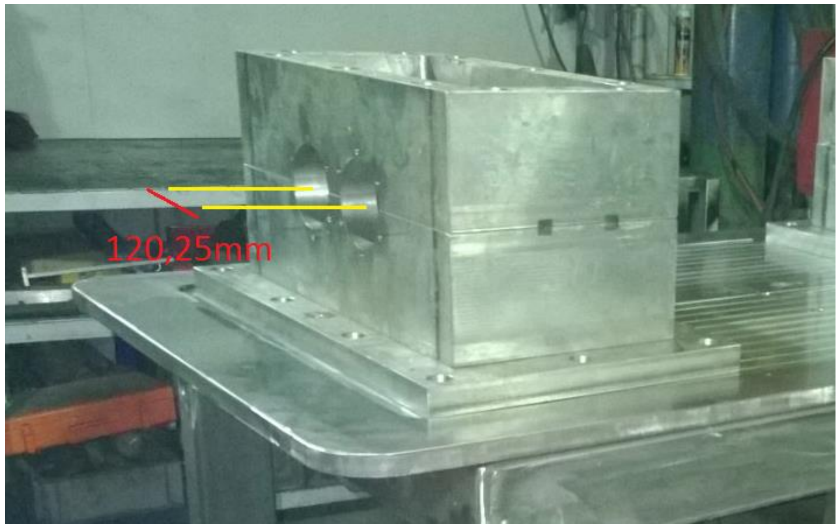

Figure 4.58: Center Distance of Gears after Production

Designers have to think this error or similar. It is very important detail for design. Otherwise this gearbox or error parts may be waste. Time, labor and cost may be loss. How does this error compensate? Simply, outer face diameter of housing and gearbox hole of housing are concentric. But outer face diameter of housing and inner face diameter of housing which are mounted bearing aren't concentric. Centers should be different from center within permitted tolerance.

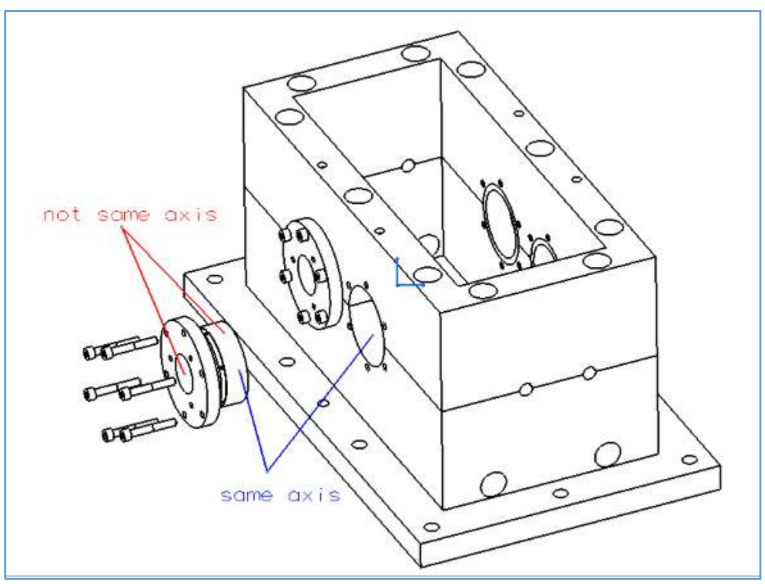

Figure 4.59: Concentric between Housing and Gearbox

This nonconcentric housing is illustrated in Figure 4.60. Different of housing's inner and outer diameter is 0.25 mm.

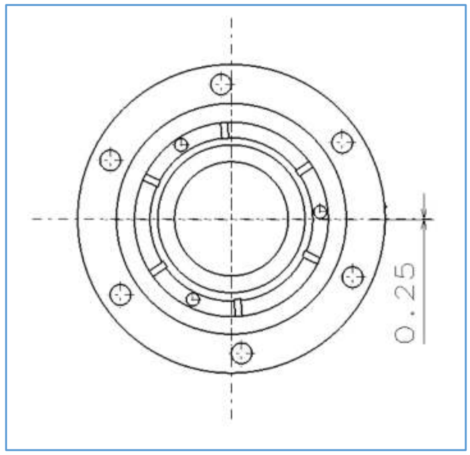

Figure 4.60: Concentric on Housing

On the contrary, non-concentric housing are used to create deliberate assembly error in center distance to study effect of manufacturing error on performance of gears. Following picture shows how it is created deliberate assembly error.

In first position center distance is 120 mm. If only right housing is rotated 90degree clockwise direction, center distance is 120.25 mm in 2.position.If right housing is rotated 90degree clockwise direction and left housing is rotated 90 degree anticlockwise direction. Center distance is 120.5 mm in 3.position.If right housing is rotated 90degree anticlockwise direction and left housing is rotated 90degree clockwise direction, center distance is 119.5 mm in 4.position (Figure 4.61).

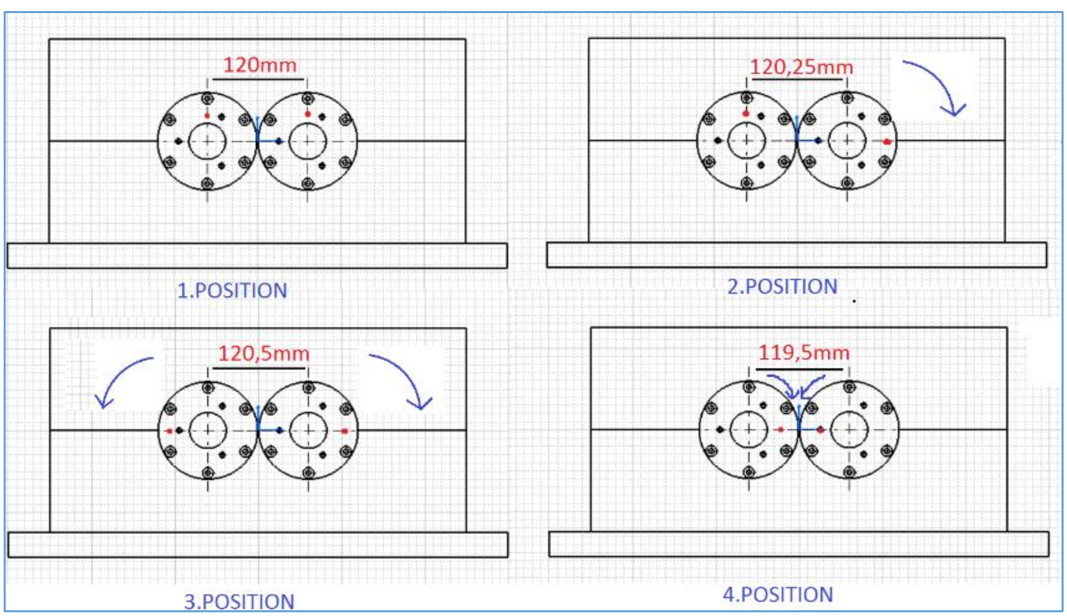

Figure 4.61: Position Center Distance Depend On Housing

Aligning of the bolted parts in assembly

Generally dimensional deviations are inevitable at connection of the bolted parts in assembly. Reason of this tip diameter of bolts and connection hole diameter are not same. There are dimensional differences between the two because of easy installation. For example for M18 bolt, hole may be 18.5 mm. So precision assembly is trouble for these connection.

In these types of connections, guide pins are often used. Typically, the guide pin can be used for positioning the die with a controlled and precise tolerance of the work piece. For instance there is a part and work in a sensitive axis of it is expected. The best solution is guide pin.

In this study as shown in Figure 4.62, especially guide pins is used between gearbox and base plate.

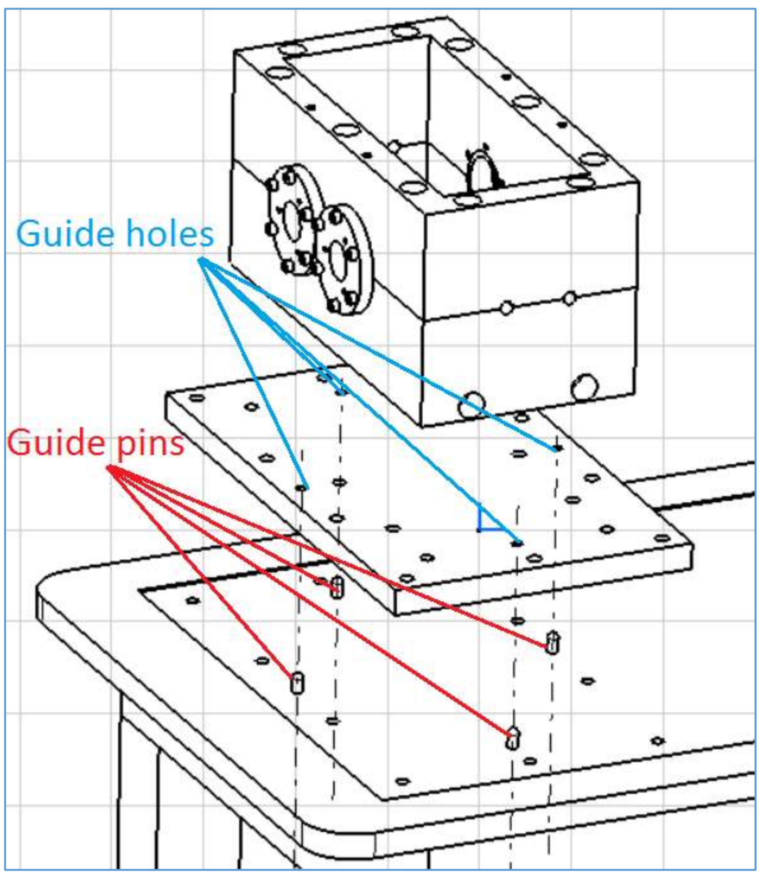

Figure 4.62: Guide Pins between Gearbox and Base plate

Other, guide pin should be between parts of gearbox. It is illustrated in Figure 4.63.

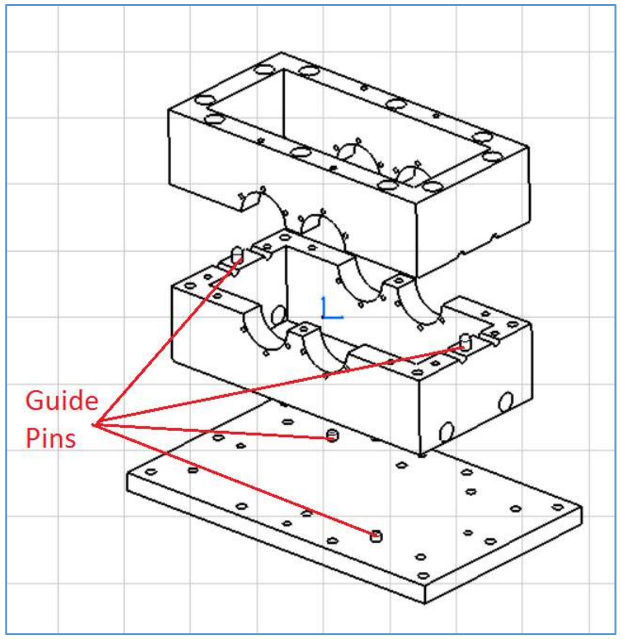

Figure 4.63: Guide Pins between Parts of Gearbox

Aligning of couplings and similar parts

Couplings are connection parts to transport power and motion. Especially alignment of rigid coupling couple is difficult not to guide. So normally one side of coupling couple is removed the extent of tolerance at the central axis direction. Other side is extruded the extent of tolerance at the central axis direction. This operation is as shown in figure 4.64.

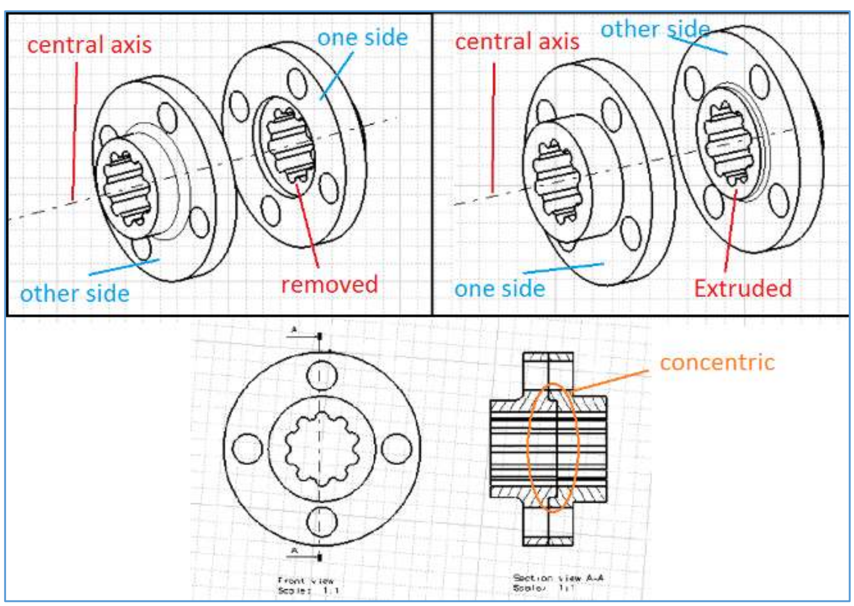

Figure 4.64: Aligning of Couplings

CHAPTER 5

MANUFACTURING PROCESS

5.1.GENERAL INFORMATION

The manufacturing industry has a very important place. Many machine parts are made and shaped by casting, removing chips or without removing chips of semi-finished with machine tools. Machine tools in machine manufacturing industry at design and manufacturing stages, with manufacturing technology, CAD (Computer Aided Design), CAM (Computer Aided Manufacturing) and CNC (Computer Numerical Control) systems are widely used. In this chapter manufacturing process of test rig are discussed part by part. Some technical drawings and some pictures of test rig components are given in Appendix D.

5.2.DETERMINATION OF THE MANUFACTURING PROCESS

Manufacturing of shafts, rods, couplings, housings, gearbox and gear are defined in this section.

5.2.1. Shaft and Rod Manufacturing

Shaft and rod is illustrated in Figure 5.1. Normally shafts are manufactured with lathe machining. However, gear pin and bolt holes placed on the test rig shaft makes it impossible to produce shaft. Reason of this best production method should be optimized.

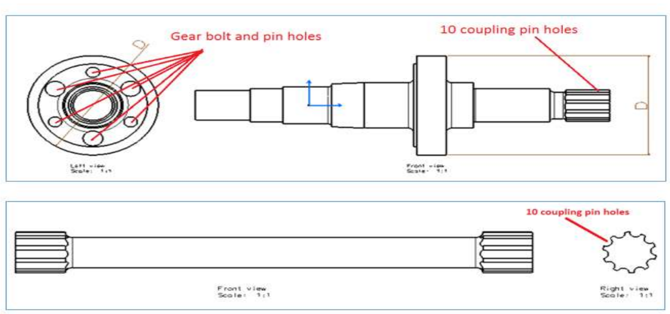

Figure 5.1: General View of Shaft and Rod

Optimized best test rig shaft and rod production methods can be defined as below.

- Optimal shaft and rod diameters (D) should be provided. Because shaft size affects to material cost and production time.

- Rough turning (Figure 5.2): This operation is usually carried out by treating the outside towards the center giving more chips. Firstly, center hole should be drilled. In cases where long work pieces should be connected between the mirror and the tailstock, centering hole is drilled for centering, bearing and supporting of work pieces. Thus provides to centering of the work piece and rotating without concentric during operation.

Figure 5.2: Rough Turning of Shaft with Universal Turning Machine

- Fine turning (Figure 5.3): Fine turning process is done after rough turning by giving small chips. Last dimensions of shaft diameter and fillets is finished with fine turning.

Figure 5.3: Fine Turning of Shaft with CNC Turning Machine

- Horizontal Machining Center: Horizontal Machining which is known as milling, relies on rotational cutters to remove metal chips from a metal work piece. Horizontal machining occurs on a HMC (horizontal machining center) and it employs a spindle which is parallel to floor. Gear bolt and pin connecting holes and couplings pin connecting holes on the shafts and rods are drilled with HMC.

5.2.2. Couplings and Housing Manufacturing

Coupling as shown in Figure 5.4. There are 4xM16 pin holes, gear and rod connecting holes and stepped diameters on the coupling.

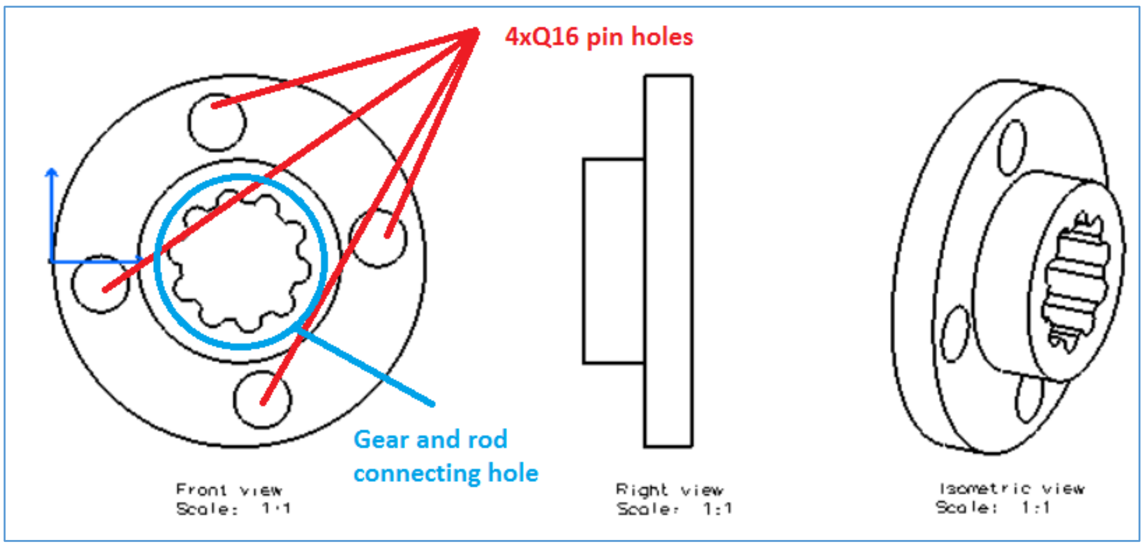

Figure 5.4: Couplings views

Optimized best test rig couplings and housing production methods can be defined as below.

- Optimal coupling diameters (D) should be provided due to material cost and production time.
- Rough turning: Purpose of rough turning is to speed up the process.
- Fine Turning: Purpose of fine turning is provided to stepped diameters of couplings (this picture is used for shaft, couplings and housing).

Figure 5.5: Fine Turning of Parts with CNC Turning Machine

- Milling Operation (Figure 5.6): Milling is the most common process of machining, a metal or another part removal process, which can create a variety of features on a part by cutting away the unwanted material. Milling is normally used to produce parts that are not axially symmetric and have many features, such as holes, slots, pockets, and even three dimensional surface contours.

  So 4xM16 pin holes, gear and rod connecting holes and stepped diameters on the coupling are removed with milling operation.

Figure 5.6: Milling Process of Couplings

5.2.3. Gearbox manufacturing

Gearbox mainly occurs from three components. Upper, bottom and base components are illustrated in Figure 5.7. Upper and bottom components consist of 4 parts. Upper, bottom and base components connect each other with bolt and pins.

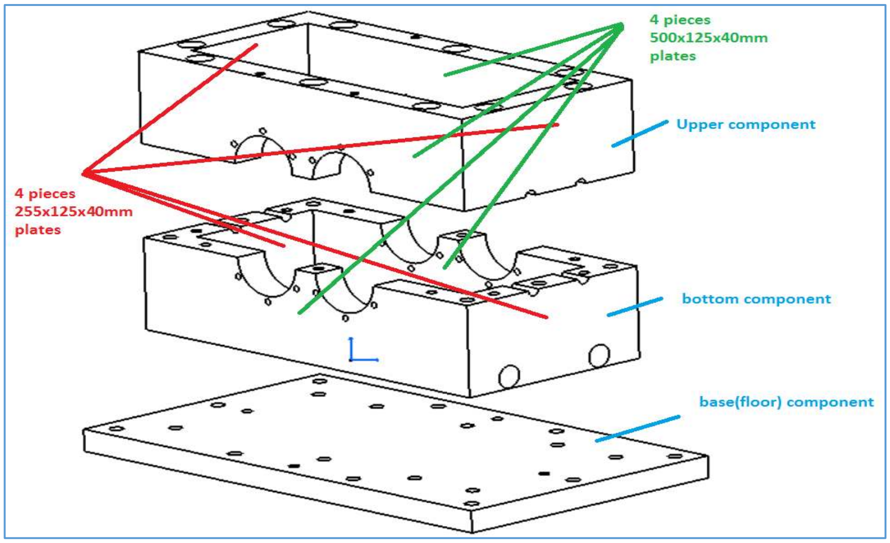

Figure 5.7: Explode view of Gear Box

Optimized best test rig gearbox production methods can be defined as below.

- Plasma cutting: upper and bottom component of gearbox consist of 4 plates as 40mm. Generally thick parts is cut with plasma. It is shown in Figure 5.8. These parts are cut as 50mm and these parts must be larger 3mm than design dimensions for milling operation.

Figure 5.8: Plasma Cutting of Gear Box Components

- Welding process: After plasma cutting, these four parts are connected with welding from inner and outer corners. Upper and bottom components are occurred as box (Figure 5.9).

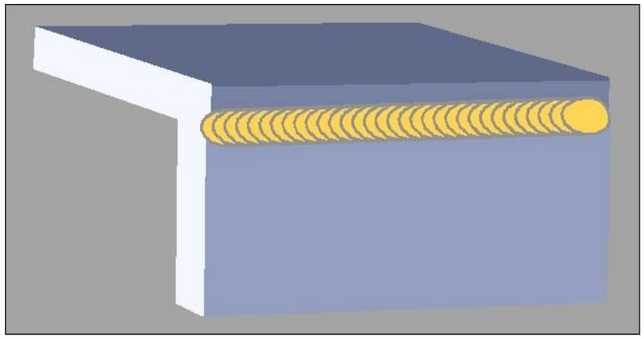

Figure 5.9: Welding Process of Gear Box

- Milling process: Upper, bottom and base components are brought design dimensions with pin and bolt holes (Figure 5.10).

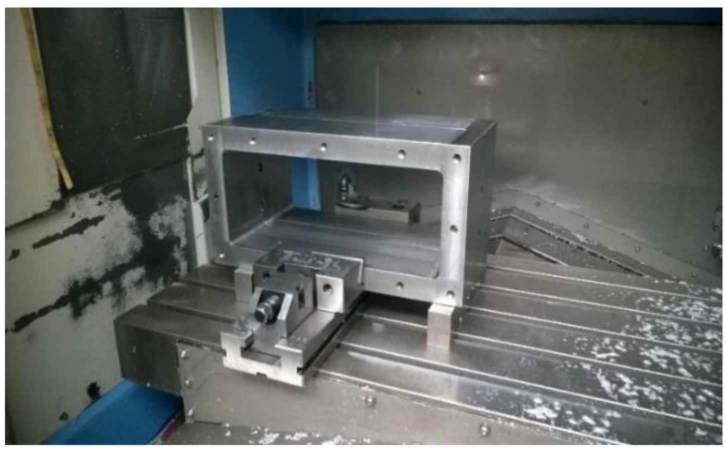

Figure 5.10: Milling Process of Gear Box

- Horizontal Machining Center: Components are assembled together with bolt and pins. After assembly housing holes are drilled with HMC (Figure 5.11).

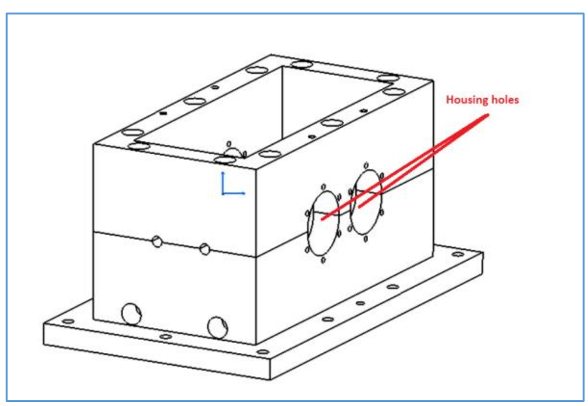

Figure 5.11: Operated Housing Holes with Horizontal Machining Center

5.2.4. Gear manufacturing

On this test there are two tips gear. These gears are spur and helical gears. They are manufactured in a gear manufacturer by giving gear production parameters (Figure 5.12). For spur gear, these parameters are modulus, pressure angle, teeth number. For helical gears, they are modulus, pressure angle, teeth number and helical angle. Technical drawing of helical gear and some pictures of gears are given in Appendix D.

Figure 5.12: Gears after Manufacturing

5.3.PROCESS ERRORS AND THEIR SOLUTIONS

Process errors and their solutions during assembly and process are defined below one by one.

- Many components of test rig (%90) are production with CNC type machine. So working with professional machine operators are required for precision production.

- It is trouble that removing pin holes on the shaft with tolerances due to long shaft. Bending can be occurred on the machine tools or shaft. Inconsistencies can be occurred in pin joints hole sizes between shaft and gears regarding to long shaft. Apparatus can be set for this holes before horizontal or vertical machining. In addition to assembly gear on the shaft easily, gear hub tolerances can be increases. It is not problem. Because pins and bolts carry the loads (Figure 5.13).

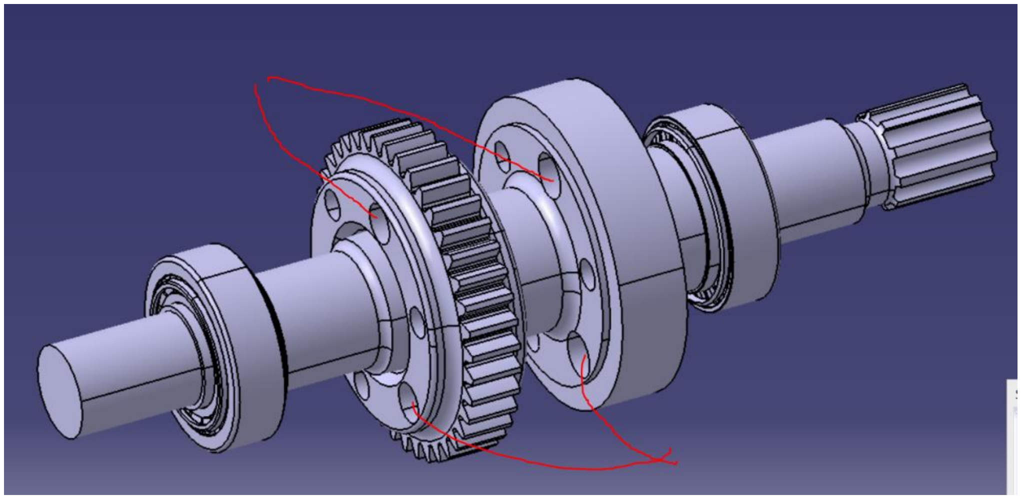

Figure 5.13: Pin and Bolt Joints on the Shaft

- Precision machining of pin joints holes (Figure 5.14) between couplings, rods and shaft can be hard. It is necessary to machining together with apparatus or can be operate with 5-axis machine one by one.

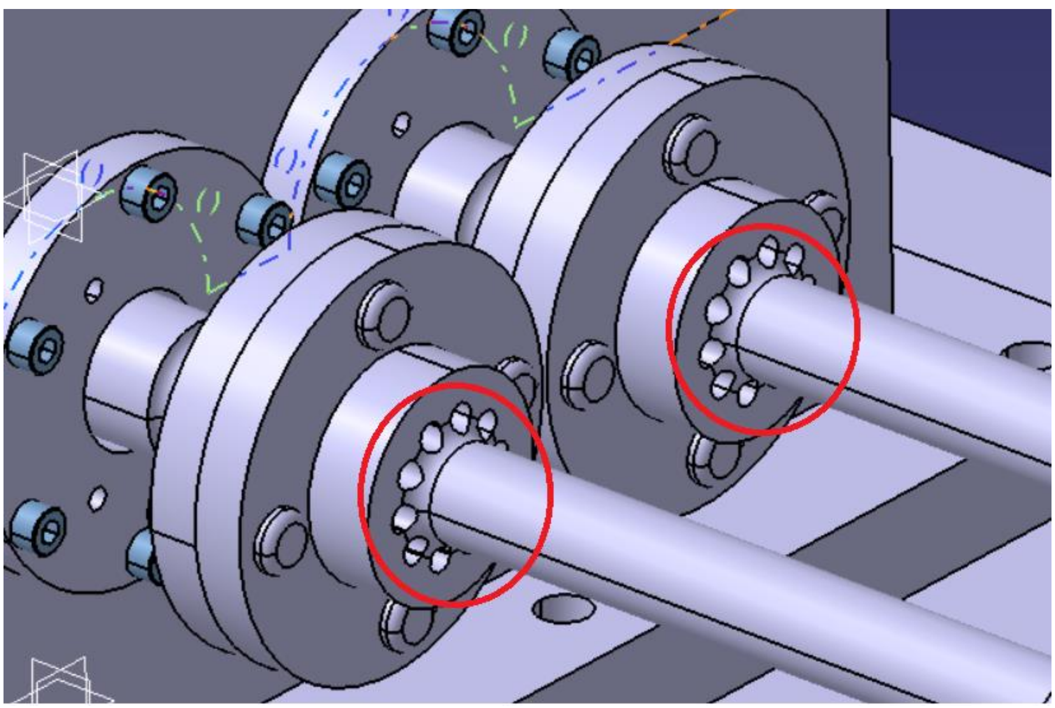

Figure 5.14: Pin Joints between Couplings and Rods

- Detection of 0,25 mm concentricity with a sign between inner and outer surface is necessary. Because tightness can be occurred on the system. In addition adding a wrench mouth is necessary to make adjustments of axis easily or to provide parallelism of center distance.

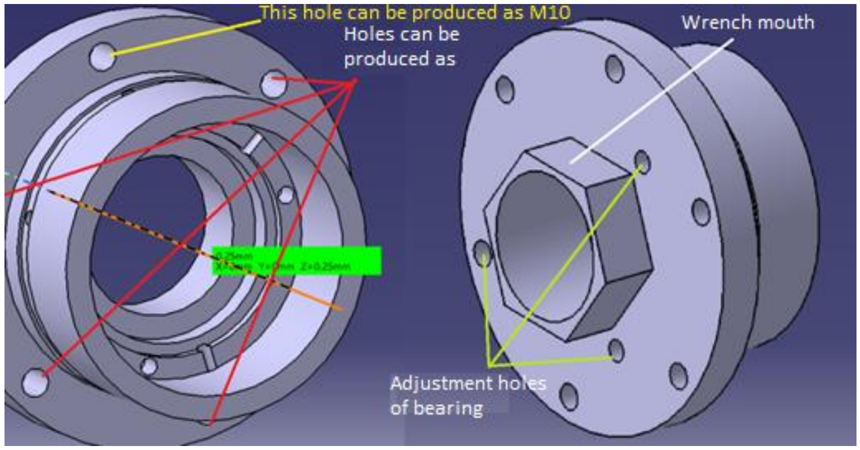

Figure 5.15: Detection of Concentricity by a Sign between Inner and Outer Surface

- Disassembly and reassembly of the gearbox takes too much time to require many bolt and pin joints. Redesign can be need. Disassembly and reassembly should be provided from only one side of gearbox (Figure 5.16).

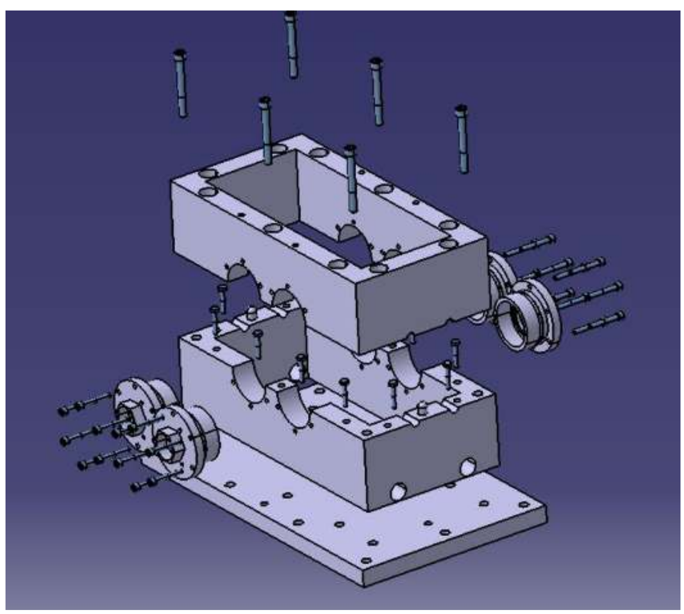

Figure 5.16: Trouble Assembly with Many Bolts

- For planarity of main plate of test rig, adding profiles and four plates should be need. Firstly, four plates are machined, after main plate side is machined (Figure 5.17).

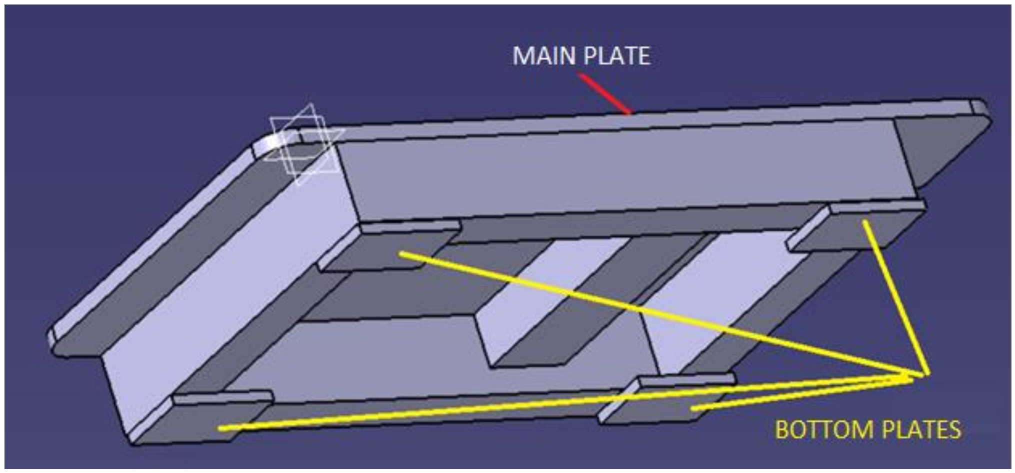

Figure 5.17: Machining After Adding Plate for the Surface Planarity

Helical gears and shaft should be manufactured as one part or helical gears (Figure 5.18) should be manufactured as herringbone gear. Result of this, misalignment of helical gears is trouble.

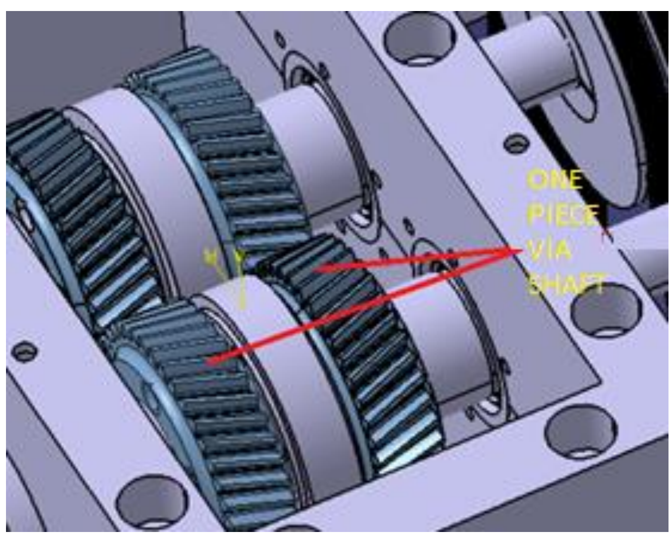

Figure 5.18: Herringbone Gear

- Because the processing time of parts needs to be extended, processing of share should be given up to 3 mm.

- All of material used on test rig should be analyzed one by one. Especially safety parts must be analyzed.

Figure 5.19: Hardness Test Of Rod

- For occupation healthy and safety, all of rationing parts must be kept under acquisition.

- After processing of parts in manufacturing, all of parts should be quality checked with technical drawing. In addition assembly parts should be controlled together for mounting.

Figure 5.20: 3-D Quality Control of Housing

- The central misalignment of connected parts with rigid couplings is hard. So in design flexible couplings should be used.

CHAPTER 6

DISCUSSION AND CONCLUSION

6.1.DISCUSSION AND CONCLUSION

Gears are one of the most important components than similar machine components. The gears have the ability of transmission of motion, power and force at parallel and nonparallel directions. So, invention of different machines and equipments are promoted by gears. Today gears are preferred for many kinds of machines and equipments to transmit motion and power. These machine may be simple home and office machines, transport machines, heavy machines, tanks, helicopters, submarines. Especially, gears can be transmit high power for many applications than similar equipments. Gears have highest efficiency and highest working life among similar between minimum and maximum rotations. In addition gears are the cheaper than the others.

Number of gear research centers is greater worldwide. Especially, in Europe there are many research centers. AGMA, BGA, FZG and CETIM are examples. Because gears are important elements to develop technology. Theoretical researches only are not enough to develop gear. It need to be supported with experimental studies. Experimental research results do activate the research subjects beyond the theoretical limits too.

After this thesis, academic collaboration were provided in Gaziantep University and other university and researches centers in Turkey and in the world. Design and production of a back to back test rig will help to start doing experimental work and supply actual test results about gear researches.

In this thesis, following studies are described chapter by chapter.

In Chapter 1, general information about thesis subjects has been given. TE and transmission error measurement techniques has been described. Advantages and disadvantages of experimental works has been discussed. At the end of thesis which parameters will be measured and after modification of test rig which parameters will be studied have been described.

In Chapter 2, kind of gears, their parameters and their failures have been explained.

In Chapter 3, literature survey of experimental studies and design and development studies have been discussed.

In Chapter 4, gear test rigs have been investigated, and for design which test rig is used and its components have been defined and described.

In Chapter 5, back to back test rig has been designed analytically. Here, center distance has been defined and shaft, couplings, gears, bolts, pins, bearings, rods, belt-pulley, motor, torque mechanism and lubrication system have been designed with analytically and 3-D.

For analytical, excel has been used mostly, for computer aided design catia and AutoCAD have been used.

In Chapter 6, Designed safety components have been analyzed with Finite Element Programmed Msc Simxpert and results has been discussed with analytical solutions.

In Chapter 7, Manufacturing processes have been defined and test rig has been produced. Occurred Manufacturing errors during manufacturing process has been defined and their solutions are described.

Following differences from other studies about test rig design are;

- 120 mm Center Distance was used (mostly used 91,5 mn- only Çakır, 120 mm was used for design)
- For coupling connection, pins was preferred instead of keywall.
- New concept torque loading mechanism designed and produced.
- Gear ratio was used as 1:1
- All of system were mounted on one chassis.(test system, lubrication system, control system)

6.2.RECOMMENDATIONS FOR FUTURE WORK

The following studies may be considered for future work.

- Modification of test rig with instruments.

- Tangential accelerometer devices
- Grating (rotary encoder) systems for digital use
- Etc.

- And some experimental studies as below,
  - Gear tooth stresses and strains
  - Gear tooth bending and surface fatique
  - Gear tooth deflections
  - Gear tooth static and dynamic loads
  - Bearing deflections
  - Bearing loads
  - Gear shaft vibrations
  - Gear torsional vibrations
  - Gear case vibrations
  - Noise radiated from a test gearbox

REFERENCES

[1] Özgüven, H.N., Houser D.R. (1998). Mathematical models used in gear dynamics—a review. *Journal of Sound and Vibration*. 121, (3) 383.

[2] Welbourn, D.B. (1979). Fundamental knowledge of gear noise. A Survey. Proc. Noise & Vibration of Eng. and Trans. I. Mech. E., Cranfield. UK. 9-14

[3] Milenkovic, V., Shmuter, S., Field N. (1983). On-Line Diagnostics of Rear Axle TE. ASME Special Publication HOO288. Computer Integrated Manufacturing.101-109

[4] Milenkovic, V., Shmuter, S. (1982). An Angular Sensor for TE Inspection. *SAE Transactions*, Vol. 91, Section 1. 202-220

[5] Krantz, T. L., Kahraman, A. (2005). An Experimental Investigation of the Influence of the Lubricant Viscosity and Additives on Gear Wear. NASA/TM. 2005-213956.

[6] Krantz, T. L. (2005). The Influence of Roughness on Gear Surface Fatigue. NASA/TM.2005-213958.

[7] Krantz, T. L., Tufts, B. (2007). Pitting and Bending Fatigue Evaluations of a New Case-Carburized Gear Steel. NASA/TM.2007-215009.

[8] Handschuh, R.F., Krantz, T. L. (2010). Engagement of Metal Debris into a Gear Mesh. NASA/TM. 2010-216759.

[9] Chase, D. R. (2005). Development of an Efficiency Test Methodology for High-Speed Gearboxes, M.Sc. Thesis in the Ohio State University.

[10] Klein, M. A. (2009). An Experımental Investıgatıon of Materıals and Surface Treatments on Gear Contact Fatıgue Lıfe. M.Sc. Thesis in the Ohio State University.

[11] Vaidyanathan, A. (2009). An Experımental Investıgatıon of Helıcal Gear Effıcıency, M.Sc. Thesis in the Ohio State University.

[12] Rossi, F. (2010). Influence of Profile Modifications on Transmission Error and Noise of Spur Gears. PhD thesis in the Politecnico di Milano.

[13] Milliren, M. R. (2011). An Experımental Investıgatıon into the Influence of Varıous Errors on the Transmıssıon Error and Root Stresses of Spur Gears. M.Sc. Thesis in the Ohio State University.

[14] Rao, S., McPherson, D., Sroka, G. (2005). Repair of Helicopter Gears. AGMA 05FTM15. ISBN: 1-55589-863-7.

[15] Yıldırım, N. (1994). Theoretical and Experimental Research In High Contact Ratio Spur Gearing. Ph.D. Thesis, School of Engineering in the University of Huddersfield.

[16] Britton R. D., Elcoate, C. D., Alanou, M. P., Evans H. P., Snidle, R. W. (2000). Effect of Surface Finish on Gear Tooth Friction, Trans. of the ASME, *Journal of Tribology* Vol. 122. 354-360.

[17] OTTO, H.P. (2009).Flank load carrying capacity and power loss reduction by minimized lubrication. Dissertation. TU München.

[18] Höhn, B.R., Otto, M., Thoma, F. (2010). Calculation of load distribution and load carrying capacity for spur and helical gears, *International Conference on Gears. VDI Berichte* 2108, 2, VDI-Verlag Düsseldorf.

[19] Höhn, B.R. Oster, P., Otto, M., Thoma, F. (2010).Tooth bending strength of helical gears, International Conference on Gears. VDI Berichte 2108, 2, VDI-Verlag Düsseldorf.

[20] Klocke, F., Gorgels, C., Vasiliou, V. (2010). Influence of Gear Properties induced by Hard Finishing Processes on the Load Carrying Capacity of Gears, Production Related Run Behavior of Gears. International Conference on Gears. V.VDI Berichte 2108.1, VDI-Verlag Düsseldorf.

[21] Brecher, C., Gorgels, C., Bagh, A. (2009). Improvement of the Efficiency of Parallel-Axis Transmissions by Means of PVD-Coatings, Friction, Wear and Wear Protection.

[22] Fetvaci, C., Imrak, E., (2008). Mathematical Model of a Spur Gear with Asymmetric Involute Teeth and Its Cutting Simulation. *Mechanics Based Design of Structures and Machines*. 36:1, 34 – 46.

[23] Fetvaci, C., Imrak, E., (2008). Computerized Cutting Simulation Of Involute Helical Gears Generated With Rack Cutters. *Int. J. Design Engineering*. Vol. 1, No. 4, 445–452.

[24] Fetvaci, C. (2010). Computer Simulation of Helical Gears with Asymmetric Involute Teeth. Journal of the Faculty of Engineering and Architecture of Gazi University, Cilt 25, No. 3,441-447.

[25] Karpat, F., Ekwaro, O. S., Cavdar, K. Babalik, F.C. (2008). Dynamic Analysis of Involute Spur Gears with Asymmetric Teeth. *International Journal of Mechanical Sciences*. 50 (12) 1598-1610.

[26] Bozca, M., Fietkau, P. (2010). Empirical model based optimization of gearbox geometric design parameters to reduce rattle noise in an automotive transmission. *Mechanism and Machine Theory*. vol. 45, 1599-1612, Elsevier.

[27] İmrek, H., Özkasap, A. D. (2001). Duz Dişli Çarklarda Aşınma Olayının Deneysel Olarak İncelenmesi. TMMOB Makina Mühendisleri Odası Konya Şubesi Makina-Tasarım ve İmalat Teknolojileri Kongresi.

[28] Yıldırım, N (2005). Some Guidelines On The Use Of Profile Reliefs Of High Contact Ratio Spur Gears. *Proc. Of IMechE, Part C*, Vol 219, 1087-1095.

[29] İmrek, H., Duzcukoglu, H. (2005). Relation Between Wear And Tooth Width Modification İn Spur Gears. Elsevier B.V, Wear 262 (2007) 390–394.

[30] Yıldırım, N., Gasparini, G., Sartori, S. (2008). An İmprovement On Helicopter Transmission Performance Through Use Of High Contact Ratio Spur Gears With Suitable Profile Modification Design. Proc. Of IMechE, Part G, Vol222, 1193-1210.

[31] İmrek, H., Duzcukoglu, H. (2008). A New Method For Preventing Premature Pitting Formation On Spur Gears. Elsevier B.V Engineering Fracture Mechanics 75 (2008) 4431–4438

[32] Başaran, B. (2001). Helisel Dişli Çarklarda Pıttıng Oluşumunun Deneysel İncelenmesi, Yüksek Lisans Tezi. Gazi Üniversitesi Makina Mühendisliği.

[33] ÇAKIR, M. V. (2003). Desıgn of A Gear Research Test Rıg. M.Sc. Thesis in Gaziantep University Mechanical Engineering Department.

[34] Korka, Z., Vela, I. (2008). Design and Execution of a Test Rig for Studying the Vibrations of a Gearbox. Analele Unıversıty, Eftımıe Murgu Resıta. Anul Xv, Nr. 1, Issn 1453 – 7397.

[35] Lomate, Amruta., Mohite, Suhas., Shinde, Rahul. (2010). Design and Development of Torque Testing Rig for a Gearbox. International Journal of Computer Communication and Information System (IJCCIS). Vol2. No1. ISSN: 0976–1349.

[36] Åkerblom, Mats. (1999). Gear Test Rıg for Noıse and Vıbratıon Testıng Of Cylındrıcal Gears. Volvo Construction Equipment Components AB SE–631 85 Eskilstuna, Sweden.

[37] Sachidananda H.K., Gonsalvis, J., Prakash, H. R., Rajesh A.R. (2011). Design and Development of Power Recirculating Gear Test Rig. CLEAR IJRET Vol-01.No-01.

[38] Tunalıoğlu, M. Ş., Tuç, B. (2012). İç Dişli Çarklarda Aşınmanın Deneysel Olarak İncelenmesi.TMMOB MMO Mühendis ve Makina Dergisi, cilt 53, sayı 632, 49-54

[39] Strama Company. Avaliable at: http://www.strama-mps.de/en/product-portfolio/test-rigs.html

[40] Newcastle University Design Unit Services in Newcastle available at: http://www.ncl.ac.uk/gears/services/test/index.htm

[41] Inui, T., Minami, H. (2004). Development of High-Speed Loading Test Rig for Gear Units of Railway Vehicles. J-Rail.

[42] Smith, J.D. (1987). Gear TE Accuracy with Small Rotary Encoders. Proc. Instn. Mech. Engr. Vol. 201, No.C2, 134-135

APPENDIX

APPENDIX A

GEARS

GEARS AND THEIR IMPORTANCE

Gear is a machine element which is used to transmit power and motion from one rotating shaft to another. Gears, which provide the advantages of engineering and cost according to others, are most critical components of power and motion transmission systems. So gears are used in different industries from machine and equipments manufacturing to automotive industry, from energy industry such as steam and hydraulic turbines, wind turbines to aeronautics such as helicopter and aero plane industries worldwide. In all of these sectors, there is an increasing demand for gears “work at high speeds and carry high loads”. So there is more need for gear research and development activities on gear subject like wear, fatigue, transmission failures, failures based on vibration and noise.

Commonly, gears can be classified into three types as illustrated in Figure A.1;

- Parallel axis gears
- Intersecting axis gears
- Non-intersecting and non-parallel axis gears

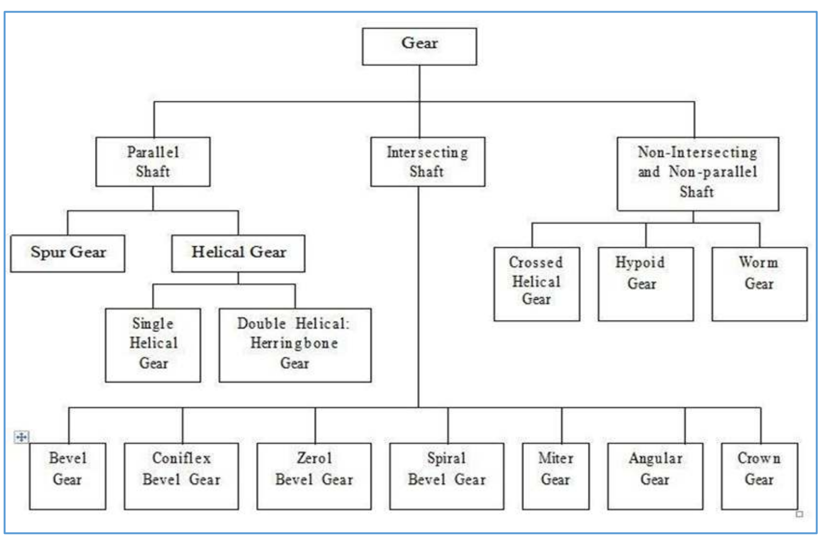

Figure A.1 Classification of gears

Parallel Axis Gears

Spur Gears

Spur gear is the most commonly used type of parallel axes one. Its teeth are perpendicular to the gear face. Spur gear is mostly available, and is generally cheaper than the others. The basic geometry of a spur gear is illustrated in the Figure A.2.

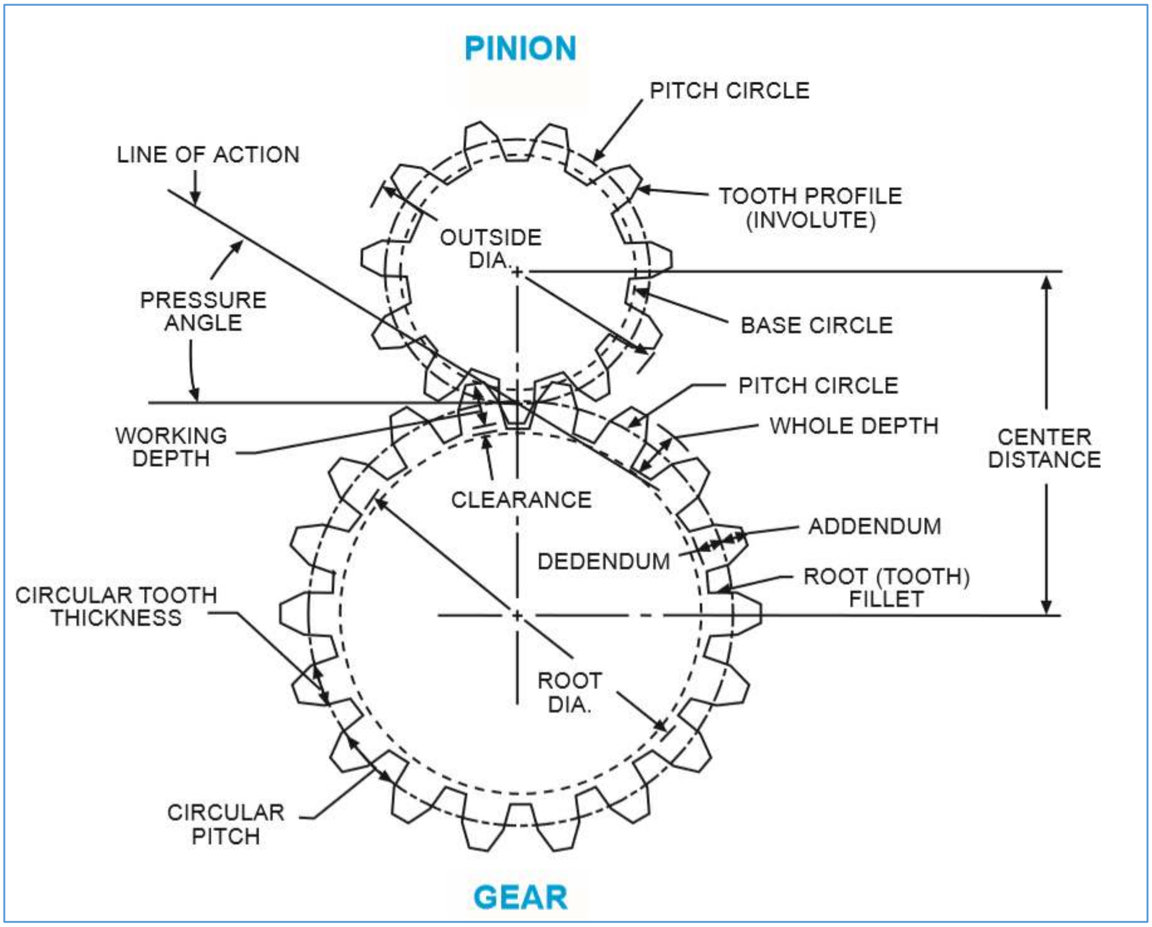

Figure A.2 Spur Gear Nomenclature

Addendum is the height on the tooth between tip circle and the pitch circle or pitch line.

Base Diameter is the base cylinder diameter.

Backlash is the amount of tooth space. This space occurs between mating gears during contact of teeth on the pitch circle diameter.

Bore Length is the total distance through gear.

Circular Pitch is the distance on the pitch circle or pitch line from the beginning of a first tooth to the beginning of a second tooth.

Circular Thickness is the length of a tooth on the pitch line of a tooth.

Clearance-Operating is the amount of tooth space between tip circle of pinion gear and root circle of driven gear.

Contact Ratio in general, ratio is the average number of tooth pairs of gear in contact on mating gears.

Dedendum is the distance from the root of the gear tooth to the pitch circle on the same tooth.

Diametral Pitch is calculated as dividing the number of teeth to the pitch diameter.

Face Width is the teeth length on axial plane.

Fillet Radius is the radius that occurs from fillet of intersection root circle and trochoid curve of tooth.

Full Depth Teeth are those in which the working depth equals 2.000 divided by the normal diametric pitch.

Hub Diameter is gear outside diameter.

Involute Teeth of spur gears are those in which the active portion of the profile in the transverse plane is the involute of a circle.

Normal Diametral Pitch is the diametral pitch value.

Normal Plane is the plane normal to the surface of tooth on the pitch point and the pitch plane and normal plane are perpendicular together.

Normal Pressure Angle in a helical tooth normal plane.

Outside Diameter is the outside circle diameter.

Pitch Circle is the circle found from a number of teeth and circular pitch.

Pitch Diameter is the pitch circle diameter.

Pressure Angle is the angle at a pitch point between normal to the tooth surface and the plane tangent to the pitch surface.

Root Diameter is the base diameter of the tooth space.

Tip Relief is a tooth profile modification.

Undercut is a condition in generated gear teeth when any part of the fillet curve lies inside a line drawn tangent to the working profile at its point of juncture with the fillet.

Whole Depth is the tooth total depth, calculated as addendum plus dedendum.

Working Depth is the the sum of gear pair addendums.

Some of geometric parameters can be calculated according to equations given in Table A.1.

Table A.1. Spur Gear Formulas

Item	Explaination	Formula
CD	center distance	$CD=(d_g+d_p)/2$
m	normal module	
a	addendum	a=m
b	dedendum	b=1,25*m
h_k	working depth	$h_k=2*m$
h_t	whole depth	$h_t=2,25*m$
t	tooth thickness	t=p/2
r_f	fillet radius	$r_f=0,3*m$
c	clearance	c=0,25*m
d_a	outside(addendum) diameter	$d_a=(Z_1+2)*m$ (Z_1: teeth number of gear1)
P	diametral pitch	P=25,4/m
p	circular pitch	p=m*3,1417

Helical Gears

Helical gears are similar to the spur gear except that the teeth are at an angle to the shaft, rather than parallel to it as in a spur gear. (See the references for more specific information). The resulting teeth are longer than the teeth on a spur gear of equivalent pitch diameter.

The longer teeth cause helical gears to have the following differences from spur gears of the same size:

- Improved tooth strength due to the elongated helical wrap- around.
- Increased contact ratio due to the axial tooth overlap.
- Helical Gears thus tend to have greater load carrying capacity than Spur Gears of similar size.
- Due to the above, smoother operating characteristics are apparent.

Helical gears may be used to mesh two shafts that are not parallel, although they are still primarily use in parallel shaft applications. A special application in which helical gears are used is a crossed gear mesh, in which the two shafts are perpendicular to each other: The basic descriptive geometry for a helical gear is essentially the same as that of the spur gear, except that the helix angle must be added as a parameter.

Helical gears have the major disadvantage that they are expensive and much more difficult to find. Helical gears are also slightly less efficient than a spur gear of the same size.

The information contained in the Spur Gear section is also pertinent to Helical Gears with the addition of the following as shown in Figure A.3.

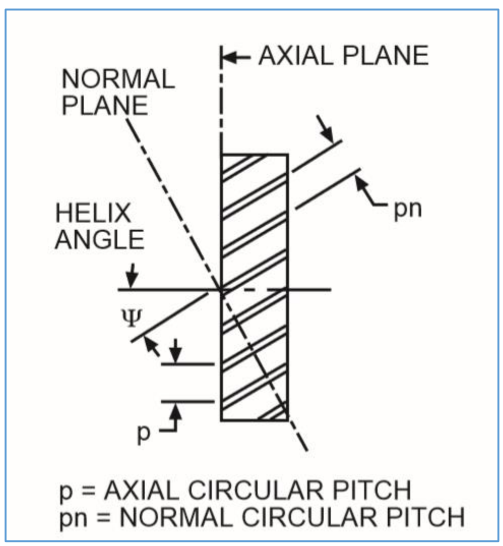

Figure A.3: Helical Gear

- **Helix Angle** is the angle between any helix and an element of its cylinder. In helical gears, it is at the pitch diameter unless otherwise specified.

- **Left Hand,** helical gear lean to the left when the gear is placed flat on a horizontal surface. (see Figure A.4)
- **Right Hand,** helical gear lean to the right when the gear is placed flat on a horizontal surface. (see Figure A.4)

Figure A.4.: Left and Right Hand Helical Gear

Some parameters of helical gears can be calculated in same manner as spur gears but some of them is calculated in different way and equations are presented in Table A.2.

Table A.2. : Helical Gear Formula

To Obtain	Having	Formula
Transverse Diametral Pitch (P)	Number of Teeth (N) & Pitch Diameter (D)	$P = \frac{N}{D}$
	Normal Diametral Pitch (P_n) Helix Angle (ψ)	$P = P_N Cos\psi$
Pitch Diameter (D)	Number of Teeth (N) & Transverse Diametral Pitch (P)	$D = \frac{N}{P}$
Normal Diametral Pitch (P_N)	Transverse Diametral Pitch (P) & Helix Angle (ψ)	$P_N = \frac{P}{Cos\psi}$
Normal Circular Tooth Thickness (τ)	Normal Diametral Pitch (P_N)	$\tau = \frac{1.5708}{P_N}$
Transverse Circular Pitch (p_t)	Diametral Pitch (P) (Transverse)	$p_t = \frac{\pi}{P}$
Normal Circular Pitch (p_n)	Transverse Circular Pitch (p)	$p_n = p_t Cos\psi$
Lead (L)	Pitch Diameter and Pitch Helix Angle	$L = \frac{\pi D}{Tan\psi}$

Nonparallel Axis Gears

Non parallel axes gears consist of bevel gears, worm gears and hypoid gears (a special type of spiral bevel) shown in Figure A.5 a, b, c respectively. Bevel gears have teeth which has a conical form. Worm gear transmits motion between non parallel and non-intersecting shafts with less efficiency due to high friction and loss.

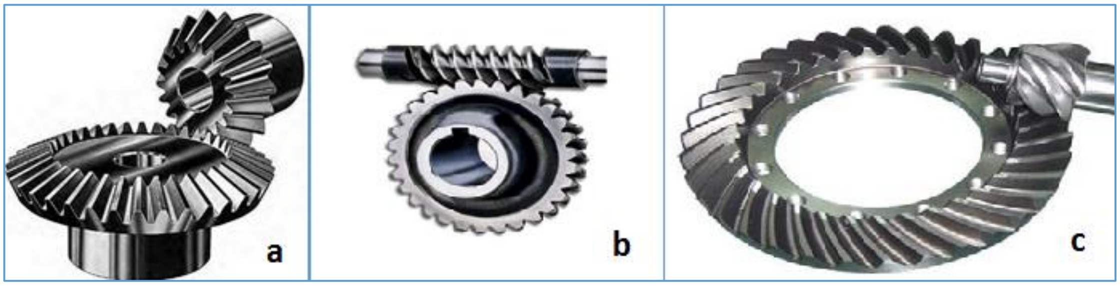

Figure A.5. a-Bevel Gears, b- Worm Gear, c- Hypoid Gears

FAILURE OF GEARS

The most important issue for designing a gear pair is to find a solution which fulfills load carrying for required power for long time service. Gears design is expected to provide enough mechanical strength to withstand force transmitted, enough surface resistance to overcome pitting failure and enough dynamic resistance to carry fluctuating loads without failure by taking limitations into consideration. There are some geometrical (space constraints), performance and economical limitations when designing a gear pair and other gearbox elements.

Gears are generally designed to operate at predefined center distance for many applications, because there is a space constraint and gearbox cases are manufactured at exact dimensions. Center distance change can be allowable for little amount or not. Designer should take this limitation and decide to apply profile shift to gears or use a standard dimension. Any change in operating center distance of gear pairs affects backlash amount which is usually very essential and sometimes undesirable depending on application. Those criteria are usually used for geometric design of gears. However gears should also be checked for a safe mechanical design.

Factor of safeties are taken into account to provide safe operation of gear pairs under loading for tooth root bending and surface contact stress. The underlying reason for purpose of using these values is to ensure that stresses occurs at gear root or surface should be less than strength values. Designing a gear pair much safer than required one is not economical. Due to this reason, engineer should be careful about economical design of gear pair.

Gear design criteria include two main points of static and dynamic performance. Static performance usually deals with global kinematic and geometric requirements and strength analysis of gear materials under load while dynamic performance usually deals with vibration and noise of gears. Although there are many different modes of gear and tooth failures (pitting, scuffing, wear, spalling, case crushing, frosting, scoring, fatigue breakage, overload fracture), there are three main causes of gear failures taken into consideration during gear mechanical designs; surface durability (pitting) due to surface contact stress and tooth breakage caused by tooth bending fatigue stress.

APPENDIX B

COMPUTER AIDED DESIGN

Spur Gear Design

There are many different methods to design a gear with 3D software. But mostly, catia, solidworks, AutoCAD and similar softwares are used. In this study, two methods are used. Ones directly gear design in catia. Other, design with gear curves regarding to coordinates. With this method real gear shapes are designed. Because you may create a lot of coordinates. Mean of a lot of coordinates is increasing of precision.

Directly Gear Desing In Catia.

Following steps are suitable for directly gear design in catia software;

- The mathematical formula of gear parameters and involute curves.

The table contains the parameters and formulas used in the parametric definition of gear in the CATIA software.

P	Formula	Description/ Units used for construction
a	20deg	Pressure angle: technologic constant (10deg ≤ a ≤ 20deg) / Angular degree
m	—	Modulue / millimeter
Z	—	Number of teeth (5 ≤ Z ≤ 200) / Integer
p	m * π	Pitch of the teeth on a straight generative rack / millimeter
e	p / 2	Circular tooth thickness, measured on the pitch circle / millimeter
ha	m	Addendum = height of a tooth above the pitch circle / millimeter
hf	if m > 1.25 hf = m * 1.25 else hf = m * 1.4	Dedendum = depth of a tooth below the pitch circle. Proportionally greater for a small modulus (≤ 1.25 mm) / millimeter
rp	m * Z / 2	Radius of the pitch circle / millimeter
ra	rp + ha	Radius of the outer circle / millimeter
rf	rp - hf	Radius of the root circle. / millimeter

P	Formula	Description/ Units used for construction
rb	rp * cos(a)	Radius of the base circle /millimeter
rc	m * 0.38	Radius of the root concave corner. (m * 0.38) is a normative formula / millimeter
t	0 ≤ t ≤ 1	Sweep parameter of the involute curve / floating point number
yd	rb * (sin(t * π) - cos(t * π) * t * π)	Y coordinate of the involute tooth profile, generated by the t parameter / millimeter
zd	rb * (cos(t * π) + sin(t * π) * t * π)	Z coordinate of the involute tooth profile / millimeter
ro	rb * a * π / 180deg	Radius of the osculating circle of the involute curve, on the pitch circle / millimeter
c	sqrt(1 / cos(a)^2 - 1) / PI * 180deg	Angle of the point of the involute that intersects the pitch circle / angular degree
phi	atan(yd(c) / zd(c)) + 90deg / Z	Rotation angle used for making a gear symmetric to the ZX plane / angular degree

Figure B.1: Spur gear Formulas

- The generative shape design workshop

Start and configure the generative shape design workshop: Since the part design workshop is not sufficient for designing parametric curves, select the generative shape design workshop Generative shape design:

Start > Shape> Generative shape Design

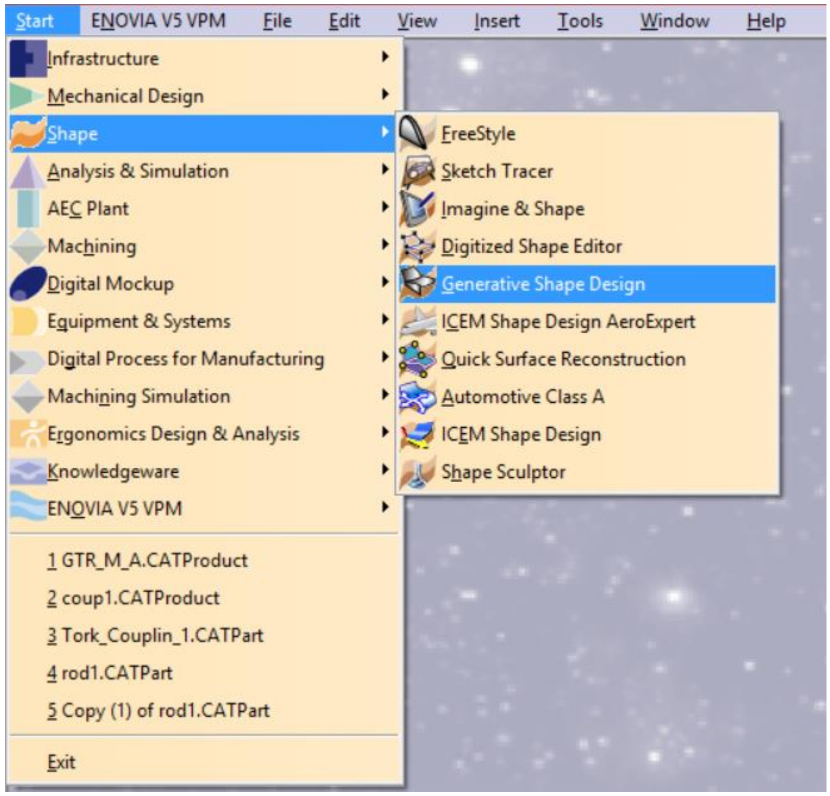

Figure B.2: Starting of Catia

- After CATIA program is initiated – select TOOLS>OPTIONS>infrastructure > part infrastructure and in Display select Parameters and Relations (Figure 4.55).

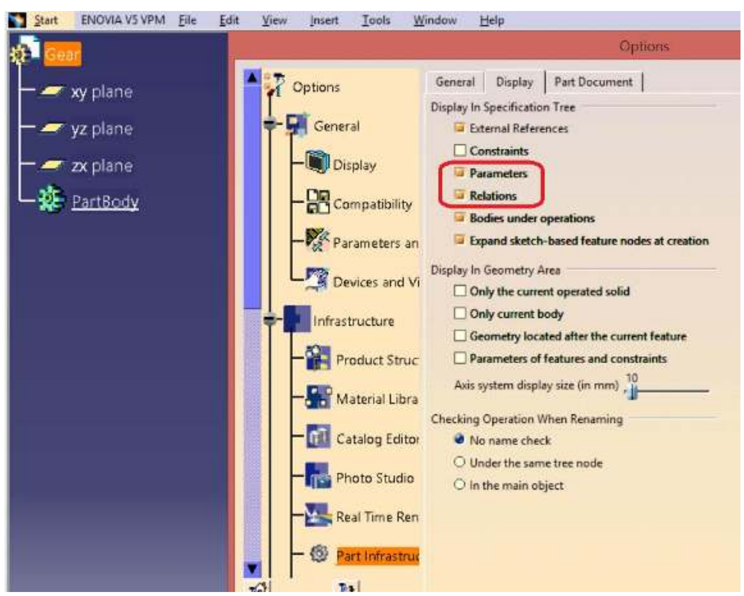

Figure B.3: Options Menu

- Then in Options>General in Parameters and Measures select with value and with formula in Parameters Tree View (Figure B.4).

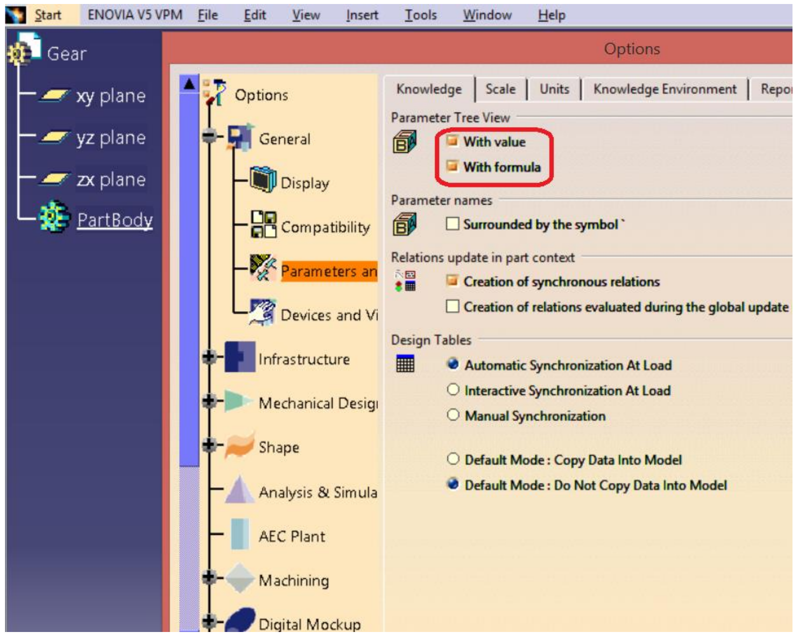

Figure B.4: Parameters and Measures

- Click on arrow pointed down near table icon. Fog and f(x) are two most important things you will use for gear design (Figure B.5).

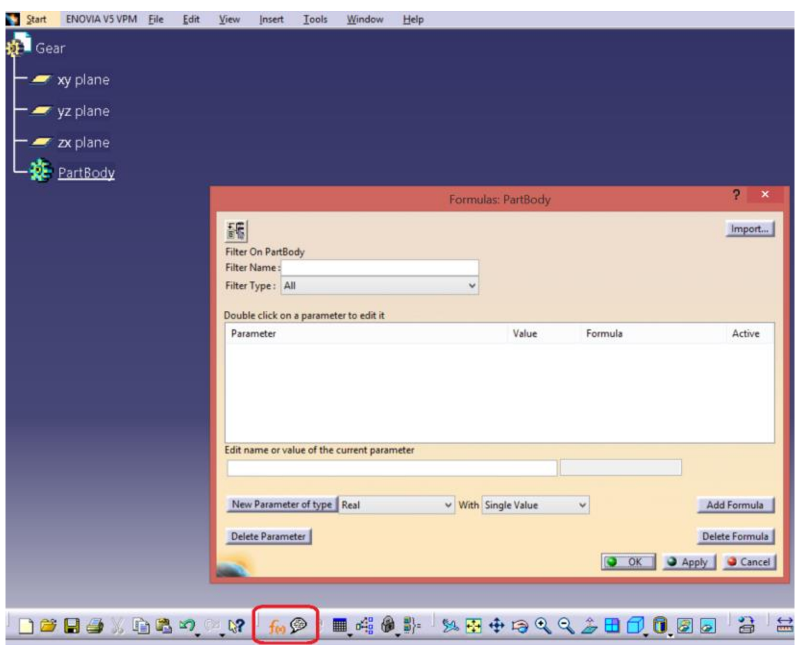

Figure B.5: Adding Formulas

- Enter the parameters.

Enter the Module (m) as length (parameter of type), number of teeth (z) as integer (parameter of type), Pressure Angle (a) as angle (parameter of type) and the other parameters are entered one by one as rb - base cylinder radius, rp - Pitch circle radius, ra - outside circle radius, rf - root circle radius, rc – bottom clearance (Figure B.6).

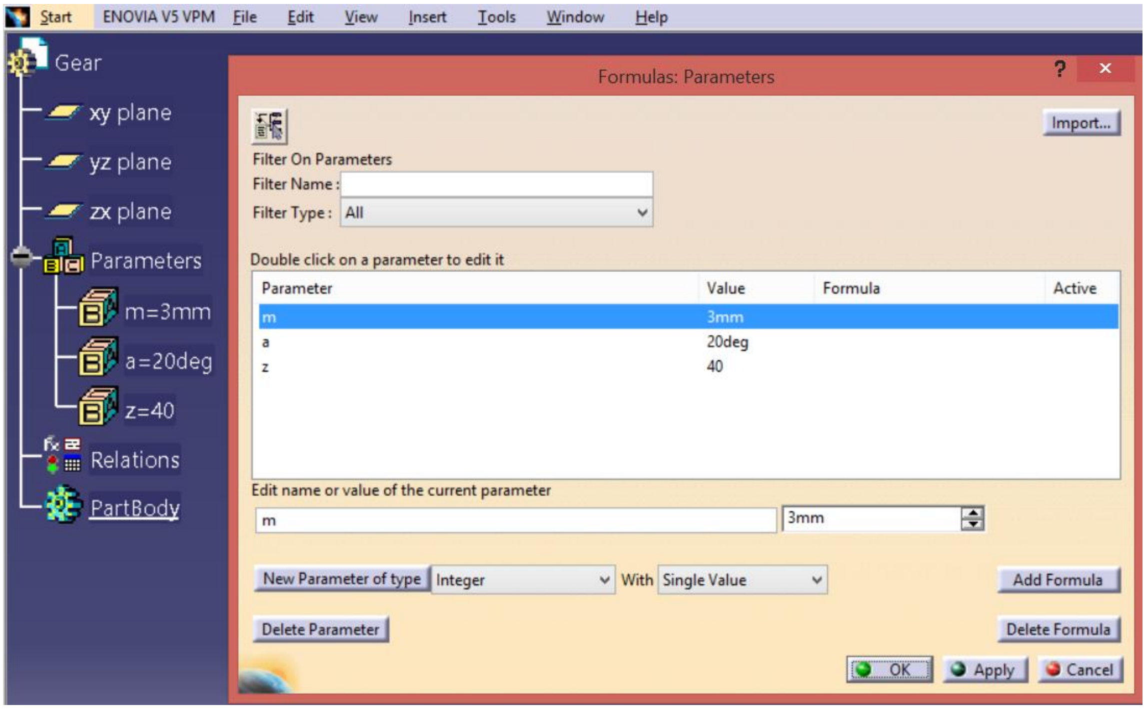

Figure B.6: Entering input values

- Entering the formula (Figure B.1).

In main windows, firstly add Formula. Then formula editor will appear:

r_p - Pitch circle radius, $r_p = m*z/2$

r_b - base cylinder radius, $r_b = r_p*\cos(a)$

r_a - outside circle radius, $r_a = r_p + m*1$

r_f - root circle radius, $r_f = r_p - 1.25 *m$

r_c – bottom clearance. $r_c = m*0{,}38$

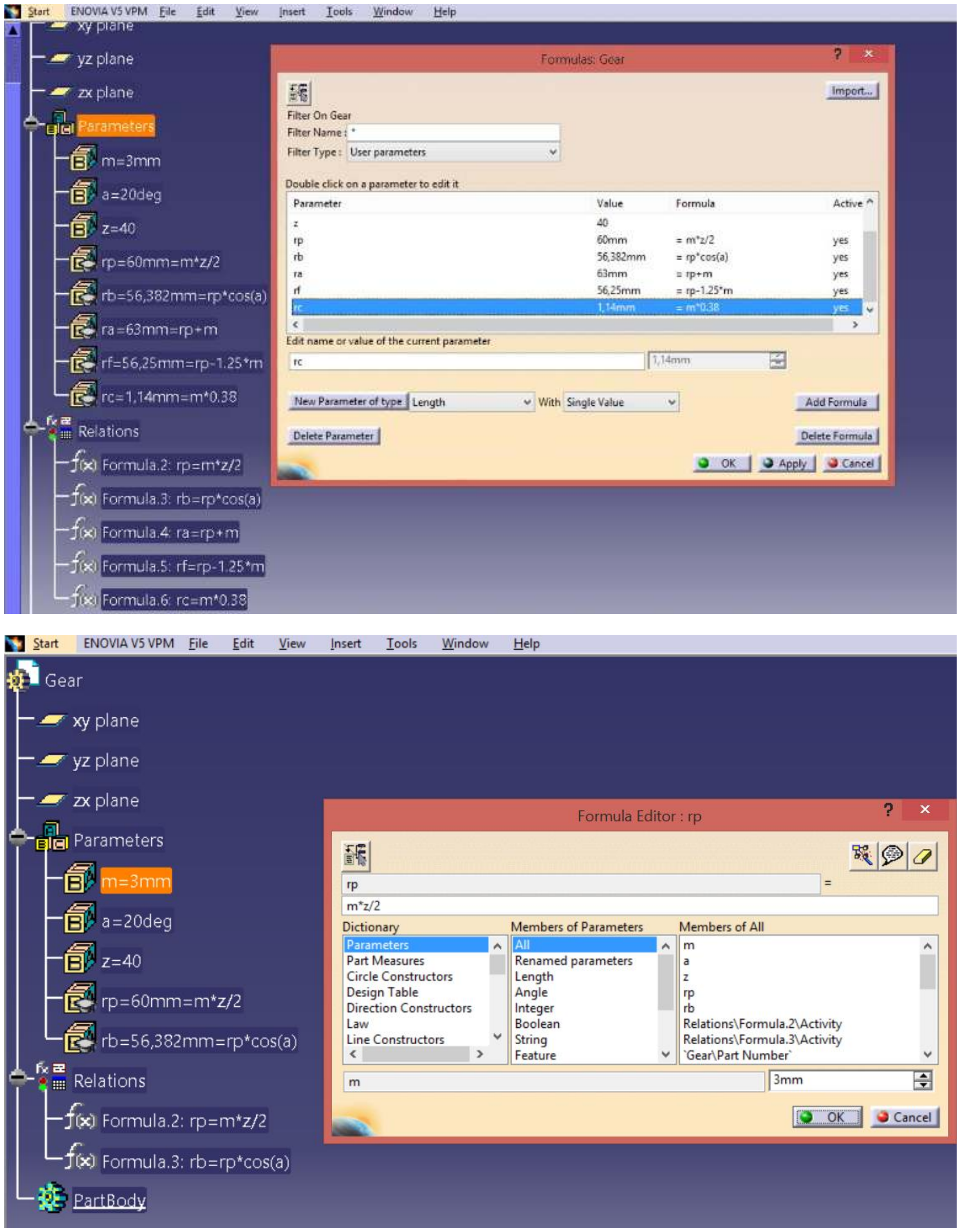

Figure B.7: Entering the formulas

- Check the primary and computed parameters
- Parametric laws of the involute curve

Define the formulas defining the (Y, Z) Cartesian position of the points on the involute curve of a tooth. We could as well define a set of parameters Y_0, Z_0, Y_1, Z_1, for the coordinates of the involute's points. Add laws that will define the involute of the gear

Figure B.8. Click on fog icon, name law as yd > select ok > add parameters, t – select real, and x - length select their types and apply > ok (Figure B.9).

Law y_d: $y_d=r_b*(\sin(t*PI*1rad)-\cos(t*PI*1rad)*t*PI)$

Same should be done for zd. This law will helps to create points that define spline for our involute. Involute is line that is trajectory of point belonging to line that is always tangent to base gear cylinder. It is used for tooth profile. If gears had profiles formed by straight lines they wouldn't work.

Law z_d:$z_d= r_b*(\cos(t*PI*1rad)+\sin(t*PI*1rad)*t*PI)$

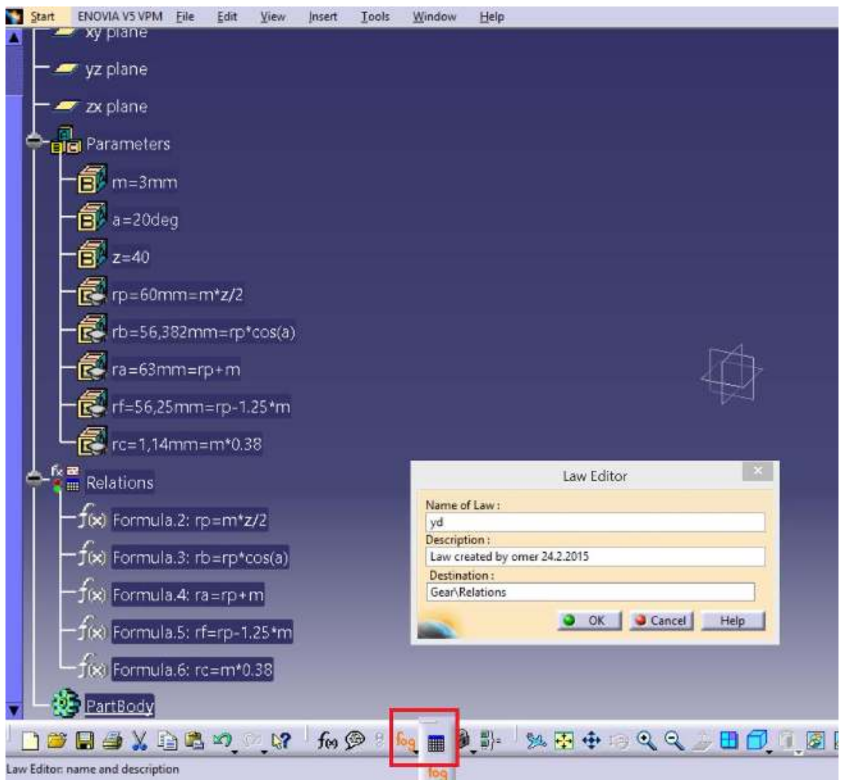

Figure B.8: Adding Laws

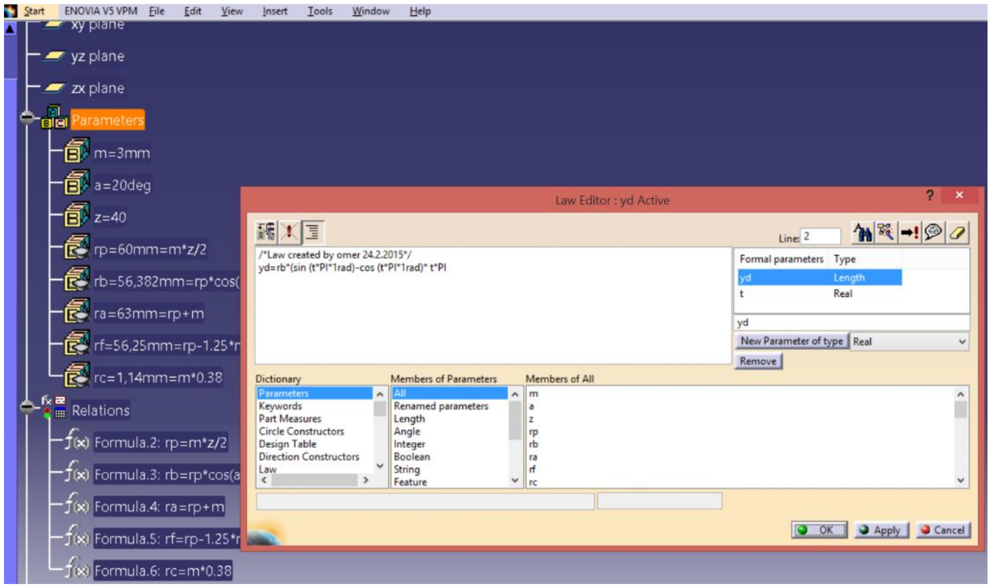

Figure B.9: Typing Laws

- Create geometric body and insert geometric elements

Creating geometric profile for the first tooth:

The position of each point is defined by the y_d (t) and z_d (t) parametric laws. 5 points are defined on the YZ plane.

Insert > Wireframe> Point> Select point type: on plane>Select YZ plane > for position Y and Z, right click and Edit formula. In order to ordinate, double click the Relations\Z_d .evaluate(0).

Click on the spline icon and connect all points (Figure B.10). Check for the spline profile on the screen.

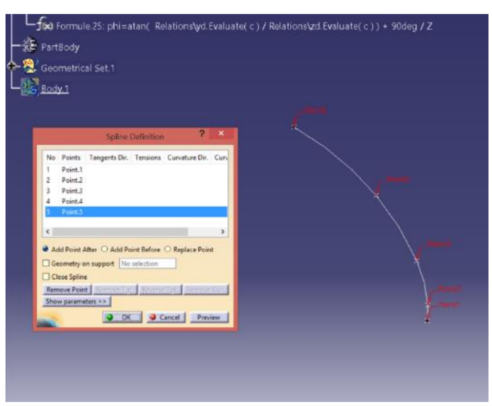

Figure B.10: Clicking Spline

- Make the geometric profile of the first tooth
- Define the parameters, constants and formulas
- Insert a set of 5 constructive points and connect them with a spline
- Extrapolate the spline toward the center of the gear

Click on the Extrapolate icon (Figure B.11) in the extrapolate dialog box key in point 2 for the boundary point and extrapolated spline.1.

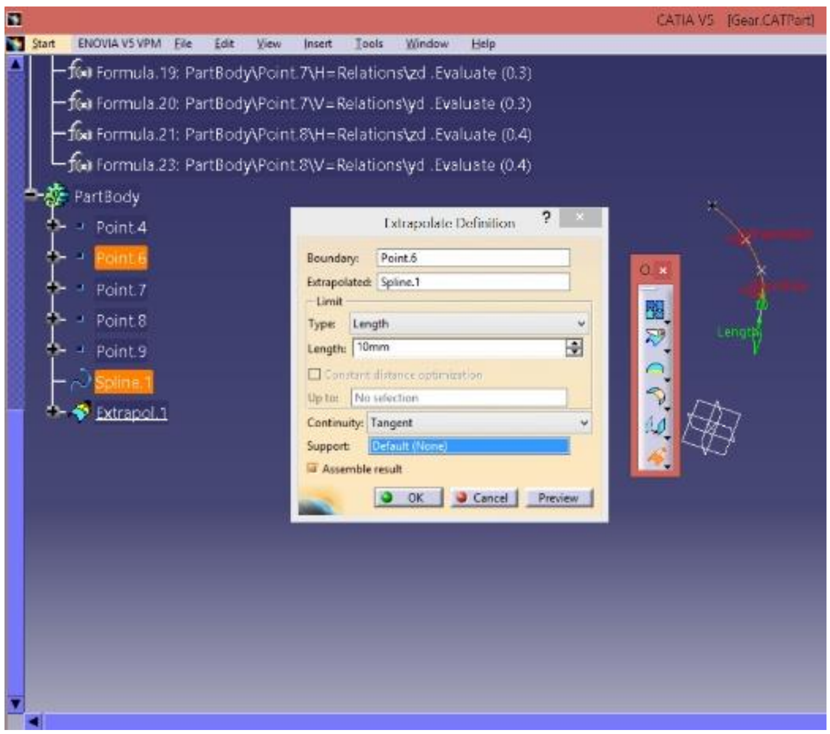

Figure B.11: Extrapolate Icon

- Rotate the involute curve for the symmetry relative to the ZX plane

The rotation angle is decided by formula, from table. Before this the value of c, the involute parameter is entered from the formula table. c=sqrt(1/(cos(a)*cos(a))-1)/PI,

and the unit should be selected as real.

Phi =atan (Relations\$y_d$ .Evaluate(c)/Relations\$z_d$ .Evaluate(c))+90deg/z.

Rotate the Extrapolated spline through an angle –Phi. The points and spline can be hidden by right click on the point menu and select hide/show menu (Figure B.12).

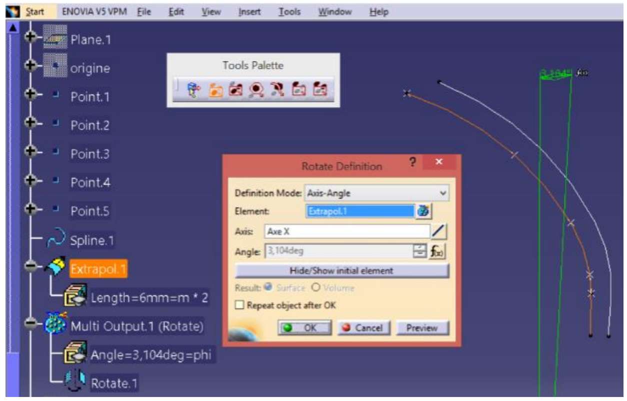

Figure B.12: Rotate the Extrapolated spline through an angle

- Draw the outer circle and the root circle (Figure B.13).

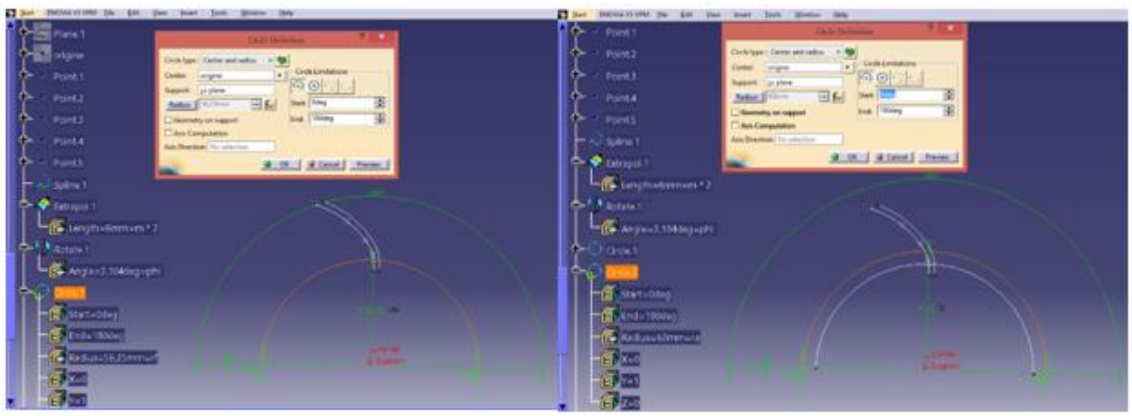

Figure B.13: Draw the outer circle and the root circle

- Insert a rounded corner near the root circle

The corner between the extrapolated involute curve and the root circle has a radius defined by the parameter r_c. Catia prompts to select an arc (in red) out of 4 possible geometric solutions (Figure B.14).

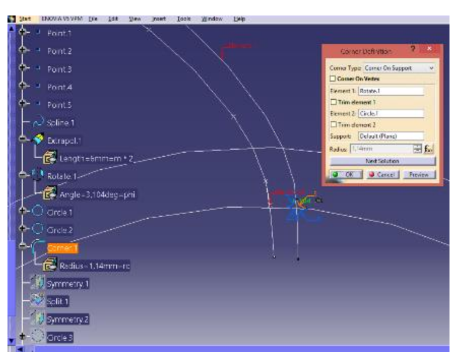

Figure B.14: Insert a rounded corner near the root circle

- Create the rounded corner of the next tooth (Figure B.15).

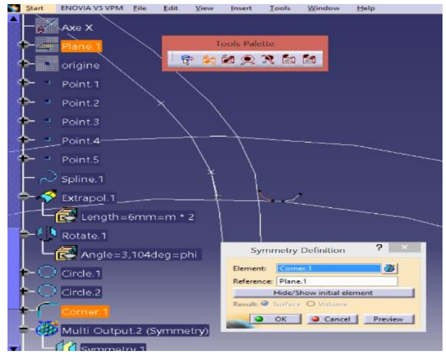

Figure B.15: Create the rounded corner of the next tooth

- Split between fillet radius and outer radius (Figure B.16).

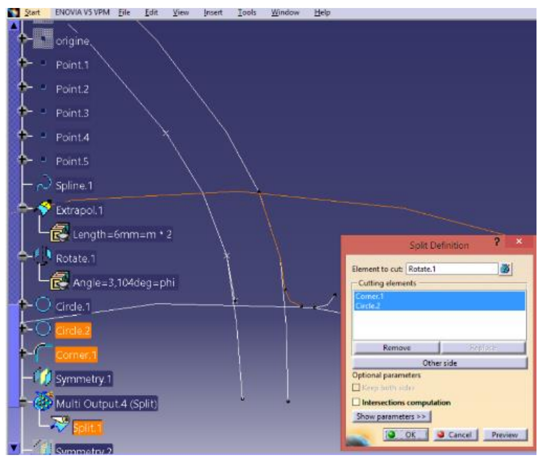

Figure B.16: Split between fillet radius and outer radius

- Symmetry of involute curves (Figure B.17).

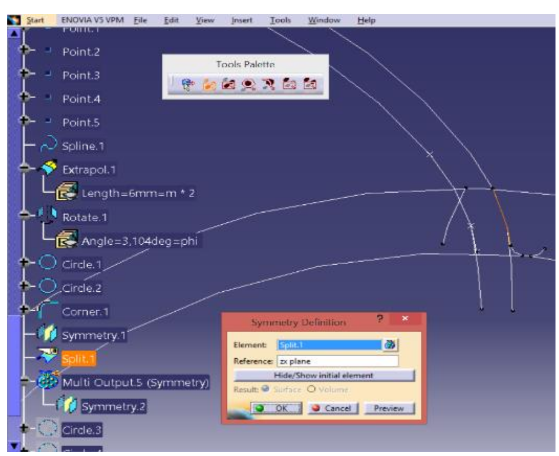

Figure B.17: Symmetry of involute curves

- Circle definition between two teeth (Figure B.18).

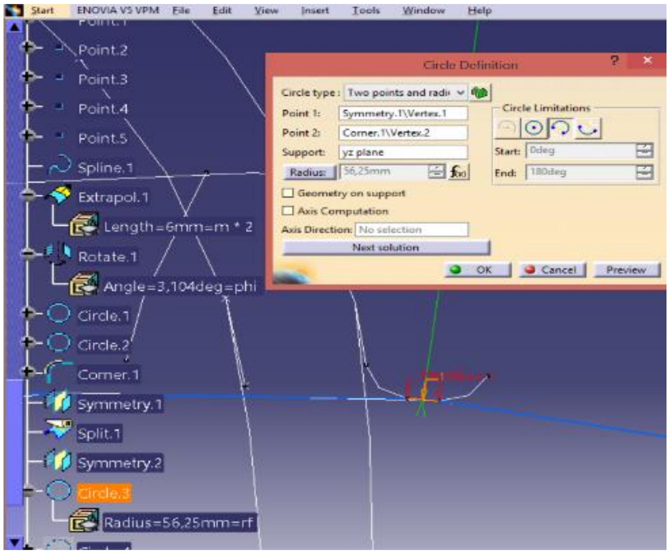

Figure B.18: Circle definition between two teeth

- Circle definition for tip radius (Figure B.19).

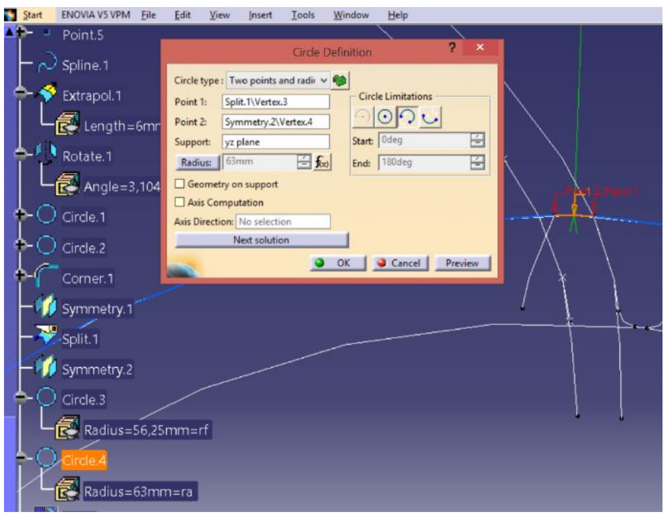

Figure B.19: Circle definition for tip radius

- Assemble the different elements of the first tooth

At this assembly stage the extrapolated spline has to be cut, fill and join the different elements of the 1st tooth: Cut the segment of the extrapolated spline between the outer circle and the rounded corner. The symmetric profile is defined relative to the ZX plane, for the other side of the 1st tooth (Figure B.20).

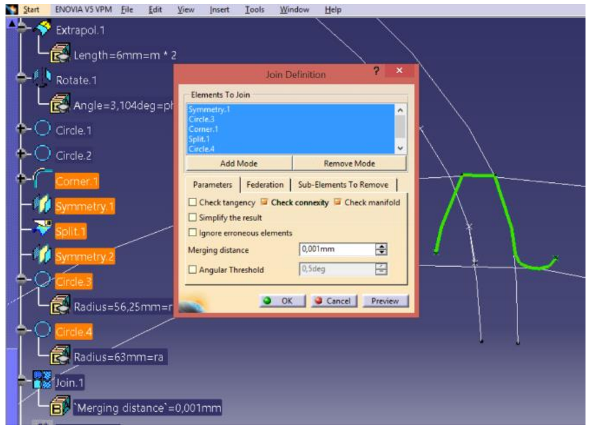

Figure B.20: Assemble the different elements of the first tooth

- Build the whole gear profile with circular pattern definition (Figure B.21).

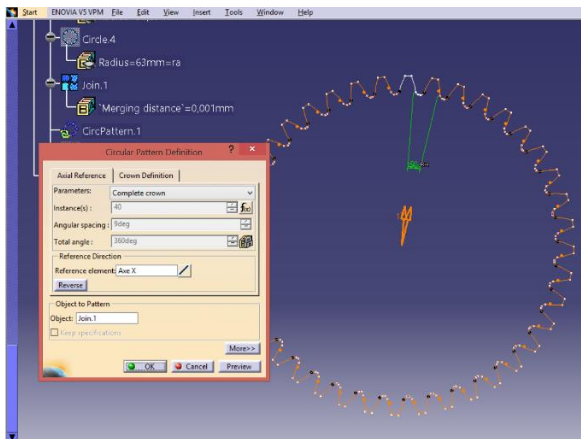

Figure B.21: Build the whole gear profile

- Extrude the whole gear profile with pad definition (Figure B.22).

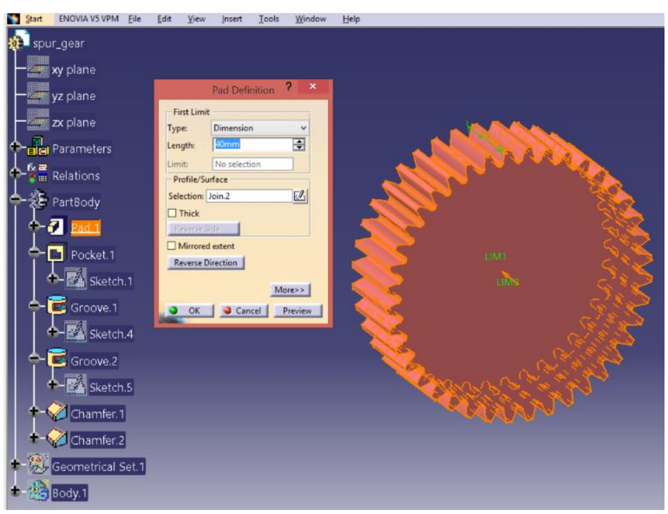

Figure B.22: Extrude the whole gear profile

- Another regulation of the geometry for test rig like pin hole, bolt hole and shaft hole (Figure B.23).

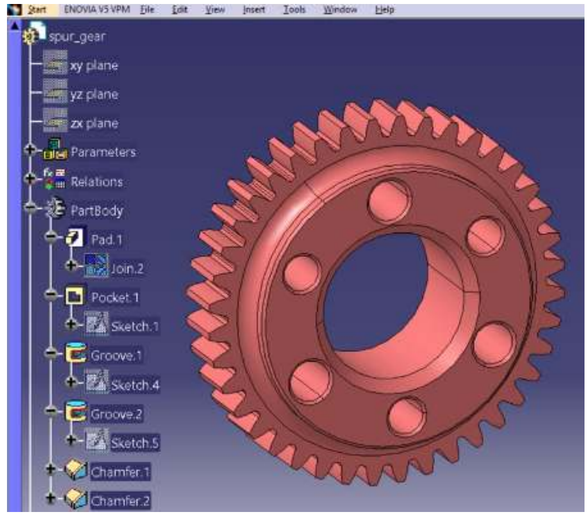

Figure B.23: Regulation of the Geometry

Design with gear curves regarding to coordinates

In this method, as shown in flowchart (Figure B.24), firstly a gear design software is used to generate coast side-drive side involute curves coordinates, coast side-drive side trochoid curves coordinates or a tooth profile coordinates or all coordinates of a gear. After that, this coordinates are arranged in excel or text files to use interface software. In this software curves of gear are created in two dimensions. After the necessary arrangements gear are created as 3D model. Generally these sofwares may AutoCAD, catia, solid works and the others. In this study two methods are applied. Ones, gear design software-excel-catia. Others, gear design software-text files-AutoCAD-catia.

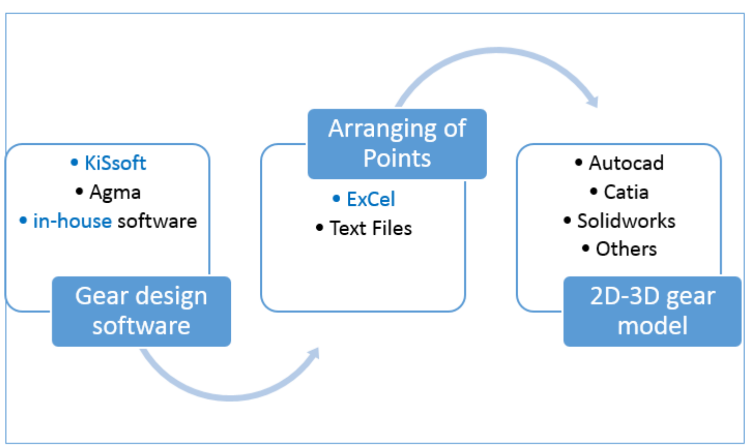

Figure B.24: Flowchart of design with gear curves regarding to coordinates

Following steps for “software-excel-catia method” are applied in this study;

- To generate tooth profile coordinates, In-house software is used. Output files of this program is shown in Figure B.25. Gear parameters are founded within this files. These coordinate points number are increased or decreased regarding to requirement. Shown parameters in this file are module, teeth number, pressure angle for coast and drive sides, tip diameter, base diameter, root diameter, tooth thickness of tip and pitch point and the other necessity parameters. In addition software allow to user that show view of the gear or gear pairs. Moreover, the movement of the gear and contact of the gear are observed by users.

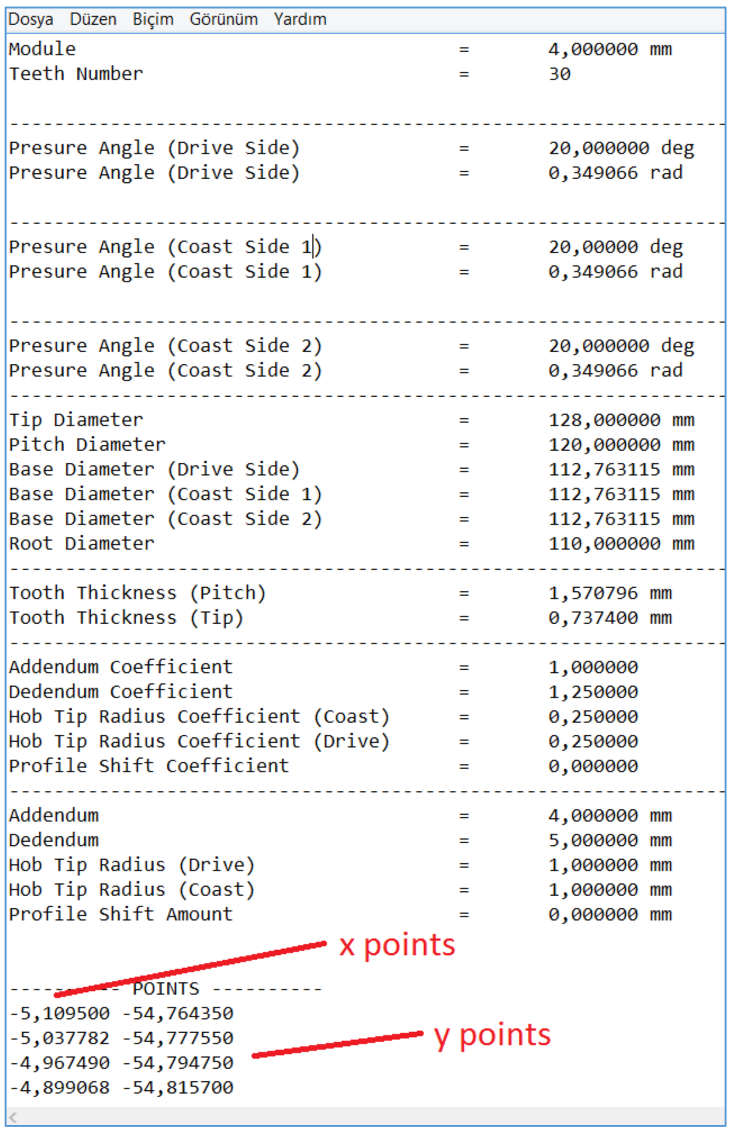

```
Dosya   Düzen   Biçim   Görünüm   Yardım
Module                                   =       4,000000 mm
Teeth Number                             =       30

----------------------------------------------------------------
Presure Angle (Drive Side)               =       20,000000 deg
Presure Angle (Drive Side)               =       0,349066 rad

----------------------------------------------------------------
Presure Angle (Coast Side 1)             =       20,00000 deg
Presure Angle (Coast Side 1)             =       0,349066 rad

----------------------------------------------------------------
Presure Angle (Coast Side 2)             =       20,000000 deg
Presure Angle (Coast Side 2)             =       0,349066 rad
----------------------------------------------------------------
Tip Diameter                             =       128,000000 mm
Pitch Diameter                           =       120,000000 mm
Base Diameter (Drive Side)               =       112,763115 mm
Base Diameter (Coast Side 1)             =       112,763115 mm
Base Diameter (Coast Side 2)             =       112,763115 mm
Root Diameter                            =       110,000000 mm
----------------------------------------------------------------
Tooth Thickness (Pitch)                  =       1,570796 mm
Tooth Thickness (Tip)                    =       0,737400 mm
----------------------------------------------------------------
Addendum Coefficient                     =       1,000000
Dedendum Coefficient                     =       1,250000
Hob Tip Radius Coefficient (Coast)       =       0,250000
Hob Tip Radius Coefficient (Drive)       =       0,250000
Profile Shift Coefficient                =       0,000000
----------------------------------------------------------------
Addendum                                 =       4,000000 mm
Dedendum                                 =       5,000000 mm
Hob Tip Radius (Drive)                   =       1,000000 mm
Hob Tip Radius (Coast)                   =       1,000000 mm
Profile Shift Amount                     =       0,000000 mm

---------- POINTS ----------
-5,109500 -54,764350
-5,037782 -54,777550
-4,967490 -54,794750
-4,899068 -54,815700
```


Figure B.25: Output files of program

- In text files, all parameters other than the x-y coordinates are delete and then save file (Figure B.26).

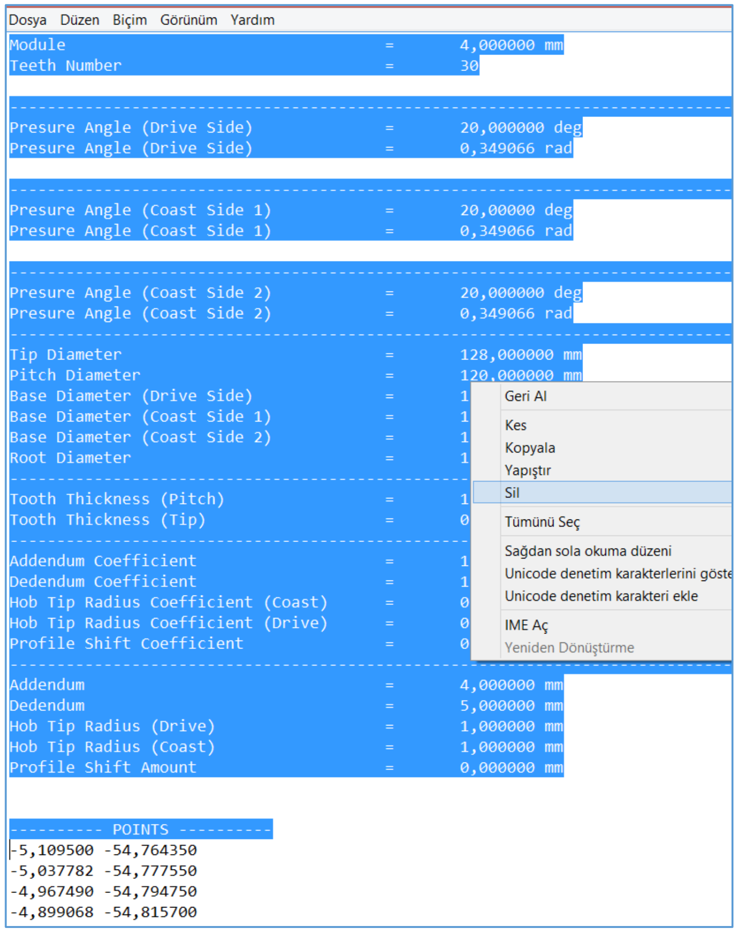

Figure B.26: Deleting parameters

- Start the excel and then to start the text import wizard, on the Data tab, in the Get External Data group, click From Text (Figure B.27).

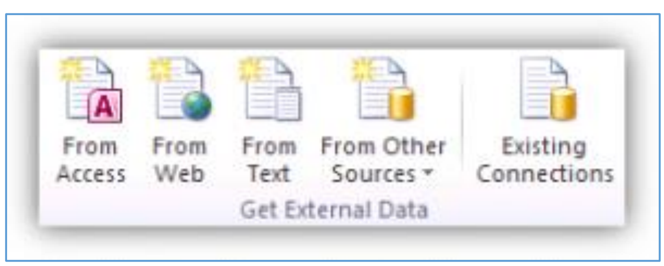

Figure B.27: Starting excel

Then, click from text. This will allow text file types such as prn, txt and csv to be imported. Browse to find the file you would like to import, select it and click Import (Figure 3.80).

Figure B.28: Imported text files

The Text Import Wizard appears to guide you through the process of importing your data (Figure B.29).

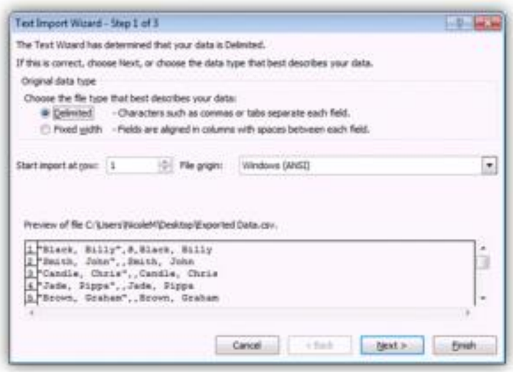

Figure B.29: The text import wizard

Select Delimited if the text contains a character such as a comma, tab, space or semi-colon to separate the various fields (Figure B.30). Otherwise select Fixed Width if there are a certain number of spaces between each field. A preview of the file is displayed below. If you would like to start the import at a row other than 1, enter the selected row number in the Start import at row field.

Tick tab-space and click next. Select type of character that separates the various fields. You can select as many as are applicable. If you would like to include your own characters that aren't listed, select the other checkbox and enter the specific character in the field provided.

Figure B.30: Second Step of text import wizard

A preview of the data in columns appears below, text is selected and click advance button. For decimal separator point and for thousands separator no one are selected. Click finish. Select where you would like the imported data to be in the workbook and click OK.

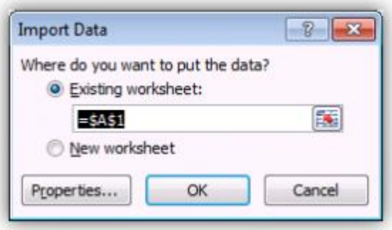

Figure B.31: A preview of the data

A view of the data in columns appears below. First column is x coordinates, second column is y coordinates and third column is empty. But in catia z coordinates need to be defined. So for third column add zero and save file.

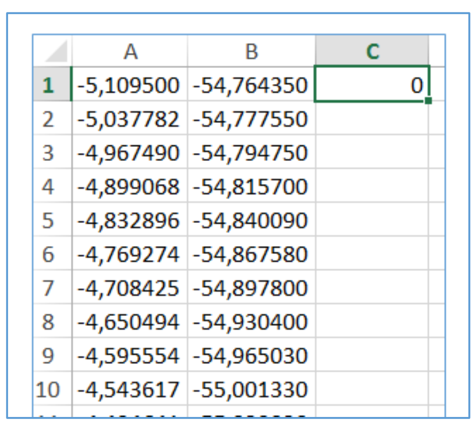

	A	B	C
1	-5,109500	-54,764350	0
2	-5,037782	-54,777550	
3	-4,967490	-54,794750	
4	-4,899068	-54,815700	
5	-4,832896	-54,840090	
6	-4,769274	-54,867580	
7	-4,708425	-54,897800	
8	-4,650494	-54,930400	
9	-4,595554	-54,965030	
10	-4,543617	-55,001330	

Figure B.32: A view of the data in columns

- Go to below command folder, where the catia is installed (Figure B.32).

C:\Program Files (x86)\Dassault Systems\B21\intel_a\code\command

GSD_PointSplineLoftFromExcel.xls excel files is found. This file is copied to another place to arrange it.

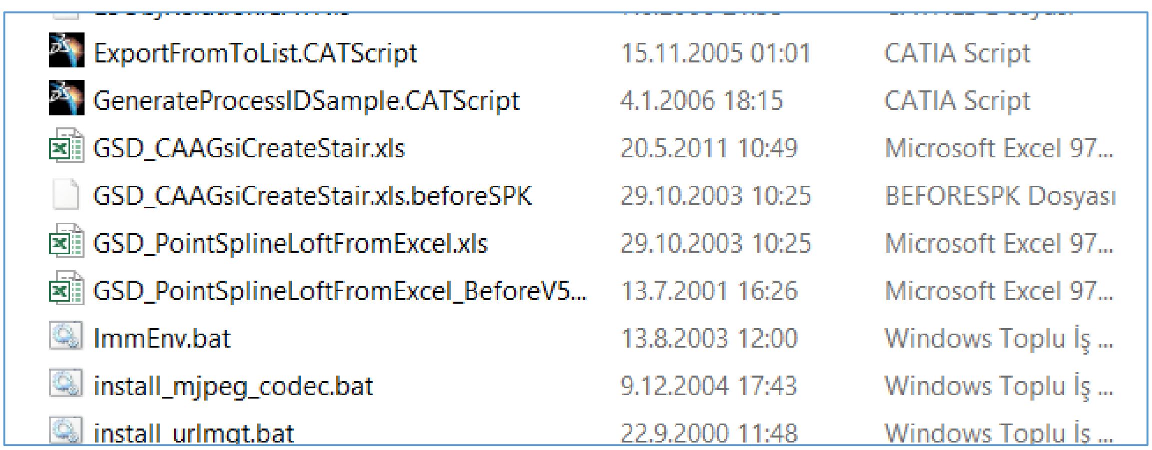

Figure B.32: Command folder of catia

Files is opened and selected area is deleted. Cells containing “EndCurve, EndLoft, End” are cut and replaced other cells different from A, B, C columns to import the data of gear.

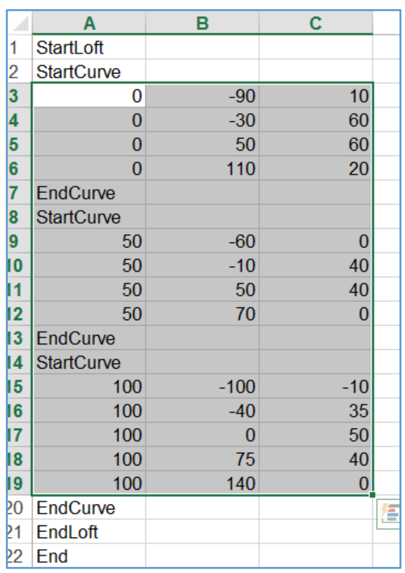

Figure B.33: Deleting of Selected Area

Excel file containing data of gear is opened. All of data are copied and replace in GSD_PointSplineLoftFromExcel.xls excel file.

	A	B	C	D
1	StartLoft			
2	StartCurve			
3	-5,109500	-54,764350	0	EndCurve
4	-5,037782	-54,777550	0	EndLoft
5	-4,967490	-54,794750	0	End
6	-4,899068	-54,815700	0	
7	-4,832896	-54,840090	0	
8	-4,769274	-54,867580	0	
9	-4,708425	-54,897800	0	
10	-4,650494	-54,930400	0	
11	-4,595554	-54,965030	0	
12	-4,543617	-55,001330	0	
13	-4,494641	-55,039030	0	
14	-4,448545	-55,077840	0	

Figure B.34: Excel file containing data of gear

Cells containing “EndCurve, EndLoft, End” are cut and replaced to end of A column.

	A	B	C
198	4,364519	-55,157970	0
199	4,405215	-55,117550	0
200	4,448545	-55,077840	0
201	4,494641	-55,039030	0
202	4,543617	-55,001330	0
203	4,595554	-54,965030	0
204	4,650494	-54,930400	0
205	4,708425	-54,897800	0
206	4,769274	-54,867580	0
207	4,832896	-54,840090	0
208	4,899068	-54,815700	0
209	4,967490	-54,794750	0
210	5,037782	-54,777550	0
211	5,109500	-54,764350	0
212	5,182149	-54,755320	0
213	EndCurve		
214	EndLoft		
215	End		

Figure B.35: Replacing of “EndCurve, EndLoft, End”

- Catia is started and new part is created.

Figure B.36: Starting of Catia

- Alt+F8 is clicked while GSD_PointSplineLoftFromExcel.xls excel file is opening. Macro windows appears. Main macro is selected and run.

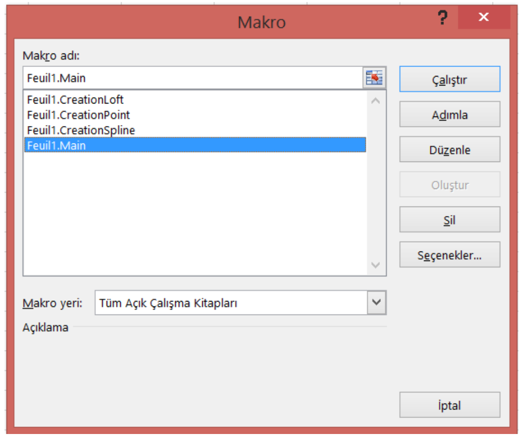

Figure B.37: Macro Window of Catia

Then a user info frame appears. In this there are 3 options. First, only points are created, second points and splines are created, third points, splines and loft are created. 2 is written in area and Ok is clicked.

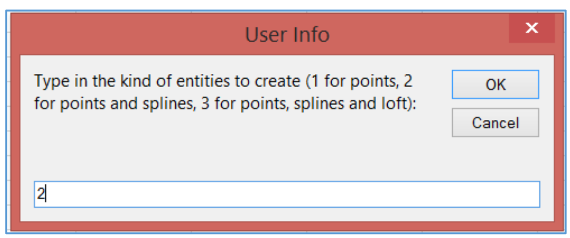

Figure B.38: Selecting of geometry command

A tooth points and spline of gear are created in catia as shown in Figure 4.94.

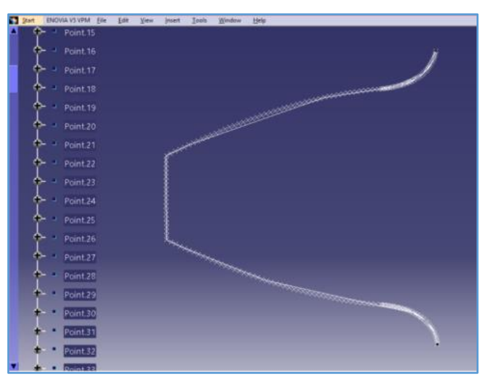

Figure B.39: View of Spline in Catia

After arranging in catia, a gear must be created illustrated in figure B.40.

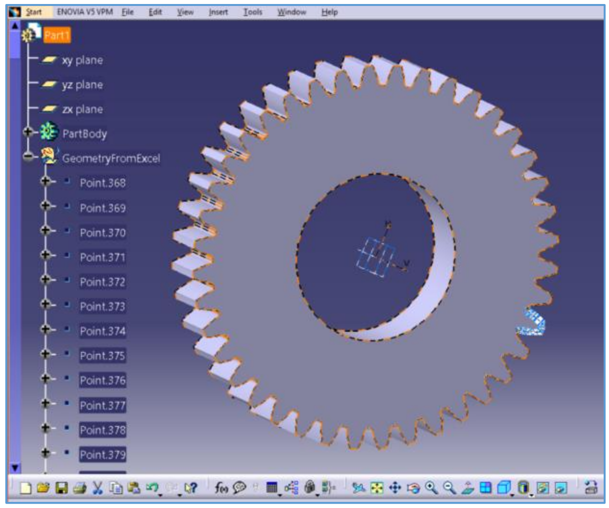

Figure B.40: Arranging of geometry in Catia

Following steps for "software-textfiles-autocad-catia method" are applied in this study;

- Output text file of B.Şahin's gear design software which is saved in previous section is opened. Spline is written to first row.

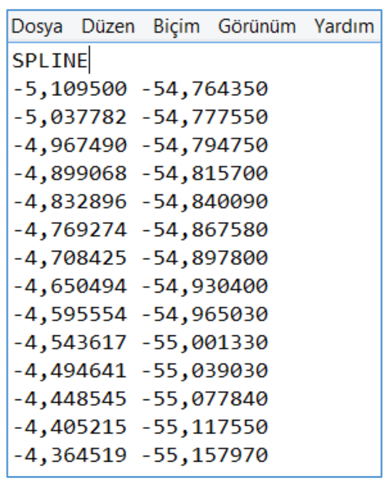

Dosya Düzen Biçim Görünüm Yardım

```
SPLINE
-5,109500 -54,764350
-5,037782 -54,777550
-4,967490 -54,794750
-4,899068 -54,815700
-4,832896 -54,840090
-4,769274 -54,867580
-4,708425 -54,897800
-4,650494 -54,930400
-4,595554 -54,965030
-4,543617 -55,001330
-4,494641 -55,039030
-4,448545 -55,077840
-4,405215 -55,117550
-4,364519 -55,157970
```

Figure B.41: Output text file of B.Şahin's gear design software

- Replace is selected within EDIT menu

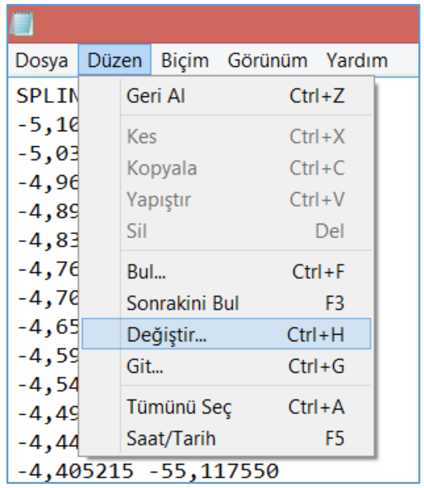

Figure B.42: Starting of replacing menu

- Replace window appears below. Sought value must be “,” (comma) and new value must be “.”(Point). Because AutoCAD recognizes the decimal symbol as point. Comma is used as coordinate recognizing. After replace all is selected.

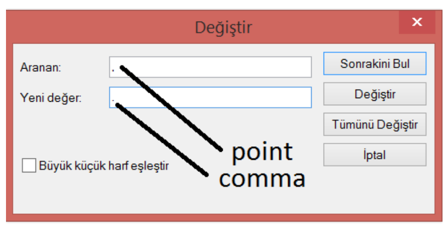

Figure B.43: Replace of comma and point

- Gap between two coordinates are copied and paste it to sought value. New value must be “,” (comma). Then click replace all.

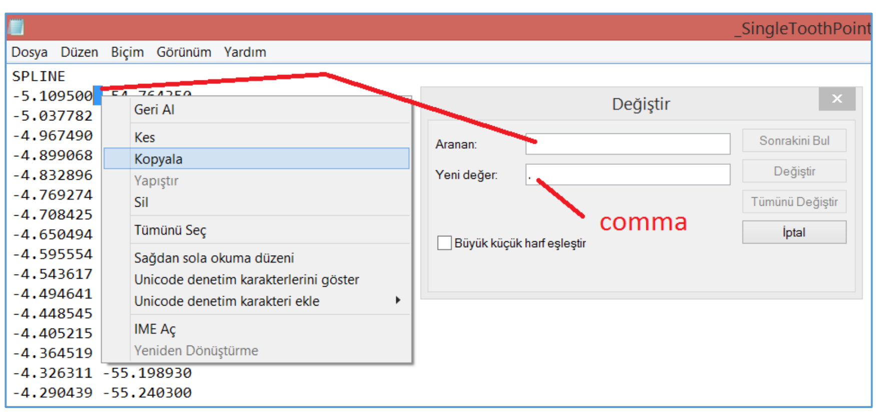

Figure B.44: Replace of comma and gap

- The file is saved as “tooth_profile.scr” anywhere.

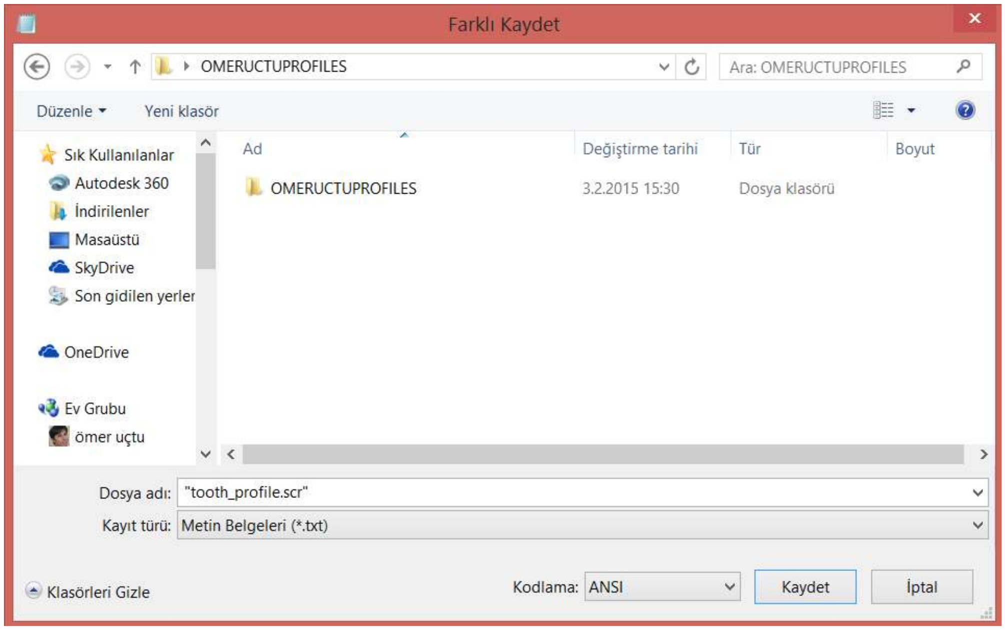

Figure B.45: Saving of File

- AutoCAD is opened and “scr” is typed on command window and entered. Then saved “tooth_profile” file is import from where is saved.

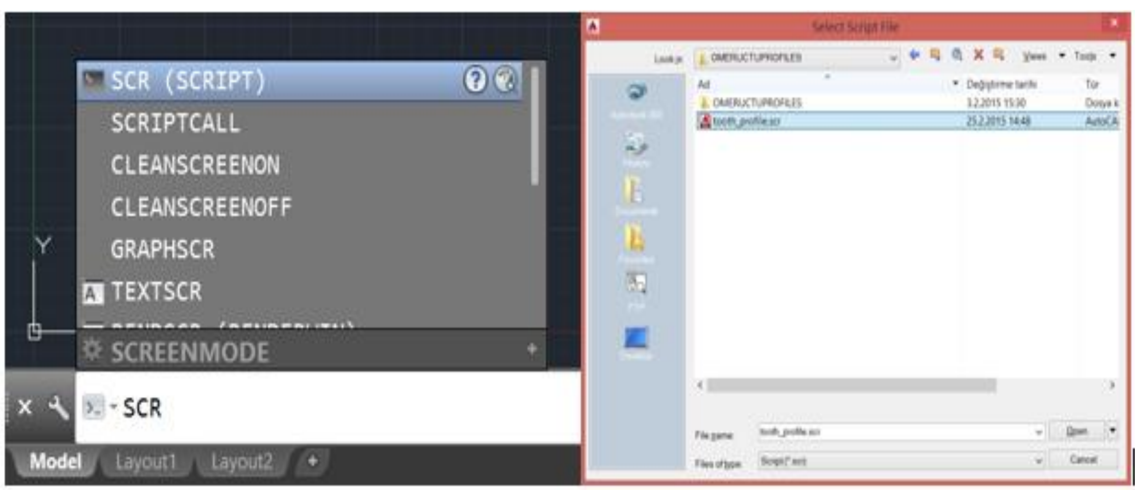

Figure B.46: SCR Command and Importing File

- When the curve is imported, push enter button twice on keyboard. Curve is shown in fig. Program draw the curve linked to 0, 0, 0 point. Main of this, center of the gear is 0, 0, 0 point.

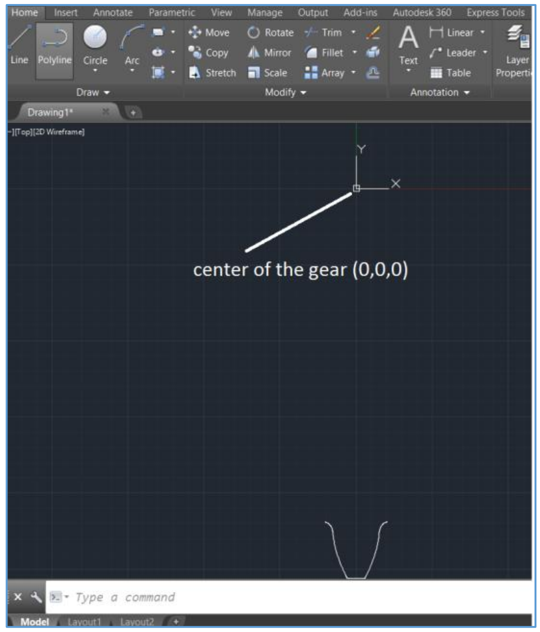

Figure B.47: View of Curve in AutoCAD

Tooth curve is increased by polar array command. In this application teeth number is 30. So each angle between two teeth is $360^0/30=12^0$. Regulating of gear, it is as shown in fig. After the AutoCAD file is saved as .dxf or .dwg format. It must be saved as 2007 version. Because 3D softwares can’t open (Figure B.48).

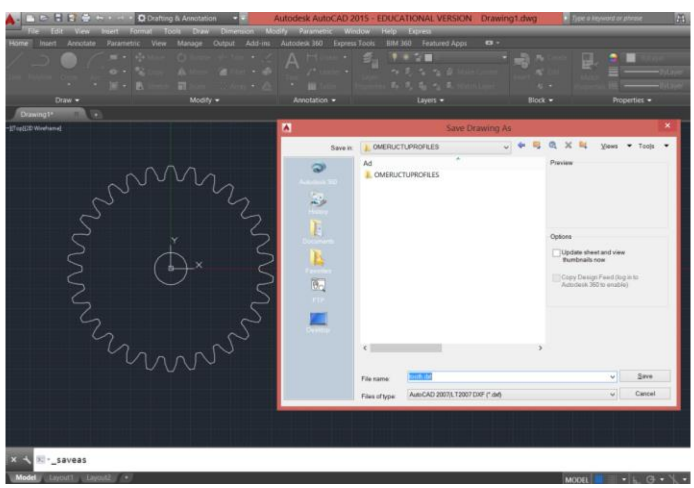

Figure B.48: Rotating of Tooth

- Catia is started and new part is created. The saved file is dragged and dropped in catia. Model appears below. Main view is copied and pastes to the part file (Figure B.49).

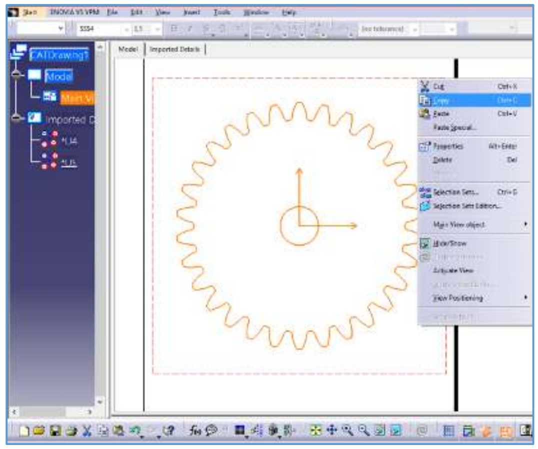

Figure B.49: Importing Geometry to Catia in Draft File

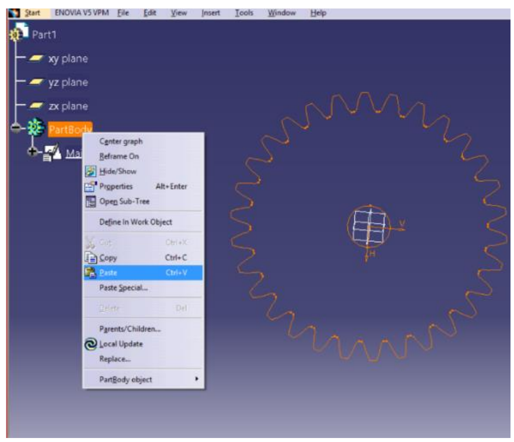

Figure B.50: Importing Geometry to Catia in Part Design

- Finally, model is padded and created as shown in figure B.51.

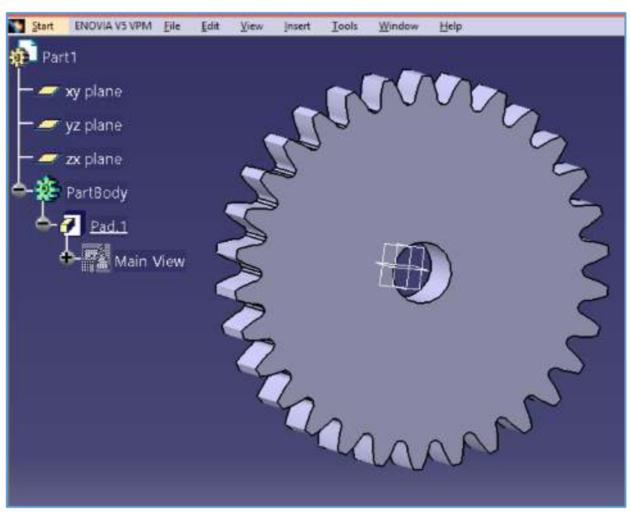

Figure B.51: Padded of Gear Geometry

APPENDIX C

FINITE ELEMENT ANALYSIS

GENERAL INFORMATION

Finite element method (FEM) is a numerical method for solving a differential or integral equation. It has been applied to a number of physical problems, where the governing differential equations are available. The method essentially consists of assuming the piecewise continuous function for the solution and obtaining the parameters of the functions in a manner that reduces the error in the solution.

Shortly, FEM is;

- A numerical method.
- Traditionally, a branch of Solid Mechanics.
- Nowadays, a commonly used method for multiphysics problems.

FEM can be applied following areas;

- Structure analysis: a cantilever, a bridge, an oil platform…
- Solid mechanics: a gear, an automotive power train …
- Dynamics: vibration of Sears Tower, earthquake, bullet impact…
- Thermal analysis: heat radiation of finned surface, thermal stress brake disc…
- Electrical analysis: piezo actuator, electrical signal propagation…
- Biomaterials: human organs and tissues…
- Others…

There are many professional softwares for FEM. Some of them, Simxpet, ansys, abacus and the others. In this study Simexpert was used.

SimXpert is a unified computer aided engineering environment for product simulation that enables manufacturers to accelerate the speed and accuracy of simulation, increase design productivity, and bring better products to market faster. SimXpert accomplishes this by integrating multidiscipline analysis capabilities, the best simulation methodologies, and a high degree of customization all into one engineering environment. Given SimXpert's unified engineering environment, analysts and designs can reduce the number of tools in their engineering workflow and better share critical information with each other.

SimXpert provides multiple workspaces for structural, thermal, explicit dynamics, systems and controls, and multibody dynamics that allow analysts to easily move from one discipline to another while sharing data models and results. This enables all the CAE teams to share the information more effectively, without data loss.

ELEMENT TYPES

Finite elements themselves are defined by both their topology (i.e., their shape) and their properties. For example, the elements used to create a mesh for a surface may be composed of quadrilaterals or triangles. Similarly, one element may be a steel plate modeling structural effects such as displacement and rotation, while another may represent an air mass in an acoustic analysis. Both the shapes and properties supported depend upon the analysis program you are using with Simxpert, as defined in your Analysis Preferences.

At this stage of using Simxpert, where you are creating a finite element mesh using the Finite Elements application form, elements are defined purely in terms of their topology. Other properties such as materials, thickness and behavior types are then defined for these elements in subsequent applications, and discussed in later chapters of this guide.

The table below describes the element topologies supported by Simxpert. The columns in the table provide the following information:

• The left-hand column lists seven element shapes and illustrates each with a common node configuration.

• The Structural Uses column describes typical usage conditions for the element shapes. For example, use Bar-shaped elements if you plan to define the element properties as bars, springs, or gap elements.

• The Mesher Support column indicates which mesher-node configuration combinations are supported for each element shape.

Table C.1: Elements Type of Mesh

Element Shape	Node Configurations and Mesh Techniques Supported	Structural Uses
Point 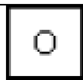		Use Point for a concentrated mass, spring, or damper to ground.
Bar 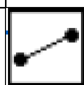	Isomesh supports Bar1, Bar2, and Bar4 elements.	Use Bar when the stress state varies in one dimension, and when properties of the element are defined along a curve or straight line.
Tria 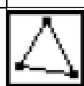	Isomesh and Paver support Tria3, 4, 6, 7, 9, and 13 elements.	Use Tria and Quad when the stress state varies in two dimensions and is constant in the third. You can also use Tria and Quad when one dimension of the area to be modeled is very small in comparison to the other two.
Quad 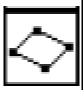	Isomesh and Paver support Quad4, 5, 8, 9, 12, and 16 elements.	
Tet 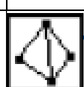	Isomesh supports Tet4, 5, 10, 11, 14, 15, 16, and 40 elements. Tet Mesh - Tet4, 10, and 16.	Use Tet, Wedge and Hex when the stress state varies in all three dimensions, and all three dimensions of the area to be modeled are comparable. Simxpert supports a variety of node configurations for each of these elements.
Wedge 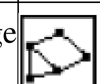	Isomesh supports Wedge6, 7, 15, 16, 20, 21, 24, and 52 elements.	
Hex 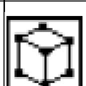	Isomesh supports Hex8, 9, 20, 21, 26, 27, 32, and 64 elements.	

MESH GENERATION TECHNIQUES

There are four basic mesh generation techniques available in Simxpert: IsoMesh, Paver Mesh, Auto TetMesh, and 2-1/2D Meshing. This section describes each meshing technique. Selecting the right technique for a particular model must be based on geometry, model topology, analysis objectives, and engineering judgment.

Isomesh

This approach creates elements within a regularly shaped region of geometry via simple subdivision (Figure C.1).

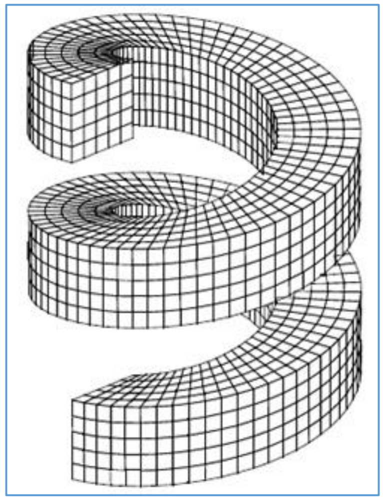

Figure C.1: Example of solid IsoMesh

Paver

The Paver is an automated surface meshing technique that you can use with any arbitrary surface region, including trimmed surfaces, composite surfaces, and irregular surface regions. Unlike the IsoMesh approach, the Paver technique creates a mesh by first subdividing the surface boundaries into mesh points, and then operates on these boundaries to construct interior elements (Figure C.2).

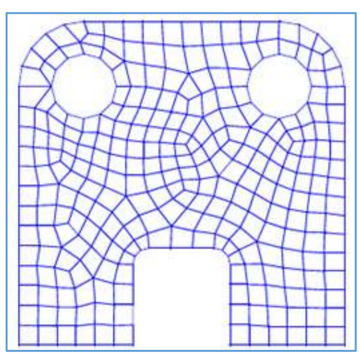

Figure C.2: Example of Paver mesh technique

Auto TetMesh

The Auto TetMesh approach is a highly automated technique for meshing arbitrary solid regions of geometry. It creates a mesh of tetrahedral (4-noded solid) elements for any closed solid, including boundary representation (B- rep) solids, as well as regular solid regions (Figure C.3).

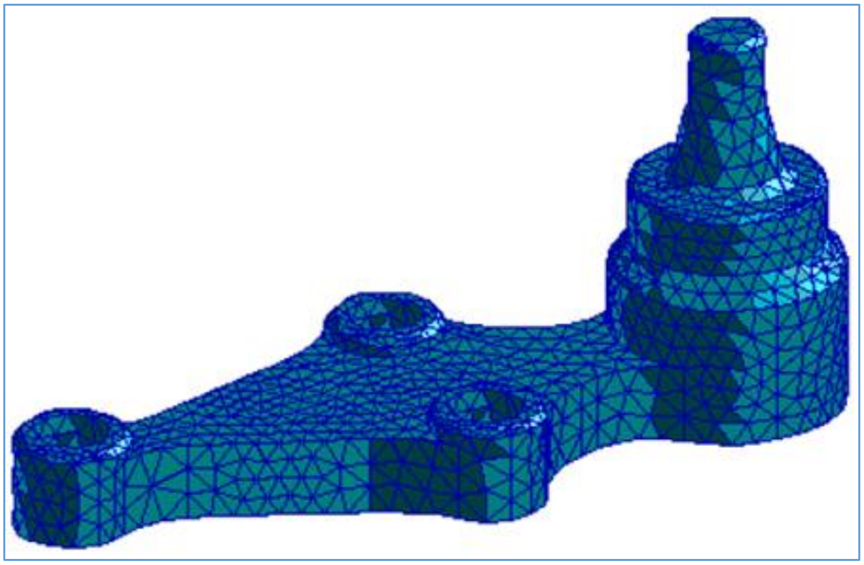

Figure C.3: Auto Tet Mesh technique

2 D Meshing

A planar 2D mesh can also be transformed to produce a 3D mesh of solid elements, using sweep and extrude operations (Figure B.4).

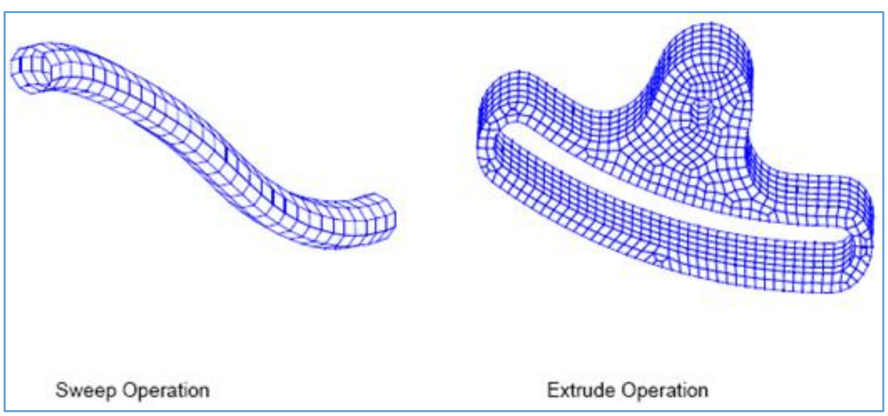

Figure C.4: Example of 2D meshing.

Important points to note are:

- The direction and element density in the sweep or extrude direction can be specified with this 2D to 3D transformation approach.

- This technique produces elements that maintain no associativity with any parent geometry. This prevents subsequent loads, boundary conditions and properties from being assigned via geometric entities for these elements.

ANALYSIS OF THE PARTS

Shaft Analysis

In this study, shaft which is the most important and precision part of gearbox is analyzed with using Simxpert software. Moment, deflection and Von-Mises Stress of Shaft is observed. For these analyses in Simxpert, following steps are applying.

- Analytical designed shaft is drawn as 3D with using Catia V5 software. Shaft is saved as suitable extension like .stp, .parasolid, .iges or others to import to Simxpert.
- Shaft is imported to Simxpert and some geometrical challenges are applied.
- Shaft material is described. Here elastic modulus and Poisson's ratio are described.
- Shaft is meshed.
- Shaft is fixed from places of bearings and loads are applied from gear placed.

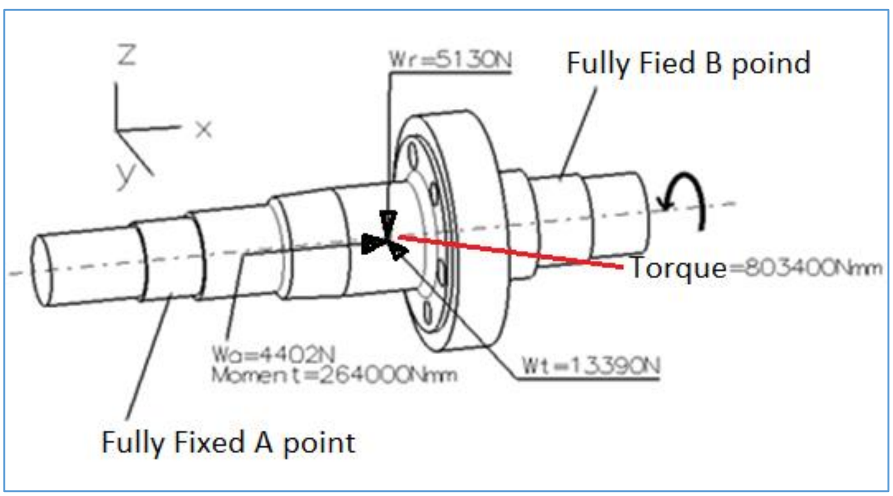

Figure C.5: Application Points of Loads

Areas is illustrated in Fig. are critical points of shaft when shaft is fixed and loads are applied as shown in Figure C.5. Shaft is meshed via CTETRA10 elements as solid in

Figure C.6. There are 505373 elements. Mesh size is 2mm.The mesh statistics are shown in Figure C.7.

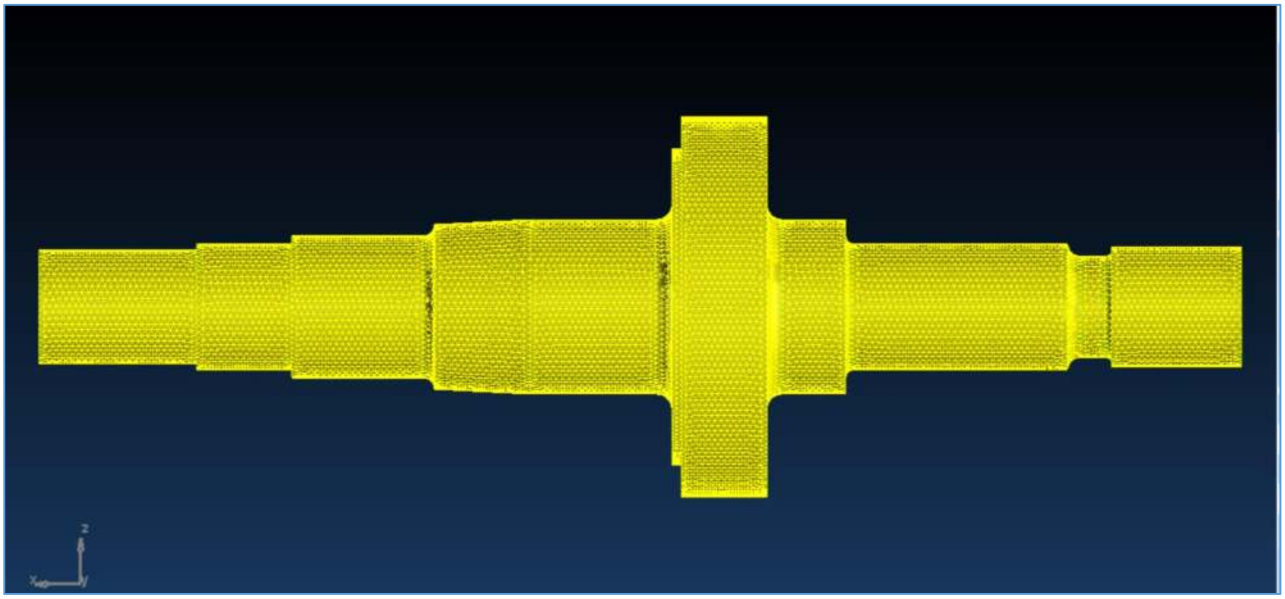

Figure C.6: Meshing of Shaft

```
Statistics
Statistics For Current Scene
=================================================================
GRID                    Entities =  717218
Parts          =    1
--------------------------------------------------------------
Solid                  Elements =  505373      100.0%
 CTETRA10                 Elements =  505373                 100.0%
--------------------------------------------------------------
Elements          =  505373
--------------------------------------------------------------
--------------------------------------------------------------
Curves        =    173
--------------------------------------------------------------
--------------------------------------------------------------
Surfaces       =    60
--------------------------------------------------------------
--------------------------------------------------------------
Solids        =    1
--------------------------------------------------------------
Statistics For Other Entities in Current Model
=================================================================
```

Figure C.7: Mesh Statistics of Shaft

According to analysis maximum Von Misses stresses are became on described points within previous chapter. In analysis on this point von-Misses stress is found as 60,5MPa (Figure C.8).

Error ratio of between finite element analysis and analytical solution is;

$$r = \frac{X_t - X_i}{X_i} * 100 \qquad \text{(C.1)}$$

$$r = \frac{60.5 - 60.1}{60.5} * 100$$

$$r = 0.6\%$$

According to this equation r is error ratio, X_t is finite element analysis solution and X_i is analytical solution.

Normally, critical points occur in applied torque area and challenge areas of shaft diameter. Critical points at analytical solution and finite element solution occur on same points. A-20 Steel 1050 CD can be used as shaft material. Yield stress of this material is 580Mpa. If safety factor is 3, yield stress of material at analytical solution is 3*60.5 MPa=181.5 MPa. So A-20 Steel 1050 CD material can be safety used.

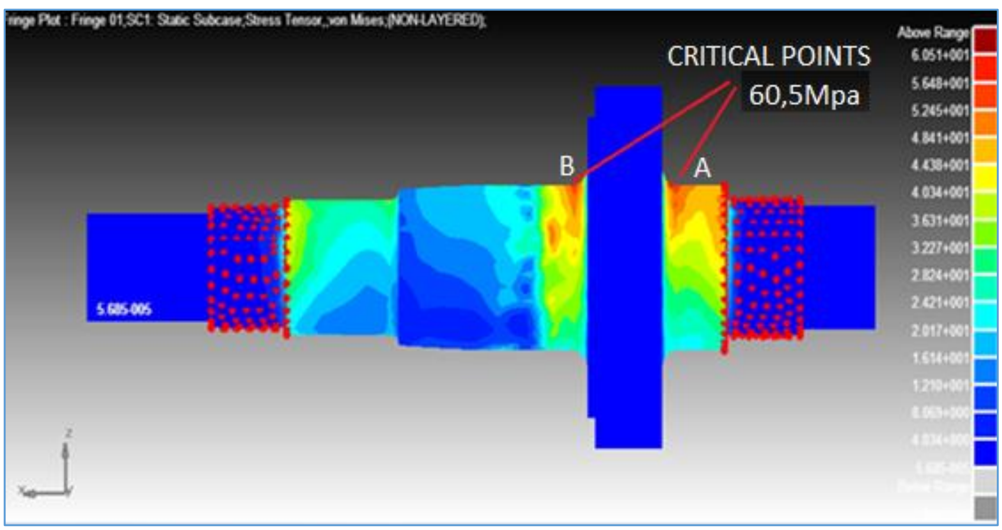

Figure C.8: Von-Mises Stress and Critical Points of Shaft

At the same conditions maximum deflection of shaft occurs in applied loads points. Maximum deflection is 24 micrometers. Deflection graph on x-axis is draw as shown in below Figure C.9. Finite element analysis and analytical solution values are nearly same.

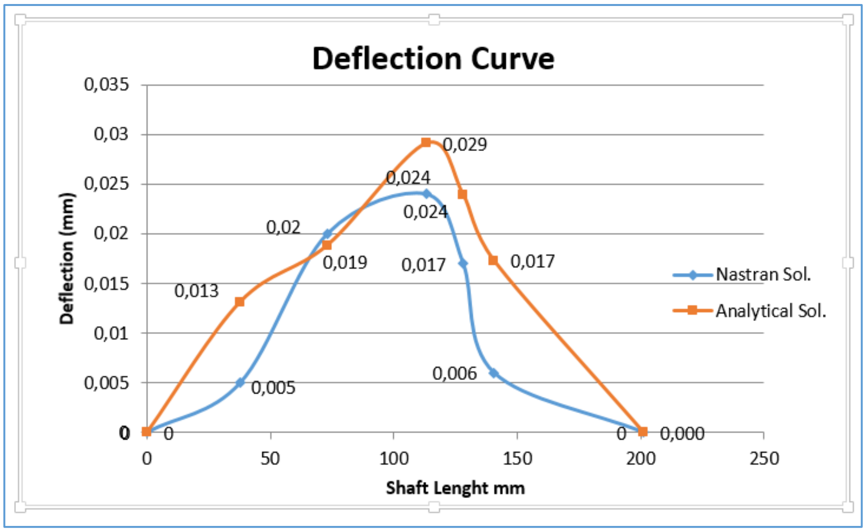

Figure C.9: Discussion of Deflection both FEM and Analytical Solution

Coupling Analysis

Coupling is fixed from four pin holes and 803.4 Nm torque is applied from x center axis as shown in Figure C.10.Von Misses stress is illustrated in Figure C.13. It is found as 35.5 MPa.

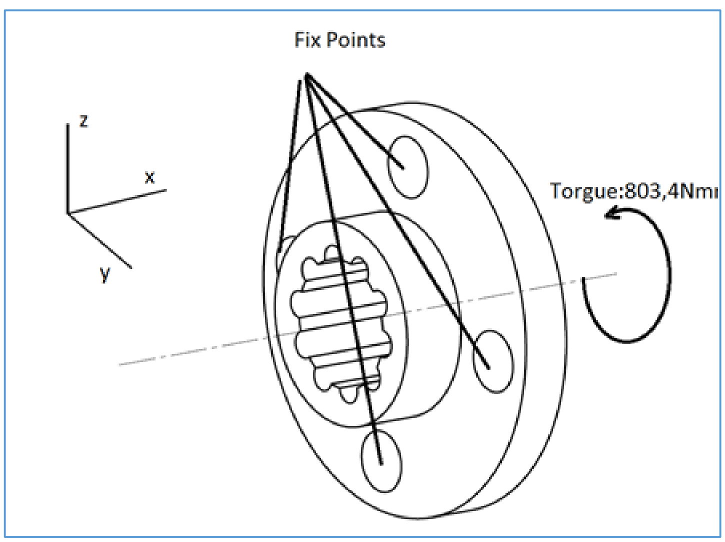

Figure C.10: Application Point of Fix and Torque for coupling

Coupling is meshed via CTETRA10 elements as solid in Figure C.11. There are 133880 elements. Mesh size is 2 mm. The mesh statistics are shown in Figure C.12.

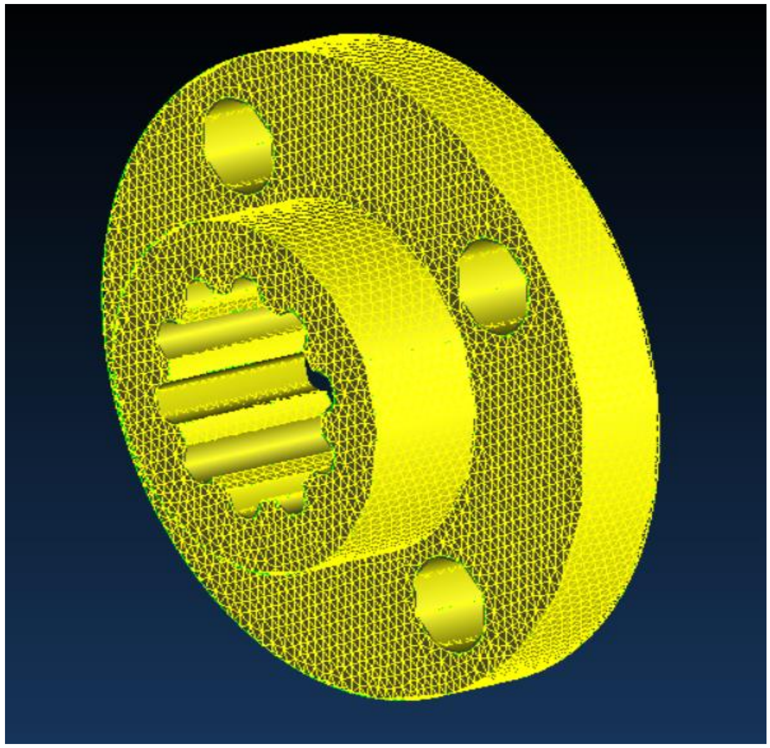

Figure C.11: Meshing of Coupling

```
                                   Statistics
Statistics For Current Scene
========================================================================
GRID                  Entities =  197028
Parts          =     1
------------------------------------------------------------
Solid                 Elements =  133880     100.0%
 CTETRA10                 Elements =  133880              100.0%
------------------------------------------------------------
Elements        =  133880
------------------------------------------------------------
------------------------------------------------------------
Curves       =    134
------------------------------------------------------------
------------------------------------------------------------
Surfaces      =    39
------------------------------------------------------------
------------------------------------------------------------
Solids       =    1
------------------------------------------------------------
Statistics For Other Entities in Current Model
========================================================================
```

Figure C.12: Mesh Statistics of Coupling

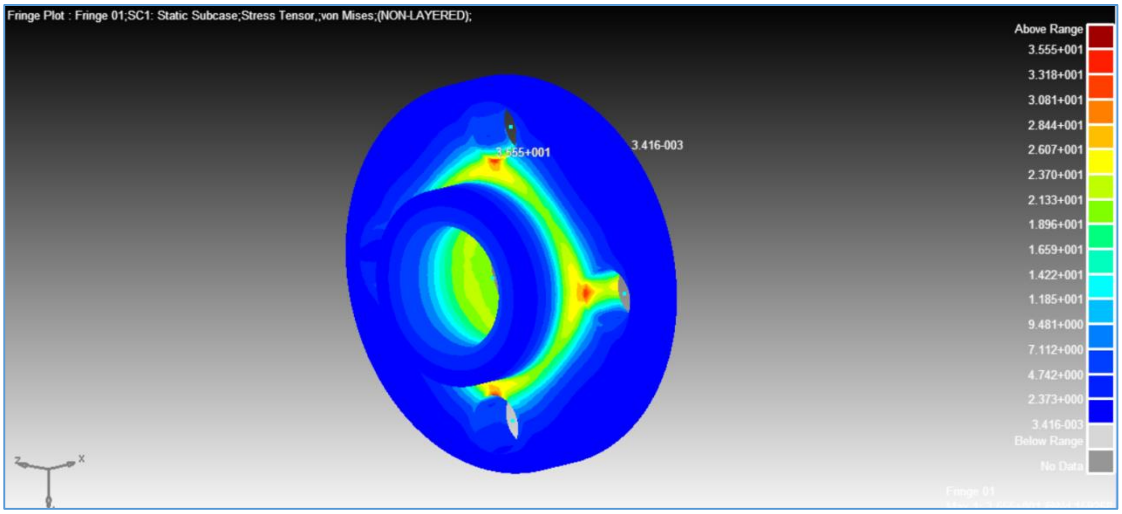

Figure C.13: Results of Coupling FEM

Rods Analysis

Rod 1 is fixed from one side which is end of rod and 803.4 Nm torque is applied from x center axis as shown in Figure C.14. Von Misses stress is illustrated in Figure C.17. It is found as 398 MPa.

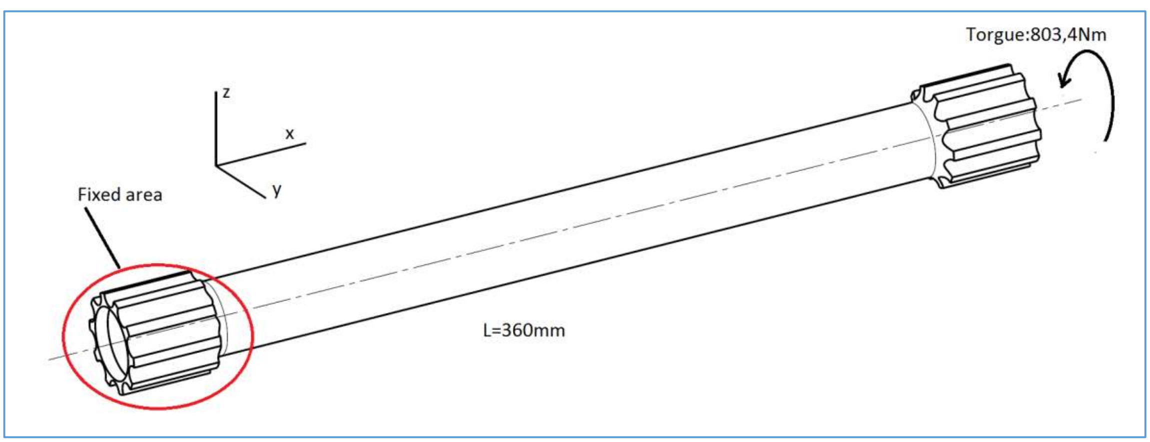

Figure C.14: Application Point of Fix and Torque for Rod 1

Rod 1 is meshed via CTETRA10 elements as solid in Figure C.14. There are 181198 elements. Mesh size is 2 mm. The mesh statistics are shown in Figure C.15.

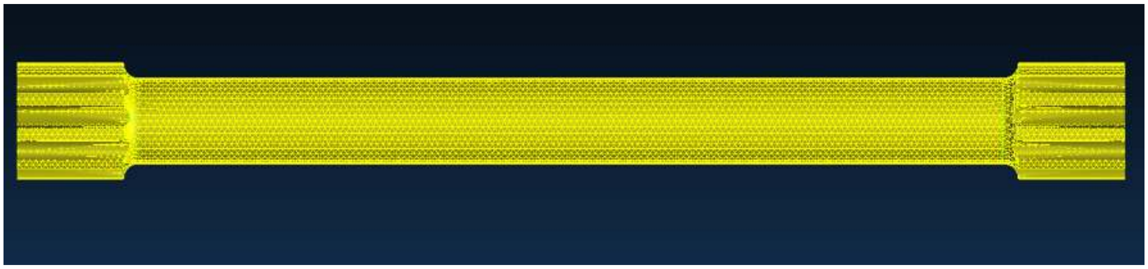

Figure C.15: Meshing of Rod 1

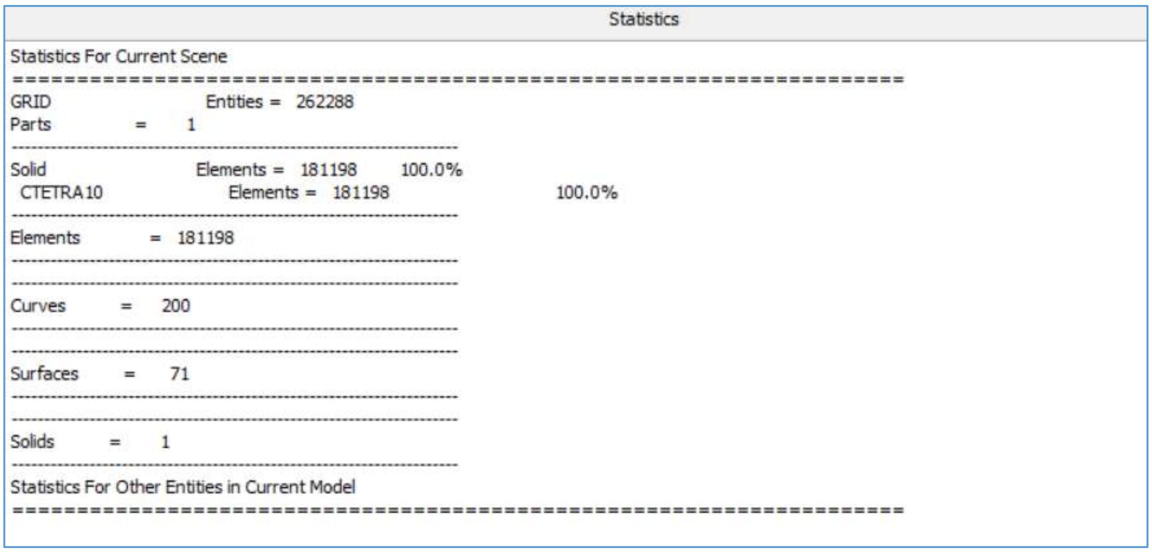

Figure C.16: Mesh Statistics of Rod 1

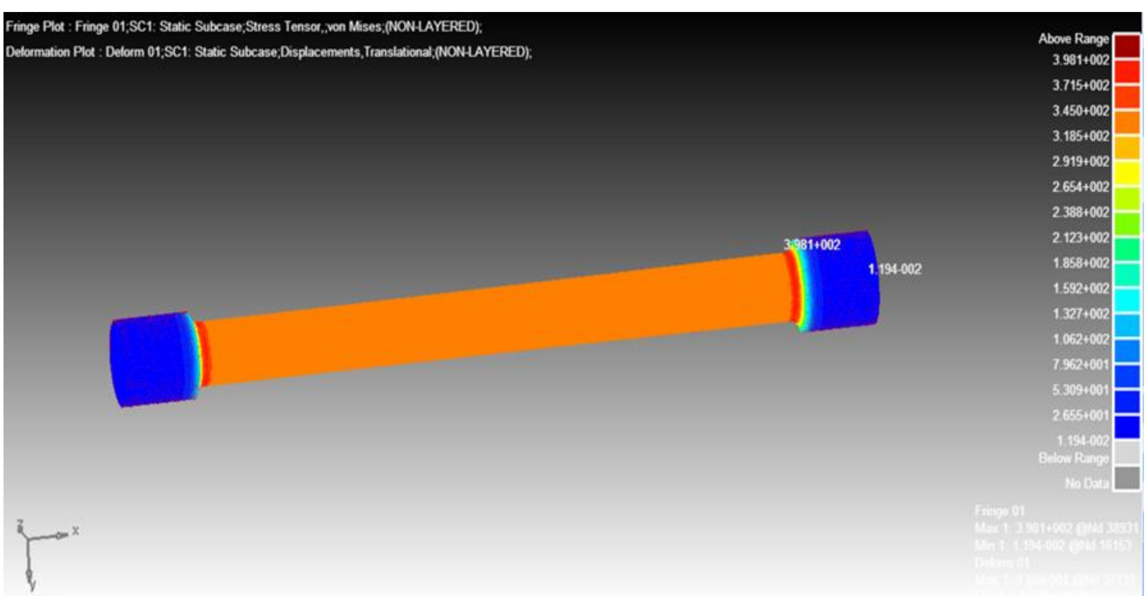

Figure C.17: Results of Rod 1 FEM

Rod 2 is fixed from one side which is end of rod and 803.4 Nm torque is applied from x center axis as shown in Figure C.18. Von Misses stress is illustrated in Figure C.20. It is found as 407 MPa.

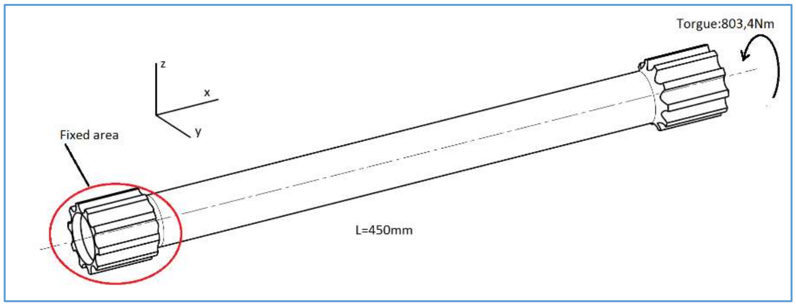

Figure C.18: Application Point of Fix and Torque for Rod 2

It is meshed via CTETRA10 and its element size is 2 mm as shown in Figure C.18.There are 215665 elements.

Figure C.19: Meshing of Rod 2

Figure C.20: Results of Rod 2 FEM

Torque Coupling Analysis

Torque Coupling is fixed from two pin holes and 803.4 Nm torque is applied from x center axis as shown in Figure C.21. Von Misses stress is illustrated in Figure C.24. It is found as 22.3 MPa.

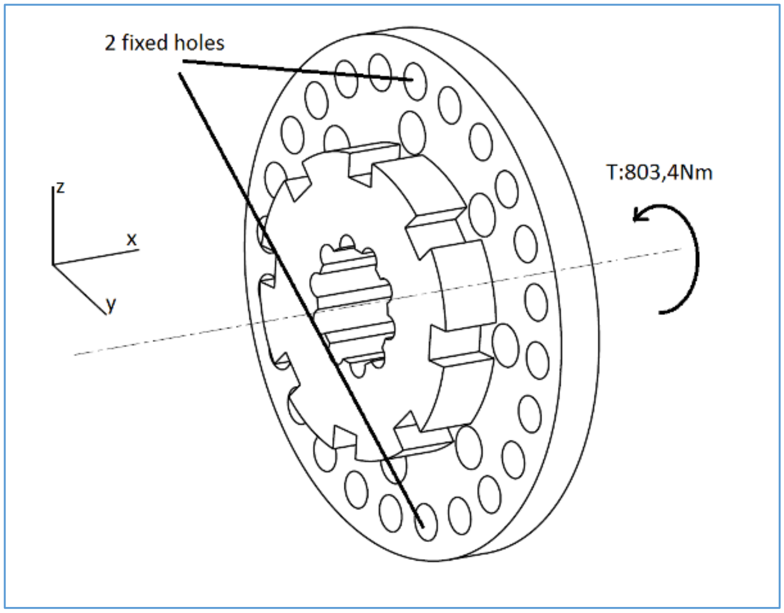

Figure C.21: Application Point of Fix and Torque for Torque coupling

Torque Coupling is meshed via CTETRA10 elements as solid in Figure C.22. There are 299455 elements. Mesh size is 2 mm. The mesh statistics are shown in Figure C.23.

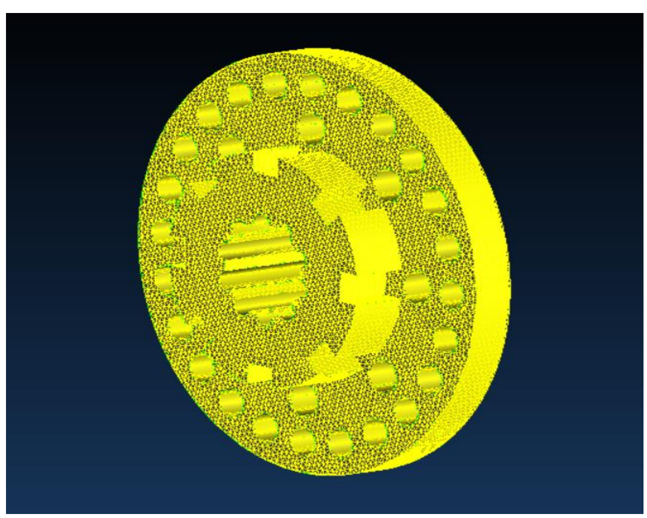

Figure C.22: Meshing of Torque Coupling

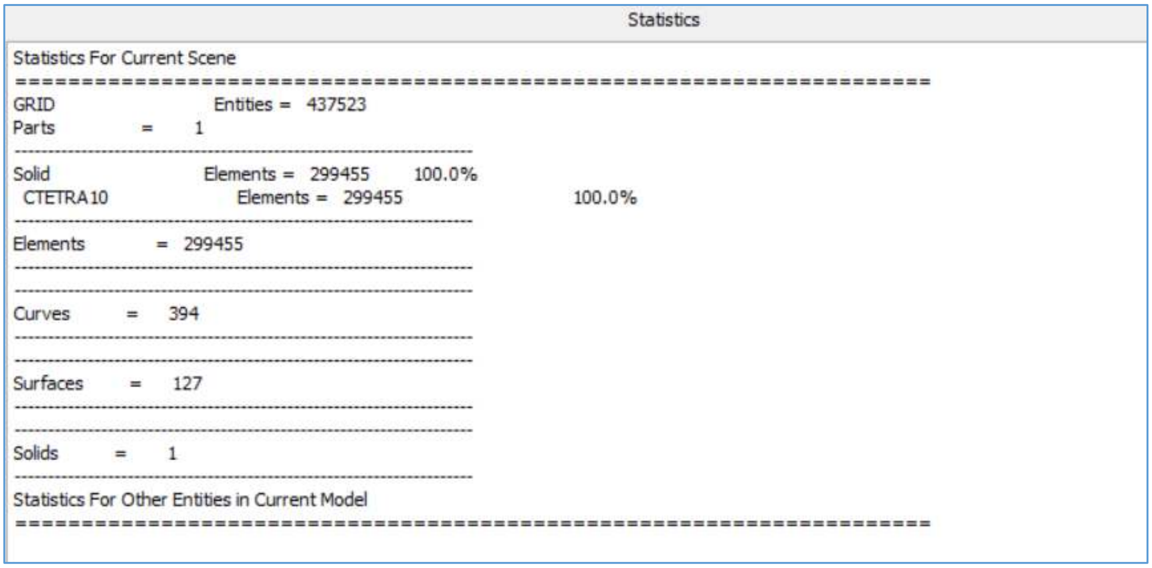

Statistics

Statistics For Current Scene

==

GRID Entities = 437523

Parts = 1

Solid Elements = 299455 100.0%

CTETRA10 Elements = 299455 100.0%

Elements = 299455

Curves = 394

Surfaces = 127

Solids = 1

Statistics For Other Entities in Current Model

==

Figure C.23: Mesh Statistics of Torque Coupling

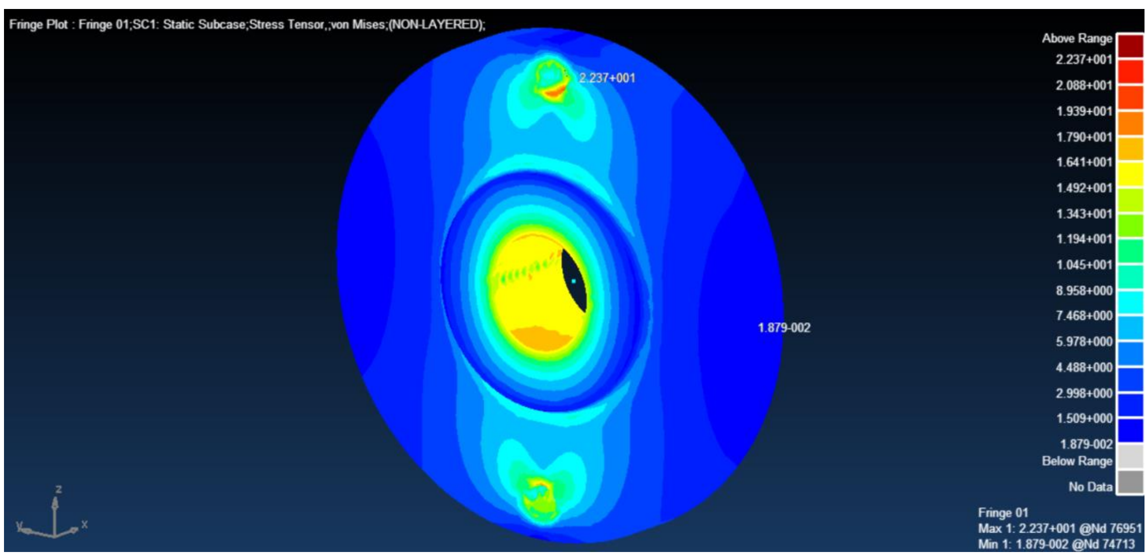

Figure C.24: Results of Torque Coupling FEM

Gear Liner Static Analysis

Spur gear liner static analysis is described step by step.

- Units is arranged (Figure C.25).

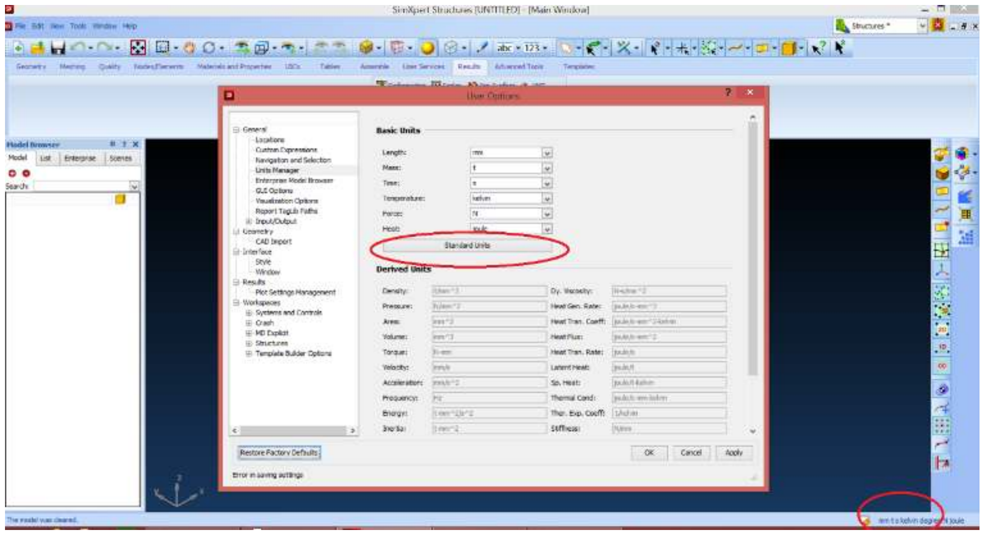

Figure C.25: Definition of Units

- Gear is imported as*.stp extension. (Figure C.26) (Parasolid extension is recommended.)

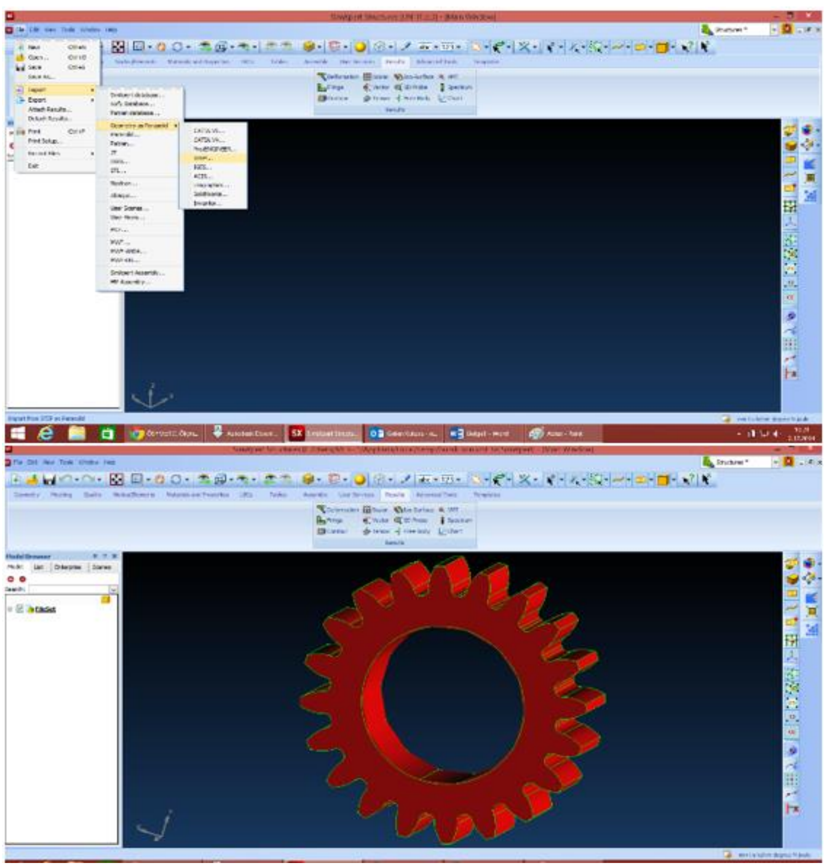

Figure C.26: Imported of Gear

- Gear is set from solid to surface with Geometry- mid-surface-automatic to solve rapidly. In extract midsurface window select gear body within solid bodies section and activate delete solid (Figure C.27).

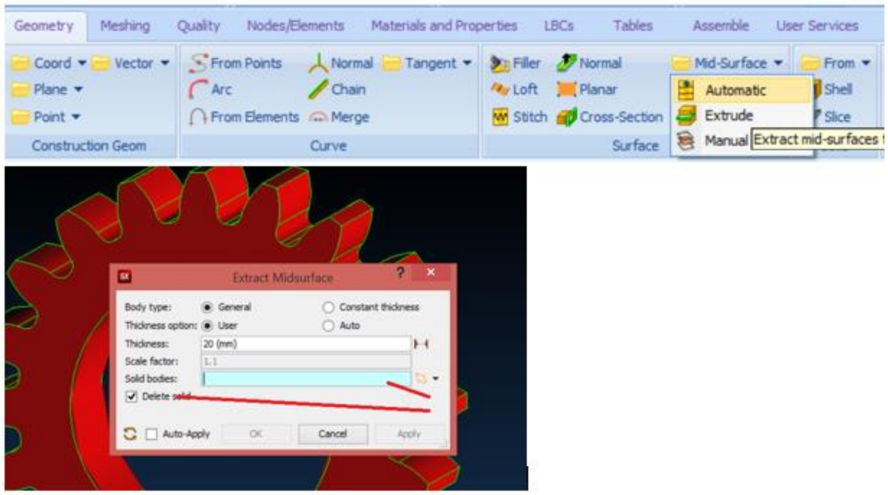

Figure C.27: Midsurface of Gear

- Center point of gear is described with Geometry-Point-Mass center (Figure C.28).

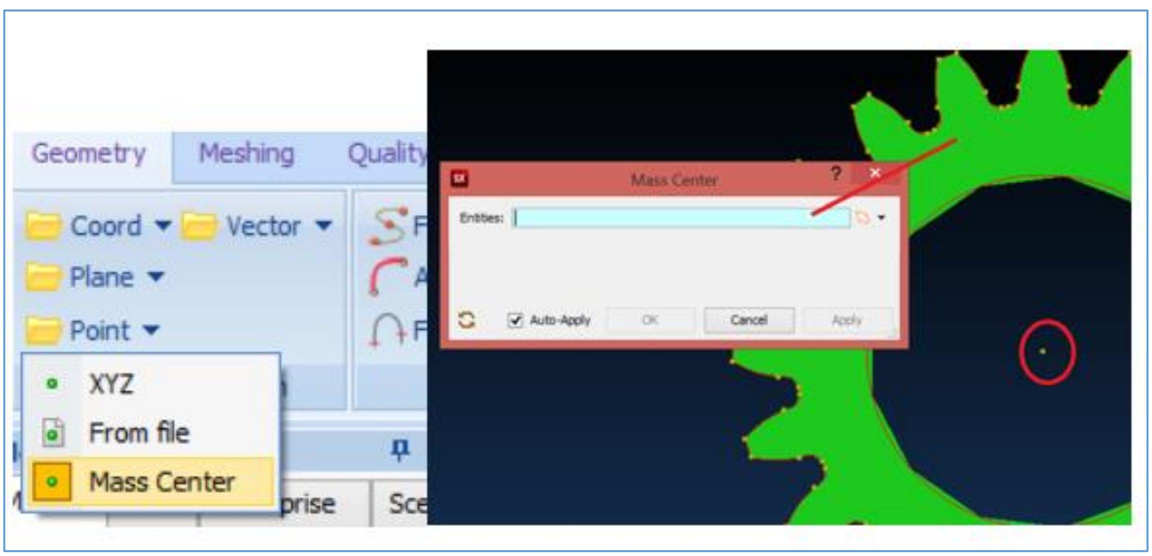

Figure C.28: Definition Center Point of Gear

- Spline is created with Geometry-From points and Polyline –N points are activated and three points are selected then Ok (Figure C.29).

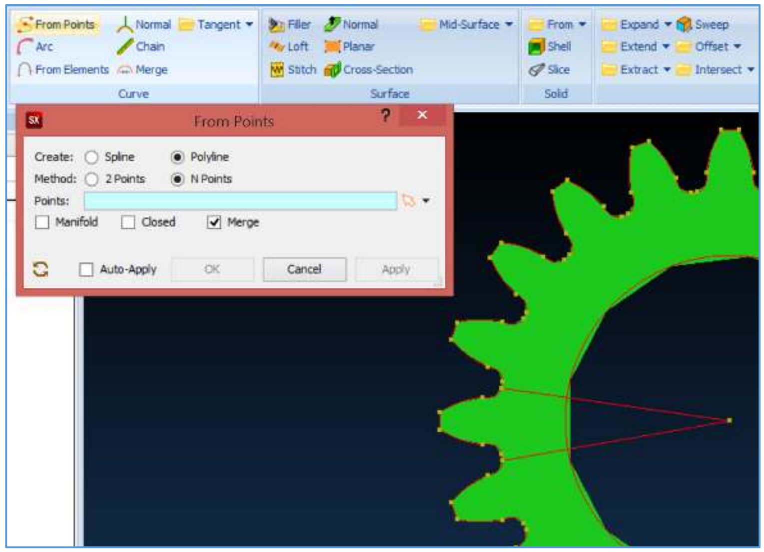

Figure C.29: Spline Creating to Split

- Area between this spline is split with Geometry-Split-Surface by Curves. Whole area is selected for entities and split curves is selected for curves. Then Ok. Gear surface is divided two parts (Figure C.30).

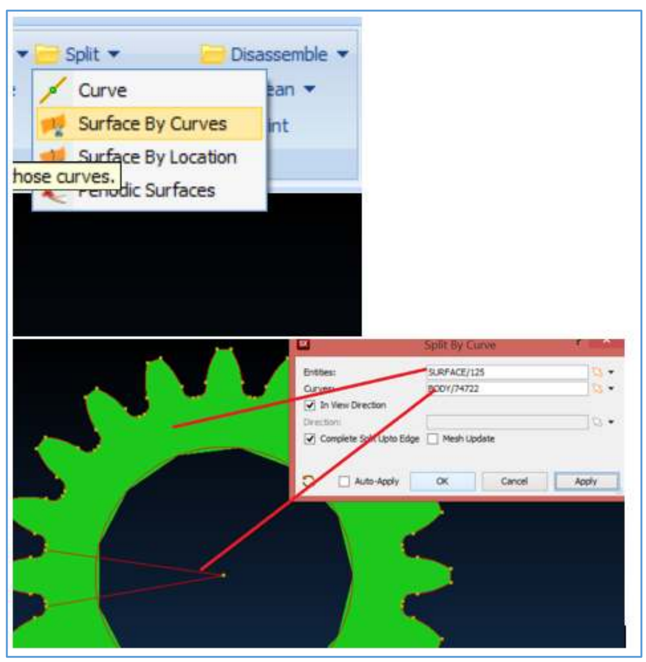

Figure C.30: Splitting a Tooth

- Material is defined under Materials and Properties selection isotropic. Young's modulus and Poisson's ratio are added. Property is defined as shell selection two surfaces in Entities, material is selected and gear thickness is added (Figure C.31).

Figure C.31: Adding Material Properties

- Meshing surface by Meshing-Auto mesh-Surface. Mesh size of first area is 1.5 and second is 1.Then OK (Figure C.32).

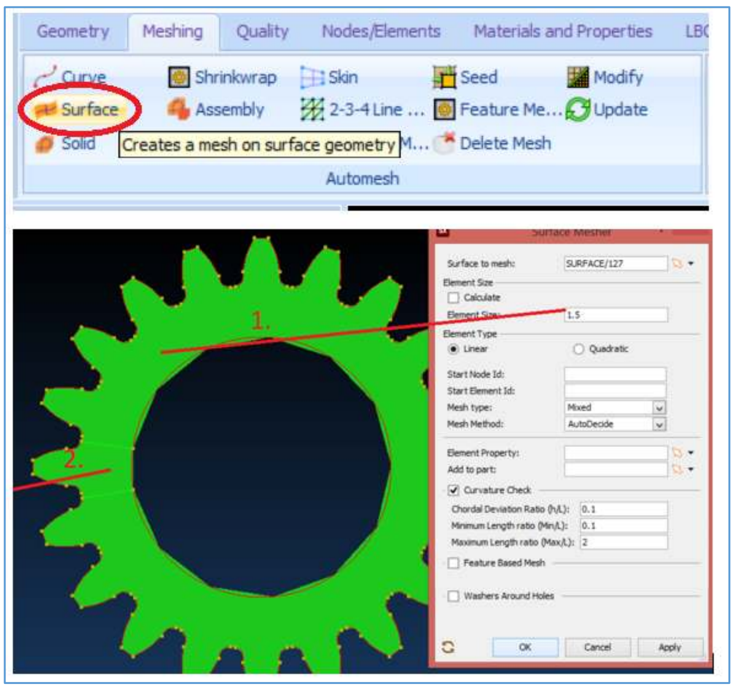

Figure C.32: Meshing

- Angle Driven, Length Degen and Connected Element should be zero or no problem under quality tab in check section (Figure C.33).

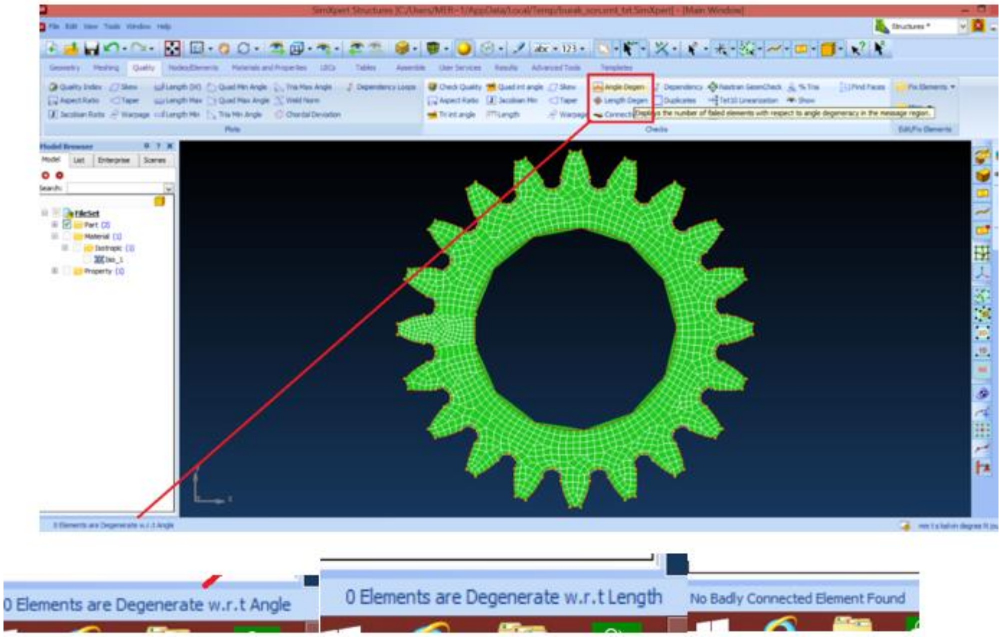

Figure C.33: Quality Check

Gear is meshed via CQUAD4 and CTRIA3 elements as solid in Figure C.33. There are 1318 CQUAD4 and 134 CTRIA3 elements. Mesh size is 1.5 mm and 1 mm mentioned in previous page in Figure C.32.The mesh statistics are shown in Figure C.34.

```
                                Statistics
Statistics For Current Scene
=======================================================================
GRID                 Entities =    1613
Parts         =     1
--------------------------------------------------
Shell                Elements =    1452      100.0%
 CQUAD4                 Elements =    1318             90.8%
 CTRIA3                Elements =    134               9.2%
--------------------------------------------------
Elements        =    1452
--------------------------------------------------
--------------------------------------------------
Points        =    127
--------------------------------------------------
--------------------------------------------------
Curves        =    126
--------------------------------------------------
--------------------------------------------------
Surfaces       =    2
--------------------------------------------------
Statistics For Other Entities in Current Model
=======================================================================
```

Figure C.34: Mesh Statistics of Gear

- Center of Gear is fixed under LBC Tab-Constraints-Fixed and load is applied from tip point under LBC Tab-Loads-Force (Figure C.35).

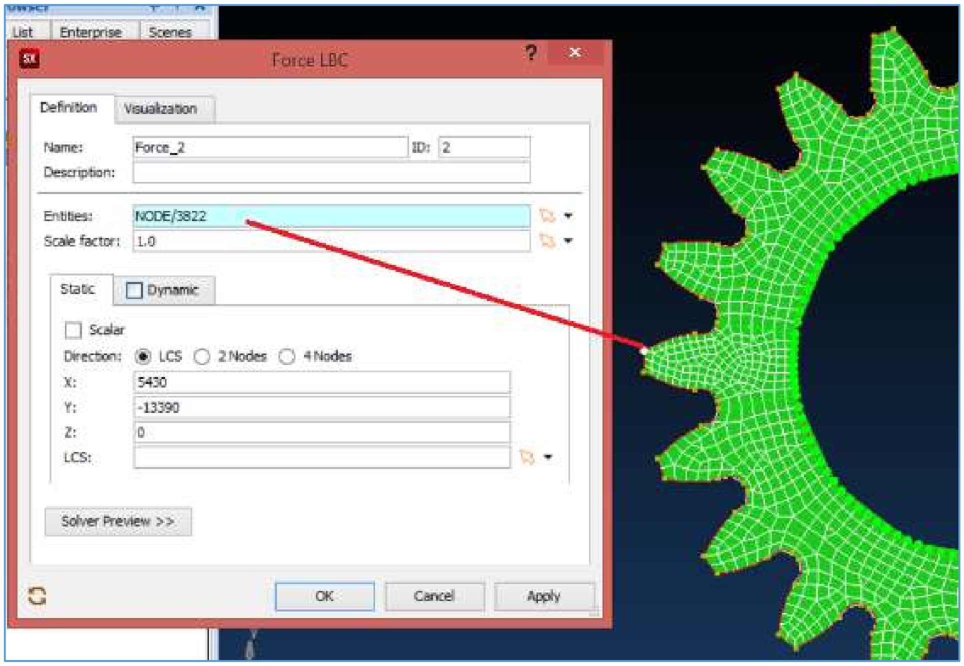

Figure C.35: Application of LBC properties

- Right mouse button is clicked on FileSet and "create new nstran job " is selected then right mouse button is clicked on the job name and program is "run" (Figure C.36).

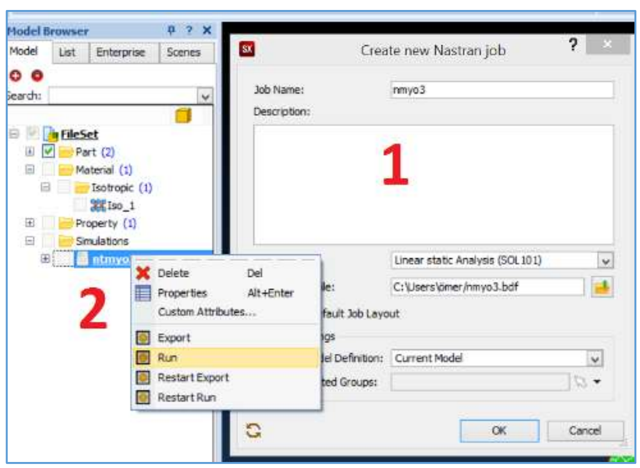

Figure C.36: Creating new Job

- Result is attached by File-attach results- "job name.xdb" (Figure C.37).

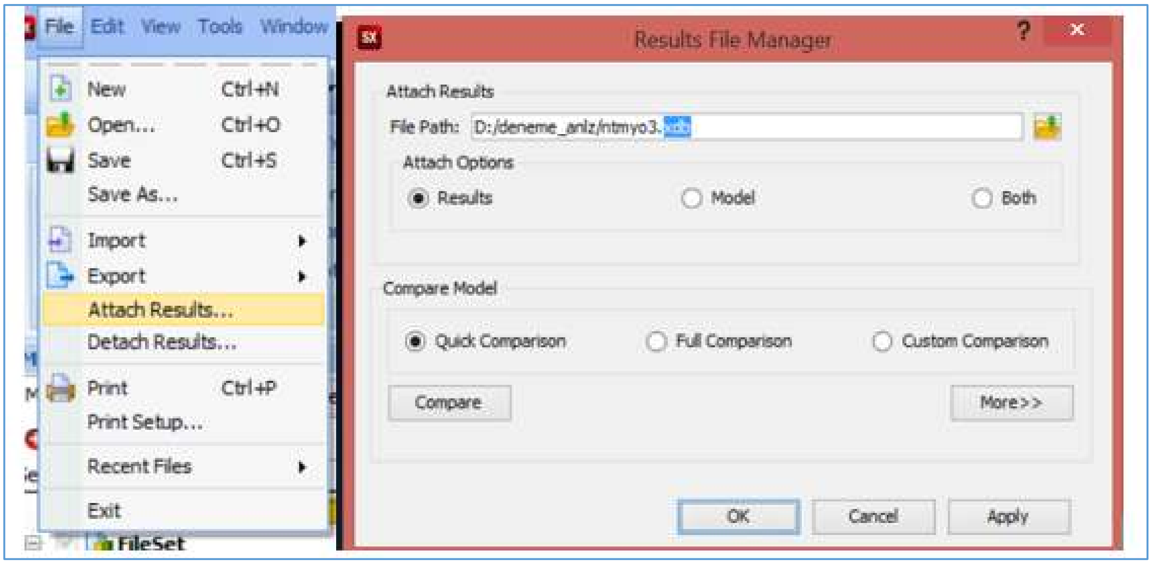

Figure C.37: Attacking results

- Result is interpreted under Result tab as stresses, deflection and etc. (Figure C.38).

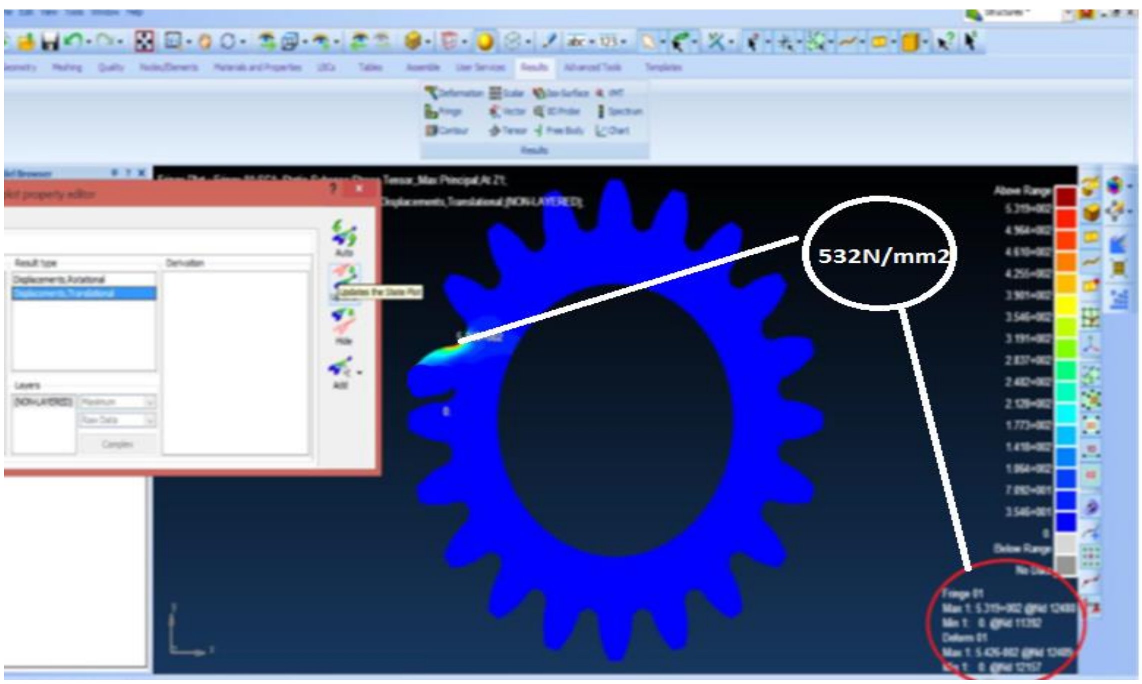

Figure C.38: Results

Bending stress of gear is defined with Lewis Equation. According to Lewis Equation;

Bending Stress is;

$$\sigma^t = \frac{W_t}{Fw * m * Y} \tag{C.2}$$

Here;

W_t: Tangential forces (13390 N defined in previous section), m: module and Y: Lewis form factor (0,4 for 40 teeth)

$$\sigma^t = \frac{13390}{20 * 3 * 0{,}4} = 557 \text{ N/mm}^2$$

In Fem, result of this value is 532 N/mm^2. Error ratio of between finite element analysis and analytical solution is;

r= $(X_t-X_i)/X_i$*100

r= ((557-532)/557)*100

r=4.4%

APPENDIX D

TECHNICAL DRAWINGS AND PICTURES OF SOME TEST RIG PARTS

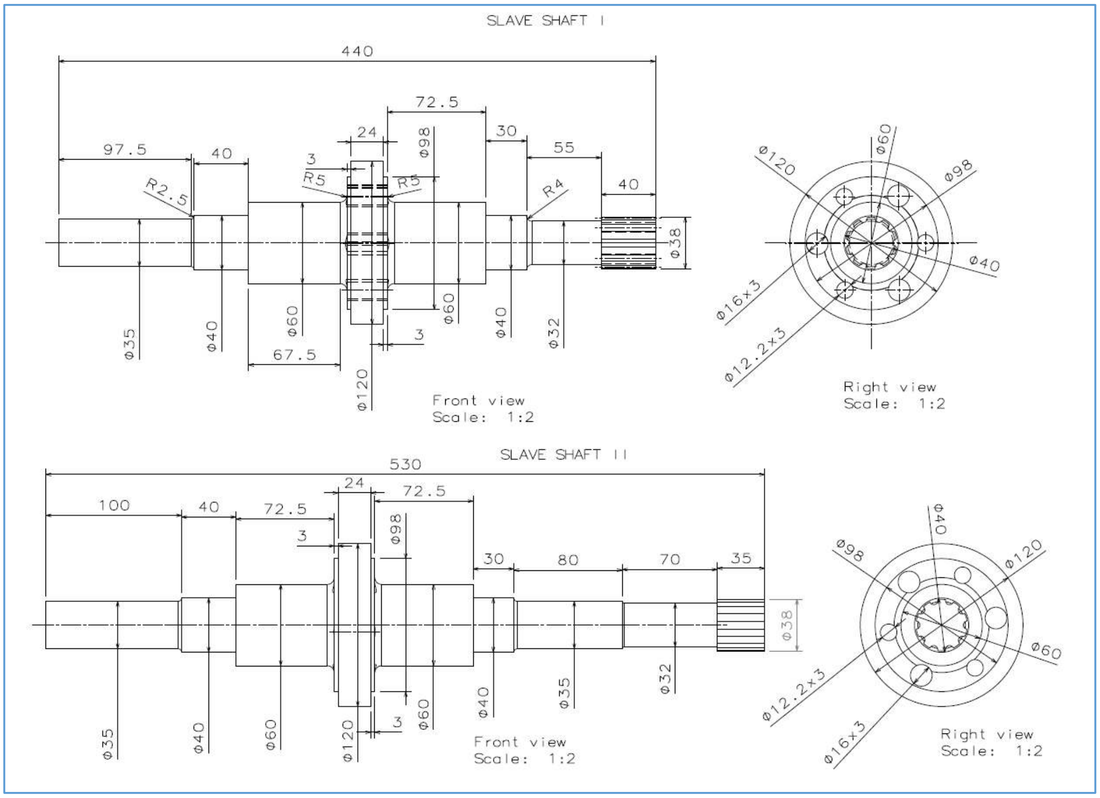

Figure D.1: Technical Drawing of Slave Shaft

Figure D.2: Picture of Slave Shaft

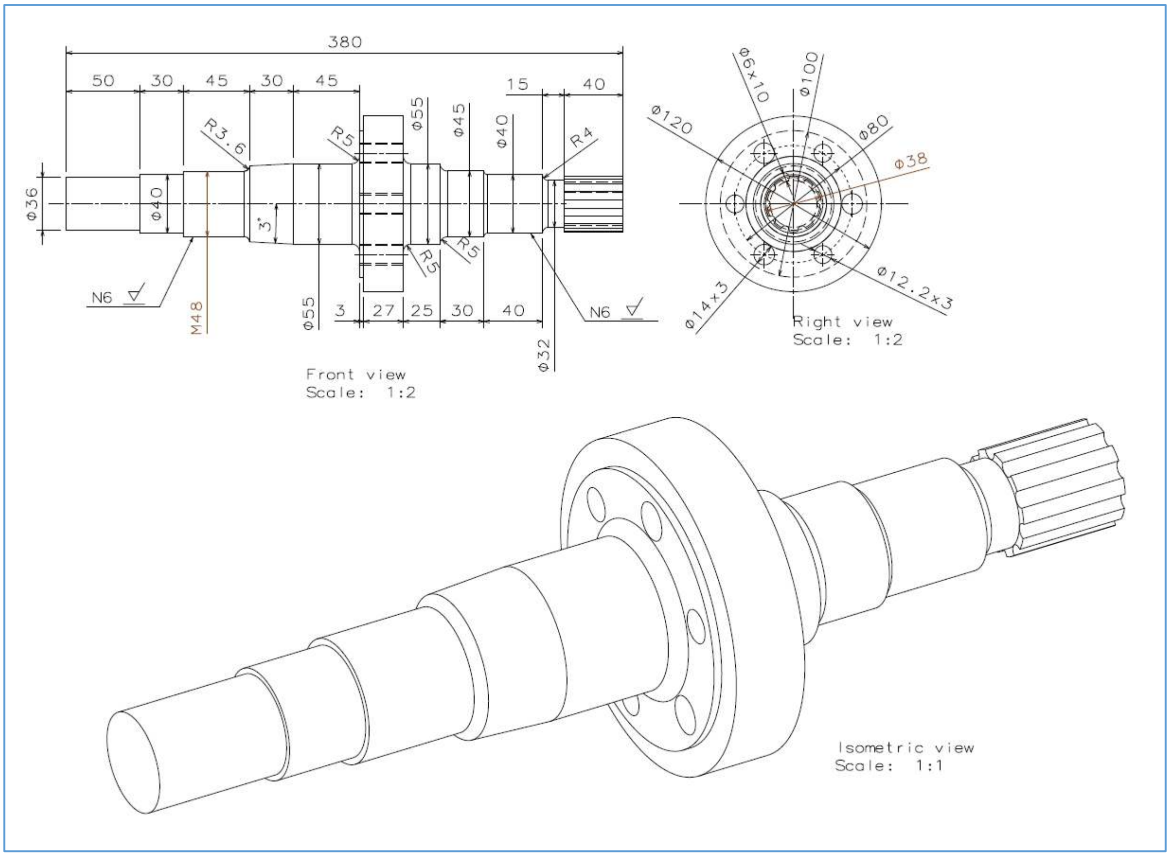

Figure D.3: Technical Drawing of Test Shaft

Figure D.4: Picture of Test Shaft

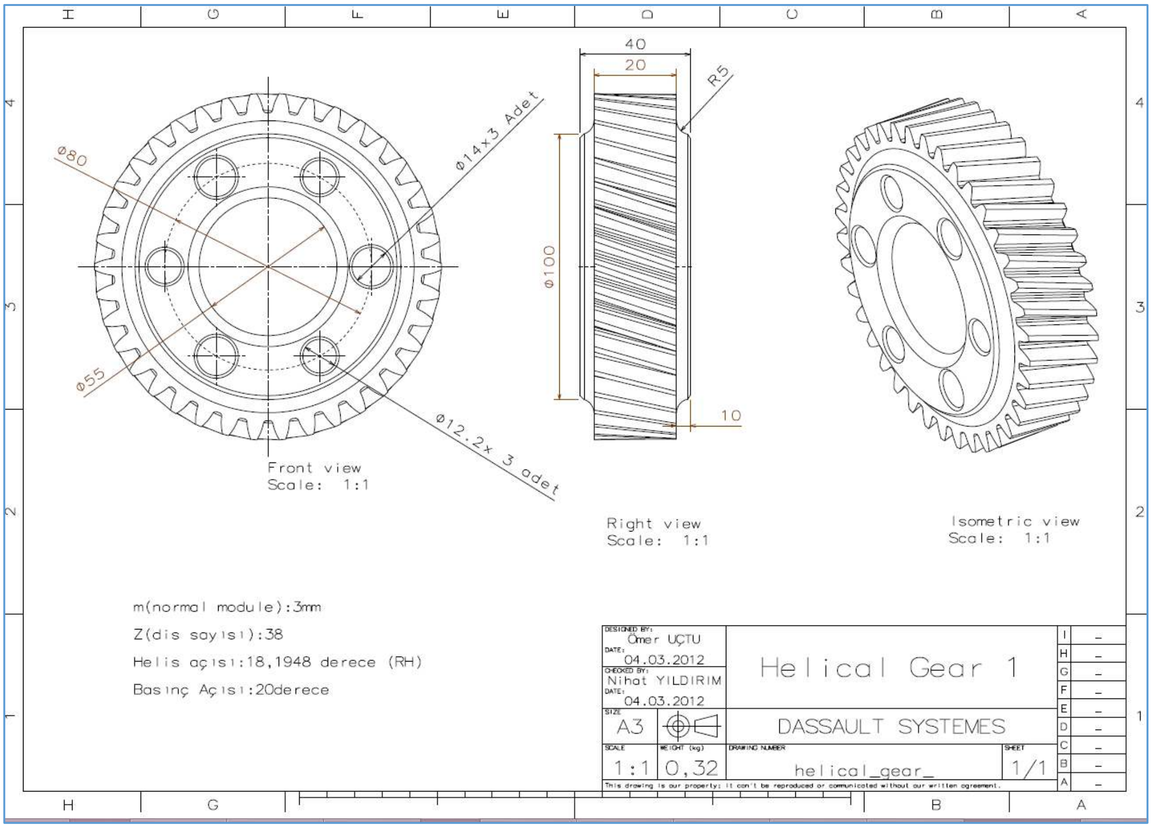

Figure D.5: Technical Drawing of Helical Gear

Figure D.6: Picture of Helical Gear

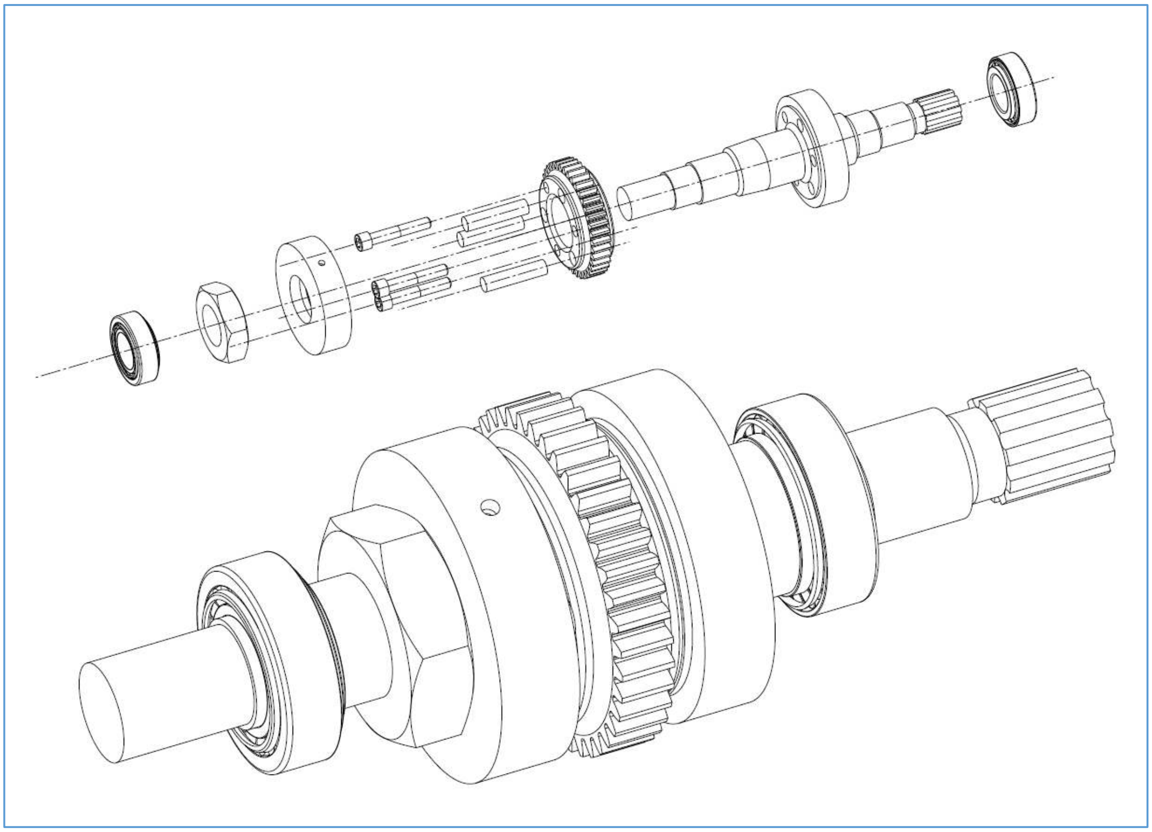

Figure D.7: Technical Drawing of Test Shaft Assembly

Figure D.8: Picture of Test Shaft Assembly

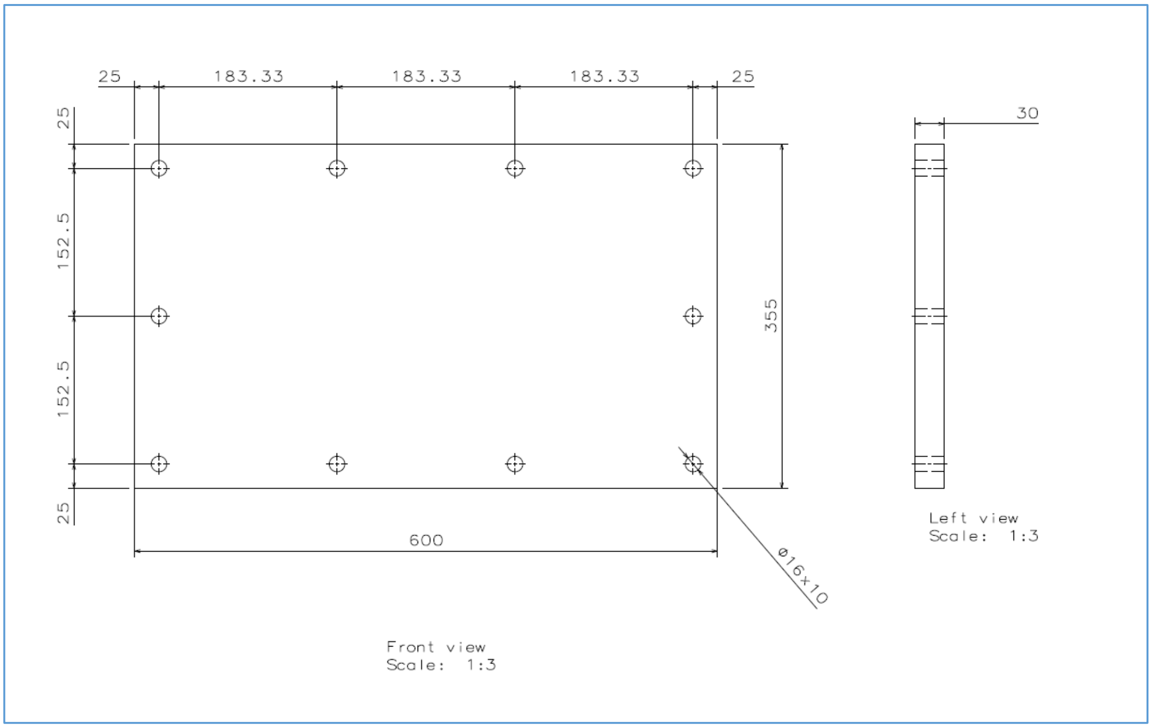

Figure D.9: Technical Drawing of Gearbox Plate

Figure D.10: Picture of Gearbox Plate

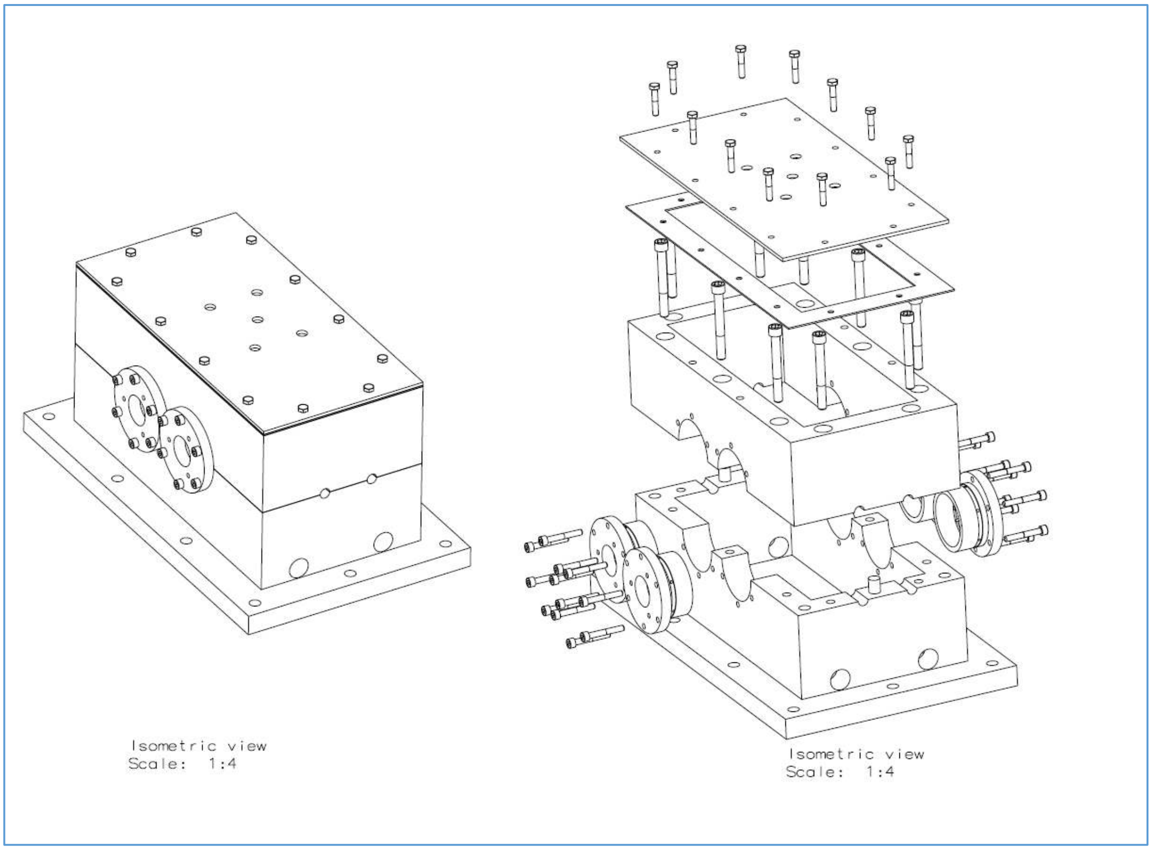

Figure D.11: Technical Drawing of Gearbox Assembly

Figure D.12: Picture of Gearbox Assembly

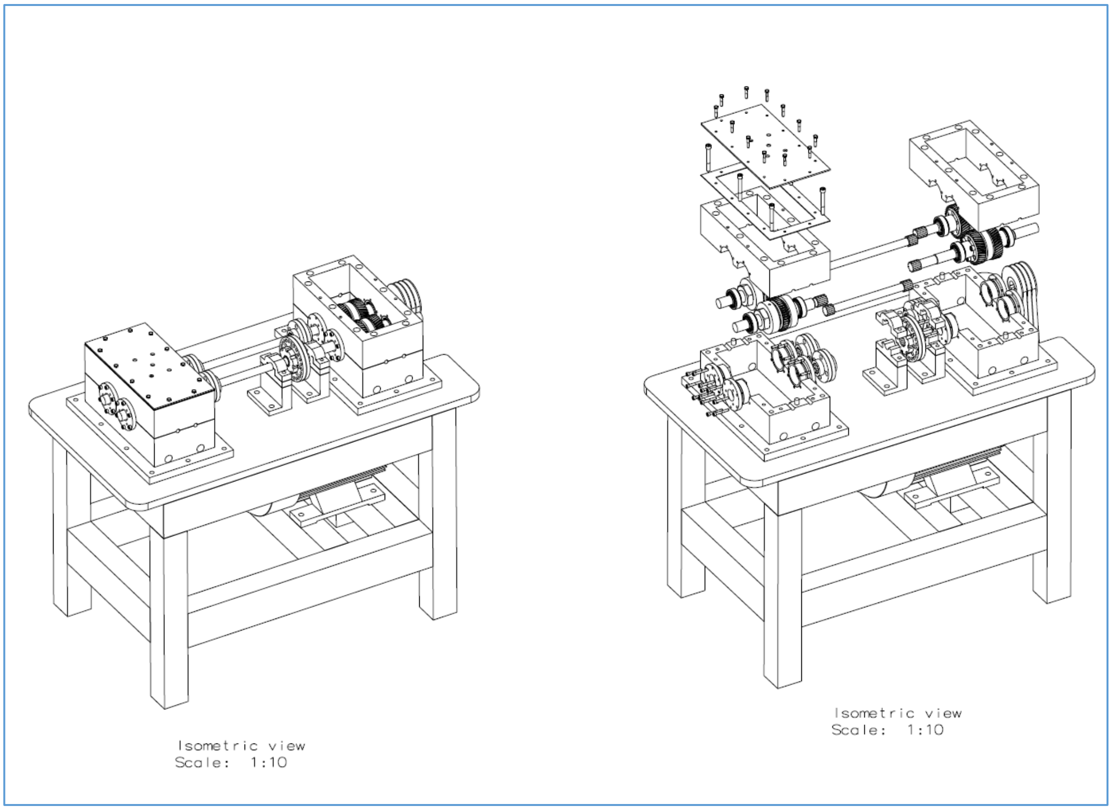

Figure D.13: Technical Drawing of Test Rig Assembly

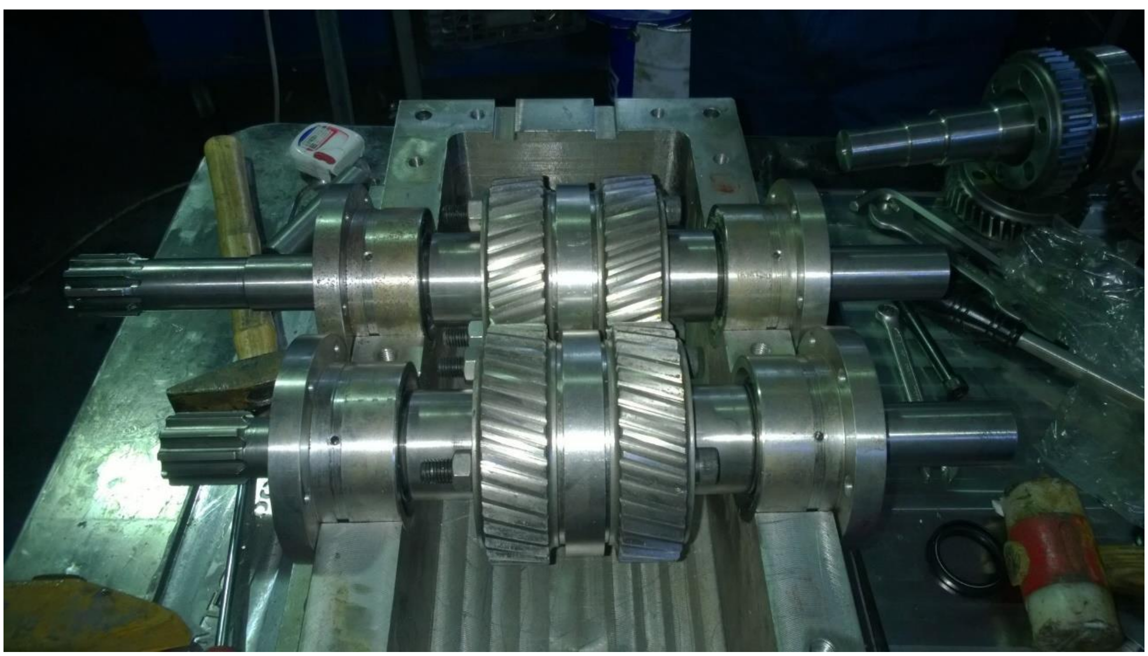

Figure D.14: Picture of Half Slave Gearbox

Figure D.15: Picture of Slave Gearbox

Figure D.16: Picture of Chasis

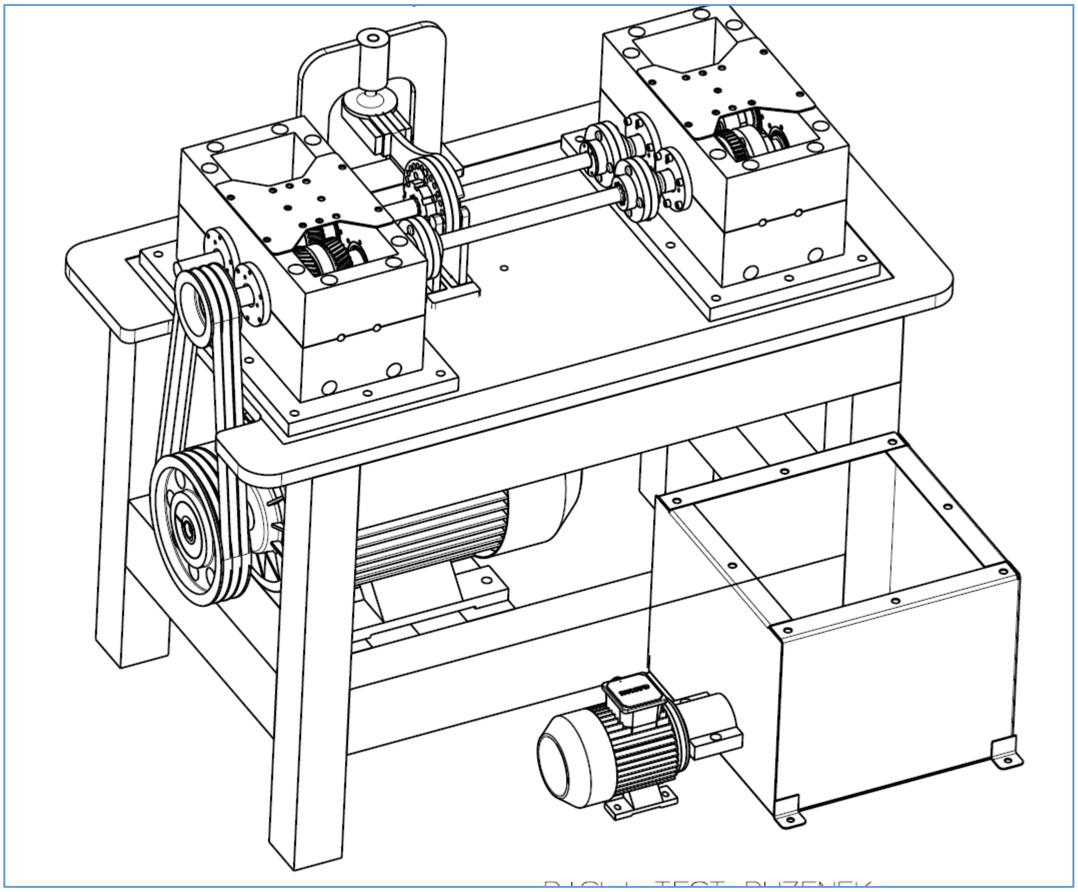

Figure D.17: Technical Drawing of Test Rig

Figure D.18: Picture of Test Rig (Front View)

Figure D.19: Picture of Test Rig (Isometric View 1)

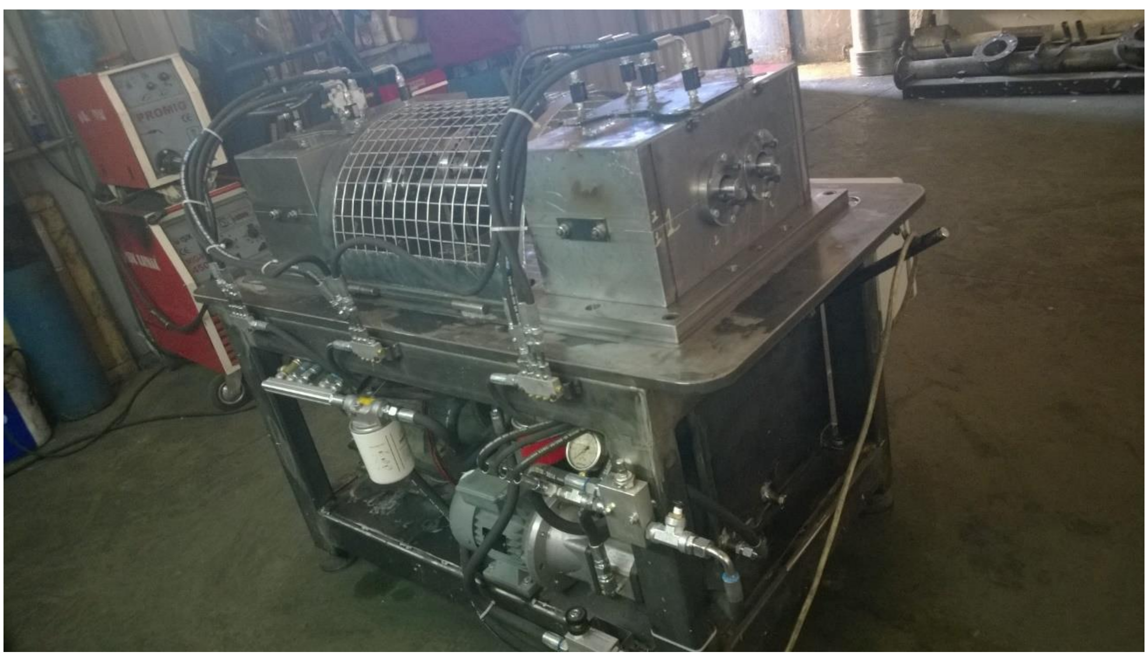

Figure D.20: Picture of Test Rig (Isometric View 2)